DEVELOPMENT OF AN IN-VITRO MODEL OF HUMAN PROSTATE

By

Bernadette Daly-Burns B.Sc.

A Thesis Submitted For The Degree Of Masters Of Philosophy To

The Faculty Of Medicine

University College London

Institute of Urology and Nephrology

Research Laboratories

University College London

ProQuest LLC
789 East Eisenhower Parkway
P.O. Box 1346
Ann Arbor, MI 48106-1346

ABSTRACT

The mechanisms controlling the growth and development of Benign Prostate Hyperplasia (BPH), the most common non-malignant disorder found in men over the age of 70, are poorly understood. There is a shortage of relevant "in vitro" models suitable for studying this disease. The aim of this project was to develop a representative "in vitro" model system for the study of BPH.

Epithelial and fibroblast cell lines (Pre2.8 and S2.13 respectively) were derived from the same biopsy of BPH and immortalised using the temperature sensitive SV40 large-T antigen construct. At 33°C the cells grow progressively under the influence of the SV40 large T-antigen, but at 39°C the conformation of the protein changes and the protein is no longer functional, so the cells stop dividing and are able to differentiate. When monolayer cultures were switched from 33°C to 37°C or 39°C, changes in morphology, cell size distribution and a reduction in cell proliferation were observed. Both cell lines expressed the 5α-reductase type I enzyme, but did not express androgen receptor (AR) and did not secrete PSA and PAP, hence they are likely to be undifferentiated cells. Pre2.8 epithelial cells have a basal cell phenotype at 33°C and undergo limited differentiation at 37°C and 39°C. DNA profiling was used to confirm the origin of the cells. The cell lines were shown to be Mycoplasma-free. Both cell lines showed amplification of DNA on chromosome 20q, a region known to be associated with cell immortalisation.

In order to develop a representative model of BPH, Pre2.8 and S2.13 cells were mixed in 3-dimensional matrigel cultures and optimised in order to obtain the most suitable culture conditions to produce prostate-specific characteristics. The three-dimensional culture system consisted of epithelial cells surrounded by a layer of stromal cells and in some cases with the formation of acinus like structures. The 3-D model showed some prostate-specific characteristics, for instance the epithelial cells expressed the androgen receptor. The epithelial cells differentiated towards a luminal phenotype, expressing K8 and 18.

In conclusion, a matched pair of epithelial and stromal BPH cell lines has been established which show some typical characteristics of prostate cells and have been

grown in a three-dimensional culture. The model may be useful for studying the cell interactions that control the growth of benign prostate Hyperplasia.

This thesis is dedicated to the wonderful men in my life, my husband Michael and son Ciaran.

Thank you for all your support and patience during this long period of time.

ACKNOWLEDGEMENTS

I am indebted to my supervisor Prof. John Masters for the training, encouragement and support he has provided during my MPhil studies at the Institute of Urology.

Special thanks to Dr David Hudson, my second supervisor for his invaluable training and support throughout the duration of the project. To other colleagues involved in this area of research, Dr. Pat Fry, Ms Tahirah Alam, Dr Rodger Tatoud, Dr Istvan Laczko and Dr Qin Wang thank you for all your technical input, advice, expertise, help and support. To all other work colleagues who have come and gone. Thank you for your support and patience during those stressful moments.

I would like to thank Dr. Mike O'Hare for transducing the primary cultures with the temperature sensitive SV40 construct.

Finally, I would like to thank my family and friends for their encouragement and support. Michael thank you for acting as father and house husband at weekends, while I was working on my MPhil. Completion of this thesis would not have been possible without your understanding, encouragement and unquestioning support.

TABLE OF CONTENTS

LIST OF FIGURES **Page**

LIST OF FIGURES **Page**

LIST OF FIGURES **Page**

LIST OF TABLES **Page**

ABBREVIATIONS

°C:	Degree Centigrade
5α-R:	5α-reductase
AR:	Aandrogen Receptor
BOO:	Bladder Outlet Obstruction
BPE:	Bovine Pituitary Extract
BPH:	Benign Rrostatic Hyperplasia
$CaCl_2$:	Calcium Chloride
CFE:	Colony Forming Efficiency
CO_2:	Carbon Dioxide
DHT:	Dihydrotestosterone
DMEM:	Dulbecco's Modification of Eagles Medium
DNA:	Deoxyribonucleic Acid
dNTP:	Deoxyribonucleotide Triphosphate
DRE:	Digital Rectal Examination
FACS:	Fluorescence Activated Cell Sorter
FBS:	Foetal Bovine Serum
GAPDH:	Glyceraldehyde-3-Phosphate Dehydrogenase
G418:	Neomycin
GC:	Growth Curve
HPV:	Human Papilloma Virus
IPSS:	International Prostate Symptom Score
IPSS:	International Prostate Symptom Score
K:	Keratins
Kb:	Kilobase
KGF:	Keratinocyte-SFM Medium
Ltag:	Large T Antigen
LUTS:	Lower Urinary Tract Symptoms
M:	Molar
$MgCl_2$:	Magnesium Chloride
ml:	Mililitre
MPD:	Mean Population Doubling

ABBREVIATIONS

NaCl:	Sodium Chloride
NaOH:	Sodium Hydroxide
NE:	Neuroendocrine
PBS :	1x Phosphate-Buffered Saline
PCR:	Polymerase Chain Reaction
PI:	Propidium Iodide
PK:	Protease K
PrEGM:	Prostate Epithelial Growth Medium
PSA:	Prostate Specific Antigen
PSAP:	Prostatic Acid Phosphatase
PSMA:	Prostate Specific Membrane Antigen
QOL:	Quality Of Life
RNA:	Ribonucleic acid
RPM:	Revolutions Per Minute
RT-PCR:	Reverse transcription –polymerase chain reaction
SE :	Standard Error
SMA:	Smooth Muscle α-Actin
SMC:	Smooth Muscle Cell
STR:	Short Tandem Repeat
TA:	Transit Amplifying
TURP:	Transurethral Resection of the Prostate

CHAPTER 1

INTRODUCTION

1.1 THE PROSTATE

The prostate gland is part of the male reproductive system, producing secretions that contribute to the ejaculate. The prostate acts a bit like a junction box. It allows the tubes that transport sperm from each testicle and the tubes that drain from the seminal vesicles to meet and then empty their contents into the urethra. Some men develop problems urinating due to an enlarged prostate. The urethra has to pass through the prostate before reaching the penis. It is only in recent years that research into understanding the diseases, cancer and benign prostate hyperplasia (BPH) of the prostate has developed. This is partly due to the lack of in vitro models of these diseases, particularly BPH. The value of such models lies in their ability to increase understanding of the biology and development of these conditions. Relying on a continuous supply of human prostate tissue for research can be limiting, due to the difficulty in obtaining human tissue and also the limited lifespan of primary cells. If the optimum prostate model was developed it could have the potential to investigate therapeutic agents for the prevention or treatment of these diseases. This thesis concentrates on developing an in vitro model for BPH, in the hope to overcome the limitations (e.g. lack of cell differentiation) of current in vitro models.

1.1.1 Development And Hormone Control

The gland begins to develop at about the twelfth week of gestation. At birth the prostate weighs approximately 4g and at puberty enlarges to approximately 20g. It continues to grow throughout adult life by 1 to 2% per year, eventually causing the symptoms of benign prostatic hyperplasia (BPH) in approximately 25% of men (McConnell, 1998). Between weeks 10 and 12 of gestation, epithelial buds begin to grow out from the urogenital sinus to form the prostatic acini and ducts. These epithelial buds grow and branch into the surrounding mesenchyme until approximately week 16 of gestation (Kellokumpu-Lehtinen and Pelliniemi, 1988).

The development of the human urogenital tract during embryogenesis is initially similar in both sexes. The urogenital tract comprises the Wolffian (mesonephric) duct and the Mullerian (paramesonephric) duct and includes the urogenital sinus and testis.

Sexual differentiation and development rely on the availability of androgens, specifically testosterone and dihydrotestosterone (Coffey and Isaacs, 1981). Testosterone is converted to a more active form dihydrotestosterone (DHT) by the

intracellular enzyme 5α-reductase (5α-R). 5α-R has two main isoforms, types 1 and 2, both of which are expressed in the human prostate (Andersson and Russell, 1990) (Jenkins et al., 1992a; Thigpen et al., 1993). When testosterone from testicular or adrenal sources reaches the prostate it can bind directly to the androgen receptor or be converted to DHT. DHT can then bind to the same androgen receptor, but with greater affinity than testosterone.

Testosterone is synthesised in the Leydig cells of the foetal testis (Wilson and Siiteri, 1973) and mediates the development of the Wolffian duct into the epididymis, seminal vesicles and the vas deferens (George and Wilson, 1986; Warwick R and Williams PL eds, 2002). DHT is required for the development of the prostate and external male genitalia. Loss of function mutations in 5α-R2 results in pseudohermaphroditism, with incomplete development of the urogenital sinus and external genitalia. Such mutations also inhibit prostate growth, but do not affect the development of the Wolffian duct (Andersson et al., 1991; Goldstein and Wilson, 1975; Imperato-McGinley et al., 1974).

1.1.2 Anatomy

The prostate is a small gland that lies immediately below the bladder (see figure 1.1). Its shape has been described as an inverted pyramid. The prostatic urethra runs from the bladder neck proximally to the membranous urethra distally. An angulation of approximately 35 degrees occurs midway along the prostatic urethra. This is called the verumontanum, and is an embryological remnant located where the ejaculatory ducts enter just below the urethral crest. The internal sphincter, which prevents retrograde ejaculation, surrounds the proximal urethra at the bladder neck. Ejaculatory contents are synthesised and stored in the seminal vesicles, which are connected to the urethra by the ejaculatory duct and are situated behind the bladder.

Currently, the most widely accepted anatomical model of the prostate is that proposed by (McNeal, 1968). He divided the prostate gland into 4 zones, the transition zone, the central zone, the peripheral zone and the anterior fibromuscular stroma (see figure 1.2). The transition zone is the smallest portion (5 to 10%) of the glandular tissue and surrounds the urethra above the verumontanum. The central zone makes up approximately 25% of the glandular prostate. It is a cone shaped region between the base of the prostate and the verumontanum, surrounding the ejaculatory ducts, making up much of the base of the prostate. The peripheral zone is the largest part (65 to 70%)

of the glandular prostate and extends towards the anterior in a horseshoe shape. The anterior fibromuscular stroma makes up one third of the prostate volume.

Figure 1.1: Anatomy Of Prostate

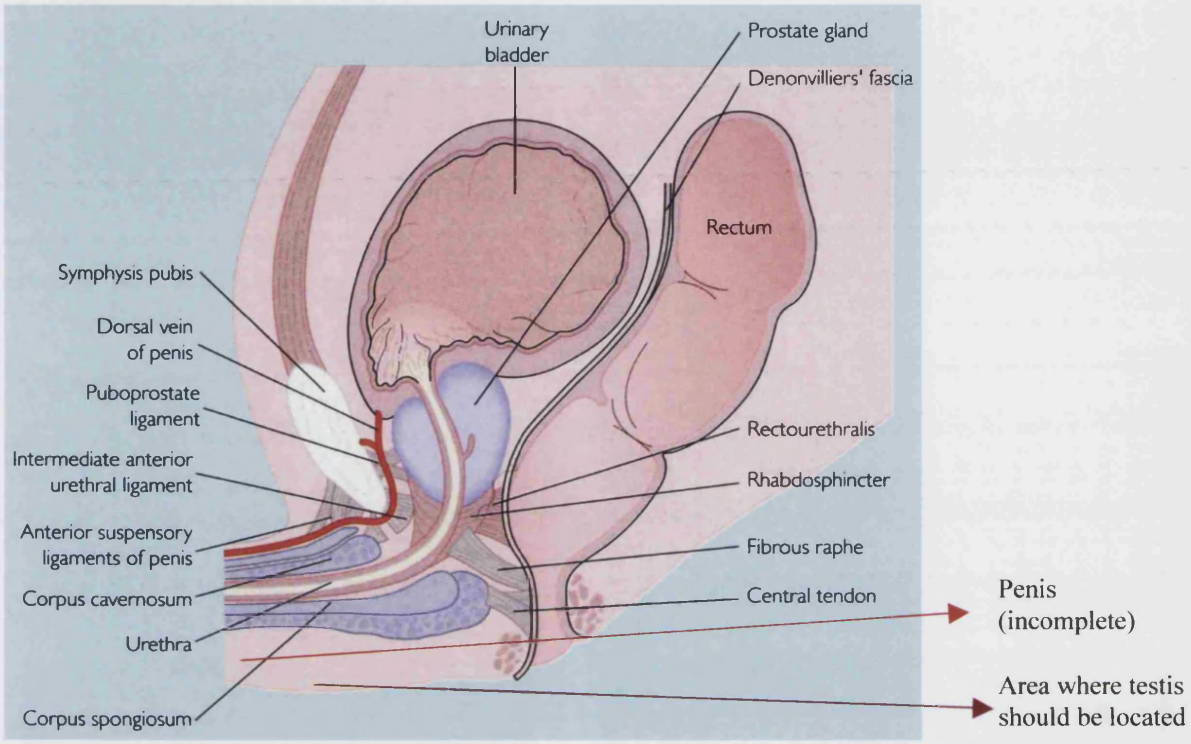

Sagittal View Of The Male Pelvis. The growth of the prostate is controlled by testosterone, the male sex hormone. Most testosterone is made by the testis, travelles into the bloodstream and finds its way to the prostate. The testis (not shown in diagram) are situated anterior to the rectum, with one to the right and left, just behind the penis.

Figure 1.2: Zonal Anatomy Of The Prostate

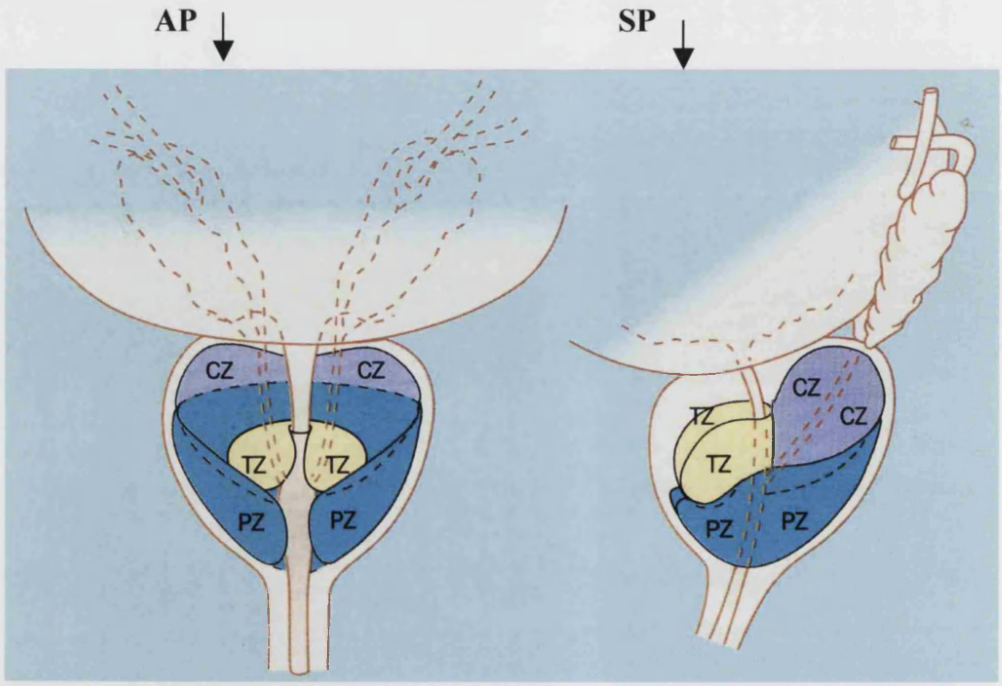

Zonal anatomy of the prostate in Antero-Posterior (AP) and sagittal planes (SP) showing central zone (CZ), peripheral zone (PZ) and transition zone (TZ).

1.1.3 Morphology And Histology

The human prostate consists of a complex array of secretory ducts and acini surrounded by stroma (see figure 1.3). The epithelium consists of two layers, the luminal and basal layers. Luminal cells are tall and columnar, and overlay flattened, elongated basal cells that rest on a basement membrane. The supporting stroma includes smooth muscle cells, fibroblasts, myofibroblasts, blood vessels, nerve terminals and lymphatics (Aumuller, 1983). The stromal cells are embedded in a loose collagenous extracellular matrix, providing mechanical support.

(McNeal, 1968) described zonal differences between the acini. The central zone contains large irregular shaped acini folding into luminal ridges. The luminal epithelial cells contain large, pale nuclei positioned in an irregular fashion within a granulated cytoplasm. The stroma of the central zone contains long tightly packed smooth muscle cells aligning the contours of the acini. The peripheral zone acini are small and round with no obvious projections. The basal cells contain a small, dark nucleus in a clear cytoplasm. The stroma contains loose, randomly arranged smooth muscle cells. The acini of the transition zone are similar to those in the peripheral zone.

The transition zone is the site of development of BPH, while the majority of cancers develop in the peripheral zone. Although the peripheral and transition zones are similar histologically, BPH does not develop in the peripheral zone.

Figure 1.3: Morphology Of BPH Tissue

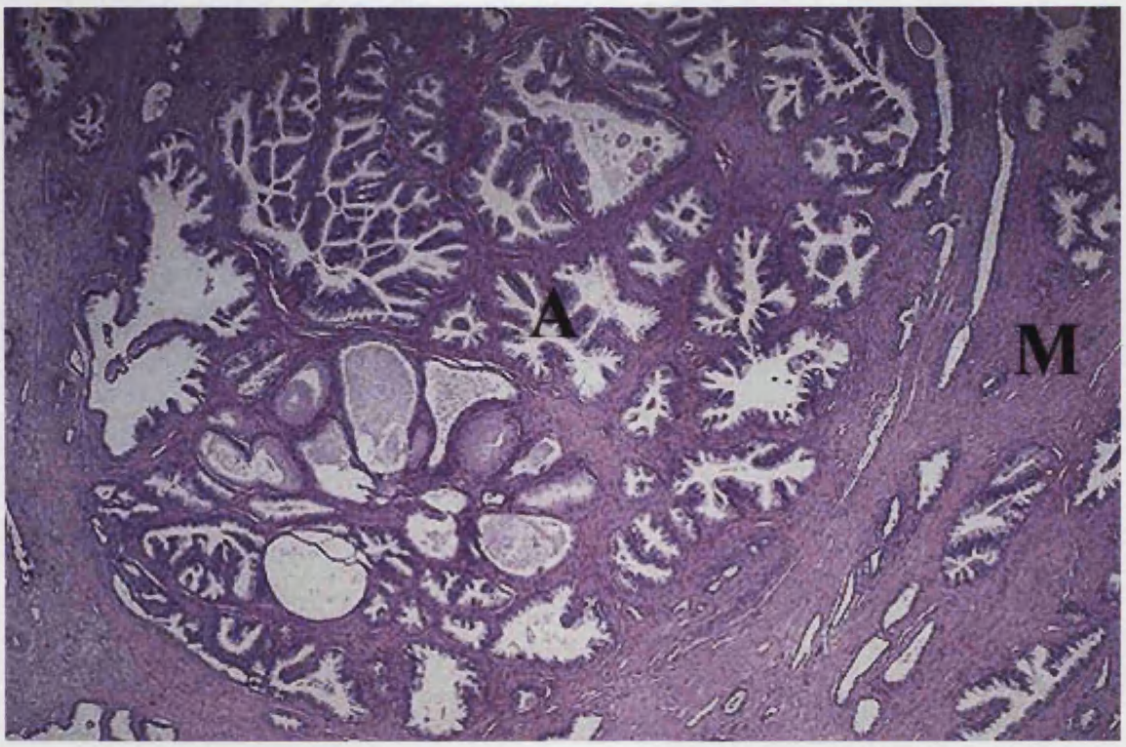

Low power magnification showing H&E staining of a Benign Prostatic Hyperplasia nodule. **A** indicates the acinus, **M** indicates the fibromuscular connective tissue/stroma.

1.1.4 Cell Types

Epithelial Cells

Prostate epithelium contains 3 distinct cell populations; the secretory luminal, the proliferative basal and the neuroendocrine (NE) cells. These cell populations can be distinguished by their proliferative capacity, hormonal sensitivity and cytokeratin expression (table 1.1).

Table 1.1: Characteristics Of Prostate Epithelial Cells

Markers	Basal cells	Luminal cells	Neuroendocrine cells
Cytokeratin	K5/K14	K8/K18	Mixed basal and luminal (complex - K5/K8)
Proliferation	Ki-67		
Secretion		PSA, PAP	Chromogranin A
Hormone Receptor		AR	Serotonin, calcitonin
Other	Bcl-2, CD44, p63	CD57	CD56

The proliferation-associated antigens Ki-67 (Gerdes et al., 1984; Hudson et al., 2001a), PCNA and MIB-1 (Cattoretti et al., 1992) have been used to measure the proliferative capacity of epithelial cells. These markers, together with DNA cell cycle distribution indicate that the basal cells are the main proliferative compartment (Bonkhoff et al., 1994; Dermer, 1978; Merchant et al., 1983). Co-expression of proliferation markers with the neuroendocrine marker chromogranin A has not been observed (Bonkhoff et al., 1991). Less than 20% of Ki-67 positive cells are in the luminal layer and most of these are in an intermediate position between the basal and luminal layers, while the remaining 80% are in the basal layer (Hudson et al., 2001a).

The luminal cells express prostate specific antigen (PSA), prostatic acid phosphatase (PSAP), prostate specific membrane antigen (PSMA) (Lilja and Abrahamsson, 1988), and androgen receptor (Masai et al., 1990). The basal cells are believed to be androgen independent, although there is evidence that the basal cells express nuclear receptors for estrogens and progesterone (Ruizeveld de Winter et al., 1991) (Wernert et al., 1988). NE cells express the secretory granules of the peptide chromogranin A (Xue et al., 1998) and serotonin, a neurotransmitter and hormone, (Capella et al., 1981; di Sant'Agnese et al., 1985; Fetissof et al., 1983). Some NE cells contain calcitonin (Abrahamsson et al., 1986; di Sant'Agnese and Mesy Jensen, 1984; di Sant'Agnese et al., 1989; Fetissof et al., 1986).

Cytokeratins are a family of 20 polypeptides that form the intermediate filaments of epithelial cells. These cell markers have been fundamental in establishing the differentiation pattern of epithelial cells. In the prostate the luminal cells express keratins (K) 8 and 18, while the basal cells express K5 and K14. An intermediate basal cell population expresses K5 with low levels of K8 (Peehl et al., 1994; Purkis et al., 1990; Xue et al., 1998). Basal cells may also express K17 (Hudson et al., 2001b; Troyanovsky et al., 1989). Keratin 19 can be expressed by luminal and basal cells (Hudson et al., 2001b; Peehl et al., 1996).

The bcl-2 proto-oncogene is expressed by the basal cells of the prostate (Hockenbery et al., 1991; McDonnell et al., 1992). The basal cells express the surface membrane marker CD44, distinguishing them from the luminal cells, which express CD57 (Terpe et al., 1994; Liu et al., 1997). The p63 gene is expressed in normal prostate basal cells only. It is thought that this gene is involved in prostate development (Signoretti et al., 2000).

Stromal Cells

The prostate stroma contains smooth muscle cells, fibroblasts, and an intermediate type called myofibroblasts (Zhang et al., 1997). Smooth muscle cells make up the largest part of prostate stroma (Shapiro et al., 1992).

Like epithelial cells, stroma can be differentially characterised using staining for intermediate filaments, including desmin, vimentin and myosin (see table 1.2). Desmin forms an interconnecting network across muscle cells. Smooth muscle α-actin (SMA) is the major constituent of the microfilaments involved in smooth muscle contraction (Darnell, 1986). Vimentin is expressed in all stromal cells and can be used to differentiate epithelial cells from stromal cells.

Further characterisation is achieved using SMA (Skalli et al., 1986), myosin and desmin, which are expressed in smooth muscle cells but not in fibroblasts (Peehl and Sellers, 1997; Zhang et al., 1997). SMA stains twice as many smooth muscle cells as desmin, indicating that desmin underestimates the number of smooth muscle cells (Peehl and Sellers, 1997; Shapiro et al., 1992). SMA is also expressed in myofibroblasts. This means that desmin negative smooth muscle cells are actually myofibroblasts.

The cell adhesion molecule CD44 is expressed in some stromal cells (Fry et al., 2000a) and androgen receptor (AR) is expressed in approximately 50% of stromal cells (Janssen et al., 1994).

Table 1.2: Characteristics Of Prostate Stromal Cells

Markers	Smooth muscle	Myofibroblast	Fibroblast
Stromal cell markers (intermediate filaments)	Vimentin, SMA, SM-Myosin	Vimentin, SMA	Vimentin
Hormone	AR, ER	AR, ER	AR, ER
Others	CD44	CD44	CD44

1.1.5 Biochemistry

Luminal epithelial cells secrete prostate specific antigen (PSA) (Sinha et al., 1987) and prostate acid phosphatase (PSAP) (Lin et al., 1992) PSA and PSAP production are under the control of androgens via the androgen receptor.

PSA is a 34 kilodalton, 240-amino acid glycoprotein and is a member of the human kallikrein (hGK-1) family (Henttu and Vihko, 1989; Riegman et al., 1989). PSA is a serine protease (Watt et al., 1986) that acts like the digestive enzymes chymotrypsin and trypsin. PSA is secreted into the seminal fluid where it plays a role in semen liquification.

PSAP is a 100 kilo-Dalton dimer (Ostrowski and Kuciel, 1994) and is the major phosphotyrosyl (p-tyr) protein phosphatase in prostate epithelial cells (Lin et al., 1992; Ostrowski and Kuciel, 1994). It is thought that PSAP is also involved in liquefaction of semen and maintenance of sperm motility.

Other secretory products of the prostate include the trace elements selenium, zinc and cadmium. The prostate has a higher concentration of zinc than any other human tissue. Zinc and selenium are important in reproduction in males and females (Zhang et al., 1997; Bedwal and Bahuguna, 1994). Zinc deficiency leads to depletion of testosterone and inhibition of spermatogenesis. It is thought that zinc extends the life span of the ejaculated spermatozoa.

Selenium is found in sperm mitochondria (Hansen and Deguchi, 1996) and its deficiency may be associated with male infertility. It is suggested that selenium may be important in prostate cancer prevention (Wynder et al., 1994).

Citrate is produced, accumulated and secreted by the mitochondria of the prostate epithelial cells. A much higher level of citrate is found in the prostate compared to other tissues in the body, probably because there is limited citrate oxidation via the Krebs cycle in the prostate (Costello and Franklin, 1997). It is thought that the high levels of zinc in prostate mitochondria inhibit citrate oxidation and hence it is an inefficient energy metabolite (Costello and Franklin, 1981). A continuous supply of aspartate and glucose is required for citrate production. Aspartate is converted to oxaloacetate (OAA), which is converted to acetyl-CoA (AcCoA) (CoA meaning coenzyme acetylation) while producing citrate. The end products of glucose metabolism are lactate and citrate, due to the conversion of glucose to pyruvate and AcCoA. It is thought that testosterone and prolactin regulate this cycle (Costello and Franklin, 1994; Costello et al., 1996; Franklin and Costello, 1990).

1.2 BENIGN PROSTATIC HYPERPLASIA (BPH)

Benign prostatic hyperplasia (BPH) develops in the majority of men as they age. BPH occurs in the transition zone (McNeal, 1978). Symptoms seldom develop before the age of 30, but the incidence increases rapidly after the age of 50. Most older men have microscopic BPH (Bartsch et al., 1979), 50% will go on to develop macroscopic BPH (enlarged prostate) and 50% of these will develop clinical symptoms (Birkhoff et al., 1976; Lytton et al., 1968). BPH seldom reduces life expectancy, but it has a major impact on quality of life.

There are only two definitive risk factors known, advancing age and the presence of androgens. The average weight of an adult human prostate with normal histology is 20g ± 6. This will slowly increase to approximately 33g ± 16 with the development of BPH in the ageing man. Only 4% of prostates with BPH will increase to 100g by the seventh decade (Berry et al., 1984). BPH does not develop in men who have been castrated before puberty (Boyle, 1990). It is thought that the change in the ratio between testosterone and estrogen may drive the growth of BPH.

Although the causes of BPH are not clear it is thought that inherited and environmental factors are involved in BPH. The incidence is lower in Asia than in Europe, but is increasing in Japan, perhaps due to the adoption of a diet containing more animal fat (Chyou et al., 1993a). Family history is also associated with BPH (Sanda et al., 1994). Diet may influence pathogenesis, but there is little supporting evidence. A high fat diet increases the levels of the hormone prolactin, which may increase the risk of BPH because of its effect on the proliferation of prostatic epithelium. An intake of greater than 25oz (equivalent to 708g or 0.74litres or 6 units) of alcohol per month may reduce the incidence of BPH (Chyou et al., 1993b).

1.2.1 Etiology Of BPH

There are three main hypotheses to explain the pathogenesis of BPH. These hypotheses are based on (1) hormones (2) stromal-epithelial interaction and (3) stem cells.

The hormonal theory

The hormonal theory is based on the fact that a testicular function is required for BPH development (Isaacs and Coffey, 1989b), as BPH does not occur in men castrated prior to puberty. Androgen withdrawal in non-castrated adults leads to a reversible decrease in prostate size (Bosch et al., 1989), also indicating a role for androgen in the development and maintenance of BPH.

One theory suggests that the main factor responsible for the development of BPH is an age associated increase in DHT levels (Salm et al., 2000). This theory was based on data suggesting that DHT levels are higher in BPH tissue than in normal tissue. However, this was proven to be incorrect because some of the tissue specimens were obtained from cadavers and hormone levels change during the period taken to collect the samples. Comparison of previous results with results obtained from BPH and normal tissue, collected immediately showed that there was no difference between DHT levels in BPH tissue and normal tissue (Isaacs et al., 1983).

Another theory suggests that synergism between oestrogen and androgen may play a role in BPH pathogenesis. BPH was induced in dogs by treatment with oestrogen androstane-3,17-diol (a DHT derivative) but not with oestrogen alone (Walsh and Wilson, 1976; Bartsch et al., 1987). BPH induced with oestradiol and oestrogen androstane-3,17-diol is more severe than with androgen alone (Walsh and Wilson,

1976). It was also shown that BPH tissue contains less oestrogen receptors than normal tissue (Isaacs et al., 1983). Alterations in the ratio of androgen to oestrogen may be associated with abnormal prostate growth (Griffiths et al., 1991).

Stromal-Epithelial Interaction Theory

The stromal-epithelial interaction theory was initially suggested by Rischemer in 1925. He suggested that BPH was a stromal nodule that induced migration of epithelial cells resulting in the formation of new acini. In 1978 McNeal suggested that the primary lesion of BPH was a glandular budding and branching mechanism that gave rise to new acini in the transition zone. He suggested that this mechanism was a reawakening of the embryonic potential of prostatic stroma to induce epithelial growth during adulthood (McNeal, 1978).

Mouse embryonic mesenchyme can induce bladder epithelial cells to form prostate-like glandular structures (Cunha et al., 1983) in the presence of a functioning testis. The mechanism of "reawakening" is unknown, but could involve growth factors (Lawson, 1997) (Griffiths et al., 1998) or the basement membrane (Mawhinney et al., 1974).

Stem Cell Theory

Stem cells are cells that have the ability to self renew and proliferate. Transit amplifying (TA) cells originate from stem cells and proliferate for a limited number of cell divisions. TA cells divide to form luminal non-proliferative cells. Clonal expansion of TA cells eventually results in the prostate growing to its maximal normal size. The stem cell theory suggests an imbalance between the growth of new cells and the maturation and death of older cells (Isaacs and Coffey, 1989a).

In the normal prostate, proliferation and cell death are in equilibrium. Some alteration in this equilibrium may cause BPH. Two possibilities have been suggested: either an abnormal increase in stem cell numbers or an abnormal increase in the number of TA cells would produce an enlarged prostate.

1.2.2 Clinical Presentation

Symptoms

Patients with BPH can present with lower urinary tract symptoms (LUTS). LUTS are very common and can be influenced by many factors (including malignancy, infection,

inflammation, neurological, mechanical and drugs), and so it is important to confirm the underlying cause (Blaivas, 1996).

LUTS symptoms are due to obstruction and/or irritation. Obstructive symptoms include hesitancy, poor stream and incomplete emptying, while irritative symptoms include nocturia, frequency and urgency. The symptoms are influenced by the increase in the size of the prostate and dysfunction of the bladder muscle (Blaivas, 1996; Madsen and Bruskewitz, 1995a).

Diagnosis

A detailed medical history including patient quality of life (QOL) must be taken. The quality of life can be examined by completing a symptom score sheet. The most common is the International Prostate Symptom Score (IPSS). Each score determines whether a patient has mild (0-7), moderate (8-19) or severe (20-35) symptoms (Barry et al., 1992).

Physical examination

A digital rectal examination (DRE) can be carried out to examine the prostate and help distinguish between BPH, prostatitis and prostate cancer. A neurologic examination would help rule out neurological disorders as a cause of LUTS (McConnell et al., 1994a; Ziada et al., 1999).

Urine Analysis

In order to rule out urinary tract infection and hematuria, urine analysis using a dipstick test or by examination of spun sediment can be done (Madsen and Bruskewitz, 1995b).

PSA levels

PSA analysis has advantages and disadvantages. It is not specific in distinguishing between BPH and prostate cancer, but it is the most sensitive and simple test available. When PSA and DRE results are combined it becomes a more reliable (Tchetgen and Oesterling, 1995). Serum PSA levels greater than 4.0 mg/ml may be indicative of BPH or cancer (McConnell JD, 1994).

Urine Flow Rate

This test is a measure of the maximum flow rate (Qmax) and the rate of flow. This test requires a fluid volume of at least 150ml in order to be accurate. A flow rate of less than 15ml per second is significant for bladder outlet obstruction (BOO) (McConnell et al., 1994a; Garraway et al., 1993; Chancellor et al., 1991).

Residual Volume

Residual volume is the volume of fluid left in the bladder after void is complete. Greater than 150ml is a significant residual volume (McConnell et al., 1994b).

Urodynamics /Pressure flow rate

Urodynamics can be carried out if there is no definitive diagnosis. This is a measurement of the pressure in the bladder during voiding. It is carried out by passing a pressure transducer into the rectum and one into the bladder to record the change in pressure as the bladder fills and as the bladder voids into the flow meter. Patients who have pressure flow obstruction due to BPH generally respond better to surgery than those who have no obstruction (Griffiths, 1996; McConnell et al., 1994b).

1.2.3 Treatment

Surgery is no longer the only option for the treatment of BPH. Initially LUTS must be confirmed as the cause of BPH. Once a diagnosis of BPH is confirmed a decision must be made between the patient and the urologist as to what treatment would be preferred. The choice of treatment is watchful waiting, medical therapies or surgery. In order to make this decision IPSS, quality of life, flow-rate and residual volume must be taken into consideration (Ziada et al., 1999; Lepor H, 2002; Altwein JE, 2002).

Watchful Waiting

If the patient has mild symptoms and there are no apparent complications then watchful waiting is often the preferred option. The doctor and patient decide not to treat the symptoms immediately. Instead they wait and see if symptoms improve or deteroriate over time. Follow-ups are carried out after 6-12 months. Improved symptoms are seen in approximately 25% of cases, 50% stay the same and 25% deteriorate (Lepor, 2002).

Medical Treatment

Medical treatment is carried out for mild or moderate symptoms. There are two classes of drug, alpha-blockers and 5-α reductase inhibitors (Lepor, 2002).

The effect of α-Blockers is to relax smooth muscle in the bladder neck and in the prostate. Smooth muscle contraction in the prostate is mediated by the alpha-1 adrenoceptor (α1-AR) (Hieble et al., 1985; Lepor et al., 1988). α-Blockers target the symptoms and their effectiveness seems to be independent of prostate size and obstruction. The first α1-blocker was Phenoxybenzamine, which had many side effects. Currently the drugs in use are Praxosin, Indoramin, Infuzosin, Doxazosin and Terazosin, all of which have fewer side effects. More recently an α_{1A} blocker has been produced, which has even fewer side effects due to α1-blockade in the brain and cardiovascular system.

The efficacy of α1-blockers is dose dependent. It is claimed that there is a 20-50% improvement of IPSS and therefore an improved QOL. Flow-rate is improved by 20-30% (2-3ml/sec). A quick response (48 hrs) is observed after treatment and effectiveness can be maintained for 3-4 years, after which the symptoms become resistant to the drug.

The most common side effects are tiredness, dizziness and headaches. Less common side effects are asthenia, palpitations and gastrointestinal disturbances (nausea, vomiting, constipation and diarrhoea). There is also a risk of postural hypertension (lowering of blood pressure).

The conversion of testosterone to dihydrotestosterone (DHT) is blocked by 5α-R inhibitors and result in reduced prostate size. 5α-R inhibitors aim to treat the disease, unlike α-blockers which treat the symptoms. There are two 5α-R isozymes (type I and II) (Jenkins et al., 1992b). The most frequently prescribed drug is Finasteride, which selectively inhibits 5α-R type II (Vermeulen et al., 1989).

Finasteride is thought to be most effective if the prostate is greater than 40ml in size. It is claimed to reduce prostate size by 20-30%. It improves IPSS by 15% and flow rates by 1.3-1.6 mL/sec and therefore QOL is improved. 5α-R inhibitors take 6 months to

achieve maximum effect, which can be maintained for 6 years, after which the disease becomes resistant to the drug. The incidence of subsequent acute urinary retention is reduced (Polat et al., 1997).

Side effects include ejaculatory disorders and impotence. PSA levels tend to be reduced by half over a 12-month period (Guess et al., 1993). This should be taken into consideration in order not to miss the possible onset of prostate cancer.

Studies comparing terazosin, finasteride and placebo showed that although finasteride caused the prostate to shrink, its effectiveness at increasing urinary flow was little better than placebo and less than terazosin. 5α-R inhibitors do not seem to be as effective at relieving symptoms as α-blockers. The drugs of choice are α-Blockers unless there is substantial prostatic enlargement. In this case treatment with finasteride may be beneficial.

Phytotherapeutic agents are chemicals derived from plant extracts that have been used for the treatment of BPH. These herbal remedies have not been sufficiently evaluated in clinical trials and the mode of action of these agents is not fully understood (Gerber, 2002; Dreikorn, 2002; Lowe, 2001).

Surgical treatment

Removal of BPH tissue using open surgery is carried out by an incision through either the abdominal wall or the perineum. It is based on the presence of a cleavage plane between the BPH tissue and the unaffected prostate tissue. BPH tissue should be easily removed using an index finger along the cleavage plane. Open surgery is very successful giving a 98% symptom improvement (Ziada et al., 1999). The main disadvantages of this procedure are bleeding and the hospitalisation period (5-10 days) required for the patient to recover from open surgery. Open surgery is usually reserved for cases with particularly large prostates or if large bladder stones are present (Tubaro et al., 2001; Servadio, 1992).

Transurethral Resection of the Prostate (TURP) has largely replaced open surgery, especially if the tissue is estimated to weigh 50g or less. A resectoscope is used to remove the BPH tissue (Holtgrewe, 1998). It has many advantages over open surgery. Hospitalisation time is reduced to 1 or 2 days (Chang et al., 1998). Bleeding is

minimised. Symptom score improvements of 80-100% and mortality risk improvement of 2% can be achieved (Ziada et al., 1999). Associated bladder conditions such as stones can easily be observed and dealt with using this technique.

New approaches are being developed in an attempt to replace TURP in order to reduce side effects. Transurethral vaporization (TVP), laser therapy, transurethral microwave therapy (TUMT), transurethral needle ablation (TUNA) and high-intensity focused ultrasound (HIFU) are other techniques that can be used to treat BPH, but none of these have replaced TURP (Ziada et al., 1999).

1.3 IN-VITRO MODELS

1.3.1 Primary Culture Systems

Primary cultures proliferate initially for up to 50 population doublings, depending on the type of cell population, and usually then undergo crisis, stop dividing and die (Hayflick, 1965). This process is called replicative senescence. In culture, cancer cells can escape senescence due to genetic changes in key genes, a process called spontaneous transformation. Normal cells can escape senescence if they are immortalised with a transforming virus, or if transfected with a plasmid containing a transforming viral gene. There are two main ways of establishing primary cultures: explant culture and enzymatic dissociation.

Explant culture is carried out by cutting tissue into approximately 1 mm^3 fragments and then placing the explants in tissue culture flasks in a suitable culture medium. Stromal and epithelial cells can grow out of the explants.

Human prostatic epithelial cells and fibroblasts from the prostates of 15 cadaveric kidney donors (aged under 40 years) and 2 fetuses (35 weeks gestation) were established using explant cultures (Cussenot et al., 1994a). Primary prostate stromal cell cultures have also been obtained using explant cultures established from BPH and prostate cancer tissue (Kooistra et al., 1995a; Planz et al., 1999).

Enzymatic dissociation is achieved by collagenase digestion, of the intercellular collagen matrix (Freshney, 1987). The standard enzymatic procedure involves chopping the tissue into small fragments, dissociating in medium containing collagenase and

trypsin and incubating with constant stirring at 37°C for a few hours or overnight. The resulting suspension can then be successively sieved through a wire mesh with decreasing pore size in order to obtain single cells (Sensibar et al., 1999a; Peehl and Stamey, 1986a; Peehl et al., 1988a; Brothman et al., 1992a; Peehl and Sellers, 1997; Fry et al., 2000b; Hudson et al., 2000a; Hayflick, 1965; Zhang et al., 1997). Variations to this method include the concentration and type of proteolytic enzymes, number of enzymatic treatments, incubation times and whether the final cell extract is sieved.

In a study of rat prostate, cells were isolated using trypsin and then collagenase for epithelial cell isolation. A higher concentration of trypsin without collagenase digestion was used for stromal cell isolation (Taketa et al., 1990a). The stromal cells digested with trypsin could only attach to tissue culture dishes pretreated with 10% FCS or fibronectin. Although these findings were made with rat prostates, the information obtained was then applied to human prostate cultures. Primary human prostate stromal cultures (PNX and BH101) were produced from normal and BPH tissue using mechanical dissociation followed by collagenase and hyaluronidase treatment (Tatoud et al., 1995). Prostatic stromal cells were isolated by collagenase digestion of BPH tissue with constant stirring at 37°C for 2-4 hours, then rinsing tissue pieces in PBS and repeating collagenase treatment for 16-18 hours (Kassen et al., 1996a).

In some cases a mixture of the two methods has been used. After mechanical dissociation fragments were digested with a collagenase solution and then small fragments were seeded onto tissue culture plates and cell outgrowths appeared (Robinson et al., 1998a; Janssen et al., 2000).

It is easier to establish stromal cells than epithelial cells in culture. Stromal cells tend to outgrow epithelial cells when grown in a basic medium such as RPMI-1640 supplemented with 10-20% FCS (Kooistra et al., 1995a; Tatoud et al., 1995). Stromal cells were isolated from explant cultures (Planz et al., 1999) in equal volumes of DU145 cell conditioned medium and RPMI-1640 supplemented with 10% FBS, insulin, transferrin and selenium (ITS). Primary stromal cell cultures were isolated in DMEM: F12 medium and 20% FCS (Fry et al., 2000b). A pure population of stromal cells is usually achieved by the second or third passage.

A human prostatic smooth muscle cell (SMC) primary culture system was developed (Zhang et al., 1997). The culture medium was modified to preferentially stimulate smooth muscle growth over myofibroblasts or fibroblasts. It was found that SMC growth was stimulated by growth factors such as insulin, dexamethasone, prostate cancer conditioned medium and horse serum (it is thought that FBS tends to stimulate fibroblasts while horse serum stimulates SMC growth). The hormones found to stimulate SMC growth were DHT and hydrocortisone. Estradiol influenced SMC differentiation, but not growth. These growth factors and hormones were used to supplement MCDB-131 medium for the maintenance of SMCs in culture. It was proposed that TGFβ is a key regulator of growth and differentiation in prostate stromal cells (Peehl and Sellers, 1997).

Pure cultures of prostate epithelial cells can be readily established in serum-free culture medium, as the absence of serum inhibits the growth of the stromal cells (Peehl and Stamey, 1986b; Peehl et al., 1988b; Brothman et al., 1992b). In a study of the growth promoting effect of BPE on rat prostate epithelial cells, McKeehan identified some of the growth factors and hormones needed to support prostate epithelial cell growth in the absence of serum. A serum-free growth medium was developed called WAJC404, supplemented with 130pM cholera toxin, 833nM insulin, 1.6mM EGF, 43nM prolactin, 1μM dexamethasone and 25μg/ml bovine pituitary extract (BPE) (McKeehan et al., 1984).

In the study of rat prostate, Taketa et al, found that dexamethasone inhibited the proliferation of epithelial cells at concentrations above 30nM. Maximum stromal cell growth was seen on addition of 2mg/ml of BSA (in addition to cholera toxin and BPE). Higher concentrations of BSA had an inhibitory effect on growth of stromal cells. Epithelial cell cultures were maintained in a modified WAJC404 medium (without dexamethasone or ovine prolactin). Stromal cells were maintained in MEM medium supplemented with 2mg/ml BSA, cholera toxin and BPE (Taketa et al., 1990b).

In order to improve epithelial cell growth a low calcium culture medium was developed which was supplemented with specific growth factors. Epithelial cells were maintained in low serum and low calcium DMEM medium, while fibroblasts were cultured in RPMI-1640 medium supplemented with serum. Two layers developed in the epithelial cultures. The cells survived four to five passages before becoming senescent. The

phenotype of the two layers could be distinguished by their cytokeratin patterns. The upper layer displayed a luminal cell pattern. Fibroblasts took longer than epithelial cells to become established in culture, but once established they grew faster and achieved up to 10 passages. Cultured cells from the transition, peripheral and central zone showed the same growth pattern and had the same phenotype (Cussenot et al., 1994b).

In an investigation of prostate stem cells, a lineage analysis was carried out on basal and secretory luminal cells by monitoring spontaneous differentiation in primary prostate cultures. Primary epithelial cultures were maintained in WAJC404 medium (McKeehan et al., 1984). The results were similar to those of Cussenot et al. (1994) where the initial monolayer expressed luminal and basal cytokeratins and was AR and PSA positive. Multilayer cultures have also been established (Robinson et al., 1998b). The upper layer consisting of highly differentiated cells contained secretory vacuoles with increased luminal cytokeratin expression.

A comparison of serum-free media for the growth of epithelial primary cultures was made (Fry et al., 2000c). PrEGM, a commercially available serum-free medium, was the only medium that permitted the long-term cultivation of epithelial cells. The epithelial cells could be passaged with 0.25% trypsin in 0.5mM/L versene by harvesting adherent cells (allowing cells to lift off the bottom of the dish). Normally epithelial cells are grown in a serum free medium but in order for these cells to re-attach to the base of the tissue culture flask, 5% FCS was added to medium for 48 hours.

Primary prostate epithelial cell cultures were grown clonally to identify prostate stem cells. Single cells were obtained by further digestion with trypsin/versene in saline buffer and growth of cells on a mouse 3T3 fibroblast feeder layer on collagen. Two types of colonies were distinguishable. Three-dimensional cultures were also developed using cells from individual colonies in matrigel using stromal cell conditioned PrEGM medium containing mibolerone. Mibolerone is a synthetic androgen and unlike 5α-DHT (5α-dihydrotestosterone) is not metabolised. The results of these investigations suggest that Type II colonies, consisting of undifferentiated rapidly dividing cells, may be the progeny of prostate stem cells. The smaller Type I colonies may be the progeny of differentiated transit-amplifying populations (Hudson et al., 2000b).

Another method used to isolate stromal or epithelial cells is the Percoll gradient. A 5-10% (increasing density) discontinuous Percoll gradient (Pharmacia) was used to separate different cell types by density after centrifugation (Kassen et al., 1996b). Stromal cells separated at the 5% interface, while the epithelial cells were between the 5 and 10% interfaces. Stromal cells were collected and cultured in phenol red-free RPMI-1640 and 10% FBS. Using this procedure, Kassen found that bFGF and BPE induced a concentration dependent proliferation of prostatic smooth muscle cells. DHT had a weak stimulatory effect on smooth muscle growth and in the presence of bFGF, and at low concentrations DHT was able to further stimulate smooth muscle growth. TGFβ had an inhibitory effect on stromal cells.

The same method was later used to isolate stromal cells from normal and BPH patients of varying ages (Sensibar et al., 1999b). Less cell proliferation was observed in cultures from older patients.

1.4 IMMORTALISATION AND CHARACTERISATION OF PROSTATE CONTINUOUS CELL LINES

Primary cultures have a limited lifespan and therefore immortalised cell lines with an unlimited lifespan have advantages. Immortalised cell lines provide a uniform, standardized and reproducable source for study. These cells retain many properties of normal cells. Spontaneous immortalisation seldom occurs for normal human cells (Macieira-Coelho and Azzarone, 1988) and therefore viral transformation (immortalisation) is used. Primary cells are infected with a transforming virus and have an extended lifespan. The cells eventually reach a state called crisis, a period of balanced cell growth and cell death. Some cells survive crisis and gain additional genetic changes and consequently become immortal.

DNA tumour viruses such as SV40, adenovirus EIA and EIB, human papilloma virus (HPV) 16 and 18 have been used. It is also possible to immortalise cells by expressing cellular oncogenes such as myc, fos, pRb and p53 (Stamps et al., 1992b).

One of the main disadvantages of immortalisation is the loss of differentiated cell characteristics. The cells are driven by the viral gene or oncogene to divide and additional morphological and chromosomal changes develop (Steinberg and Defendi, 1979; Taylor-Papadimitriou et al., 1982). Virally immortalised cells often become

neoplastically transformed, likely to be due to genetic alterations. However, such cell lines have been exploited to study the neoplastic process.

Continuous cell lines (whether immortalised or derived directly from cancers) must be characterised and authenticated (table 1.1 and 1.2). Various immortalised normal prostate cell lines (table 1.3) have been developed.

Prostatic cells characterized as basal cells may express K5, K15, K14, K17 and K19 but are negative for K8 and K18 while more differentiated luminal-like cells can express K8, K18, K17 and K19 but are negative for K15 and K14. K17 and K19 can be expressed by basal and luminal cells. Smooth muscle cells are positive for vimentin, SM-actin, SM-myosin and SM-desmin. Myofibroblasts are positive for vimentin, SM-actin, SM-myosin and negative for SM-desmin. Fibroblasts are positive for vimentin and negative for SM-actin, SM-myosin and SM-desmin. The luminal epithelial and stromal cells can be positive for AR. Prostate specific characteristics include luminal epithelial cell expression of PSA, PSMA and PSAP (table 1.1 and 1.2).

The proportion of proliferating cells can be determined using Ki67 staining (table 1.1 and 1.2). During transformation chromosomal alterations occur and karyotypic analysis can be used to identify large chromosomal alterations and to determine if a normal Y-chromosome is present (Stacey et al., 1990).

Neoplastic characteristics include the loss of anchorage dependence allowing growth in semi-solid agar and the development of xenografts in nude mice. The presence of the transforming gene can be detected (e.g. expression of SV40 large T-antigen).

1.4.1 Immortalised Epithelial Cell Lines

Two prostate epithelial cell lines from neonates, NP-2s and NP-2e, were established by immortalisation with HPV16 (Lechner et al., 1978). The cells have a typical epithelial phenotype with a "cobblestone" appearance. They have a normal human male karyotype, are non-tumorigenic and express 5α-R. Both cell lines became senescent after 30–35 population doublings. In order to extend the lifespan of NP-2s cells they were transformed with the SV40 virus (Kaighn, 1980). The transformed epithelial cell lines T1, T2 and T5 consisted of small cells with a tendency to overlap and had altered morphological, ultrastructural, chromosomal and growth characteristics compared to

NP-2s cells. The morphology of T2 was similar to PC-3, a prostate cancer cell line. All 3 cell lines became anchorage independeant over time and had reduced serum requirements, although each line had a different response to growth factors. Kaighn later stated that these cell lines were not tumorigenic and were not immortalised (Kaighn et al., 1989). Further attempts to immortalise NP-2s cells used a plasmid, pRSV-9, containing the SV40 early region genes (Kaighn et al., 1989). Transformed cell lines 267B1, 272E1 and 272E4 were characterised as luminal epithelial cells, expressing PSA and PSAP markers. This pattern was similar to that seen in NP-2s cells, except for the fibroblast markers. The cell lines 267B1, 272E1 and 272E4 had ultrastructural features of epithelial cells, were pseudodiploid and non-tumorigenic. TGF-β and EGF stimulated growth in clonal assays. In conclusion, these 3 cell lines are immortalised non-tumorigenic human epithelial cell lines. However, these cell lines have been transformed twice and therefore a lot of chromosomal abnormalities are likely to have occured. The 3 cell lines are differentiated epithelial cells and are therefore of no use for the study of epithelial cell differentiation.

Primary cultures of normal prostatic luminal cells were established from a 35-year old male donor (Cussenot et al., 1991). Liposomal transfection with a plasmid, pMK16, containing the SV40 genome with a defective replication origin gene (SV40 ori-) resulted in an immortal cell line. The cell line, PNT1, expressed KL1, a luminal marker, SM cell markers and was weakly positive for PSA and PAP. The PNT1 cell line was used to develop a new cell culture model for studying the progression of non-malignant to malignant prostate cells (Degeorges A et al., 1995). Three cell lines, PNT1A and PNT1B from one patient, and PNT2 from another were. All the lines were positive for SV40 T-antigen, cytokeratin 8 and 18 and negative for cytokeratin 14. PNT2 was positive for cytokeratin 19 and negative for vimentin, while PNT1A and PNT1B were negative for cytokeratin 19 and positive for vimentin. All cell lines were non-tumorigenic. The population doubling times for PNT2, PNT1A and PNT1B were 36, 30 and 28 hours respectively. Their serum dependency was high, medium and low respectively and their EGF response was positive, positive and negative respectively. A fibroblastic cell line did not survive crisis. PNT2, PNT1A and PNT1B cell lines have no added advantage as a prostate epithelial cell line compared to 267B1, 272E1 and 272E4 cell lines, previousely described. PNT2 may be useful for studying intermediate epithelial cells due to its expression of K19.

Human papilloma virus (HPV) type 18 DNA was used to transform cells isolated from the peripheral zone of a normal prostate (Weijerman et al., 1994). The resulting cell line PZ-HPV-7 had a typical epithelial morphology with small cuboidal cells in a cobblestone pattern. The cells were positive for cytokeratin 8 and 5 and negative for PSA. Karyotyping revealed a diploid pattern at passage 30, which became close to tetraploid at passage 99. Following xenotransplantation into nude mice, small growths made up of squamous cells developed. The majority of prostate cancers develop in the peripheral zone so this cell line may be useful for comparative studies of normal peripheral zone cells with peripheral zone cancer cells. To my knowledge there is no other normal prostate cell line specifically from the peripheral zone.

Another cell line was developed by immortalisation of cells isolated from BPH tissue with a construct containing the SV40 large-T antigen gene (Hayward et al., 1995). A single clone, BPH-1, grew as a monolayer culture and had a typical epithelial cobblestone appearance. These cells express markers of intermediate epithelial cells. Karyotyping demonstrated that the cells are aneuploid with a structurally normal Y chromosome. DNA cell cycle distribution for BPH-1 cells is 51% (G_0/G_1), 26% (G_2.M) and 23% (S phase). The cells are not tumorigenic in nude mice. Androgen receptor, PSA and PSAP are not detected by biochemical assays or RT-PCR. Immunocytochemical analysis shows weak staining for AR, while PSA and PSAP are undetectable. Cells proliferate in serum-free medium. Previousely described normal prostate cell lines were luminal epithelial cells. BPH-1, an intermediate epithelial cell line may be useful for the study of epithelial cell differentiation, although a basal cell line would be most advantageous. This cell line has been useful for the study of expression and effect of growth factors on prostate epithelial cells. EGF, TGFα, FGF1, αFGF and FGF-7 (KGF) increase and FGF2 (bFGF), TGFβ1 and TGFβ2 inhibit BPH-1 cell proliferation. Testosterone has no effect on proliferation rate.

Human prostate epithelial cells derived from a patient undergoing cystectomy for bladder cancer were transformed with a hybrid virus composed of adenovirus 12 and SV40, resulting in the cell line PWR-1E (Webber et al., 1996). Another cell line, RWPE-1, was established from non-neoplastic adult human prostatic epithelial cells immortalised with HPV 18 (Bello et al., 1997). The parental epithelial cells could not be maintained in culture beyond 5 passages. RWPE-1 was further transformed by the oncogene v-Ki-ras to establish a tumorigenic cell line, RWPE-2. RWPE-1 is positive for

cytokeratin 8 and 18, and weakly positive for 5 and 14. Mibolerone is a synthetic androgen and unlike 5α-DHT (5α-dihydrotestosterone) is not metabolised. It was used to stimulate growth and PSA and AR expression. Cell growth was also stimulated by bEGF and bFGF, while it was inhibited by TGFβ. The non-tumorigenic cell line RWPE-1 was also transformed with N-methyl-N-nitrosourea (MNU). Four cell lines were established called WPE1-NA22, WPE1-NB14, WPE1-NB11 and WPE1-NB26, in order of increasing malignancy (Webber et al., 2001). RWPE-1 has similar advantages to the BPH-1 cell line, as it also appears to be an intermediate epithelial cell line and may be useful for studying prostate epithelial cell diferentiation. In addition this cell line has the added advantage of successfully being transformeded from normal epithelial cells to maignant epithelial cells. They could be used for comparative studies of normal and malignant prostate epithelial cells.

BRF-55T is a human prostatic epithelial cell line developed from BPH tissue (Iype et al., 1998). Primary cultures were initiated from cellular outgrowths of explanted tissue, and immortalised with a pRSV-T plasmid. The cells are positive for cytokeratin 8 and 18, PSA and AR markers. H-ras, K-ras and p53 are expressed. The cells are thought to be pre-malignant as they have some capacity for anchorage-independent growth.

Primary cell cultures obtained from radical prostatectomy specimens were immortalised with a recombinant retrovirus encoding the E6 and E7 genes of HPV-16 (Bright et al., 1997b). 1532N, 1535N and 1542N cells have doubling population times of 32h, 41h and 48h respectively. The cells have a low serum requirement and are androgen insensitive. The cells do not form tumors in athymic mice and do not form colonies in semi-solid agar. This cell line does not appear to have any advantages over other immortalised epithelial cell lines, discussed above.

Although all of the above mentioned prostate epithelial cell lines retain some of their normal prostate characteristics, such as PSA and AR expression they all tend to be differentiated luminal epithelial cells. In order to study prostate epithelial cell differentiation it would be ideal to have a prostate basal cell line that has the ability to differentiate into luminal cells that should be able to express prostate specific characteristics. To my knowledge there is no such prostate cell line. The aim of this thesis was to develop such a prostate cell line using a temperature sensitive model.

1.4.2 Immortalised Stromal Cell Lines

Relatively few immortalised human prostatic stromal cell lines have been established.

DuK50, a human prostate stromal cell line was stained positive for vimentin and fibronectin with weak smooth muscle alpha-actin staining (Roberson et al., 1995). Staining was negative for desmin antibody, epithelial cytokeratins and prostate-specific antigen, which ruled out contamination with prostatic epithelial cells. This staining pattern was suggestive of myofibroblasts. This cell line has a diploid karyotype and is non-tumorigenic in nude mice and does not form colonies in semi solid agar. Cell proliferation was stimulated by androgens.

A stromal cell line, WPMY-1 (Webber et al., 1999) was derived from the same prostate tissue specimen as the epithelial cell line, RWPE-1 (Bello et al., 1997). Immortalisation was carried out with the SV40 large-T antigen, using the pRSVT plasmid. The cells have an elongated, spindle-shape morphology and are characterised as myofibroblasts. WPMY-1 has a hyperdiploid karyotype with chromosome numbers of 58-68. These cells are stimulated in a dose-dependent manner with Mibolerone, EGF, b FGF, PDGF-BB and PDGF-AA. A dose dependent inhibition was observed with TGFβ, in the presence and absence of serum, although it is thought that TGFβ stimulates stromal growth. WPMY-1 cells did not form tumors in nude mice, but they did form colonies in soft agar. A differential of 0.7% CFE with 10% donor calf serum (DCS) compared to 4.6% with 10% FCS shows that the serum type is an important factor when setting up cell culture experiments.

These two cell lines have been useful for studying expression and effect of growth factors on prostate stromal cells. As with prostate epithelial cells it would be useful to have a stromal cell line where stromal cell differentiation could be switched on. Although the main aim of this thesis was to develop a prostate epithelial model, a temperature sensitive prostate stromal cell line was developed along side the temperature sensitive epithelial cell line.

Table 1.3: Characteristics of Immortalised Normal Prostate Cell Lines

Epithelial Cell Line Name	Reference	Immortalising Genes	Derivation	Phenotype
NP-2s and NP-2e NP2-T1, T2, T5 267B1, 272E1, 272E4	(Lechner et al., 1978) (Kaighn, 1980) (Kaighn et al., 1989)	HPV 16, E6 & E7 SV40 virus SV40 ori$^-$	Normal neonatal	Non-t, anc-d, epit. $5\alpha R^+$ Non-t, anc-d, Imm, non-t, lum, PSA^{w+}, PAP^{w+}
PNT1 PNT1A, PNT1B, PNT2	(Cussenot et al., 1991) (Degeorges et al., 1995)	SV40 ori$^-$ defective gene SV40 large T and small t antigens	Normal adult	Luminal epit PSA^{w+}, PAP^{w+} Imm, non-t, luminal
PZ-HPV-7	(Weijerman et al., 1994)	HPV type 18	Normal adult	Imm, non-t, epit PSA^+
BPH-1	(Hayward et al., 1995)	SV40 large T antigen	BPH	Imm, non-t, I-luminal
PWR-1E	(Webber et al., 1996)	Adenovirus 12 and SV40 Hybrid	Non-neoplastic	Imm, epit
RWPE-1	(Bello et al., 1997)	HPV type 18	Normal	Non-t, anc-d, I-luminal, PSA^+, AR^+
BRF-55T	(Iype et al., 1998)	SV40 large T antigen	BPH	Pre-mal luminal PSA^+, AR^+
1532N, 1535N, 1542N	(Bright et al., 1997b)	E6 & E7 genes of HPV-16	Normal	Non-t, anc-d, epit.
Stromal Cell Line Name	**Reference**	**Immortalising Gene**	**Derivation**	**Cell Characterisation**
DuK50	(Roberson et al., 1995)		Normal	Non-t, anc-d, SM, AR^+
WPMY-1	(Webber et al., 1999)	SV40 large-T	Non-neoplastic	Non-t, anc-id, myofib, AR^+

Non-tumorigenic (non-t); anchorage dependent (anc-d); anchorage independent (anc-id); epithelial (epit); luminal (lum); intermediate luminal (I-luminal); weak positive (w+); pre malignant (pre-mal); smooth muscle cells (SM); myofibroblast (myofib)

1.5 3-DIMENSIONAL CULTURE SYSTEMS

In order to overcome the limitations of monolayer culture systems, co-cultures and 3-dimensional cultures of prostate epithelial and stromal cells have been developed.

Bayne and colleagues set up co-cultures in which epithelial and stromal cells derived from BPH were grown on opposite sides of microporous membranes (Bayne et al., 1998). Although there was no direct interaction between stromal and epithelial cells, this culture system maintained many prostate characteristics, including response to androgens, secretion of PSA by epithelial cells and expression of 5α reductase types I and II. This co-culture model was used to study cellular interactions between BPH stromal and epithelial cells (Habib et al., 2000).

Although these co-cultures express prostate specific characteristics, they lack the architectural structure and cell-cell contacts of the stromal and epithelial cells in vivo. These culture systems also lack contact with a basement membrane (Drubin and Nelson, 1996). Basement membranes are thin extracellular matrices underlying epithelial cells in tissue and are important for normal development (Kleinman et al., 1987b).

3-Dimensional in-vitro models have been developed to enable direct stromal and epithelial cell interaction. Matrigel culture systems provide a substitute for basement membrane components. Matrigel is extracted from the Engelbreth-Holm-Swarm (EHS) mouse sarcoma, a tumour that is rich in extracellular matrix proteins. Approximately 60% of Matrigel consists of laminin, an essential component of the basement membrane (Malinda and Kleinman, 1996; Kleinman et al., 1987a). The remaining 40% of Matrigel is made up of collagen-IV, heparin sulphate proteoglycans, and nidogen. Matrigel also contains varying concentrations of growth factors.

Matrigel cultures of RWPE-1 (normal epithelial cell line) and RWPE-2 (tumorigenic epithelial cell line derived from RWPE-1) were used in a study of acinar differentiation (Webber et al., 1997). The normal prostate cells underwent acinar morphogenesis, but the tumorigenic cells had lost this ability.

Using rat prostatic epithelial cells, 3-dimensional collagen gel cultures were successfully constructed which provided a useful means for investigating prostatic disease and hormone and growth factor influences on prostate cells. Epithelial cells

formed acinus-like structures in these models (Ma et al., 1997). Hall et al. used this 3-D collagen co-culture model to study the interaction of human benign (PNT1) and tumour (PC3) prostate cells with primary benign and tumor epithelial and stromal cells. Differences were observed between tumour and normal cells, in particular the formation and acinus-like structures. There was stronger expression of luminal markers by the immortalised cell lines and stronger basal expression by the primary cells. PSMA was present in all cultures, while PSA was positive in all cultures except the PC3 cell line (Hall et al., 2002).

1.6 IMMORTALISATION AND CONDITIONAL IMMORTALISATION

Polyoma viruses can cause infections in humans, often in the kidney, and can induce cancer in animals. Because these viruses have a simple structure and contain a small genome they are used in genetic engineering. One of the first polyoma viruses to be studied was the simian virus 40 (SV-40) (Carbone, 2001; Barton S, 2002; Watson et al., 1992). Other viral genes that have been used to immortalize cells are adenovirus E1a (Seigel GM, 1996), human papilloma virus (HPV) E6 and E7 (Peters et al., 1996; Le Poole et al., 1997) and Epstein Barr Virus (EBV) (Zeidler et al., 1996). Most of these genes probably act by blocking the inhibition of cell cycle progression by inhibiting the activity of genes such as CCIP-1/WAF-1/21, Rb, p53 and p16, therefore giving cells an increased life span and allowing further mutations if desired. These viruses are relatively easy to maintain and work well in the laboratory, although health and safety rules should be adhered to when working with any of these viruses.

SV40 was first isolated from monkey kidney cells, hence its name (Carbone, 2001; Barton S, 2002; Watson et al., 1992). A Hind II restriction enzyme map of SV40 was produced in 1971 and it was shown that DNA replication always began at the same Hind II site and continued in two directions (Nathans and Danna, 1972; Danna and Nathans, 1971; Danna and Nathans, 1972; Bryan and Reddel, 1994).

The SV40 genome is a double-stranded circular DNA of 5243bp (figure 1.4). The genome is divided into two regions, the early and late genes. These regions are expressed respectively before and after DNA replication begins. The origin of DNA replication (ori) and the early and late promoters are situated between the coding sequence of the early and late gene regions (Saenz-Robles et al., 2001).

The early region encodes three proteins, large T antigen (LTAg), small t antigen (stAg) and 17K T antigen (17KT) that are 708, 174 and 135 amino acids respectively. The LTAg, a 90kDa protein, has a number of functions, including DNA binding, nuclear localisation, ATPase activity and helicase activity. It binds to ATP, replication protein A and DNA polymerase α for initiation of DNA synthesis (Dornreiter et al., 1990; Smale and Tjian, 1986). LTag recognises the viral replication of origin (ori^-) in the presence of ATP and acts as a DNA hilicase by opening the double helix. The LT Ag also interacts with the protein products of the retinoblastoma (Rb) and p53 tumour suppressor genes. Rb and p53, cell cycle regulatory genes are iactivated during immortalisation, probably by blocking the inhibition of cell proliferation caused by tumour suppressor genes. The product of the SV40 LT gene, the T antigen binds the P53 and Rb proteins and allows an extended proliferative life span of these cells, i.e. immortalisation. This action also restricts the DNA surveillance activity of genes like p53 (Finlay et al., 1989). Small t antigen, a 17kDa protein, is not essential for productive infection in cells. It is involved in activating protein phosphatase 2A, which stimulates cell proliferation through a protein kinase pathway. The role of the 17KT antigen in transformation is not fully understood (Saenz-Robles et al., 2001; Ali and DeCaprio, 2001; Pipas and Levine, 2001; Rundell and Parakati, 2001).

The late region of the SV40 gene encodes the viral coat proteins (VP1, VP2 and VP3). Immortalisation can be carried out using both early and late genes, although the late gene region is not required (Saenz-Robles et al., 2001; Ali and DeCaprio, 2001; Pipas and Levine, 2001; Rundell and Parakati, 2001).

Figure 1.4: Schematic Diagram Of The SV40 Genome

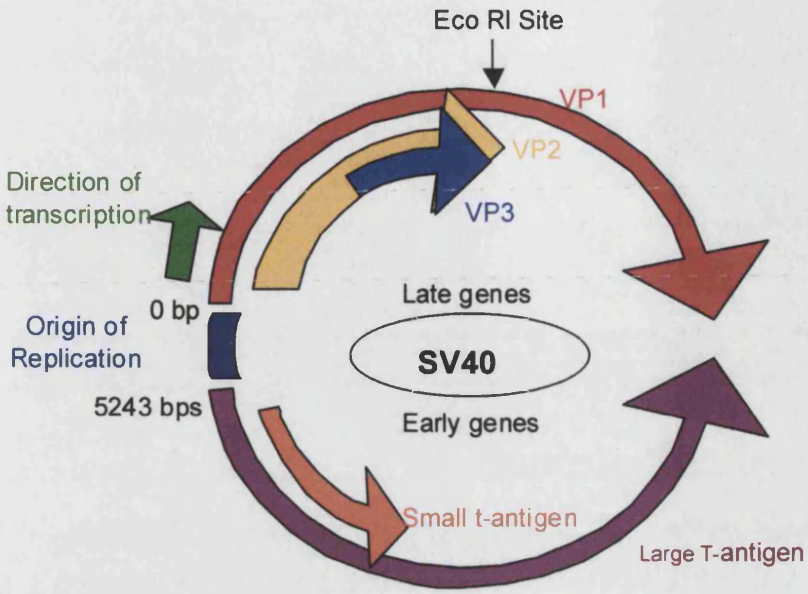

The SV40 genome is divided into an early and late gene region. The early region consists of small and large T antigen proteins that are involved in DNA replication. The late region encodes for 3 viral coat proteins. The number of nucleotides synthesised start and end at the origin of replication (ori). The green arrow indicates the direction of DNA synthesis. Contains a single EcoRI site, 1700bps away from the DNA replication site. Schematic diagram of the SV40 genome – information taken from text books (Brock and Madigan, 2002; Barton S, 2002).

DNA replication on the SV40 viral genome is initiated by the large T-antigen protein, which specifically recognises the viral origin of replication in the presence of ATP (Dean et al., 1987b). The T-antigen, a product of the viral A gene, acts as a DNA helicase, opening the double helix as it moves along, forming a replication bubble. The host cell components of the replication machinery assemble in the replication bubble and two replication forks are formed, which move away from the origin in the opposite direction (Parsons et al., 1990; Wessel et al., 1992; Dodson et al., 1987; Dean et al., 1987a; Pipas and Levine, 2001).

The most important step for achieving immortalisation is the inactivation of p53 and Rb cell cycle regulatory genes (Stamps et al., 1992a; Ozer et al., 1996). Other DNA tumour viruses also bind to these tumour suppressor genes and are sometimes used to immortalise cells. Adenovirus 5, E1B and HPV and E6 bind to p53 and adenovirus E1A

and HPV E7 bind to Rb causing inactivation of these cell cycle regulatory genes. SV40 appears to be the most common DNA tumour virus used for immortalisation of cells.

The differentiated characteristics of cells, such as AR and PSA expression in prostate epithelial cells, tend to be lost in immortalised cells. The loss may be due to cells proliferating and not differentiating in culture (Parker et al., 1999), and this limitation might be overcome using temperature sensitive cell lines.

Temperature-sensitive mutants in LTAg (tsA mutants) were used to show that T antigen function is necessary to initiate and maintain immortalisation in cells. Several temperature sensitive mutants of the SV40 A gene have been established (Chou et al., 1974; Tegtmeyer, 1972; Tevethia and Tevethia, 1977; Tevethia and Ripper, 1977). The temperature sensitive SV40 large T antigen behaves as wildtype LTag at permissive temperatures (33°C), initiating DNA replication. LTag becomes conformationally inactive at non-permissive temperatures (39°C) and can no longer initiate DNA replication due to the temperature sensitive A58 mutation inserted into the SV40 virus at 3504bp (Stamps et al., 1994). The cell line should proliferate at 33°C and this proliferation should be switched off at 39°C, allowing cell differentiation to occur. Using this technology it may be possible to maintain cell proliferation at the permissive temperatures and switch to cell differentiation at a non-permissive temperature and hence retain tissue specific characteristics.

This thesis describes the characterisation of two immortalised cell lines grown from BPH tissue, a stromal (S2.13) and epithelial (Pre2.8) cell line, derived from the same individual. The cells were immortalised by transfecting primary stromal and epithelial cells with the temperature sensitive immortalizing oncogene, Simian Virus 40 large T-antigen carrying both the tsA58 and U19 mutations (SV40U19tsA59). The Bgl1-Hpa1 fragment of the early region of SV40 large T-antigen was inserted into the single BamHI restriction site of the pZipNeoSV(X)1 shuttle vector, which replaces a region of the wildtype gene. The temperature sensitive mutants are on nucleotides 4364, 4345 (U19) and 3504 (tsA58). The infected cells were selected with the antibiotic G418 (Cepko et al., 1984; Jat and Sharp, 1989; Stamps et al., 1994) (figure 1.5).

Figure 1.5: Schematic Diagram of the temperature-sensitive SV40 construct, ZipneoSVU19tsA58

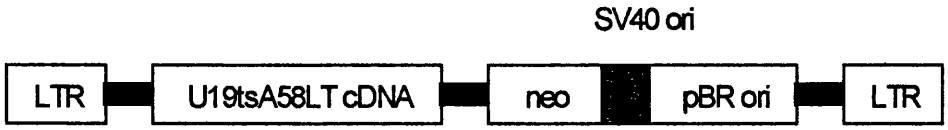

The U19tsA58 LT virus was constructed by using the pZipNeoSV (X)1 backbone and encodes a full-length LT cDNA from U19tsA58 and confers resistance to G418. The U19tsA58 LT is a combination the two mutants, U19, which encodes a LT that does not bind specifically to SV40-origin DNA sequences, and tsA58, which encodes a thermolabile LT antigen that is wild type at 33.5°C but inactive at 39.5°C (O'Hare et al., 2001).

1.7 RATIONALE FOR THIS STUDY

Until recently very little research has been carried out to study the human prostate and associated diseases. Primary cultures will only survive for a limited time and hence their usefulness as human prostate models is limited. For long-term studies immortalised cell lines are required, but there is a lack of representative in vitro models of the human prostate, particularly BPH. In this study immortalised epithelial and stromal cells, obtained from the same BPH patient, were immortalised using the temperature sensitive SV40 large T antigen (O'Hare et al., 2001). Temperature sensitive cell lines were established to try and overcome some of the problems associated with immortalisation procedures, i.e. loss of prostate specific characteristics. Because the T-antigen is switched off at 39°C, cell proliferation is switched off and cell differentiation may proceed and express prostate specific characteristics, such as PSA, PSMA and AR.

The first aim in this study was to authenticate and characterise this immortalised BPH epithelial cell line (Pre2.8) and determine to what extent they can express prostate specific characteristics. A comparison at 33°C, 39°C and 37°C, as an intermediate temperature was necessary to determine that these cells were temperature sensitive and that they do differentiate at 39°C. The cell lines were never passaged beyond 10 passages to insure stability. A new vial of the same passage number was used after every 10 passages.

Stromal-epithelial interactions, is an important factor in prostate development and is one of the hypothesised theories (McNeal, 1978) for the development of BPH. Epithelial cells alone may not be sufficient to induce differentiation. They may require the presence of stromal cells.

The aim of the second part of this project was to recombine epithelial and stromal cells to produce a BPH model that mimics in vivo conditions. Initially the immortalised BPH stromal cell line (S2.13) should be authenticated and characterised. Once an appropriate co-culture method for recombining prostate epithelial and stromal cells has been established, characterisation at 33°C, 39°C and 37°C must again be carried out in order to determine its prostate specific capabilities.

CHAPTER 2

MATERIALS AND METHODS

2.1 COSHH REGULATIONS

The COSHH (Control Of Substances Hazardous To Health) regulations require that before the start of any research project, the risks involved must be assessed and a code of practice drawn up by which the work may be carried out with the minimum amount of risk. All experiments were carried out following COSHH regulations, ensuring that the Departmental Code of Practice (containing Health and Safety regulations) was adhered to.

Immortalisation of cell lines, Pre2.8 and S2.13 was carried out by Pref M O'Hare, Dept of Surgery, Middlesex Hospital. Transformation with SV40 viral genes were carried out in Safety Level 3 tissure culture labs. Cell lines were not transferred to our laboratory until they were safe to work with, in a Safety Level 2 tissure culture laboratory. All GMO (genetic modified organisms) regulations were adhered to and GMO risk assessment forms were completed for all new lines generated.

2.2 CELL CULTURE

Cell culture is the growth and maintenance of cells, which have been established from pieces of tissue, in the laboratory. Various cell lines that were established from human prostate and one mouse cell line were used in this study and are detailed in table 2.1.

Table 2.1: Details Of Cell Lines Used In Study

Cell Line	Derivation	Culture medium	Routine Temp	Reference
LNCaP	Lymph node metastasis of prostate cancer	RPMI-1640 +10%FCS	37°C	(Horoszewicz et al., 1980)
DU145	CNS metastasis of prostate cancer	RPMI-1640 + 10%FCS	37°C	(Stone et al., 1978)
Pre2.8	SV40 large T antigen conditionally immortalised normal human epithelial cell line.	PrEGM	33°C	This thesis
S2.13	SV40 large T antigen conditionally immortalised normal human epithelial cell line	DMEM + 10%FCS	33°C	This thesis
1542-NPTX	Normal prostate epithelial cells immortalised with the E6 and E7 transforming proteins of human papilloma virus	Keratinocyte-SFM + 5%FCS	37°C	(Bright et al., 1997a)
1542-FT	Normal prostate stromal cells immortalised with E6 and E7 transforming proteins of human papilloma virus	RPMI-1640 +10%FCS	37°C	(Bright et al., 1997a)
3T3	The NIH/3T3, a continuous cell line of highly contact-inhibited fibroblast cells was established from NIH Swiss mouse embryo	DMEM + 10%FCS	37°C	(Todaro and Green, 1962)
MDA-MB-435	Metastatic human breast cancer cell line	RPMI-1640 +10%FCS	37°C	(Glinsky et al., 1996)
PC3	Epithelial cell line from a human prostatic adenocarcinoma metastatic to bone.	RPMI-1640 +10%FCS	37°C	(Kaighn et al., 1979)

2.3 CELL LINE AUTHENTICATION AND PURITY

When a new cell line has been derived it is important to authenticate its origin and also to characterise the cell line in order to determine its functionality, purity and stability. The main problems associated with continuous cell lines are cross-contamination, microbial contamination and changes in phenotype.

2.3.1 Cross-Contamination

Cross-contamination between cell lines, particularly with HeLa cells has been the cause of misrepresented scientific data since the 1960s (King et al., 1994; Gartler, 1967; Nelson-Rees et al., 1981). Short tandem repeat (STR) profiling (Masters et al., 2001) was used to confirm origin of the cell lines used in this study (Table 2.1).

Procedure

DNA was extracted from a confluent $80cm^2$ flask of each cell line, using phenol/chloroform extraction procedures. DNA samples (1g/ml) were sent to the analytical centre, LGC (Queens Road, Teddington, Midddlesex TW11 0LW) for DNA profiling.

DNA Extraction from Cultured Cells

A confluent $80cm^2$ flask was trypsinised and washed with 1x phosphate-buffered saline (PBS). Cells were lysed in 10ml lysis buffer, containing 100µl Protease K (final conc. 1mg/ml of PK), mixed well and incubated at 37°C, overnight. Sample was transferred to a 15ml polypropylene tube. Phenol was equilibrated in 10mM Tris-HCl (pH 8.0) and 0.1% Hydroxyquinoline (yellow colour) was added. Chloroform was prepared adding 1ml Iso-Amyl alcohol to 24ml of chloroform and mixing. A solution with equal volumes of phenol and chloroform was prepared by mixing together. 5ml of phenol/chloroform (1:1) was added to sample, mixed well and centrifuged at 4°C, at 9000 rpm for 20 min. Supernatant was transferred to a new tube. Extraction was repeated once with phenol/chloroform and centrifuged for 10 minutes and once with chloroform and centrifuged for 10 minutes. 10 µl of RNase (10mg/ml) was added to the sample and incubated for 1h at 37°C. DNA precipitation was carried out by adding equal volumes of isopropanol to the sample tube and then gently mixing, by inverting tube up and down. Precipitated DNA was lifted out using a blunted pasteur pipette and washed in 1ml of 70% ethanol and air dried. DNA was dissolved in 0.5 –1.0 ml of sterile water, depending on viscosity of DNA sample.

Lysis buffer

150 mM NaCl, 10 mM Tris (pH 8.0), 10 mM EDTA (pH 8.0), 0.5% SDS

Proteinase K

10mg/ml stock solution in sterile water and stored at -20^{0}C.

RNase

10mg/ml solution in sterile water, boiled for 10 minutes, allowed to cool to room temperature and stored at -20^{0}C.

Measurement of DNA concentration

DNA concentrations were measured by UV spectophometry using a DU650 series spectrophotometer (Beckman Ltd., UK). 5µl of DNA was diluted to 500µl with sterile water (1/100) and added to a clean cuvette. The spectrophotometer was blanked with water using a clean cuvette. The yield of DNA was calculated by measuring the optical density (OD) at 260nm and at 280nm and the DNA concentration was calculated as follows:

OD_{260} x 50µg/ml x dilution factor = DNA concentration µg/ml

An absorbance of 1 unit at 260nm corresponds to 50µg/ml of DNA. The ratio of the readings at 260nm and 280nm provides an estimate of the purity of DNA with respect to contaminants that absorb in the UV spectrum, such as protein. The 260nm/280nm ratio of pure DNA in water is approximately 1.8.

STR Profiling

The DNA was analysed using two sets of primers: Second Generation Multiplex (UK Forensic Science Service) (Thomson et al., 1999) and Powerplex 1 (Promega) (Lins et al., 1998) by LGC to investigate the presence of cell line cross-contamination. STRs used had tetranucleotide repeat sequences. Multiplex PCR reactions were carried out using fluorescent dye-linked primers. PCR products for each cell line were separated and analysed using a Perkin-Elmer-ABI Prism 377 Genetic Analyser and Genescan and Genotyper analysis software. The amplified product is measured according to its fluroscence and is then converted to a representative peak on a graph. These peaks are assigned allele values corresponding to the number of repeat units. Cell lines originating

from the same source should have 80% similarity for DNA profile, i.e. the same size peaks on a graph.

2.3.2 Mycoplasma Testing

Contamination of cell culture by microorganisms remains one of the major problems in routine tissue culture. One of the most problematic contaminants is mycoplasma, an organism that resides on or within individual cells presenting no overt signs of contamination like fungus or yeast.

Mycoplasma is one of the smallest living cells known. They are generally spherical in shape with a diameter varying from 0.3 to 0.8μm. Filament forms also exist with diameters of 0.1 to 0.3μm and lengths of up to 150μm. They have no cell wall and are therefore insensitive to cell wall-active antimicrobial agents. They have a small amount of genetic material and have limited biosynthetic capabilities, although they are cholesterol dependent. Their growth requires an enriched medium and they exist symbiotically with growing cells. There are more than 100 species, of which approximately 85% of all cell line infections can be attributed to 5 species (M. orale, M. arginini, M. hyorhinis, M. fermentans and Acholeplasma laidlawii).

Mycoplasma contamination can lead to misleading data, wasting valuable time and resources. DNA, RNA and protein synthesis can be altered and changes in enzyme patterns. Selection of mutant mammalian cells can be interfered with and the host cell's plasma membrane can be modified.

2.3.3 Mycoplasma Testing Of Cell Lines

Different companies and research scientists have established various kits and techniques to carry out mycoplasma testing. After investigating the possible use of various methods we concluded that the PCR based techniques were most efficient and reliable for our requirements. One technique was not sufficient to detect all types of mycoplasma contamination therefore two different PCR methods were used. The use of two different PCR methods also helps to overcome the disadvantages associated with PCR analysis. PCR is a very sensitive technique and in order to rule out any false positives it is always necessary to include a negative control. Cross contamination can be avoided by preparing template DNA in a separate room to where reagents are aliquoted. Amplified DNA should also be kept in a separate room. It is always an advantage to test your PCR

samples in duplicate as false positives and cross contamination is less likely to be repeated in both samples. A reagent only sample at beginning of your sample preperation and at the end of your sample preperation should indicate any contamination that occured throughout your preparations. Pipette tips should be changed after every reaction tube. Nested PCRs are particularly sensitive and susceptible to cross contamination due to the involvement of a second amplification round, although the second round uses a separate set of primers. In addition to two different types of PCR methods being used to test for the presence of Mycoplasma contamination in cell lines, a Stratagene PCR was used to identify the type of Mycoplasma present. To my knowledge no other procedure can easily identify Mycoplasma type. A detailed description of PCR analysis can be found later in this chapter.

The supernatant from a confluent flask of cells (table 1.3) was used to extract DNA. This supernatant could be stored at 4°C for up 1 month. A "Coriell PCR" was used to check for the presence of mycoplasma and results were confirmed using a "Drexler Multiplex, Nested PCR". The "Stratagene PCR" was used to determine the type of mycoplasma contamination. When a cell line is contaminated, ideally it should be thrown away, but alternatively this contamination can be treated with antibiotics to eliminate mycoplasma infection and re-tested for mycoplasma contamination after antibiotic treatment.

Procedure

Cell cultures were grown in antibiotic free medium, for at least 2 passages, until confluent. The supernatant was removed and stored at 4°C, until ready to use. DNA was extracted using "Strata-Clean" resin. Briefly, 100µl of supernatant was transferred to a 1.5ml tube, incubated at 95°C for 10 minutes and quickly spun to bring supernatant down from sides of tube. The Strata-Clean resin was vortexed for 30 seconds to resuspend resin and 10µl of resin was added to sample tube, well mixed and quickly spun to pellet resin. The final preparation was diluted 1:10 times and this was used as the DNA template for the PCR reaction.

2.3.3.1 Coriell PCR

Two highly conserved r-RNA sequences are used as primers. The expected size fragment, after amplification is approximately 500bps. (Toji et al., 1998)

Primer Seqences:

Primer A – 5' GGC GAA TGG GTG AGT AAC ACG 3'

Primer B – 5' CGG ATA ACG CTT GCG ACC TAT G 3'

PCR Reaction

A 25µl PCR reaction was prepared in a 200 µl tube by adding;

1x Reaction Buffer, 1.5mM $MgCl_2$, 200µm of each dNTP, 0.6U Taq Polymerase, 0.2µM of each Coriell primer, dH_2O up to 25µl and 10µl DNA template.

Perkin Elmer Thermocycler conditions for Coriell PCR

1 Cycle	95°C - 5 min	
	55°C – 1 min	45 sec
3 Cycles	72°C – 3 min	
	94°C -	45 sec
	55°C - 1 min	45 sec
40 Cycles	72°C - 3 min	
	94°C -	45 sec
	55°C -	45 sec
1 Cycle	72°C – 10 min	
	27°C – 10 min and Hold @ 4oC	

2.3.3.2 Drexler Multiplex, Nested PCR

A number of different primer sequences were chosen from the 16S r-RNA gene region. These oligonucleotide sequences do not cross-react with non-mycoplasma contaminants or with eukaryotic DNA from the cell lines. The 5 most common mycoplasma species + 20 additional species can be detected. The expected size fragment for Round I is 500 – 520bp. The expected size fragment for Round II is 310 – 330bp. (Hopert et al., 1993b; Hopert et al., 1993a)

Primer Sequence

Outer primers: Myco 9 *(A, B, C, D, E and F)*

CGC CTG AGT AGT ACG TTC GC

CGC CTG AGT AGT ACG TAC GC

TGC CTG AGT AGT ACA TTC GC

CGC CTG GGT AGT ACA TTC GC

CGC CTG AGT AGT ATG CTC GC

TGC CTG GGT AGT ACA TTC GC

Myco 3 *(A, B and C)*

GCG GTG TGT ACA AGA CCC GA

GCG GTG TGT ACA AAA CCC GA

GCG GTG TGT ACA AAC CCC GA

Inner primers: Myco 8 *(A and B)*

TGG TGC ATG GTT GTC GTC AG

TGG TGC ACG GTT GTC GTC AG

Myco 5 *(A, B, C, D, E, F and G)*

GAA CGT ATT CAC CGC AGC ATA

GAA CGT ATT CAC CGT AGC GTA

GAA CGT ATT CAC CGC AGC GTA

GAA CGT ATT CAC CGC AAC ATG

GAA CGT ATT CAC CGC AGT ATA

GAA CGT ATT CAC CGC GAC ATA

GAA CGT ATT GAC CGC GAC ATG

Reaction mix

For Round 1 of the Nested PCR, a 25µl reaction was prepared in a 200µl tube by adding:

1x Buffer (inc. 1.5mM $MgCl_2$), 1.5mM $MgCl_2$, 200µM of each d NTP, 90nm of each primer (outer & inner Drexler primers), 1.25U Taq Polymerase, dH_2O up to 50µl per reaction and 10µl of DNA template.

For Round 2 of Nested PCR, a 25µl reaction was prepared in a 200µl tube by adding;

1x Buffer (inc. 1.5mM $MgCl_2$), 1.5mM $MgCl_2$, 200µM of each d NTP, 90nm of each primer (outer & inner Drexler primers), 1.25U Taq Polymerase, dH_2O up to 50µl per reaction and 10µl of the first round product.

Perkin Elmer Thermocycler conditions:

1 Cycle	90°C – 10 min
30 Cycles	94°C – 30 sec
	60°C – 30 sec
	72°C – 60 sec
1 Cycle	72°C – 10min and Hold @ 4O°C

2.3.3.3 Stratagene PCR *Catalogue Number: 302007*

The Stratagene PCR kit is used to determine the type of Mycoplasma found.

A different fingerprint pattern distinguishes between the 5 most common causes of contamination, as follows;

M. orale	600bp
M. hyorhinis	700bp, 620bp, 280bp
M. fermentans	630bp
M. arginine	600bp, 230bp
Acholeplasma laidlawii	280bp, 100bp
Internal Control	420bp
Kit pos control	600bp, 230bp
House control (KK47)	600bp, 230bp

If an unrecognised fingerprint is obtained, the cell line may be infected with a strain that has not been characterised yet or with an organism other than Mycoplasma. An internal control and a positive control are provided with the kit.

Reaction mix

A 50µl PCR reaction was set up by adding the following:

1X buffer, 1.5mM Mg Cl_2, 0.2mM of each dNTP, 1U of Taq DNA polymerase, ddH_2O up to 50µl volume and 10µl of DNA template.

Thermocycler conditions for Stratagene PCR

1 Cycle	95°C - 5 min	
	55°C – 1 min	45 sec
3 Cycle's	72°C – 3 min	
	94°C -	45 sec
	55°C - 1 min	45 sec
40 Cycle's	72°C - 3 min	
	94°C -	45 sec
	55°C -	45 sec
1 Cycle	72°C – 10 min	
	27°C – 10 min and Hold @ 4°C	

Thermocycler Type

The same thermocycler, a Perkin Elmer 2800 was used for all PCR optimisations and sample testing. By consistently using the same type of thermocycler, for all PCR reactions, the need for further optimisation required when using different PCR machines was avoided.

2.4 CELL LINE MAINTENANCE

Complete medium was stored at 4°C. The cell lines were media-changed 2 or 3 times per week. Cultures were examined under an inverted light microscope to check for bacterial or fungal contamination. The medium additives were thawed at 37°C, added to 500ml of medium and mixed. See table 2.2 for details of medium used and additives required for the different types of medium. The medium was aspirated and replaced with the appropriate volume, carefully pipetted into the flask or plate. The cell cultures were returned to a 5% CO_2 incubator with the lid loosened (vented lids were not used due to extra expense) one half turn in order to allow gas exchange. Only one cell line was allowed at a time in the flow cabinet, in order to avoid the risk of cross-contamination.

Table 2.2: Cell Culture Medium

Medium Type	Additives (nutrients)	Additive Quantity
PrEGM (500mL) *Prostate Epithelial cell medium* Supplier: *Cambrex (BioWhittaker)*	Bovine Pituitary Extract (BPE)	2ml
	Insulin	0.5ml
	human-Epidermal Growth Factor (h-EGF)	0.5ml
	Transferrin	0.5ml
	Retinoic Acid	0.5ml
	Gentamicin sulfate amphotericin-B (GA)	0.5ml
	Epinephrine	0.5ml
	Hydrocortisone (HC)	0.5ml
	Triiodothyronine (T3)	0.5ml
RPMI-1640 w/o L- Glutamine (500mL) *For mammalian cells* Supplier: *Invitrogen (Gibco BRL, Life Technologies)*	8% Foetal Calf Serum (FCS)	40ml
	2mM of L-Glutamine	5ml
DMEM (500mL) *Dulbeccos Modified Eagle medium for mammalian cells* Supplier: *Invitrogen (Gibco BRL, Life Technologies)*	8% Foetal Calf Serum (FCS)	40ml
	2mM of L-Glutamine	5ml
Keratinocyte-SFM (500mL) Supplier: *Invitrogen (Gibco BRL, Life Technologies)*	1.5 ml Bovine Pituitary Extract (BPE)	
	2.5μg Epidermal growth factor (EGF)	
	4% Foetal Calf Serum (FCS)	
Opti-MEM 1 *Reduced serum medium* Supplier: *Invitrogen (Gibco BRL, Life Technologies)*	No additives	

2.4.1 Cell Line Passaging

The cell lines were passaged when necessary. The cultures were washed with 1x PBS and detached using a trypsin-versene (T/V) (contains 0.5g/L trypsin 1:250 and 0.2g/L versene in a buffered saline solution) treatment. 1-2ml of 1x T/V was carefully added, spread across the monolayer and removed by aspiration. The culture vessel was transferred to an incubator for a period of a few minutes to allow cells to detach. The cells were resuspended in the required volume of fresh medium.

Pre2.8 cells were treated differently because they grow in serum-free medium. 2-5ml of T/V was carefully pipetted onto cells and spread across the monolayer and flasks transferred to a 33°C incubator for up to 15 minutes to allow the cells to detach. The cells were suspended in 20ml of PrEGM medium (diluting trypsin/versene) and centrifuged at 1000 x g. The supernatant (containing T/V) was removed. Therefore inactivation of trypsin was not required. Cells were resuspended in the required volume of fresh PrEGM medium.

A single cell suspension was obtained by pipetting the cell suspension up and down approximately 5 times. For routine maintenance, the cell lines were split at appropriate ratios, depending on their growth rate. Pre2.8 cells are slow growing and density dependent and therefore they were split at an approximate ratio of 1:3. S2.13 cells are fast growing and were therefore split at a ratio of 1:20. New culture vessels were labelled with cell line name, passage number and date. Cell cultures were inspected daily.

2.4.2 Haemocytometer Cell Counting

The haemocytometer (improved Neubauer) must be clean and free of grease. If necessary, the surface of the counting chamber and the coverslip can be cleaned using a 70% alcohol-soaked tissue. When the coverslip has been correctly attached on top of the counting chamber, a rainbow effect ("Newton's rings") should be seen on either side of the central chamber.

After a single cell suspension was obtained, an equal volume (e.g. 0.2ml) of this suspension was added to 0.4% trypan blue (e.g. 0.2ml) and sample was thoroughly mixed. Trypan blue is a viability stain and is excluded by viable cells. This relates to cell semipermeability. Trypan blue enables exclusion of dead cells from the count.

Using the tip of a pipette a small volume from the mixture was transferred to the edge of the coverslip and drawn under the coverslip by capillary action. Inaccuracies in cell distribution will occur if the chamber is overfilled or underfilled. Both sides of the chamber were loaded. The grid lines of the haemocytometer chamber were focused and viable cells were counted at low power (10X objective), using a light phase microscope. For fewer numbers of viable cells all 9 large squares were counted and for larger numbers of cells, counting the 4 large corner squares was sufficient (figure 2.1). For routine subculture 100-300 cells per mm^2 should be counted. The more cells that are counted the more accurate the count will be. This was repeated for both sides of the haemcytometer.

Figure 2.1: Schematic Diagram Of A Haemocytometer Chamber

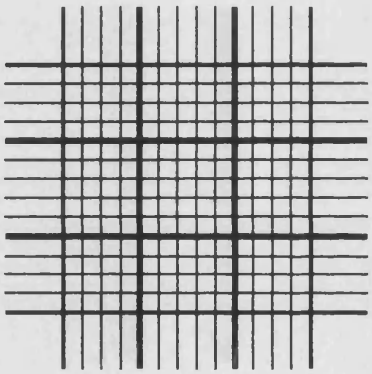

The chamber is divided into 9 large squares and each large square is divided into 16 small squares. There are 2 chambers on a haemocytometer.

Calculation of cell numbers

The formula is:

Number of cells counted ÷ number of large squares counted x 2 x 10^4

This gives the number of cells/ml of the cell suspension.

This is derived from the following:

The area of each square is 1mm and the depth of the counting chamber is 0.1mm.

Therefore, the volume of each large square is $0.1mm^3$ i.e. 10^{-4} ml

The cell suspension is diluted at a ratio of 1:1 in trypan blue therefore, the cell count must be multiplied by 2 to allow for this (Cell Number = mean x 2 x 10^4). The desired cell concentrations can then be calculated and the assay set up.

2.5 MEASUREMENT OF CELL GROWTH RATES

Growth curves for Pre2.8 cells were obtained using two procedures, an MTT assay and cell counts, while growth curves for S2.13 cells were carried out using cell counts only.

2.5.1 MTT Assay - Growth Curves

The MTT assay is a relatively rapid colorimetric assay using a dye that is reduced only by viable cells. The dye, a tetrazolium salt (MTT, (3-4,5-dimethylthiazol-2-yl)-2,-diphenyltetrazolium bromide), is reduced by mitochondrial dehydrogenase to purple formazan crystals. The crystals are dissolved in dimethyl sulphoxide (DMSO) and the intensity measured colorimetrically to give an estimate of the relative number of viable cells.

The appropriate number of cells was added in a volume of 150µl of medium to the selected wells of a 96-well plate. 150µl of medium without cells was added to column 1 in order to provide a "blank" for background subtraction.

A stock of MTT reagent at a concentration of 5mg/ml in medium was prepared and filter-sterilised using a 0.22µm filter. The stock was stored at 4°C in the dark for no more than 3 weeks.

The final MTT concentration (0.5mg/ml, 1.0mg/ml or 5.0mg/ml) was optimised for each cell line used. The medium was removed from each well, being careful not to dislodge the cells, 100µl of 0.5-5.0mg/ml MTT reagent was added and the plate was incubated at 37°C for 3 hours. Supernatant was gently removed and plate was blotted on tissue paper to ensure that all solution was removed. 100µl of DMSO was then added and incubated on a tilting platform at room temperature for 30 minutes to allow the precipitate to dissolve. The plates were read at 540nm (filter 6) on an ELISA reader (Titertek Multiskan MCC/340). Results were saved onto a disc and "Macro-transposed" (computer program to subtract blank results from sample results) and a graph of optical density (OD) versus cell seeding number was obtained (table 2.3 and figure 2.2).

The experimental conditions were optimised for each cell line, including cell number and MTT concentration. The columns (8 wells) of a 96-well plate were seeded with 1250, 2500, 5000, 10000, 15000, 20000, 30000, 40000, 50000 and 60000 cells in a volume of 150µl of medium per well and grown for 2 days (table 2.3). MTT

concentrations of 0.5mg/ml, 1.0mg/ml and 5.0mg/ml were prepared. 50µl of medium was removed from each well and replaced with100µl of 0.5mg/ml MTT for the first 2 rows of the 96-well plate. 100µl of 1.0mg/ml MTT was added to the row 3, 4 and 100µl of the 5.0mg/ml MTT was added to the last 3 rows of the 96-well plate (table 2.3).

Table 2.3: Experimental Lay Out For MTT Optimisation

MTT conc. (mg/ml)	Pre2.8 cell number per well										
0.5	0	1250	2500	5000	10000	15000	20000	30000	40000	50000	60000
0.5	0	1250	2500	5000	10000	15000	20000	30000	40000	50000	60000
1.0	0	1250	2500	5000	10000	15000	20000	30000	40000	50000	60000
1.0	0	1250	2500	5000	10000	15000	20000	30000	40000	50000	60000
5.0	0	1250	2500	5000	10000	15000	20000	30000	40000	50000	60000
5.0	0	1250	2500	5000	10000	15000	20000	30000	40000	50000	60000
5.0	0	1250	2500	5000	10000	15000	20000	30000	40000	50000	60000

Figure 2.2: Optimsation of MTT Assay for Pre2.8 Cells

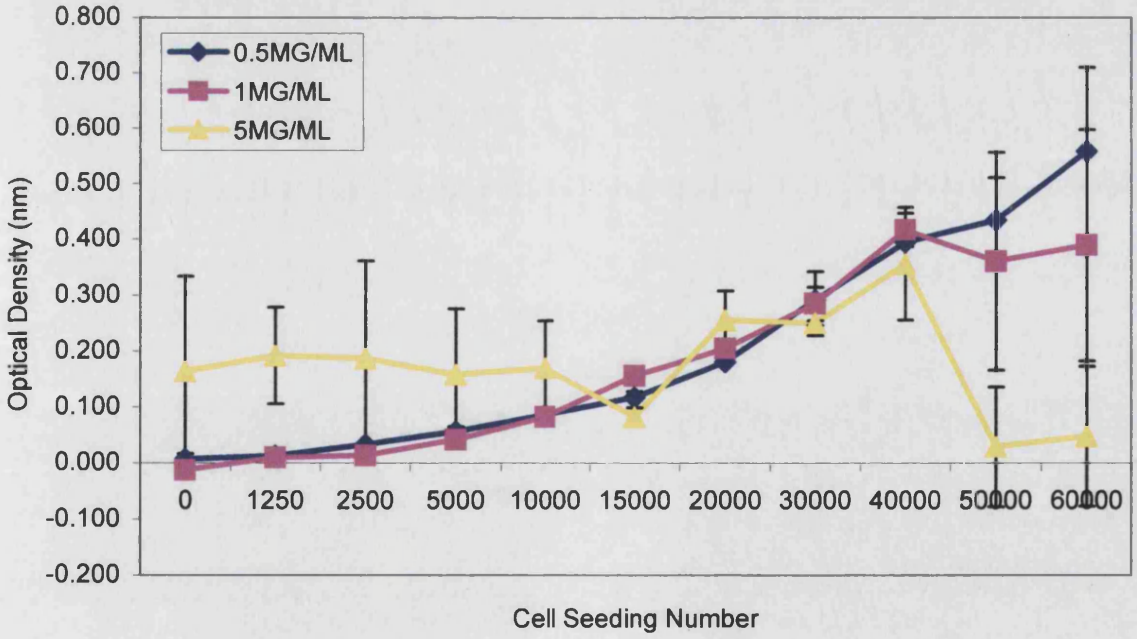

Optimisation of cell number and MTT concentration for the MTT assay with Pre2.8 cells. MTT results were obtained at 540nm on an ELISA reader and sample results were subtracted from blank results. A graph of optical density versus cell seeding number was obtained. The best results were obtained with 0.5mg/ml and 1mg/ml of MTT solution. Results from 5mg/ml had very large standard errors and there was no linearity. 1mg/ml of MTT solution was chosen as the optimum concentration for an MTT assay with Pre2.8 cells. Optical densities were linear between 2500 and 40,000 cells with MTT concentrations of 0.5mg/ml and 1mg/ml. 10,000 Pre2.8 cells were chosen as an optimum seeding concentration for Pre2.8 MTT assays.

The plates were then processed as described above. This optimisation assay was repeated twice and the mean and standard deviation was calculated for each concentration of MTT solution. A graph of optical density versus cell number seeded for each MTT concentration was obtained using Microsoft Excel. The optimum seeding number for Pre2.8 cells and the optimum MTT concentration were determined (figure 2.2).

The best results were obtained with 0.5mg/ml and 1mg/ml of MTT solution. Results from 5mg/ml had very large standard errors and there was no OD linearity. 1mg/ml of MTT solution was chosen as the optimum concentration for an MTT assay with Pre2.8 cells. Optical densities were linear between 2500 and 40,000 cells with MTT concentrations of 0.5mg/ml and 1mg/ml. 10,000 Pre2.8 cells were chosen as an optimum seeding concentration for Pre2.8 MTT assays. The OD for 10,000 cells was estimated taking into account the length of time it takes for the number of cells seeded to be regenerated (a certain number of cells seeded will die). Calculation: If 10,000 cells are seeded and it is expected that after 2 days, approximately the same number of cells (10,000) is present, then the ELISA OD reading can be estimated using the MTT assay. The mean OD for 10,000 cells from both plates was obtained (0.123 +0.084 = 0.207) (0.207/2=0.104). The OD for 10,000 cells is approximately 0.104nm.

Optimised Assay

In order to construct a growth curve using the MTT assay, 10,000 Pre2.8 cells were seeded in quadruplicate. Separate plates were incubated at 33°C, 39°C and 37°C. The cells were harvested at days 3, 5, 7, 10, 12, 14 and 18, using 1.0mg/ml MTT reagent for colour development. The mean colour intensity was calculated for the four replicates at each time point. The experiment was repeated 4 times. The mean and standard deviation were calculated for each assay.

2.5.2 Cell Counts – Growth Curves

Cell counts were used to obtain a growth curve for Pre2.8 and S2.13 cells. Triplicate T25 flasks were seeded with 100,000 Pre2.8 cells or 200,000 S2.13 or FT cells and incubated at 33°C, 39°C and 37°C. The medium was changed three times weekly and the cells were harvested after 3, 5, 7, 10, 12, 14 and 17 days incubation. The experiment was repeated three times. Viable cells (trypan blue exclusion) were counted on an inverted phase microscope using a haemocytometer. The mean cell number was calculated for each set of triplicate samples and the mean, standard deviation and standard error was calculated.

2.5.3 Statistics

In general there are 2 types of statistics: (i) descriptive or (ii) inferential. No conclusions are drawn from descriptive statistics. They simply reduce the acquired information to a manageable size and present a summary of the data. Inferential statistics draw conclusions from the data, e.g. the conclusion that there is a significant difference in some measurable response between two drugs. The mean and standard deviation was calculated using Microsoft Excel software and from these results the standard error was calculated using a standard formula.

Average

An "average" is a general term used to describe a value of a variable that is typical or representative of the data. Common types of average are arithmetic mean, median and mode. Excel returns the average (arithmetic mean) of the numbers. The arithmetic mean is the sum of all the observations divided by the number of observations (an average number is obtained by adding two or more amounts together and dividing the total by the number of amounts).

Standard deviation

Excel estimates standard deviation based on a sample. The standard deviation is a statistical measure of how widely values are dispersed from the average value (the arithmetic mean). It is calculated as the square root of the variance (a measure of the spread or variation of a group of numbers in a sample, equal to the square of the standard deviation). The more widely the values are spread out, the larger the standard deviation. For example, say we have two separate lists of exam results from a class of

30 students; one ranges from 31% to 98%, the other from 82% to 93%, then the standard deviation would be larger for the results of the first exam.

Standard Error

Standard error is a measure of variability, calculated by dividing the standard deviation of the sample in a frequency distribution by the square root of the number of values in the sample. It is a measure of the variability that a constant would be expected to show during sampling.

$SE = SD/\sqrt{n}$

2.6 CELL SIZE DISTRIBUTION

Cell size distribution for Pre2.8 and S2.13 prostate cells were measured using a Graticule under a light phase microscope and using a Beckman "Z2 Coulter Counter and size analyzer".

2.6.1 Graticule And Light Phase Microscope

Flattened cells growing on a petri dish were measured using a 1mm grid graticule, showing markings of 0.01mm on a slide. This grid is equated to similar unlabelled markings on a microscope eyepiece grid (graticule) at the different magnifications on the Light Phase Microscope.

Procedure

Semi-confluent plates of Pre2.8 and S2.13 cells, incubated at 33°C, 37°C and 39°C at day seven in culture were used for measurement. The grid on the eyepiece graticule was used as a guide for a straight line. The diameter of the cell was measured by making a note of the number of markings for each cell and its nucleus, along this line. This was repeated until a minimum of 100 cells for each cell line was measured. The number of markings was then converted to mm using the measurements worked out for that particular magnification. These figures were entered onto a Microsoft Excel worksheet and the mean and standard deviation was calculated for each group. A graph of "cell number versus size" was obtained from these measurements.

2.6.2 Beckman Z2 Coulter Counter And Size Analyzer

Cells are in suspension when size is measured using a Coulter Counter. Unlike older counters the Beckman Z2 does not require calibation. It has an analogue display and the lower threshold can be set manually on th read-out, usually at 7μm, while the upper is normally set at 30μm or infinity. After completing a trial run with Pre2.8 cells grown at 33°C, a size range was set between C1 and C2 (e.g. 10μm and 30μm) in order to avoid counting debris. This range can be altered depending on cell type. A digital display unit displays the total number of cells counted within this size range, the number of cells counted per ml, the mean, median, mode and standard deviation of cell size.

Beckman Coulter Counter

Particles suspended in a weak electrolyte solution are drawn through a small aperture separating two electrodes between which an electric current flows. The voltage applied

across the aperture creates a "sensing zone". As each particle passes through the aperture (or "sensing zone") it displaces its own volume of conducting liquid, momentarily increasing the impedance (resistance of an electric circuit to the flow of current) of the aperture. This change in impedance produces a tiny but proportional current flow into an amplifier that converts the current fluctuation into a voltage pulse large enough to measure accurately. The amplitude of this pulse is directly proportional to the volume of the particle that produced it. Scaling these pulse heights in volume units enables a size distribution to be acquired and displayed. In addition, if a metering device is used to draw a known volume of the particle suspension through the aperture, a count of the number of pulses will yield the concentration of particles in the sample.

Procedure

A single cell suspension was obtained using 0.5ml of trypsin for Pre2.8 cells grown at 33°C, 37°C and 39°C, and for S2.13 cells grown at 33°C. Cells were resuspended in 9.5ml of medium. A suitable dilution of this cell suspension was prepared in an isotonic (having the same or equal osmotic pressure - usually used with regards to describing solution on either side of a membrane.) electrolyte (e.g. PBSA). An electrolyte is a substance that, when dissolved in water, gives a solution that can conduct electricity. A minimum of 100,000 cells was sufficient for the Coulter counter. A graph of "cell number versus size" was obtained from results produced by the Coulter counter.

2.7 ANCHORAGE INDEPENDENT GROWTH IN AGAR

Anchorage independent growth is a suspension cloning procedure. Pre2.8 and S2.13 prostate cells were tested for their ability to grow in semi-solid agar, an indication of neoplastic transformation (Honjo et al., 2001; Menter et al., 2000). A breast cancer cell line, MDA-MB-435 (Glinsky et al., 1996) was used as a positive control. The assay was carried out in 6-well plates. Semi-solid agar was prepared at a concentration of 0.75% (base agar) and 0.28% (top agar) in RPMI-1640 medium.

Base Agar

Agar, 1.5% (DNA grade) was melted in a microwave and then cooled to 40°C in a waterbath. Appropriate medium was warmed to 40°C in a waterbath and allowed to equilibrate for at least 30 minutes. Equal volumes of the two solutions were mixed to give 0.75% Agar in medium, 1.5ml was added per 35mm petri dish and allowed to set.

The plates could be stored at 4°C for up to 1 week. It is best to remove the base agar plates from 4°C 30minutes before adding top agar.

Top Agar and Cell Preparation

Agar, 0.5% (DNA grade agar) was melted in a microwave and cooled to 40°C in a waterbath. Medium was warmed to the same temperature. A single cell suspension of Pre2.8, S2.13 and MDA-MB-435 was obtained from semi-confluent T80 flasks. Cell concentrations of $1.25x10^4$, $2.5x10^4$, $5.0x10^4$ and $1.0x10^5$ were prepared in triplicate, for each cell line and 0.1ml was added per 15ml conical tube. Equal volumes of medium and 0.5% agar was added to each 15ml conical tube and contents were gently mixed. 1.5ml of each sample was added per base agar plate. The assays were incubated at 37°C for 10-13 days. Colony formation was examined under a light microscope.

2.8 COLONY FORMING ASSAYS

The colony forming efficiencies (CFE), a monolayer cloning procedure, of Pre2.8 cells were measured at 33°C and 39°C. A single cell suspension of Pre2.8 cells was prepared and resuspended in 10ml of PrEGM medium. From this suspension 10,000, 15,000 and 20,000 cells were added, in triplicate to 5cm petri dishes and incubated at 33°C and 39°C for at least 14 days. Each experiment was repeated a minimum of 3 times. The cultures were fixed with 70% IMS for 5 minutes and stained with 10% Giemsa for 30 minutes. Colonies containing greater than 50 cells per colony were counted under a dissecting microscope. The average of each triplicate set was determined and the percentage colony forming efficiency (%CFE) was calculated.

2.9 IMMUNOHISTOCHEMISTRY

2.9.1 Cultures On Coverslips

Preparation of coverslips for growing cells for immunocytochemical staining, 3ml of 7X detergent was added to 1 litre of deionised water, mixed and added to a microwave bowl. Coverslips were added to the boiling solution and microwaved for 10 minutes. They were then cooled and rinsed in 10 changes of water, the first 3 times with tap water and the last 7 with deionised water. Finally, the coverslips were rinsed once with 95% ethanol, dried and sterilised by autoclaving.

To grow cells on the coverslips, the desired numbers of coverslips were placed into individual wells of a 24-well plate. A single cell suspension of the selected cell line was prepared and added to each well. To fix the cells, the medium was carefully aspirated and the monolayers washed twice with PBS. The cells were then fixed in ice-cold methanol and acetone (1:1 ratio) for 10 minutes, on ice. For storage, 1ml of a 0.1% sodium azide solution was added and the fixed cells were stored at 4°C until use. The preservative solution was prepared by dissolving 0.1g of BSA and 0.1g of sodium azide in 100ml of PBS. This reagent was stored at 4°C.

2.9.2 Cutting Paraffin Sections For Immunohistochemistry

The paraffin blocks were placed faced-down on ice for half an hour and 7-10μm sections cut on a microtome and collected on Vectabond coated slides. The slides were incubated at 60°C for 20 minutes to remove water and soften the wax to aid adherence to the glass. The slides were stored at room temperature until use.

When required, the tissue sections were de-waxed twice in xylene for 3 minutes. They were then rehydrated by incubating twice in 100% alcohol for 1 minute, followed by 2 incubations in 70% alcohol for 1 minute. The sections were then washed twice for 1 minute in distilled water and stored in water. The tissue sections were circled with a Dako resin pen to delineate the area for immunocytochemisty.

Antigen retrieval of paraffin embedded tissue sections was required for most of the antibodies used. The retrieval, using a chemical reaction was carried out using a Vector™ Antigen Unmasking Solution. The specific chemical identity of the chemical in this product is withheld as a trade secret. The protocol for laboratory made citrate buffer, for antigen retrieval is a final concentration of 0.01M sodium citrate made in distilled water to pH 6.0 with concentrated HCl.

2.9.3 Antigen Unmasking Solution

Based on a citric acid formula, this solution is can reveal antigens in formalin-fixed, paraffin-embedded tissue sections when used in combination with a high temperature treatment procedure. The Antigen Unmasking Solution is supplied as a concentrated stock at pH 6.0. Rehydrated slides were placed in glass racks and carefully lowered into boiling retrieval solution and microwaved at full power for 15 minutes. The slides were then washed twice for 5 minutes in PBS and stored in 1x PBS until the next step.

2.9.4 Monoclonal Antibodies

Antibodies are immunoglobulins (Ig) produced by the body's immune system. Each antibody is produced by lymphocytes as a result of exposure to specific chemical substances called antigens, usually on the outside of an invading organism. They are proteins of molecular weight 150,000 - 900,000 kd, consisting of two heavy chains and two light chains. The structure of their antigen binding sites has great variation, which enables different antibodies to bind to structurally different epitopes. There are 5 classes (isotypes) of immunoglogulin: IgM, IgG, IgA, IgD and IgE, plus 4 subtypes of IgG (IgG1-4), and 2 of IgA (IgA1, IgA2).

Cesar Milstein and co-workers developed monoclonal antibodies for use in the laboratory (Kohler et al. 1975). They overcame the problem that lymphocytes cannot be grown independently in the laboratory. Briefly, an animal (e.g. a mouse) is exposed to a foreign substance, which after a few days results in the production of a mixture of antibodies in response to the antigens responsible. White cells are then extracted from the animal and are fused with cells taken from a cancerous tumour (for rapid growth), usually an immortal myeloma cell line. The hybrids are then cloned. Each clone is then tested to see if they are producing antibodies for the particular target substance. Since the cells in the clone are genetically identical, all the cells produce the same antibody, which builds up in the nutrient medium surrounding the cells. This is purified, resulting in a product containing molecules of a single antibody.

Due the specificity of their binding properties, monoclonal antibodies may have a wide variety of possible uses. We have used monoclonal antibodies in our studies (table 2.4), for immunocytochemistry and for flow cytometry procedures.

Table 2.4: Primary Antibodies For Immunocytochemistry And Dilutions Used In This Study

Antigen	Clone	Species	Source	Working Dilution	Ig Subtype
Androgen receptor (AR)	F.39.4.1	Mouse	Biogenex	1/200 (DAB) 1/100	IgG1
Prostate specific antigen (PSA)	ER-PR8	Mouse	Dako M0750	1/30 (DAB) 1/20	IgG1
Prostatic acid Phosphatase (PAP)	PASE-4LJ	Mouse	Dako	1/100 (DAB) 1/50	IgG1 Kappa
Cytokeratin 8 (K8)	35βH11	Mouse	Dako	1/100 (DAB) 1/200 (Fluores)	IgM
Cytokeratin 14 (K14)	LL002	Mouse	Gift, EB Lane	1/20 (Fluores)	IgG3
Cytokeratin 17 (K17)	E-3	Mouse	Sigma	1/100 (Fluores)	IgG2b
Cytokeratin 19 (K19)	Rck108	Mouse	Gift, EB Lane	1/50 (Fluores)	IgG1
Cytokeratin 18 (K18)	LE61	Mouse	Gift, EB Lane	1/10 (Fluores)	IgG1
Smooth muscle actin (SMA)	1A4	Mouse	Sigma	1/100 (DAB) 1/200 (Fluoers)	IgG2a
Vimentin	VIM-13.2	Mouse	Vim 13.1 – Sigma	1/200 (Fluores)	IgM
Fibroblast	AOO2		Gift, M O'Hare	(Fluores)	IgM
Ki67	Anti-Ki67	Rabbit	Dako	1/100 (Fluores)	IgG2A

Abbreviations: Fluores – fluorescence; Ig – Immunoglobulin

2.9.5 Immunocytochemistry Using The Vectastain Elite ABC Kit

The Vectastain Elite ABC kit, based on the avidin biotin method of immunostaining was used. Briefly, this method employs unlabelled primary antibody, followed by biotinylated secondary antibody and an Avidin and Biotinylated horseradish peroxidase macromolecular complex.

Fresh 0.3% hydrogen peroxide in 70% methanol was prepared for each experiment. 300µl of hydrogen peroxide was added to 100ml of 70% methanol in PBS and kept at 4°C. This solution was used to saturate endogenous peroxidase, in order to avoid non-specific background staining. The peroxide solution was added to each coverslip or slide, and incubated for 30mins at room temperature, followed by two washes in 1x

PBS for 5mins each. Normal horse serum (NHS) was used to block non-specific antibody binding and was added for 20 minutes at room temperature. Then primary antibody (mouse anti-human Ab) diluted in NHS was added at a volume of 50µl of antibody to each coverslip or 100-200µl to each slide and incubated for 1-2hrs at room temperature, followed by three 5 minute washes in PBS.

Biotinylated secondary antibody was diluted and 50µl added per coverslip, or 100-200µl added per slide and incubated for 30 minutes at room temperature. Vectastain ABC reagent was prepared 30mins before use. One drop was added to each coverslip and 2 drops to each slide and then incubated for 30 minutes, followed by three washes in PBS for 5 minutes each.

The coverslips or slides were incubated in ABC reagent for 30mins at room temperature, followed by two washes in PBS for 5 minutes each. Peroxidase substrate (3,3'-diaminobenzidine tetrahydrochloride) was prepared following DAB kit instructions and 50µl was added to each coverslip or 100-200µl was added to each slide. Once the preparation was stained, the DAB was pipetted from the coverslips or slides and placed in a universal containing 12% (w/v) sodium hypochlorite solution for disposal. The coverslips or slides were carefully washed in tap water, as there is some evidence that DAB is carcinogenic.

The preparations were counterstained with Mayer's haematoxylin for about 30 seconds and then carefully washed with tap water, and then dehydrated by immersing twice in 70% alcohol for 5mins each, twice in 100% alcohol for 5mins each and twice for 5 minutes in xylene. Coverslips were mounted cell side down on a slide with a drop of DPX and slides were mounted with a coverslip with DPX.

Immunofluorescent staining

Paraffin-embedded sections were dewaxed and rehydrated and cells on coverslips were fixed before staining. PBS containing 10% foetal calf serum (FCS)/foetal bovine serum (FBS) is required for blocking of non-specific antibody binding and also for antibody dilution. Serum used should contain sufficient immunoglobulins to competitively inhibit the binding of antibodies (being tested) to cells, via interactions not involving the specific recognition of an epitope by the antigen binding region of the antibody (being tested), referred to as non-specific or background staining. Each section or coverslip

was covered with a suitable volume (50µl-300µl) for 30 minutes. Primary antibody was diluted in serum solution. 50µl was added per coverslip and 50-200µl was added per tissue section and incubated at 4°C overnight, followed by two washes in PBS for 5 minutes each. The secondary antibody was diluted and applied to sections or coverslips and incubated in the dark for 45 minutes, followed by two washes in PBS for 5 minutes each. Hoechst (25mg/ml) nuclear stain was applied and incubated in the dark at room temperature for 5 minutes, followed by two washes in PBS for 5 minutes each. The slides were mounted in Gelvatol and stored in the dark at 4°C until ready to examine under the fluorescence microscope.

Hoechst nuclear stain

Hoechst 33258, chemically known as bisbenzimide is a DNA intercalator that excites in the near UV (350 nm) and emits in the blue region (450 nm). Hoechst 33258 binds to the AT rich regions of double stranded DNA. It is a membrane-permeable fluorescent DNA stain, only when cells are fixed and it has low cytotoxicity.

Gelvatol Mounting Medium

Gelvatol is a product of the "Monsanto Indian Orchard" plant. Mounting solution was prepared by mixing 6g of Glycerol and 2.4g of Gelvatol in 6ml of distilled water in a 50ml tube. The mixture was incubated at room temperature for 30 minutes and then 12.5ml of a 200mM Tris (pH 8.5) buffer was added and heated at 50°C for 10 minutes. This process was repeated 4 times and the solution was placed on a rotating platform overnight at room temperature. The solution was then cenrifuged at 400rpm, the supernatant removed, and stored at 4°C until required.

2.10 FLUORESCENCE MICROSCOPY AND DATA CAPTURE

Fluorescence describes light emission that continues only during the absorption of the excitation light by a chromophore or other conjugated molecule that is capable of emitting secondary fluorescence. A fluorescence microscope uses high-energy, short-wavelength light (usually ultraviolet) to excite electrons within certain molecules inside a specimen, causing those electrons to shift to higher orbits. When they fall back to their original energy levels, they emit lower-energy, longer-wavelength light (usually in the visible spectrum), which forms the image.

Ultraviolet Light Action

A fluorescence microscope uses a mercury or xenon lamp to produce ultraviolet. The light comes into the microscope and hits a dichroic mirror, a mirror that reflects one range of wavelengths and allows another range to pass through. The dichroic mirror reflects the ultraviolet light to the specimen. The ultraviolet light excites fluorescence within molecules in the specimen. The objective lens collects the fluorescent-wavelength light produced. This fluorescent light passes through the dichroic mirror and a barrier filter (that eliminates wavelengths other than fluorescent), going it to the eyepiece to form the image.

Fluorescence-microscopy techniques are useful for seeing structures and measuring physiological and biochemical events in living cells. Antibodies that are specific to various biological molecules can be chemically bound to fluorescent molecules and used to stain specific structures within cells.

Fading or bleaching of fluorescence in specimens during exposure limits the time available to examine stained samples and hence limits its usefulness. To minimize the effects of photobleaching, fluorescence microscopy combined with phase contrast illumination was used for this work. This was achieved by locating the specific area of interest in a specimen using the non-destructive contrast enhancing technique (phase) then, without relocating the specimen the microscope was switched to fluorescence mode. Adobe Photoshop 5.0 was the software used to transform the captured image into the fluorescent photograph.

2.11 CYTOGENETICS

The normal karyotype of humans consists of 23 pairs of chromosomes. During the development of cancer and immortalisation of normal cells, chromosomal changes can occur. Identification of chromosome patterns can be carried out using fluorescent staining methods. A standard map of the banding pattern of each chromosome was established for the human chromosome from the prometaphase stage of mitosis.

The cytogenetics was carried out by Dr R McLeod, DSMZ, Braunschweig, Germany. Cytogenetic harvesting, slide preparation, trypsin G-banding (GTG) and fluorescence in-situ hybridisation (FISH) were performed as described previously (MacLeod et al., 2000). FISH was performed according to manufacturers' protocols using single-locus

and whole-chromosome ('painting') probes, including Octachrome paints obtained from Cambio (Cambridge, UK), AGS (Heidelberg, Germany), Vysis (Bergishe Gladbach, Germany), Q-Biogene (Illkirch, France), and Roche Molecular Biochemicals (Mannheim, Germany).

Preparations were counterstained with 4' 6-diamidino-2-phenylindole (DAPI) (Camon, Wiesbaden, Germany). Probe signals were detected directly (Octachrome) or indirectly using anti-digoxigenin-FITC (Q-Biogene) or avidin-Texas-Red (AGS). Octachrome FISH enables panoptic analysis of all 24 chromosomes on a single slide using 8 triplet probe combinations. For more detailed analysis based on G-banding and Octachrome analysis, FISH was performed using optimised single locus and painting probe combinations.

2.12 FLOW CYTOMETRY AND FLUORESCENT ACTIVATED CELL SORTING (FACS) ANALYSIS

Flow cytometery is a generic term, while FACS (Fluorescence Activated Cell Sorter) is a trademark of the Becton-Dickinson Corporation. Flow cytometry uses fluorescent probes which bind to specific cell associated molecules, allowing measurements of various phenotypic, biochemical and molecular characteristics of individual cells (or particles) suspended in a fluid stream. As the cells flow past a focused laser beam of appropriate wavelength, the probes fluoresce and the emitted light is collected and directed to appropriate detectors. These detectors, in turn, translate these light signals into electronic signals, proportional to the amount of light collected. Information regarding the relative size and granularity of a cell, for example, is also obtained as these characteristics influence the deflection (or scattering) of laser light as the cell passes through the laser beam. Flow cytometers have the ability to evaluate cells at an extremely rapid rate (e.g. up to 20,000 events per second).

Flow cytometric data can be displayed using either a linear or a logarithmic scale. The simplest type of experiment involves an immunofluorescent marker to look for a positive sub-population of cells. For example, when lymphocytes are stained with an inappropriate antibody (figure 2.2A), there is no cell expression and when lymphocytes are stained with an appropriate marker, for example CD3-FITC (figure 2.2B) the percentage of cells expressing the specific marker can easily be determined by subjectively applying a marker (M1).

Figure 2.3: Example Of Flow Cytometric Data

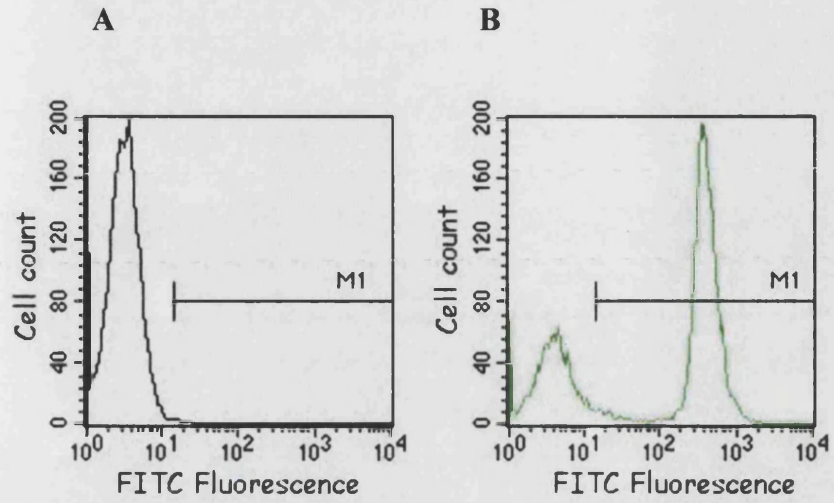

Distinguishing between non-expression and expression of antibodies for the same cell. Graph A shows distribution when a particular cell does not express an antibody. Graph B shows distribution when it expresses a particular antibody. Figures were taken from FACS Laboratory (Cancer Research) website.

Cytometry becomes more complicated when the level of fluorescence is required (figure 2.3). It may be necessary to determine the level of expression of two different populations of cells in a particular group of cells.

Figure 2.4: Example Of Flow Cytometric Data

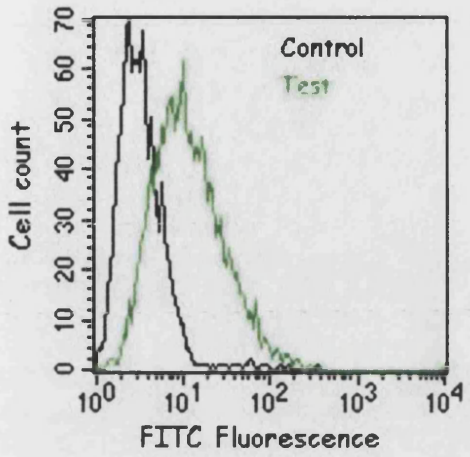

Graph showing distribution of two different levels of fluorescence. Figures were taken from FACS Laboratory (Cancer Research) website.

One of the problems associated with FACS is achieving a single cell suspension, which could potentially cause inaccurate readings (figure 2.4B top & bottom). Good cell preparations are necessary for accurate results. When large clumps are present the flow cytometer will stop counting until the block is cleared, which is achieved by flushing the system. Smaller clumps, such as two cells stuck together will pass through the capillary but the flow cytometer has the ability to exclude these cell doublets (figure 2.4A). A single cell will have a smaller width than a cell doublet passing through the beam consecutively (figure 2.4B).

Figure 2.5: Flow Cytometric Data Distribution

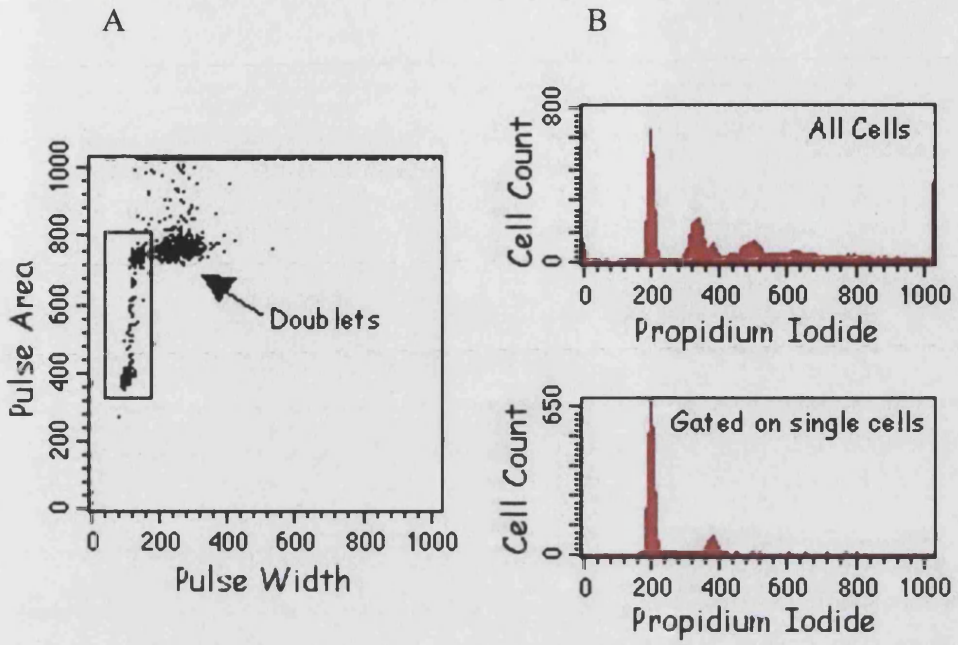

Effect of graph distribution when cell doublets are present when put through the flow cytometer. A, shows gating of cell doublets from single cells in order to achieve accurate readings. B top, shows cell distribution when cell doublets are not gated out, compared to B bottom, showing the distribution when only single cells are counted. Figures were taken from FACS Laboratory (Cancer Research) website.

FACS and Cell Cycle Distribution

The measurement of the DNA content of cells was one of the first major applications of flow cytometry. The DNA content of the cell provides information about the cell cycle and ploidy (the basic number of chromosomes can vary within an organism) of the cell. Ideally all cells in the G1 phase should take up the same amount of dye and all fluoresce in a single channel, but there can be minor conformational variations in the DNA leading to slightly different amounts of dye being taken up. This is quantified by using the coefficient of variation (CV) of the G1 peak. It is assumed that by measuring fluorescence from a DNA-binding fluorochrome, it is the same as DNA content. Although propidium iodide is probably the most commonly used dye to quantitatively assess DNA content, there are several different dyes that are available which bind stoichiometrically to DNA. Using a DNA binding dye such as propidium iodide a successful DNA profile, or cell cycle distribution can be achieved (figure 2.5).

Figure 2.6: Example Of A Successful DNA Profile Using Propidium Iodide

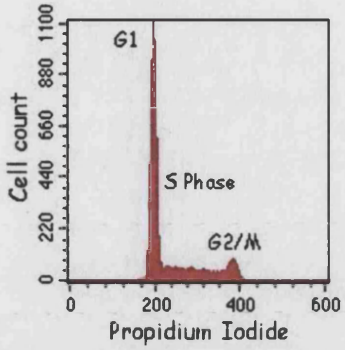

Figures were taken from FACS Laboratory (Cancer Research) website.

Once a single cell population has been obtained an estimate of the percentage of cells in G1, S phase and G2/M can be determined. This can be determined by subjectively applied markings (figure 2.6A) or by using a program that will mathematically construct a DNA histogram and thus give a more accurate measurement of the percentage of cells in each phase. The method used in this study was by subjectively applying markings (M1, M2, and M3) equivalent to cell cycle stages (G1, S, and G2/M).

Figure 2.7: Cell Cycle Distribution Using Propidium Iodide With And Without Markings

A **B**

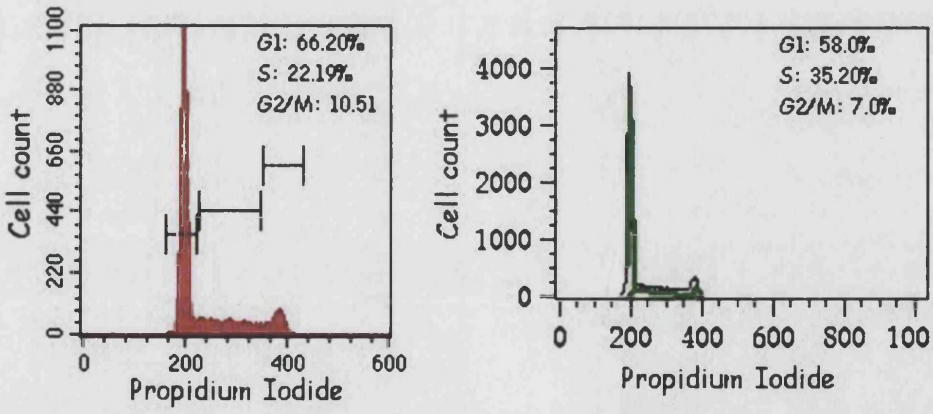

A, shows the gating of peaks in order to distinguish between G1, S and G2/M. B, shows example of cell cycle distribution pattern and percentages, without markings. Figures were taken from FACS Laboratory (Cancer Research) website.

2.13 CELL CYCLE DISTRIBUTION

For studies of the cell cycle distribution, T80 flasks of Pre2.8 cells were cultured at 33°C, 37°C and 39°C for 7 and 10 days. The cells were harvested and a single cell suspension was obtained, counted and washed in cold PBS. After centrifuging at 1500 x g for 5 minutes, the cells were resuspended in 800µl of PBS at -20°C and, while vortexing, 800µl of 70% ethanol (-20°C) was added. The cells were then stored at 4°C.

Prior to analysis, the cells were centrifuged at 2500 x g for 5 minutes and resuspended in 800µl of PBS. 100µl of 1mg/ml of RNase and 100µl of 400µg/ml propidium iodide were added and the cells were incubated at room temperature for 30 minutes.

For studies of keratin distribution, Pre2.8 cells were incubated at 33°C, 37°C and 39°C for 4 days. The cells were harvested, single cell suspensions obtained and cell counts carried out. The cells were then centrifuged and resuspended in 100µl of PBS containing 10% serum, before fixation in 4% paraformaldehyde on ice for 10 minutes. The cells were centrifuged at 1200 x g for 5 minutes, resuspended in 100µl saponin buffer (from Quillaja bark, it permeabilises cells) and incubated on ice for 10 minutes. Non-specific staining was blocked by incubating the cells in 50µl of L15 medium containing 10% serum for 30 minutes and then 50µl of primary antibody (see table 2.4) was added and incubated on ice for 45 minutes. The cells were washed in 100µl of saponin buffer three times. 50µl of secondary antibody (see table 2.4) in saponin buffer was added and the cells were incubated on ice, in the dark for 30 minutes. 50µl of saponin buffer was added to cells to produce a final volume of 100µl. The cells were washed twice in saponin buffer and twice in PBS and resuspended in 100µl of saponin buffer and stored at 4°C for a maximum of 48 hours.

2.14 3-DIMENSIONAL CULTURES

For Matrigel cultures, pipette tips and 24-well plates were cooled to -20°C for 1hr before use. 200µl of Matrigel, diluted 1:1 with culture medium was added per well and allowed to set at 39°C for 30mins. Epithelial and stromal cell suspensions were placed on top of the Matrigel. Cultures were incubated at 33°C, 39°C and 37°C for different periods. The medium was changed three times a week and the cultures were monitored routinely using an inverted phase microscope.

For fixation, the cultures were washed twice with PBS and fixed with 4% formaldehyde for 30 minutes at room temperature, followed by 2 washes with PBS. For processing, the gels were wrapped in single ply tissue paper and placed in an embedding cassette and stored in 70% ethanol overnight. The following day, the gels were dehydrated and then embedded in increasing percentages of molten paraffin. Paraffin blocks were allowed to solidify and 7-10μm sections were cut on a microtome. Haematoxylin and eosin (H&E) staining (Hine, 1981) was carried out on a sample section from each paraffin block. Immunohistochemistry was used to study prostate specific markers, cytokeratins and proliferation markers (table 2.4). Normal prostate tissue sections were used as positive controls. Sections from fixed 3-D paraffin blocks were used as negative controls (primary antibody was omitted from these sections, leaving staining with only secondary antibody).

Ethical approval was obtained for all tissue used in these experiments and the correct process for obtaining tissue samples were adhered to. These experiments were covered under study number 98/0082: "development of conditionally immortalized cell lines from human prostate tissue", which was approved by Joint UCL/UCLH committees on the ethics of human research.

In pilot studies, Matrigel and monolayer cultures were set up using mixtures of 100,000 Pre2.8 cells and 25,000 S2.13 cells in equal volumes of PrEGM and DMEM (8% FCS + 1% Glutamine) and incubated at 33°C, 39°C and 37°C for 18 – 20 days. Mibolerone, a synthethetic androgen was added to half the cultures at a final concentration of 10^{-8} or 10^{-9} M in 0.0001% ethanol. Frozen stocks of Mibolerone were prepared in 100% ETOH to a final concentration of 10^{-8}M. Unlike dihydrotestosterone (DHT), mibolerone in not metabolised, i.e. there are no enzymes in the cells to break it down. It works like DHT, binding AR and secreting PSA and PAP in the same way. Mibolerone simply mimics the effect of natural androgens.

A comparison was made of different media (PrEGM, PrEGM/DMEM and S2.13 supernatant) using reduced growth factor Matrigel. Incubation was carried out at the permissive (33°C) and semi-permissive (37°C) temperatures for 23 days. Matrigel cultures were paraffin embedded and 7μm sections were cut. Immunohistochemistry was carried out (table 2.4).

To prepare the supernatant from S2.13 cells, PrEGM medium was added to an $80cm^2$ flask, containing S2.13 cells and incubated for 3 days at 33°C. The medium was collected, designated as S2.13 supernatant and stored at 4°C for no longer than 1 week.

Few S2.13 cells survived in the 3-dimensional culture pilot studies. Therefore different proportions of S2.13 cells were tested. In addition, mouse 3T3 cells were co-cultured with Pre2.8 cells. For comparison each cell line was cultured in Matrigel alone. Cultures were set-up following the procedures described above and incubated at 37°C for 3 weeks (table 2.5).

Table 2.5: 3-D Experimental Variations

Cell Line	Ratio	Cell concentration	Medium
Pre2.8/S2.13	4:1	$1x10^5/2.5x10^4$	Equal volumes of PrEGM/DMEM
	1:1	$1x10^5/1x10^5$	
	1:4	$1x10^5/4x10^5$	
	1:8	$1x10^5/8x10^5$	
	1:10	$1x10^5/10x10^5$	
Pre2.8/3T3	1:1	$1x10^5/1x10^5$	Equal volumes of PrEGM/DMEM
	1:4	$1x10^5/4x10^5$	
Pre2.8 only		$1x10^5$	PrEGM only
S2.13 only		$1x10^5$	DMEM only
		$4x10^5$	
		$10x10^5$	
3T3 only		$1x10^5$	DMEM only
		$4x10^5$	

2.15 RT-PCR

RT-PCR can provide a semi-quantitative measure of gene expression at the mRNA level. This technique involves an enzyme, reverse transcriptase that has the ability to synthesise complementary DNA (cDNA) from mRNA. The cDNA is then used as a template for PCR analysis. PCR selectively amplifies a region of DNA, using oligonucleotide primers synthesised from a selected sense and an antisense DNA sequence. Codes of practice (for example, wearing gloves) should be carried out to ensure that RNases are not introduced during RNA extraction procedures.

2.15.1 RNA Extraction

Ribonucleases (RNases) are very stable and active enzymes that do not require cofactors to function. Since RNases are difficult to inactivate and even minute amounts are sufficient to destroy RNA, it is important that all materials are RNase free.

RNA was extracted from the Matrigel cultures using the silica-gel-based RNeasy Mini kit (Qiagen Ltd., UK). MatriSperse Cell Recovery solution was used to remove cells from Matrigel matrix for mRNA isolation. The MatriSperse solution depolymerises Matrigel at 2-8°C without enzymatic digestion. Manufacturer instructions were followed except for two minor modifications. 0.5ml of MatriSperse was added per well instead of the 2ml suggested, and 1ml of MatriSperse solution was added per dish for rinsing.

The RNeasy mini kit was used to isolate up to 100μg of total RNA. A high-salt buffer system enables RNA at least 200 bases long to bind to a silica-gel membrane. The protocols provided by the manufacturer, Qiagen were followed.

RNeasy Mini kit

Cells were harvested by trypsinisation and then lysed in the presence of a denaturing guanidine isothiocyanate (GITC) and β-mercaptoethanol containing buffer (RLT buffer) (350μl added to maximum $5x10^6$ cells) that inactivates RNases to ensure isolation of intact RNA. The RLT buffer is highly denaturing and immediately inactivates RNases to ensure isolation of intact RNA. Complete lysis or disruption of plasma membranes of cells and organelles is required to release all the RNA contained in the sample (incomplete disruption results in significantly reduced yields).

The cell lysate was homogenized using a "QIA shredder" spin column (manufactured by Qiagen). Homogenization is necessary to reduce the viscosity of the cell lysates produced by disruption. Homogenisation shears the high molecular weight genomic DNA and other high-molecular-weight cellular components to create a homogeneous lysate, so that a pure solution of RNA can be extracted. Incomplete homogenization results in inefficient binding of RNA to the RNeasy membrane and therefore significantly reduces yield. The lysate (maximum volume of 700μl) was loaded onto a "QIAshredder" spin column in a 2ml collection tube. The column was centrifuged for 2

minutes at 13,000rpm in a microcentrifuge and the homogenized lysate was collected. One volume of 70% Ethanol was added to the homogenate, mixed and added to the RNeasy mini spin column (on a 2ml collection tube) and spun at 10,000 rpm for 15 seconds.

The RNeasy mini column was transferred to a new tube and washed twice with 500µl of RPE buffer (solution containing ethanol) to remove sheared genomic DNA and protein contaminants by centrifuging at 10,000 rpm for 15 seconds. The column was then transferred to a dry 1.5ml tube and 30µl of RNase-free water was added and the column was centrifuged at 10,000 rpm for 1 minute. RNA samples were stored at –20°C until ready to use.

2.15.2 Measurement of RNA concentration

RNA concentrations were measured by UV spectrophometry using a DU650 series spectrophotometer (Beckman Coulter Ltd., UK). 4µl of eluted RNA was diluted with sterile water to 400µl (1/100) and added to a clean cuvette. The spectrophotometer was blanked with water using a clean cuvette. The yield of RNA was calculated by measuring the optical density (OD) at 260nm and at 280nm and the RNA concentration was calculated as follows:

OD_{260} x 40µg/ml x dilution factor = RNA concentration µg/ml

An absorbance of 1 unit at 260nm corresponds to 40µg/ml of RNA. This relation is valid only for measurements in water. The ratio of the readings at 260nm and 280nm provides an estimate of the purity of RNA with respect to contaminants that absorb in the UV spectrum, such as protein. The 260nm/280nm ratio of pure RNA in water is approximately 2.0.

2.15.3 Reverse Transcription

1µg of RNA was reverse transcribed into cDNA in a 20µl reaction volume. 1µl Oligo (dT)12-18 (500µg/ml) and 1µg RNA were made up to 12µl with distilled water. This mixture was heat-inactivated at 70°C for 10 minutes, rapidly chilled on ice and spun down. 4µl of 5x first strand buffer, 2µl of 0.1M DTT and 1µl of 10mM dNTP mix were added and gently mixed and incubated at 42°C for 2 minutes. 1µl of 200units of Superscript II was added and mixed gently and incubated for 50 minutes at 42°C. The

reaction was terminated by heat-inactivation at 70° C for 15 minutes. The cDNA was stored at –20°C.

2.15.4 PCR

The polymerase chain reaction (PCR) is an in vitro technique, which allows the exponential amplification of a specific region of deoxyribose nucleic acid (DNA) by repeating a 3 step process of denaturation, annealing and synthesis.

2.15.4.1 Primer Design

A poorly designed primer can result in little or no product due to non-specific amplification and/or primer-dimer formation. Several variables must be taken into account when designing PCR Primers. Among the most critical are primer length, specificity, complementary primer sequences, G/C content and polypyrimidine (T, C) or polypurine (A, G) stretches and 3'-end sequence. It is important to take time at the beginning to optimise PCR conditions to ensure efficient amplification of PCR product. See table 9 for sequences of primers used in this study.

Specificity, temperature and time of annealing are partially dependent on primer length. In general, oligonucleotides between 18 and 24 bases are sequence specific if the annealing temperature is optimal. The optimal annealing temperature tends to be at least 50°C. The annealing temperature tends to be 5°C below melting temperature, therefore an optimal primer melting temperature (T_m) tends to be 55°C. The easiest way to find the best annealing temperature is by using a gradient thermal cycler.

Primers should have a unique sequence within the template DNA that is to be amplified. A primer designed with a highly repetitive sequence may result in a smear when amplifying genomic DNA

Primers need to be designed with no intra-primer homology beyond 3 base pairs. If a primer has a region of self-homology partially double-stranded structures can occur which will interfere with annealing to the template. Inter-primer homology may cause partial homology in the middle regions of two primers that can interfere with hybridization. If the homology occurs at the 3' end of either primer, primer-dimer formation may occur which could prevent the formation of the desired product due to competition.

Primers should have between 45% and 55% GC content. The primer sequence should be chosen so that there are no G or C stretches that can cause non-specific annealing. A and T stretches should also be avoided as they could open up stretches of the primer-template which can lower the efficiency of amplification. The addition of a G-C complex at the 3'end of a primer will ensure correct binding at the 3' end due to the stronger hydrogen bonding of G/C residues.

2.15.4.2 PCR analysis

For PCR analysis, primers that had previously been optimised in our laboratory were used. All primers were synthesised by Invitrogen (GibcoBRL, UK) and supplied as lyophilised samples. Each primer was reconstituted in sterile water to a stock concentration of 100μM. 2μl of cDNA from a 20μl reverse transcriptase reaction was added per 10μl PCR reaction. PCR amplification was carried out on a Perkin Elmer-Gene Amp 2400 thermal cycler (Perkin Elmer Ltd., UK).

A typical PCR reaction mixture contained 1x PCR reaction buffer, 1.5mM magnesium chloride, 0.2mM dNTP, 5U Red Hot Taq polymerase, 50% Glycerol, antisense primer, sense primer, distilled water and cDNA. All "thermal cycling" conditions started with a denaturation step at 94°C for 10 minutes and a final annealing step at 72°C for 5 minutes (table 9). β-Actin is present in all eukaryotic cells and was used as a PCR loading control, to confirm that RNA was present in equal concentrations in all samples.

Table 2.6: Primer Sequences And Their PCR Conditions

Name	Sequence 5'→3'	Cycling conditions	Cycle No	PCR product
AR S AR A	CGAAATGGGCCCCTGGATGGATAG AGTCGGGCTGGTTGTTGTCGTGTC	94°C for 30 sec 65°C for 30sec 72°C for 40sec	40	524bp
PSA S PSA A	ACTGCATCAGGAACAAAAGCGTGA CGCACACACGTCATTGGAAATAAC	94°C for 30 sec 65°C for 30sec 72°C for 40sec	40	362bp
Keratin 5 S Keratin 5 A	GGGGTGTCGGCCTAGGTGG ACTGCGGCACGGGAGACC	94°C for 30 sec 60°C for 60sec 72°C for 90sec	35	350bp
Keratin 14 S Keratin 14 A	GAGCCGCATTCTGAACGAG GTGCACATCCATGACCTTGG	94°C for 30 sec 60°C for 60sec 72°C for 90sec	35	525bp
Keratin 8 S Keratin 8 A	CAGCAGAAGACGGCTCGAAGC TCTCAGTCTTTGTGCGCCGC	94°C for 30 sec 60°C for 60sec 72°C for 90sec	35	538bp
Keratin 18 S Keratin 18 A	GACCGTGGAGGTAGATGCCCC CACTATCCGGCGGGTGGTG	94°C for 30 sec 60°C for 60sec 72°C for 90sec	35	544bp
5α- R2 A 5α-R2 S	CCACCCATCAGGGTATTCAG CCTTGTACGTCGCGAAGC	96°C for 90 sec 52°C for 60sec 72°C for 90sec	35	350bp
5α-R1 A 5α-R1 S	GTTGGCTGCAGTTACGTATTC TGCTGATGACTGGGTAACAG	96°C for 90 sec 52°C for 60sec 72°C for 90sec	35	170bp
β-Actin s β-Actin a	GCCGAGCGGGAAATCGTGCGTG CGGTGGACGATGGAGGGGCCG	94°C for 30 sec 60°C for 60sec 72°C for 90sec	35	266bp
GAPDH A GAPDH S	CCACCCATGGCAAATTCCATGGCA TCTAGACGGCAGGTCAGGTCCAC	94°C for 45sec 65°C for 45sec 72°C for 60sec	25	597bp

2.15.5 Gel Electrophoresis

Agarose gel electrophoresis was used to visualise PCR products. For PCR products, the amplified DNA was run on a 2% agarose gel in a horizontal gel tank (Hybaid, UK), using 1x TAE buffer. The required amount of agarose was dissolved in 1x TAE buffer in a microwave oven, cooled to 60°C, supplemented with 1μg/ml ethidium bromide, poured onto a gel plate and allowed to set at room temperature. DNA loading buffer (5x dilution in 1x TAE buffer) was added to the DNA samples prior to loading. The gels were loaded and run at 150volts for 1 hour and then viewed on a UV transilluminator. Images were captured using a Gel Documentation System (Quantity One software, Biorad Ltd., UK) and printed on thermal paper (Mitsubishi P91 thermal printer). Each gel was loaded with appropriate controls and with electrophoresis size markers, either φX174 DNA digested with Hae III marker or a 1kb DNA marker. The fragment size of these markers (in base pairs) were as follows:

φX174 DNA marker:	1353, 1078, 872, 603, 310, 281, 271, 234, 194, 118, 72
1kb DNA marker:	12216, 11198, 10180, 9162, 8144, 7126, 6108, 5090, 4072, 3054, 2036, 1636, 1018, 517, 506, 396, 344, 298, 220, 201, 154, 134, 75

2.16 APPENDIX: MATERIALS AND SOURCES

Company	Materials
Griffith & Nielsen	10ml, 25ml, 50ml pipettes
	2.5ml Pasteur pipette
	30ml Universal tubes
	5ml bijous tubes
Radleys	CLP 10µl, 200µl, 1000µl tips
	CLP aerosol barrier 10µl, 200µl, 1000µl tips
VWRI (Merck)	200µl, 500µl, 1.5ml tubes
	50ml polypropelene tubes
	15ml polypropelene tubes
	0.22µm sterile filters
	Nunc 60mm dishes
	Nunc 25cm^2 flasks
	Nunc 80cm^2 flasks
VWRI (Merck)	Nunc 6-well plates
	Nunc 24-well plates
	Nunc 96-well plates
	Agarose
	Formaldehyde
	Absolute Ethanol
	Methanol (Analytical grade)
	Acetone
	Giemsa's stain
	DPX mounting medium
	Formamide
	Glacial acetic acid
	Harris' haemotoxylin
	0.4% Trypan Blue

	Xylene
	Sodium hydroxide
	Chloros, a solution of sdium hypochloride
Invitrogen	DMEM medium
(Gibco BRL, Life Technologies)	RPMI-1640 medium
	10X Phosphate buffered saline (PBS)
	Opti-MEM 1 medium
	Keratinocyte-SFM medium + supplements
	L-Glutamine (0.2M sterile solution)
	10X Trypsin (2.5%)
	Versene
	100mm dNTPs
	Superscript II (RT-PCR system)
	Oligo dT (12-18 primer) (kit)
	1kb DNA marker
	φX174 DNA digested with Hae III marker
BioWhittaker	Clonetics prostate epithelial cell growth medium (PrEGM medium + supplements)
Imperial Laboratories Andover, Hants, UK	Foetal calf serum (Heat Inactivated)
AB Gene	Red Hot Taq DNA polymerase
(Advanced Biotechnologies)	10x PCR reagent buffer
	Magnesium chloride
Unichem	Hibiset
Sigma	MTT (3-4,5-dimethylthiazol-2-yl-2-diphenyltetrazolium bromide)
	5α-Dihydrotestosterone

	Collagenase Type 1A (C9891)
	EDTA
	Ethidium Bromide
	Mineral oil for PCR
	Formaldehyde
	Propidium iodide
	Sodium Azide
	Sodium chloride
	Saponin buffer
	DMSO
	Glycerol
	Hydrogen Peroxide
	Hoechst Stain
Vector Laboratories	Vectastain Elite ABC kit / DAB substances
	Antigen Unmasking Solution
	Haematoxylin Counterstain
	Vectashield Mounting Medium for Fluorescence (DAPI)
	Vectabond Reagent
Marathon Laboratory Supplies	Basement membrane matrigel
Dako	Dako Resin Pen
Becton Dickinson	MatriSpere Cell Release Solution
Qiagen	RNeasy Mini Kit
	QIAshredder
National Diagnostics	Histoclear

Stratech Scientific	Matrigel
	Matri Sphere Cell Recovery Solution
	Gelvatol
	DPX

CHAPTER 3

RESULTS

DERIVATION AND AUTHENTICATION AND PURITY

3.1 INTRODUCTION

Two new BPH cell lines, Pre2.8 epithelial and S2.13 stromal cells have been established using a construct containing a temperature sensitive SV40 large T antigen gene. This mutant viral gene produces a protein that is conformationally normal at permissive temperatures (33°C) and is conformationally inactivated at non-permissive temperatures (39°C) (Stamps et al., 1994). Consequently the cells should replicate under the influence of the LTAg at the permissive temperature, but at the non-permissive temperature, stop dividing and differentiate. This chapter describes the derivation of the cell lines. The presence of the viral gene was confirmed using immunocytochemistry.

Authentication is essential when a new cell line is established. It must be demonstrated that the cell line has been derived from the individual claimed. The cell line may be authenticated using DNA profiling (Masters et al., 2001), a method that measures the sizes of a number of alleles containing short tandem repeat (STR) sequences. The number of times the sequence is repeated varies from person to person. The STR profile of the two cell lines was compared with that of the patient from whom the cells were derived and shown to be identical.

Contamination of cell lines with microorganisms is a potential problem with tissue culture. Unlike bacteria, yeasts, fungi and moulds, mycoplasma can not be readily detected under the microscope. Mycoplasma exists parasitically with growing cells, mostly in parasite form, growing on the cell membrane and exerting a pathological effect on the host cell. These infections can alter DNA, RNA and protein synthesis, change enzyme patterns, interfere with the selection of mutant mammalian cells and modify the host cell's plasma membrane. Hence it is important to ensure that cell lines are free of mycoplasma. PCR was used to confirm the absence of mycoplasma.

3.2 DERIVATION OF PRE2.8 EPITHELIAL AND S2.13 STROMAL CELL LINES

3.2.1 Prostate Tissue

Human prostate tissue was obtained from a 71 year-old male with symptoms of BPH, undergoing transurethral resection of the prostate (TURP). A diagnosis of BPH was subsequently confirmed by histopathology. The biopsy was transferred to a 30ml Universal plastic container containing RPMI-1640 medium supplemented with 20mM HEPES, 5% fetal calf serum (FCS), 1% penicillin - streptomycin, 1% fungizone (Amphotericin B) and 1% L-glutamine. Some of the original biopsy was frozen for future analysis, such as DNA STR profiling. Remaining tissue was used to establish immortal cell cultures.

Ethical approval was obtained for all tissue used in these experiments and the correct process for obtaining tissue samples were adhered to. These experiments were covered under study number 98/0082: "development of conditionally immortalized cell lines from human prostate tissue", which was approved by t Joint UCL/UCLH committees on the ethics of human research.

3.2.2 Primary Culture

The tissue was minced into small fragments less than $1mm^3$ using crossed scalpel blades, rinsed twice in PBS and incubated in serum-free L-15 medium with 0.3% collagenase type 1A for 3.5h on a rotating platform. The partly digested tissue was filtered through 70 and 40μm filters and the filtrate was centrifuged. The cells were plated in prostate epithelial growth medium (PrEGM) medium in $25cm^2$ flasks and grown at 37.5°C with 5% CO_2. Primary cell cultures were transferred to safety level III for retroviral transduction, which was carried out by Professor Michael O'Hare, Department of Surgery, Middlesex Hospital. GMO (genetic modified organisms) risk assessments for this work were completed by personnell within the Department of Surgery. Potentially immortalised cell cultures established and returned to our department, by Professer M O'Hare were no longer under safety level III risk. They were rendered safe to work with and were transferred to the safety level II tissue culture laboratory.

3.2.3 Transduction

Semi-confluent proliferating cultures (labelled LWE0) were exposed to filtered (0.4μm) supernatants from the retroviral packaging line, Clone8/8PB (a clone of the virus-producing cell line that was selected with 0.5mg/ml G418). The retroviral construct consisted of a defective SV40 oncogene, pZipSVtsa58 plasmid (figure 1.5). Infection was carried out for 18h with 8μg/ml polybrene and cells were grown to confluency. Infected cells were selected with 0.5mg/ml G418. Infection and selection was carried out at 33.5°C. Successful growth of epithelial-type cells was obtained.

3.2.4 Development Of Epithelial Cell Line (Pre2.8)

A semi-confluent monolayer of epithelial-like cells was obtained approximately 3 weeks after G418 had been withdrawn. These cells (passage 1) were split into two tissue culture flasks ($25cm^2$) and grown at 33°C. When these cells were semi-confluent, one flask of cells was frozen (briefly, PBS wash, trypsin, aspirate off, 10% DMSO in medium, frozen on dry ice) and the remaining cells were passaged as passage 2 (p2) at 1:2, 1:4 and 1:8 dilutions in PrEGM medium at 33°C. As these cells became confluent, growth slowed and many of the cells developed a squamous phenotype (large flat cells with a tendency to lift off the substrate).

In addition to the passaging on plastic, passage 1 cultures were also split at a 1:200 dilution on irradiated mouse 3T3 cells, as clone 1 passage 0 (cl1p0). The mouse 3T3 cells are used as a feeder layer, providing growth factors and extracellular matrix support for clonal growth of epithelial cells. See figure 3.1 for summary of derivation of Pre2.8 cells.

3.2.5 Development Of Stromal Cell Line (S2.13)

The cells grown on 3T3 feeder layers had both epithelial and stromal phenotypes. Surplus cells from cl1p0 were replated as cl1p1 at dilutions of 1:2 and 1:4 without feeders in PrEGM medium. After approximately 2 months the Cl1p1 cells had grown enough to freeze the 1:2 dilution flask. Cells from the 1: 4 dilution flask were differentially trypsinised to rapidly detach the stromal cells, leaving the epithelial cells attached to the dish. The stromal cells were replated as p2 in DMEM/FCS, in $12.5cm^2$ flasks. See figure 3.2 for summary of derivation of S2.13 cells.

Figure 3.1: Derivation Of Pre2.8 Cells

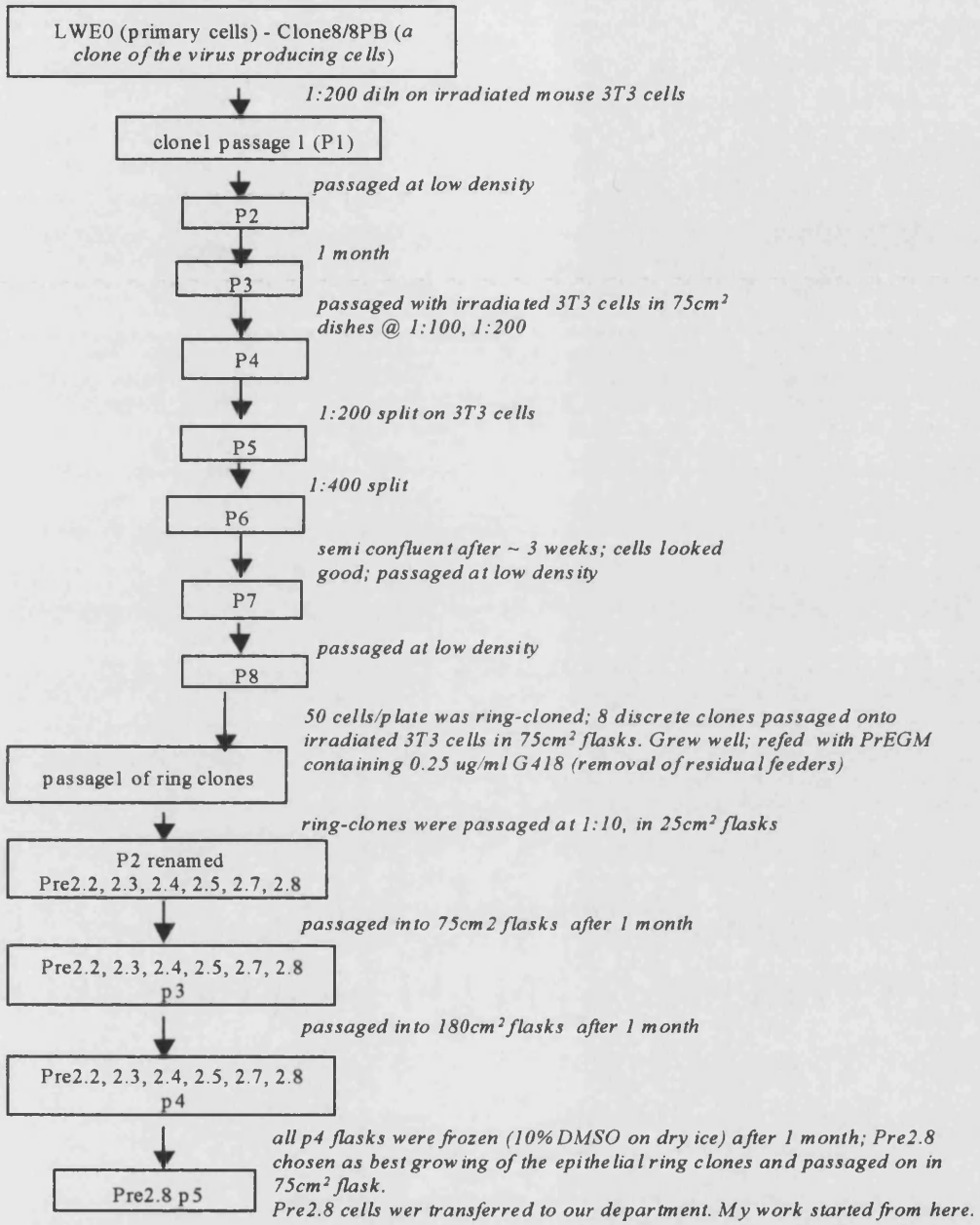

Figure 3.2: Derivation Of S2.13 Cells

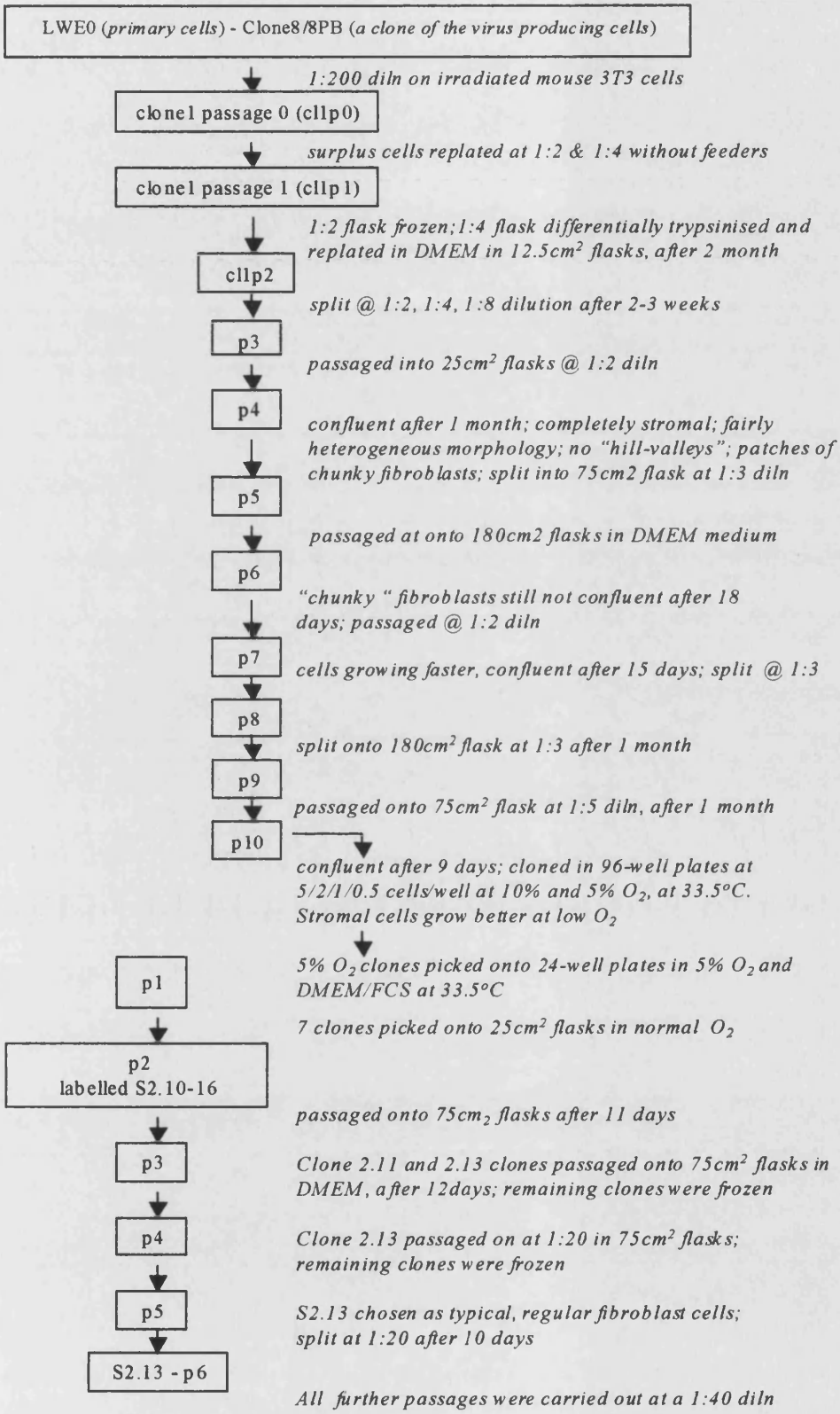

3.3 MORPHOLOGY OF LIVING CELLS

3.3.1 Pre2.8 Cells

Pre2.8 prostate epithelial cells were grown as a monolayer on plastic at 33°C, 37°C and 39°C. PrEGM medium (table 2.1 and 2.2) was used for growing prostate epithelial cells (Fry et al., 2000b). The epithelial cells, Pre2.8, attach slowly to the surface of culture plates and are relatively slow growing cells. At 33°C and 37°C the cells are small, tightly compact and irregular in shape with a cobblestone appearance (figure 3.4). When cells are transferred to 39°C the morphology alters. The cells become irregular in shape, no longer grow as tightly compact cells, and increase in size.

Figure 3.4 Morphology Of Pre2.8 Cells

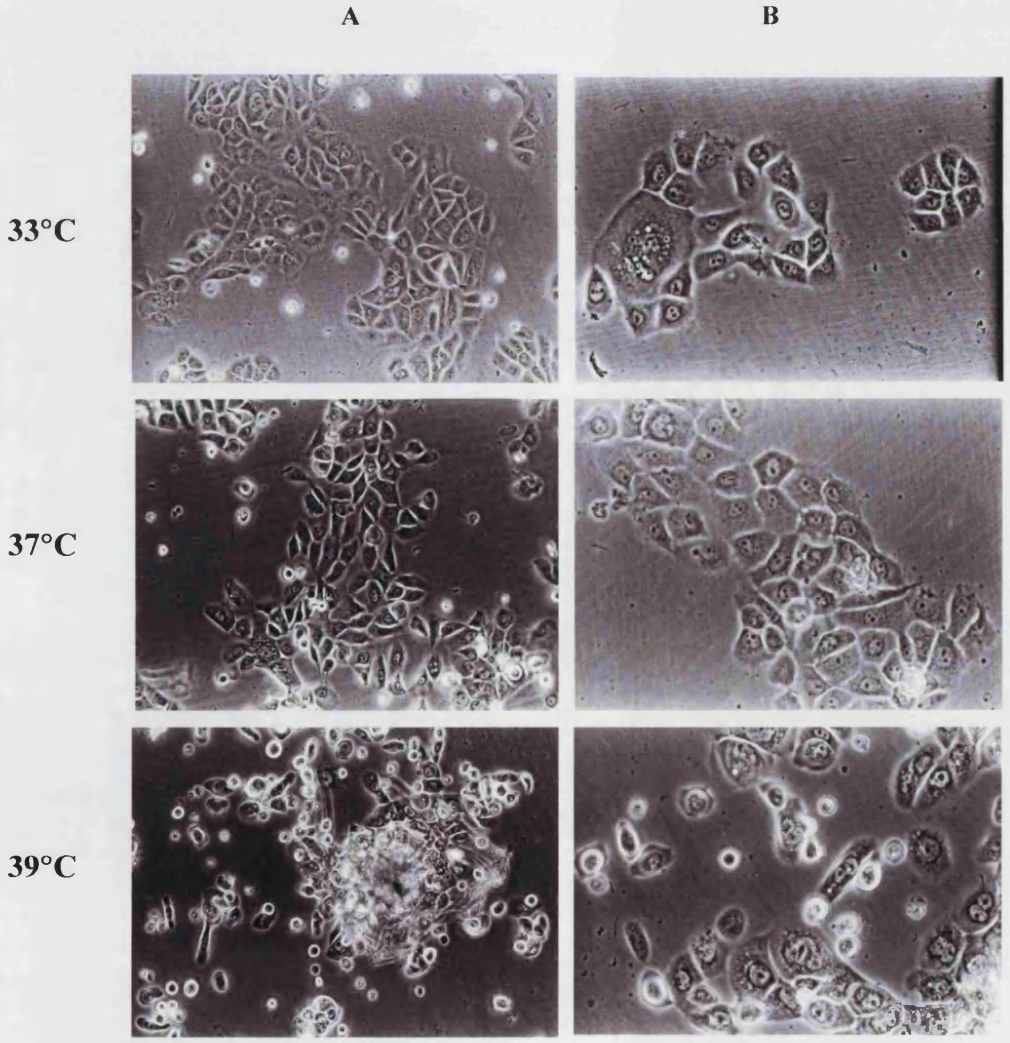

Day 6 Pre2.8 epithelial cells growing on plastic tissue culture flasks, at seeding densities of 200,000 cells/T25 flask, at 33°C, 37°C and 39°C.

Phase contrast microscopy; Original magnification: (A) x200 and (B) x400

3.3.2 S2.13 Cells

S2.13 prostate stromal cells were grown as a monolayer on glass coverslips at 33°C, 37°C and 39°C. RPMI/FCS (table 2.1 and 2.2) was used for growing prostate stromal cells. The stromal cells, S2.13, rapidly attach to the surface of culture plates and are fast growing cells relative to Pre2.8. They are slightly elongated in appearance, which is more pronounced at 37°C and 39°C than at 33°C and are loosely associated until they become confluent (figure 3.5).

Figure 3.5: Morphology Of S2.13 Cells

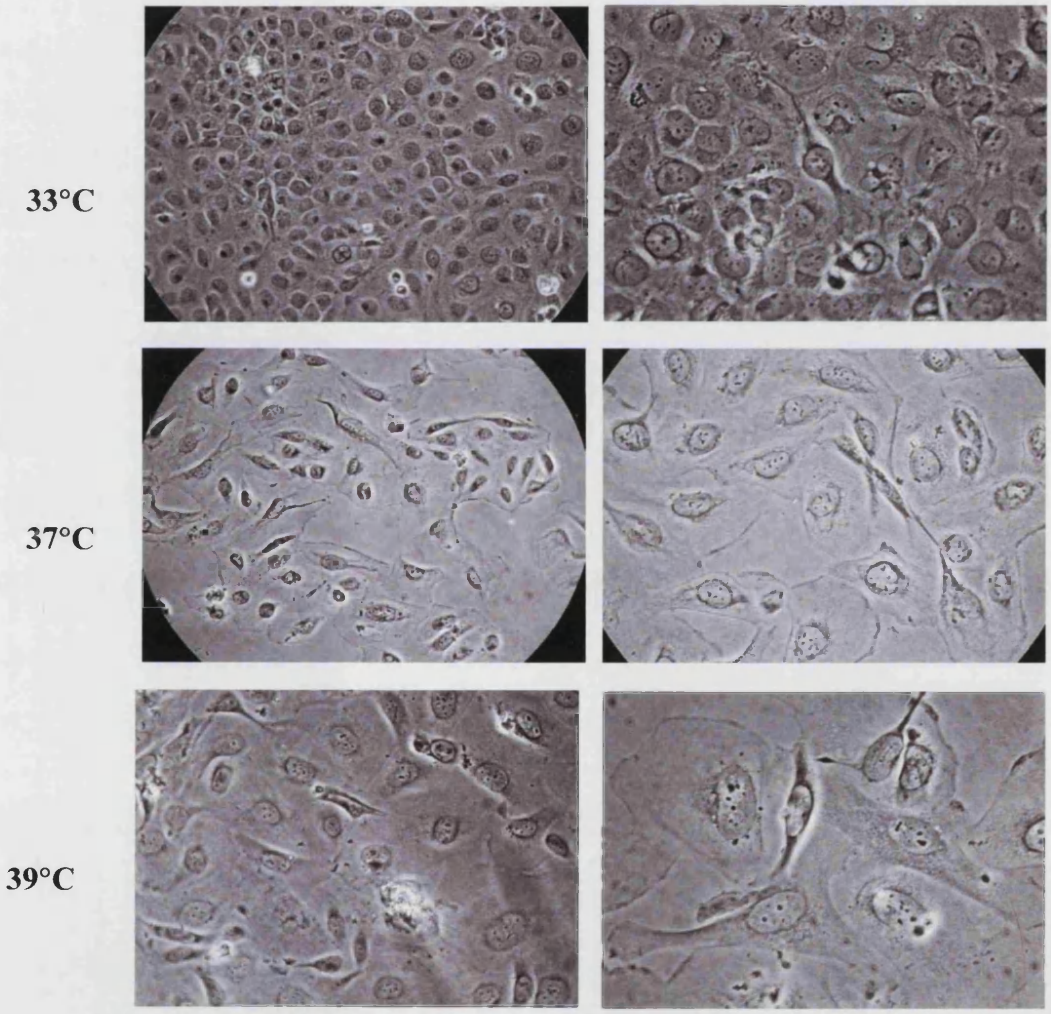

Day 4 S2.13 stromal cells grown on coverslips, at seeding densities of 40,000 cells/coverslip, at 33°C, 37°C and 39°C. Original magnification (A) x200 and (B) x400

3.4 PRESENCE OF SV40 LARGE T-ANTIGEN

Immunocytochemistry for Large T antigen (LTag) was carried out to confirm the presence of SV40 large T-antigen. Using DAB, Large T-antigen shows brown nuclear staining. Pre2.8 and S2.13 cells expressed SV40 large T antigen at 33°C (figure 3.6).

Figure 3.6: Pre2.8 And S2.13 Large T Antigen Expression

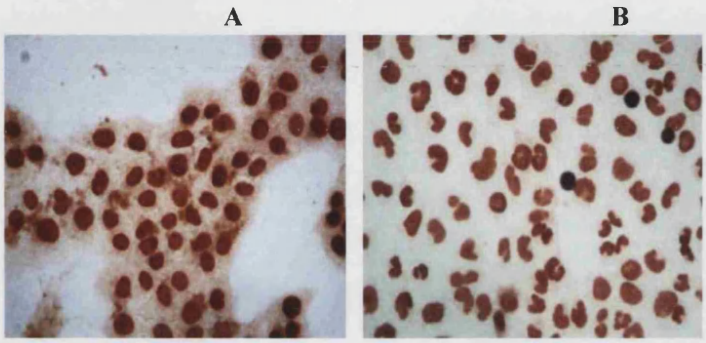

SV40 expression of Pre2.8 at 33°C (A) and S2.13 cells at 33°C (B). Immunocytochemistry shows positive staining of LTag (brown). Original magnification of A and B was x200

3.5 DNA PROFILING

DNA profiling was carried out on Pre2.8 and S2.13 cells and the tissue of origin by the LGC (Laboratory Government Chemist, Teddington, Middlesex) to confirm the origin of these cells from the individual who provided the BPH tissue.

DNA profiling was carried out by amplification of STR (short tandem repeats) regions using the Second Generation Multiplex (SGMPlus) System (United Kingdom Forensic Science Service). The number of repeats at each locus was determined by electrophoresis of the PCR products and analysed using Perkin Elmer Genescan andGenotyper computer software. STR profiling consisted of a number of primers for the loci, D18S51, D21S11, D8S1179, HUMFIBRA (FGA), HUMTHO1, HUMVWFA31/A and the sex chromosome marker amelogenin, HUMAMGX/Y (see table for description of markers).

The same STR profile was found for Pre2.8 and S2.13 cells, which was identical to DNA of the patient they were derived from (table 3.1). The three samples were heterozygous for D18S51 and D21S11, and homozygous for HUMAMGX/Y, D8S1179, HUMFIBRA (FGA), HUMTHO1 and HUMVWFA31/A loci.

	STR locus name and allele designation									
Source	*Sex marker ch Amelogenin, HUMAMGX/Y (Xp22.1-22.3 & Yp11.2)*		*D18S51 (18q21.3)*		*D21S11 (21q11.2-1q21)*		*D8S1179 (Ch 8)*	*α Fibrinogen, HUMFIBRA (4q28)*	*HUMTHO1 (11p15.5)*	*(Von Willebrand factor, vWA) HUMVWFA31/A (12p12pter)*
	Amg_1	Amg_2	D18_1	D18_2	D21_1	D21_2	D8_1	FGA_1	TH_1	VW_1
DNA from Pre2.8 Cell Line	X	Y	12	14	29	30	13	20	9	17
DNA from S2.13 Cell Line	X	Y	12	14	29	30	13	20	9	17
DNA from original Patient Tissue	X	Y	12	14	29	30	13	20	9	17

3.6 MYCOPLASMA SCREENING

Pre2.8 and S2.13 cells were negative for mycoplasma using both the Coriell PCR and the Drexler nested PCR. See figures 3.7, 3.8, 3.9 and 3.10 for results. Reagent only controls were negative and the expected size bands were present for positive controls (in-house control, KK47) in all PCR analyses, 500bps for Coriell PCR, 500-520bp for round 1 Drexler PCR and 310-330bp for round 2 Drexler PCR. The Drexler nested PCR sometimes produces two bands in round II, a 500bp – 520bp band being the outer primer product of round I and a 310bp – 330bp band being the inner primer product of the second PCR round. PCR results are shown in figure. All samples were carried out in duplicate.

The mycoplasma contaminating the positive control, KK47 is one of the 5 most common mycoplasma associated with cell line infections, Acholeplasma laidlawii. This was determined using the Stratagene multiplex PCR kit, producing a 280bp and a 100bp PCR fragment. The Stratagene kit was used to determine mycoplasma species when positive samples were detected using the Coriell and Drexler PCR screening procedures.

Figure 3.7: Coriell PCR Results For Pre2.8 Cells

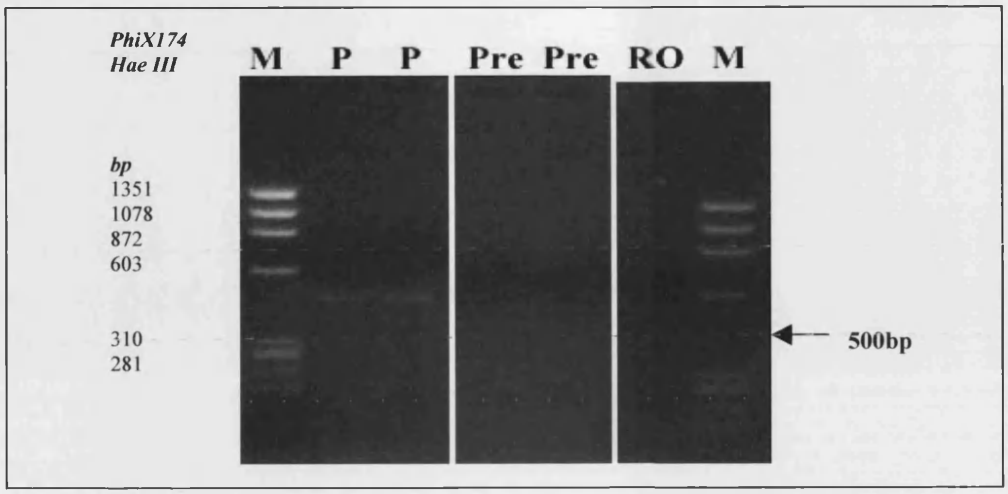

Figure 3.8: Drexler PCR (Round I And II) Results For Pre2.8 Cells

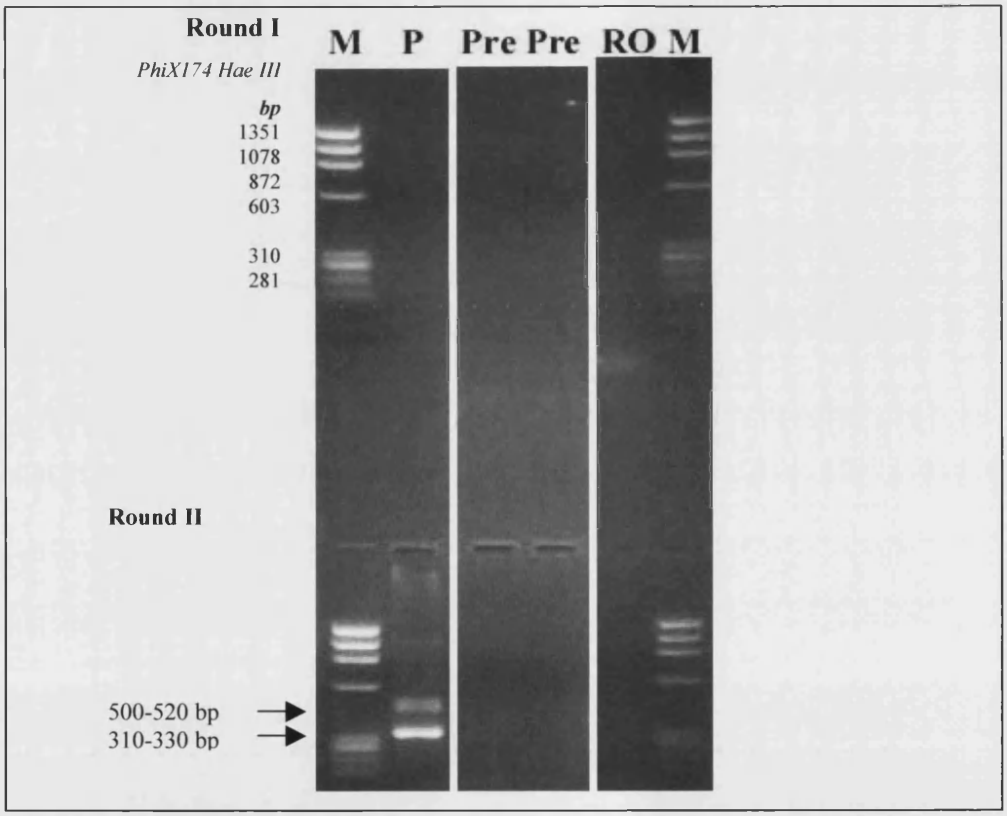

Duplicate Pre2.8 and control DNA PCR products run on a 3% agarose gel, after amplification with Coriell PCR primers (fig. 3.7) and Drexler nested PCR primers (fig. 3.8). Product size determined against a known DNA marker (M), phiX174 Hae III. In-house positive (Pos), KK47 and reagent only controls were used. The in-house positive control is a mycoplasma contaminated, human bladder-cancer cell line, KK47 which was previousely used in our laboratory. The letters representing each lane are M (marker), P (positive control), Pre (Pre2.8 cells) and RO (reagent only). Although the positive controls in figure 3.7 are a bit faint the test is repeated with the Drexler nested PCR, producing strong positive bands and confirming a negative result for the test samples. **NOTE:** Pre2.8 test samples and controls shown in figure 3.7 and figure 3.8 are from the same gel. These large gels also contained other test samples from different cell lines. They were removed in order to avoid any confusion.

Figure 3.9: Coriell Results For S2.13 Cells

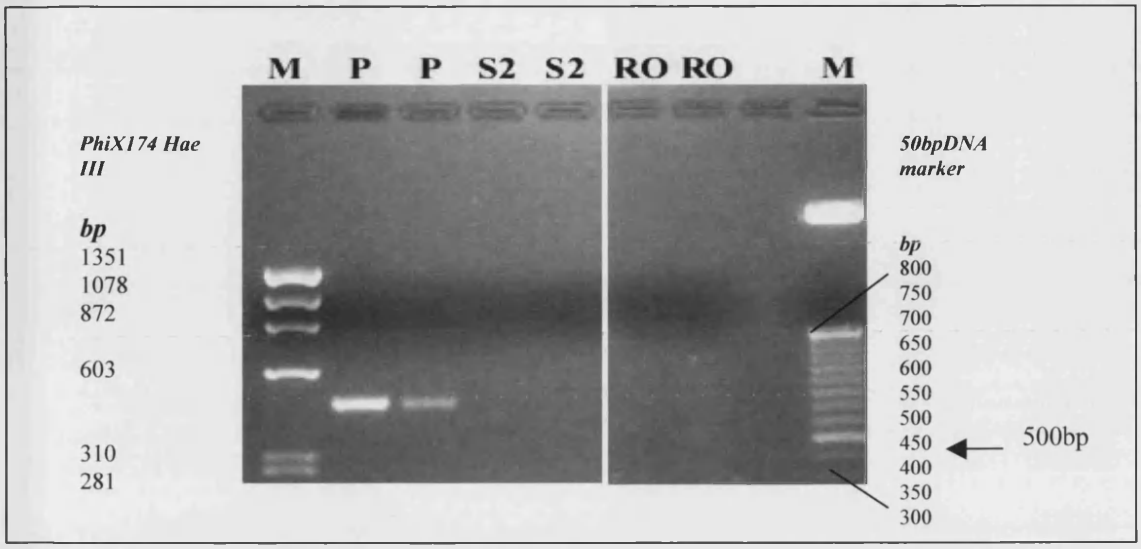

Figure 3.10: Drexler PCR (Round I And II) Results For S2.13 Cells

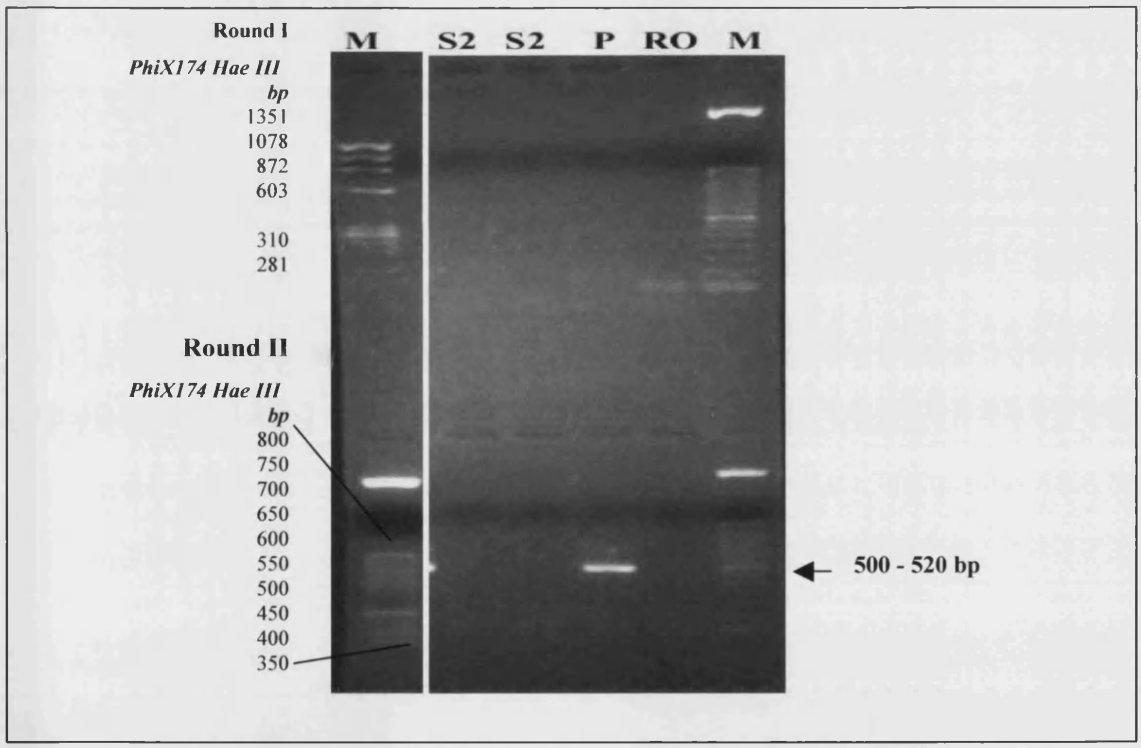

Duplicate S2.13 and control DNA PCR products run on a 3% agarose gel, after amplification with Coriell PCR primers (fig. 3.9) and Drexler nested PCR primers (fig. 3.10). Product size was determined against a known DNA marker (M), phiX174 Hae III and a 50bp marker (fragments every 50bps). In-house positive (Pos), KK47 and reagent only controls were used. The in-house positive control is a mycoplasma contaminated, human bladder-cancer cell line, KK47 which was previousely used in our laboratory. The letters representing each lane are M (marker), P (positive control), S2 (S2.13 cells) and RO (reagent only). The band observed for reagent only in fig. 3.10 was seen in the first round of the nested PCR (samples were negative) but not in the second round. **NOTE:** S2.13 test samples and controls shown in figure 3.9 and figure 3.10 are from the same gel. These large gels also contained other test samples from different cell lines. They were removed in order to avoid any confusion.

CHAPTER 4

RESULTS

CHARACTERISATION

4.1 CYTOGENETICS

Cytogenetic analysis was carried out by Dr Rod McLeod (DSMZ, Braunschweig, Germany) using slide preparation trypsin G-banding (GTG) and fluorescence in situ hybridisation (FISH). Dr Rod McLeod provided all of the Cytogenetic results and photography. Pre2.8 (passage 50) and S2.13 (passage 14) cells displayed significant cell-to-cell variation and some cells carried numerical and occasional structural rearrangements additional to those described in the consensus karyotypes, described `below.

4.1.1 Pre2.8 Cells

46<2n>X, -Y, +5, i(8)(q10)x1-2, der(9) (9qter→p11::4q25→q33::8p10→pter), der(14)ins(14;20)(p12;q1), der(15)t(10;15)(q25;p11), der(20)dup ins(20;14)(q11q13;p12), der(21)(qter→p11::4q11→q25:)

4.1.2 S2.13 Cells

93-97<4n>XXYY/XXYYY, +Y, der(2)t(2;16)(p25;p12), +3, der(3)(3qter→p11::ish20 (wcp20+) ::19q10→qter::19q10→qter::hsr::10q24→qter), der(3)t(3;10)(p24.2;q24.2), der(3)t(3;17)(q27;q23.), +4, +5, -8, der(8)(8pter→q24::hsr::5q23→qter), +9, +14, +14, +15, +17, +18, der(19)(19pter→q11::hsr), +20, i(20)(p10) + mar.

The chromosome structures of both cell lines carry relatively few changes, although both are dominated by rearrangements leading to amplification of chromosome 20.
GTG karyotypes representing typical metaphase chromosome spreads from Pre2.8 and S2.13 are presented in figures 4.1 and 4.2 respectively.

Pre2.8 cells displayed a near diploid karyotype with mostly straightforward numerical and structural rearrangements, including loss of the chromosome Y and formation of an isochromosome for the long arm of chromosome 8, i(8q). In addition, however, genomic amplification of part of chromosome 20 had been generated via a pair of apparently related rearrangements. GTG staining properties (figure 4.1) show material derived from the long arm of chromosome 20 inserted into the short-arm (p12) region of one chromosome 14, together with partial duplication of one chromosome 20 homolog (figure 4.3). Demarkating this duplication was a short piece of material from chromosome 14 (figure 23 inset) shown to be derived from p12, by silver staining and specifically detects the rDNA repeat clusters present at the p12 regions of the

acrocentric chromosomes. These findings imply that both der(14) and der(20) changes had participated in a complex non-reciprocal exchange resulting in a net increase of material derived from chromosome 20q. A second complex change involved redistribution of material covering 4q among two markers, der(9) and der(21).

The karyotype of S2.13 was hypertetraploid and in addition to numerical and several minor structural changes included three highly complex marker chromosomes bearing sizeable homogeneous staining regions (HSR), add(3)(p11), add(8)(q24) and add(19)(q11) (figure 4.2 arrows). The HSR in these markers appeared dissimilar in G-banded preparations and FISH analysis and showed all three to derive from distinct intercalary (inserted between) gains of material, in each case from chromosome 4, 19 and 20 (figure 4.4), terminating in two of these markers with segments deriving from chromosome 5q and 10q. FISH analysis showed that the most intense signals were those detected by the chromosome 20 probe. Comparison of FISH images (figures 4.3 and 4.4) revealed decidedly greater amplification in S2.13 than in Pre2.8 cells.

Summary

Cytogenetics of Pre2.8 and S2.13 cell lines exhibited multiple rearrangements, although amplification of material from chromosome 20 was the most striking change in both cell lines. Genetic instability is common in cell lines due to immortalisation procedures, but genetic instability is also associated with tumorigenesis. The amplification of material within HSR in tumor cell lines can imply selective amplification targeting genes, particularly oncogenes. Mechanisms underlying HSR formation is poorly understood, but may implicate unstable repeat DNA sequences susceptible to slippage (Macleod et al., 2000). Other research groups have associated isochromosome formation in chromosome 8 (i(8)) and alterations in chromosome 20q, particularly gain of chromosome 20 have been associated with many cancer types including prostate, bladder, melanoma, colon, pancreas and breast (Brothman et al., 1990; Richter et al., 1998; Bastian et al., 1998; Korn et al., 1999; Mahlamaki et al., 1997). It may be useful to repeat this analysis at a later passage level in order to show cell stability and to determine if passaging produces further chromosomal alterations.

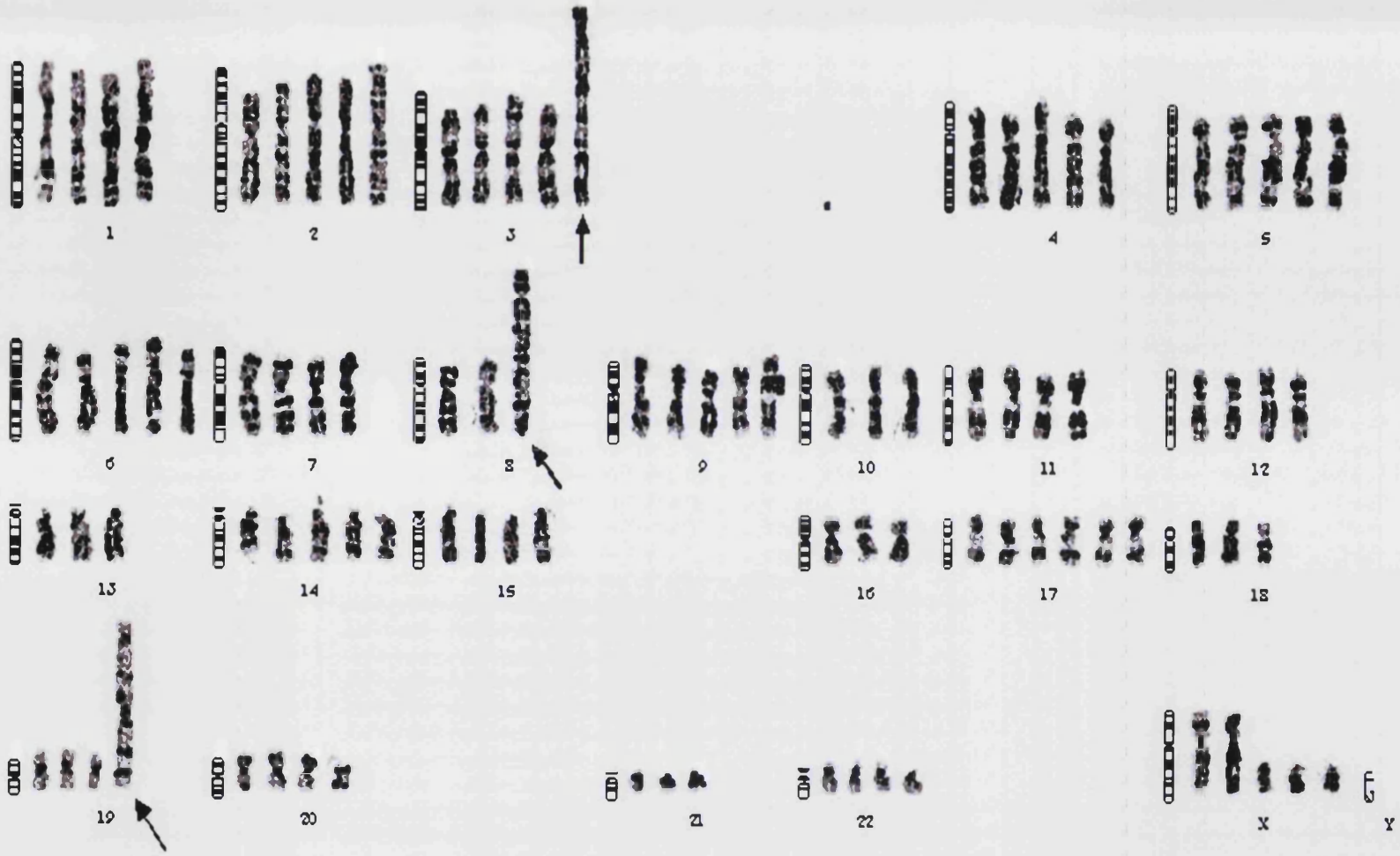
1
2
3
4
5
6
7
8
9
10
11
12
13
14
15
16
17
18
19
20
21
22
X
Y

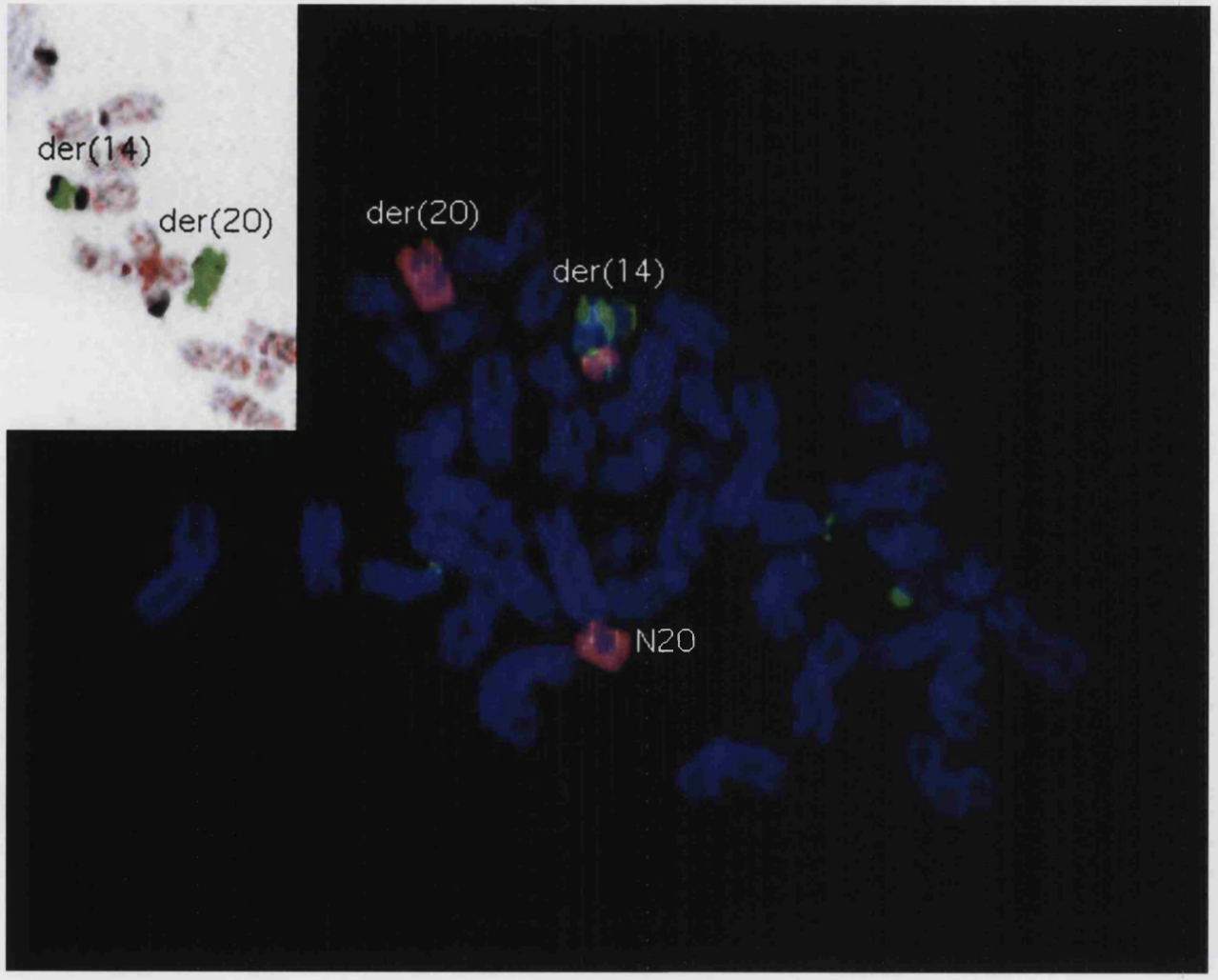
der(14)
der(20)
der(20)
der(14)
N20

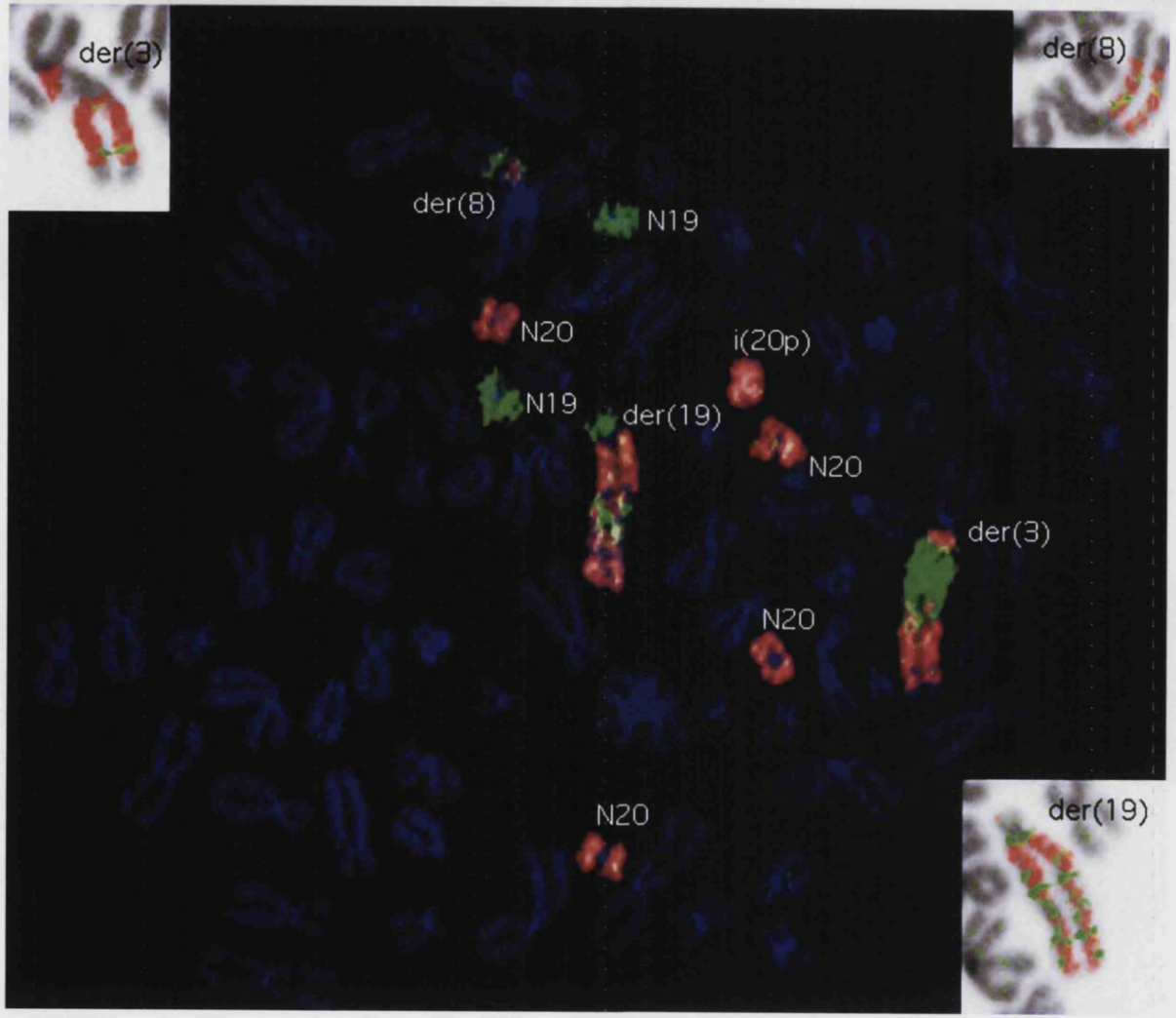
der(3)
der(8)
der(8)
N19
N20
i(20p)
N19
der(19)
N20
der(3)
N20
N20
der(19)

4.1.3 Figure Legend For Figure 4.1, 4.2, 4.3 and 4.4

Cytogenetic analysis showing amplification of chromosome 20. Dr Rod McLeod (DSMZ, Braunschweig, Germany) provided all of the Cytogenetic analysis and photography.

Karyograms illustrating dominant clones present in Pre2.8 (figure 4.1, 4.3) and S213 (figures 4.2 and 4.4) cell lines where rearrangements leading to amplification of chr.20 are indicated by large arrows.

The main colour figures show FISH analysis with probes for chr. 20 (red fluorescence) together with chr.14 (green fluorescence) in figure 4.3 and chr. 19 (green fluorescence) in figure 4.4, however the inset in figure 4.3 shows chr. 20 hybridised with green fluorescence.

The markers are indicated as follows: in Pre2.8 cells (figure 4.3), ders(14) / (20) (red and yellow arrows, respectively); and in S2.13 cells (figure 4.4), ders(3) / (8) / (19) (red, yellow and green arrows, respectively).

Interestingly both Pre2.8 and S2.13 utilise intercalary chromosomal material (co-amplification) to facilitate amplification of chr. 20 rDNA (shown black, inset figure 4.3) and material derived from chr. 19 (green fluorescence in figure 4.4) together with material from chr. 4 (data not presented).

FISH analysis and immunodetections were performed according to manufacturers' protocols and slides counterstained using DAPI. Monochrome FISH images were captured, merged and enhanced using Vysis Quips imaging system (Applied Imaging, Sunderland UK) configured to a Zeiss Axioplan microscope equipped with a Ludl filterwheel using narrow bandpass filters.

4.2 CELL PROLIFERATION

Analysis of cell cycle distribution was carried out for Pre2.8 cells initially using propidium iodide staining and Flow Cytometry analysis to determine the percentage of cells at G1, S (proliferating cells) and G2/M phases. In order to clarify flow cytometry results, immunocytochemistry for Ki-67, proliferation-associated antigen was carried out and quantified to determine percentage of cells proliferating at 33°C, 37°C and 39°C.

4.2.1 Flow Cytometry

Consistent results were not obtained for repeated FACS analysis of PI stained cells at 33°C, 37°C and 39°C. Experiments were repeated 3 times and once by a second party. 10,000 events (cells) were analysed for the initial experiment, while 20,000 events were analysed for remaining experiments (including the example shown in table 4.1 and figure 4.5). This inconsistency may be due to loss of larger, differentiated cells not getting through the capillary tube or to inaccurate gating caused by greater amounts of granularity at 39°C. It was difficult to accurately gate between G1, S and G2/M phases. An example given (table 4.1 and figure 4.5) shows that there was no clear variation in percentage of Pre2.8 proliferating cells at the three temperatures. In this example cell population was gated for G1-phase and G2 and S phases together.

4.2.2 Ki-67 Expression

Pre2.8 cells were grown on coverslips at a seeding density of $1x10^5$ cells per well at 33°C, 37°C and 39°C and stained with Ki-67 antibody after 4 days in culture. Total number and Ki-67 positive cells were counted from 3-4 coverslips at 33°C and 37°C, while 5-7 coverslips were counted at 39°C due to fewer cells per coverslip at this temperature. The average of these cells were calculated. This assay was repeated 3 times, the average and standard error calculated (table 4.2) and a histogram (figure 4.6) of percentage Ki-67 positive Pre2.8 cells obtained (photograph in figure 4.7).

There is a 60% decrease in growth when Pre2.8 cells are transferred from 33°C (93% proliferating cells) to 37°C (26% proliferating cells) and a further 10% decrease at 39°C (15% proliferating cells).

4.2.3 Summary

Results from PI stained cells using flow cytometry were unreliable with this cell line in comparison to counting of Ki-67 stained Pre2.8 cells. Proliferation is being switched off at 37°C and to a greater extent at 39°C.

It would be of interest to compare the substantial Pre2.8 proliferating population with the original tissue and with S2.13 cells, at a later stage (were mainly concentrating on characterisation of Pre2.8 cells in the time allowed for this thesis).

Table 4.1: Percentage Of Cells In G1 And G2/S Phases Of Proliferation In Pre2.8 Cells

Cell Proliferation	33°C	37°C	39°C
G1 Phase	59%	77%	55%
G2/S Phase	25%	18%	35%

One example of Pre2.8 cells from 33°C, 37°C and 39°C which were fixed and stained with propidium iodide (PI) and analysed on a Fluorescent Activated Cell Sorter (FACS) for percentage of cell proliferation, S-phase of the cell cycle.

Table 4.2: Percentage Of Ki-67 Positive Pre2.8 Cells

Cell Population	33°C	37°C	39°C
Ki-67 positive	420	174	58
Ki-67 negative	38	468	296
Total number	458	641	354
% Ki-67 positive (±SE)	93±2	26±2	15±2

Ki-67 immunocytochemistry of Pre2.8 cells, grown on coverslips at 33°C, 37°C and 39°C. Three separate assays were carried out and each assay consisted counts on 3-4 coverslips at 33°C and 37°C, and 5-7 coverslips at 39°C. Mean and standard error (SE) for each cell population, and percentage Ki-67 positive cells with standard error (SE) are displayed in table.

Figure 4.5: Percentage Of Cells In G2/S Phases Of Proliferation In Pre2.8 Cells

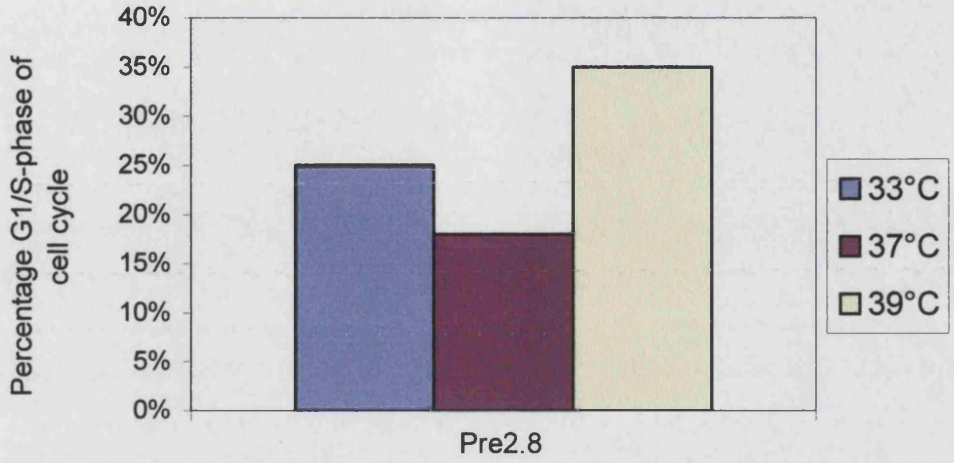

One example of Pre2.8 cells from 33°C, 37°C and 39°C which were fixed and stained with propidium iodide (PI) and analysed on a Fluorescence Activated Cell Sorter (FACS) for percentage of cell proliferation, S-phase of the cell cycle. No error bars are present, as this is just one example and not an average of a number of experiments.

Figure 4.6: Percentage Of Ki-67 Positive Pre2.8 Cells

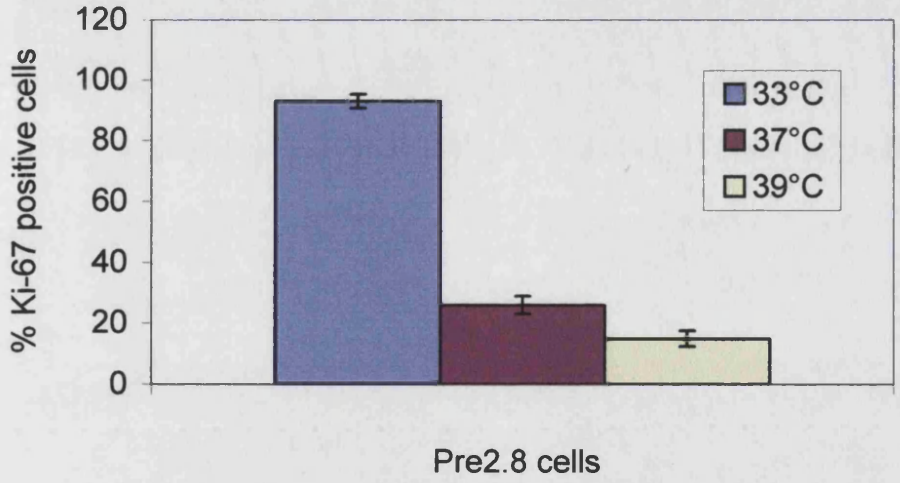

Histogram showing percentage of Ki-67 positive Pre2.8 cells with standard error (SE). Immunocytochemistry of Ki-67 antibody was carried out on Pre2.8 cells, grown on coverslips at 33°C, 37°C and 39°C. Three separate assays were carried out and each assay consisted counts on 3-4 coverslips at 33°C and 37°C, and 5-7 coverslips at 39°C. Mean and standard error (SE) for each cell population, and percentage Ki-67 positive cells with standard error (SE) are displayed in table.

Figure 4.7: Ki-67 Expression In Pre2.8 Epithelial Cells At 33°C, 37°C And 39°C

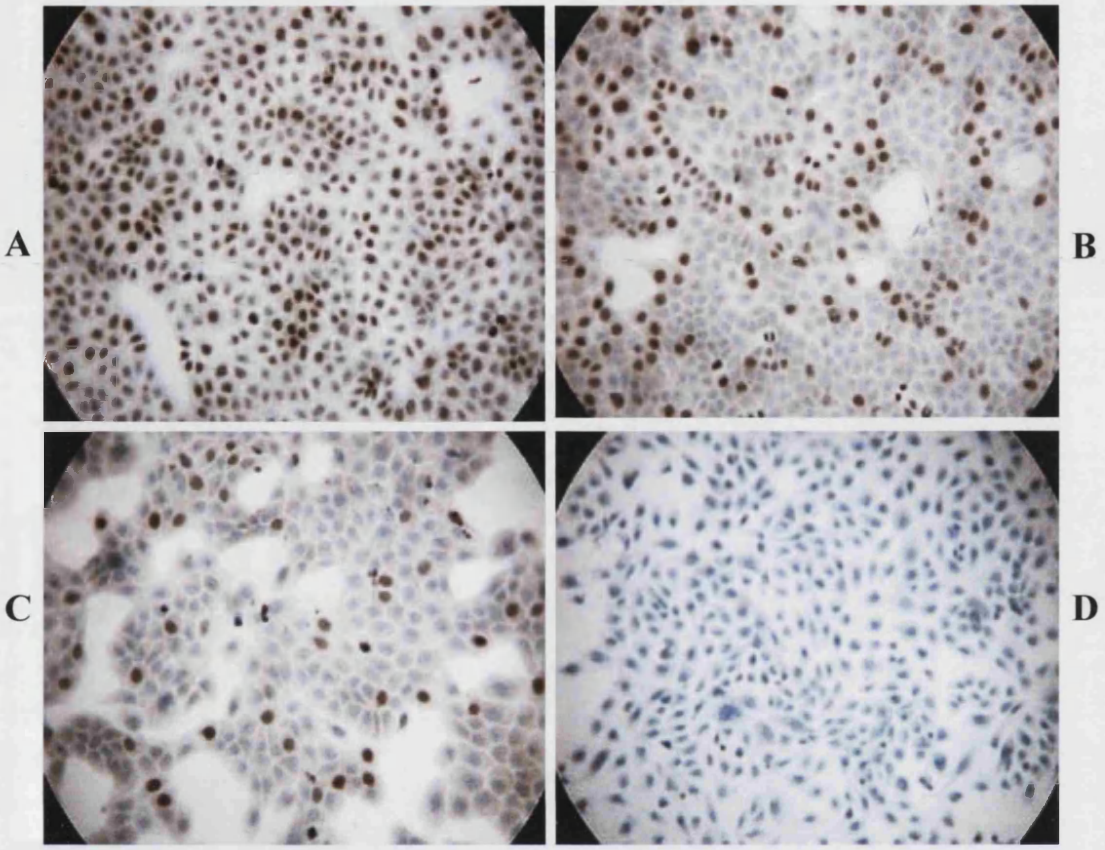

Immunoperoxidase stain of Pre2.8 cells at 33°C (A), 37°C (B) and 39°C (C) showing positive staining of the proliferative marker Ki67. Experiments were setup on coverslips with a seeding density of $1x10^5$ cells per well for each temperature and harvested for Ki67 staining at day 4. Negative (secondary antibody only) control (D) was setup using a coverslip from 33°C.

Ki67 stain – DAB/peroxidase (brown); Nuclear stain –Hoechst (blue)

Magnification: original magnification x20

4.3 GROWTH RATES

Growth curves were constructed by plating 100,000 cells per 25cm^2 flask in triplicate. Cell numbers were estimated at 2-3 day intervals up to 17 days using a haemocytometer (table 4.3 and figure 4.8).

4.3.1 Pre2.8 Growth Assays Using Cell Counts

Pre2.8 cells grow at a similar rate at 33°C and 37°C for the first 11 days. At 37°C cell numbers plateau after 11 days, while at 33°C cell number continues to increase exponentially. At 39°C, proliferation continued over the 17-day culture period at a slow rate.

Table 4.3: Proliferation Of Pre2.8 Cells, Showing The Mean And Standard Error Of Cell Numbers Derived From Three Independent Experiments

Days in Culture	Cell Number x 10^5 (±SE)		
	33°C	37°C	39°C
3	1.04 ± 0.09	1.77 ± 0.38	0.54 ± 0.06
5	2.56 ± 0.48	8.13 ± 0.33	0.78 ± 0.25
7	7.85 ± 3.02	18.03 ± 1.33	1.50 ± 0.60
10	21.72 ± 4.86	24.34 ± 2.47	1.87 ± 0.25
12	32.08 ± 4.01	30.01 ± 4.35	2.85 ± 0.60
14	38.98 ± 7.12	29.17 ± 6.43	3.39 ± 0.64
17	52.37 ± 3.27	26.67 ± 2.91	3.67 ± 0.63

4.3.1.1 Mean Population-Doubling Time for Pre2.8

The mean population doubling for Pre2.8 cells, derived from growth curves using a logarithmic scale was 36 and 24 hours, at 33°C and 37°C respectively. Cells do not grow exponentially at 39°C. Figure 4.9, below shows extrapolation of data from the exponential phase of a log curve of Pre2.8 cells.

Figure 4.8: Growth Curve Of Pre2.8 Prostate Epithelial Cells

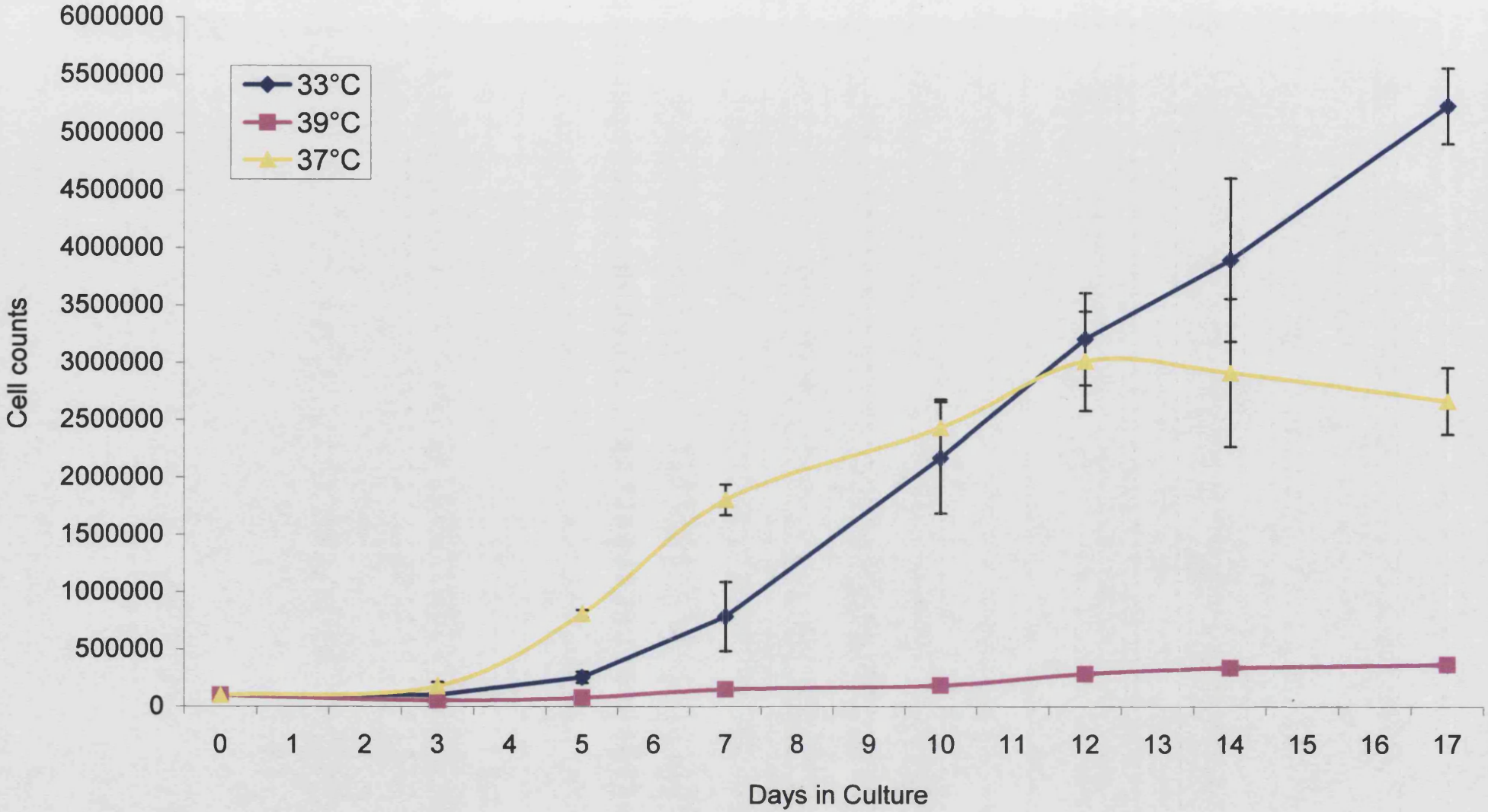

Pre2.8 cell counts for 3 separate growth assays, at 33°C, 37°C and 39°C. Cells were set up in triplicate at a density of 100,000 cells per 25cm^2. The mean and standard error were calculated and a growth curve was obtained.

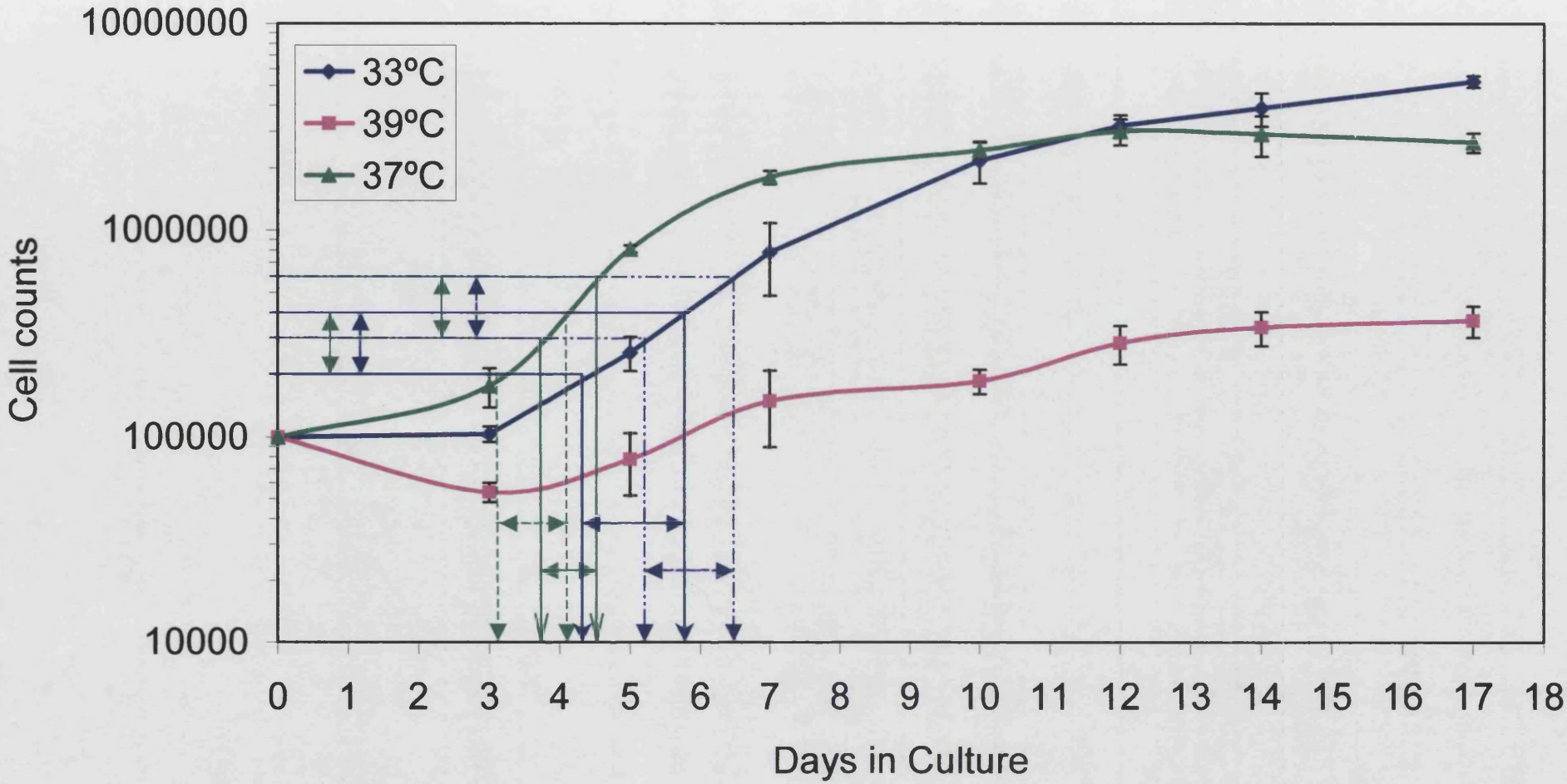

Log plot of the increase in cell concentration (y-axis) versus days in culture (x-axis), following subculture from cultures counted on regular intervals. The population-doubling time (PDT) was extrapolated from the straightest area of the exponential phase. A straight line was drawn from a particular cell count, on the y-axis in the log phase, to the plotted line. Then another straight line was drawn from a point that was double the first cell count on the y-axis to the plotted line. These two lines were then continued from the plot towards the x-axis in a straight line. The distance between these two points on the x-axis represents the length of time for one cell population to double. This was carried out at 33°C, 37°C and 39°C.

4.3.2 S2.13 Growth Assays Using Cell Counts

Growth curves were constructed by plating 200,000 cells per 25cm^2 dish in triplicate and cells were counted at 2-day intervals up to 10 days. Assays grown at 33°C and 37°C were repeated 3 times and replicated twice at 39°C, and the mean and standard errors obtained (table 4.4). A graph of cell count versus days in culture was obtained (figure 4.10). At 33°C cells grow slowly until approximately day 6 and then start growing at an exponential rate. S2.13 cells also go through a lag phase at 37°C, until day 6 and then grow at an exponential rate, but they have fewer cell numbers than at 33°C. Cells grown at 39°C were dead by day 5.

Table 4.4: Proliferation Of S2.13 Cells, Showing The Mean And Standard Error Of Cell Numbers Derived From Three Independent Experiments

Days in Culture	Cell Number x 10^5 (±SE)		
	33°C	37°C	39°C
2	1.71 ± 0.22	1.99 ± 0.25	1.58 ± 0.068
4	3.04 ± 0.88	1.91 ± 0.33	0.52 ± 0.00
5	4.79 ± 0.69	2.52 ± 0.02	0.45 ± 0.08
8	12.66 ± 03.54	10.61 ± 3.49	
10	21.0 ± 5.0	16.45 ± 3.85	

4.3.2.1 Mean Population-Doubling Time for S2.13 Cells

The mean population doubling for S2.13 cells from the exponential phase of cell count assays, using a logarithmic scale is 48 and 36 hours, at 33°C and 37°C respectively. Cells do not grow exponentially at 39°C. Figure 4.11, below shows extrapolation of data from the exponential phase of a log curve of S2.13 cells.

Figure 4.10: Cell Count Growth Curve Of S2.13 Stromal Cells

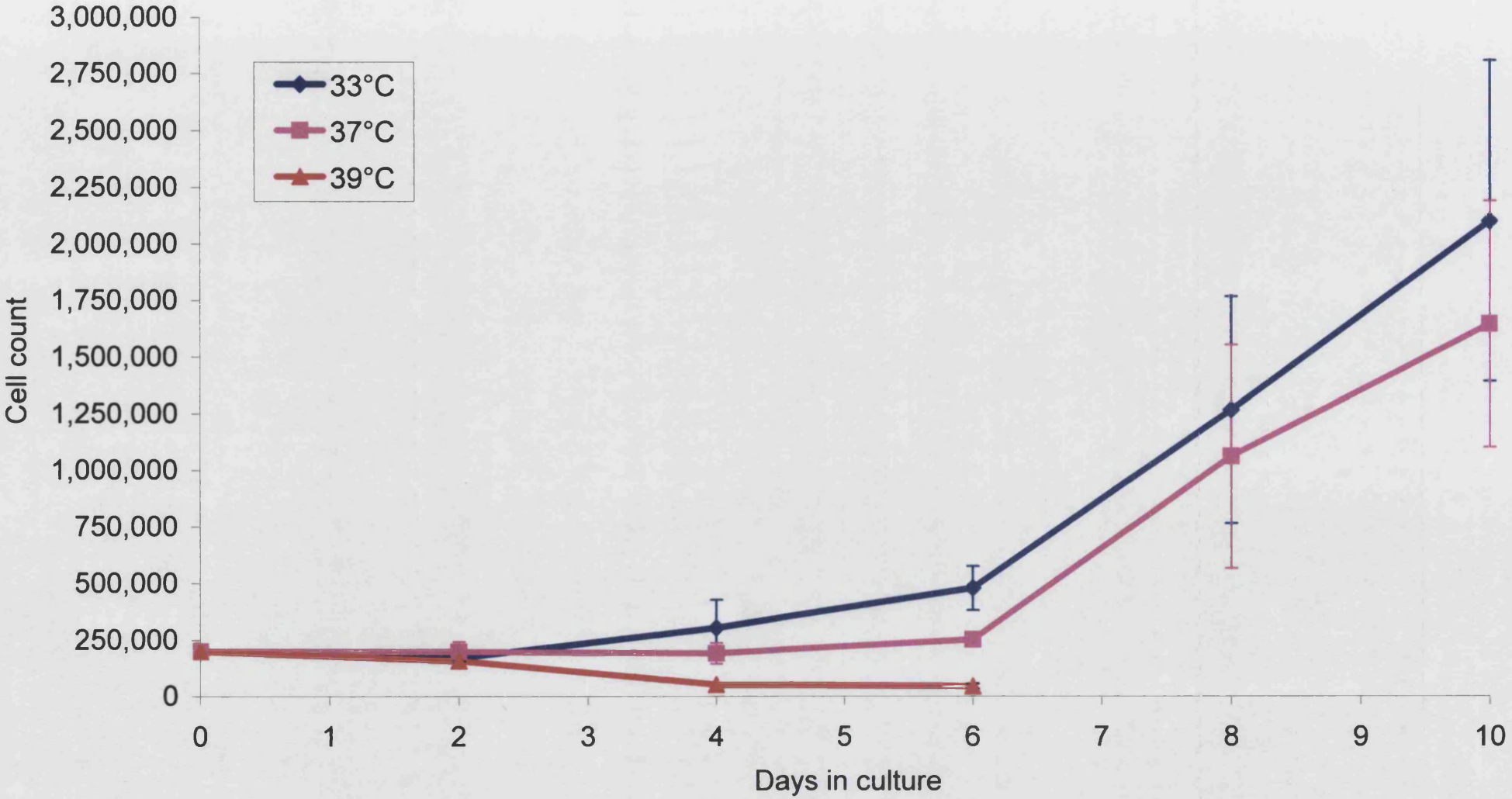

S2.13 cell counts for 3 separate growth assays, at 33°C, 37°C and 39°C. Cells were set-up in triplicate at a density of 200,000 cells per 25cm^2. The mean and standard error were calculated and a growth curve was obtained.

Figure 4.11: Extrapolation Of Mean Population-Doubling Figures For S2.13 Cells

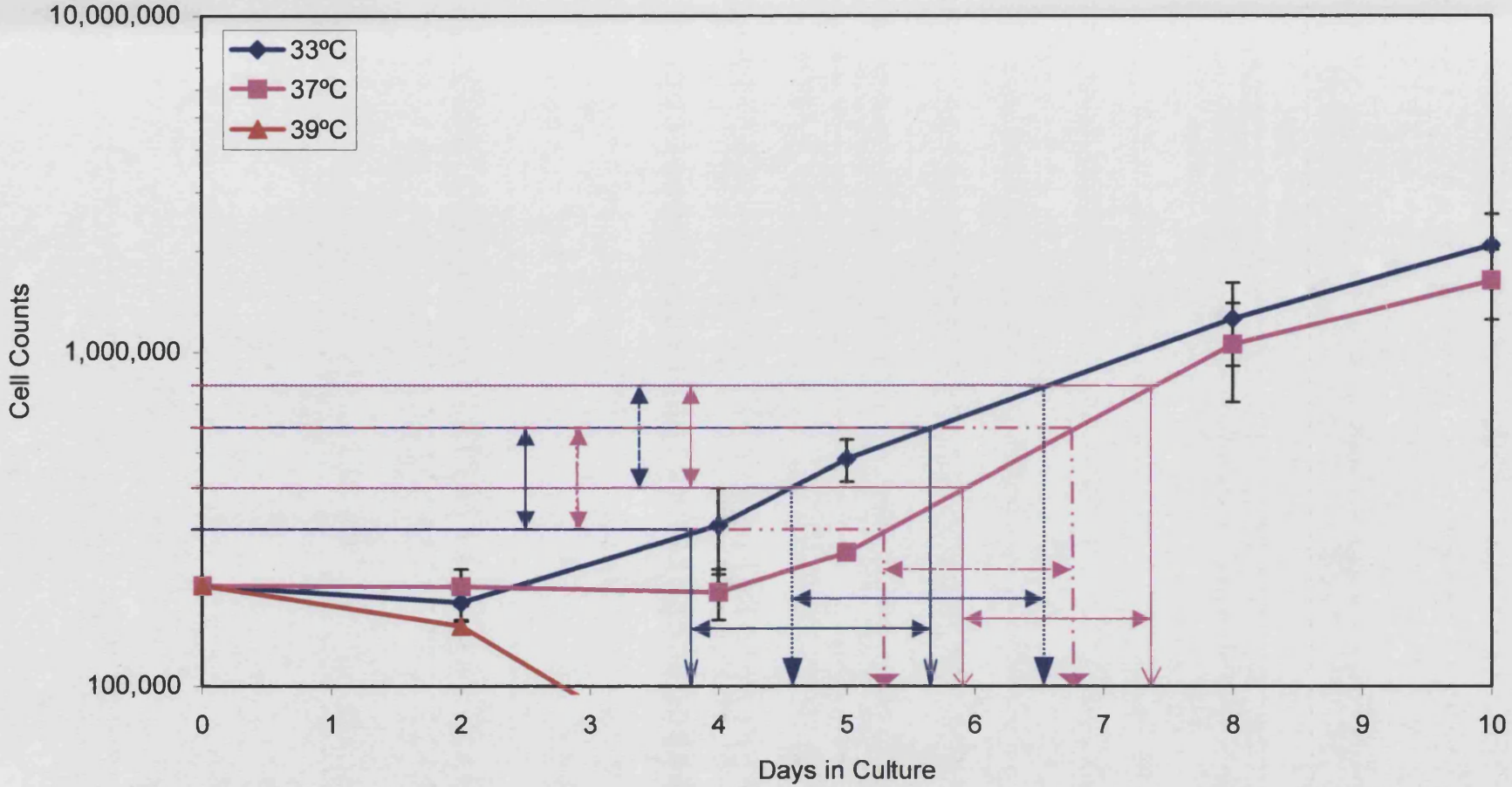

Log plot of the increase in cell concentration (y-axis) versus days in culture (x-axis), following subculture from cultures counted on regular intervals. The population-doubling time (PDT) was extrapolated from the straightest area of the exponential phase. A straight line was drawn from a particular cell count, on the y-axis in the log phase, to the plotted line. Then another straight line was drawn from a point that was double the first cell count on the y-axis to the plotted line. These two lines were then continued from the plot towards the x-axis in a straight line. The distance between these two points on the x-axis represents the length of time for one cell population to double. This was carried out at 33°C, 37°C and 39°C.

4.3.3 Comparison Of The Growth Patterns Of Immortalised (1542-NPTX) And Conditionally Immortalised (Pre2.8) Prostate Epithelial Cell Lines

The growth patterns of the conditionally immortalised prostate epithelial cell line Pre2.8 was compared with those of the immortalised cell line 1542-NPTX, in order to confirm the differences in response to temperature shift.

Cells were plated at a density of 10,000 per well in 96-well plates, and MTT assays were used to estimate growth after 3 and 10 days in culture. The results are shown in figures 4.12 and 4.13.

After 3 days growth, the 1542-NPTX cells had grown fastest at 39°C and slowest at 33°C. In contrast, the Pre2.8 cells had grown fastest at 37°C, but there were few surviving cells at 39°C.

After 10 days growth, 1542-NPTX cell number at 39°C was similar to that at 3 days, indicating that the high temperature had inhibited cell growth in the longer term. At 37°C, the optical density was 3-4 times that seen at 3 days, indicating exponential growth at this temperature. In contrast and as expected, the greatest increase in growth of Pre2.8 cells was seen at the permissive temperature, 33°C.

4.3.5 Comparison of the growth patterns of immortalised (1542-FT) and conditionally immortalised (S2.13) prostate stromal cell lines

Cells were plated at 200,000 cells per $25cm^2$ flask and grown for 5 and 9 days at 33°C, 37°C and 39°C in triplicate. The results are shown in figures 4.14 and 4.15, and are similar to those obtained with the epithelial cells. 1542-FT cells grew best at 37°C, while S2.13 cells grew best at 33°C after 5 and 9 days in culture.

Figure 4.12: Comparison Of Pre2.8 Cells With 1542-NPTX At Day 3

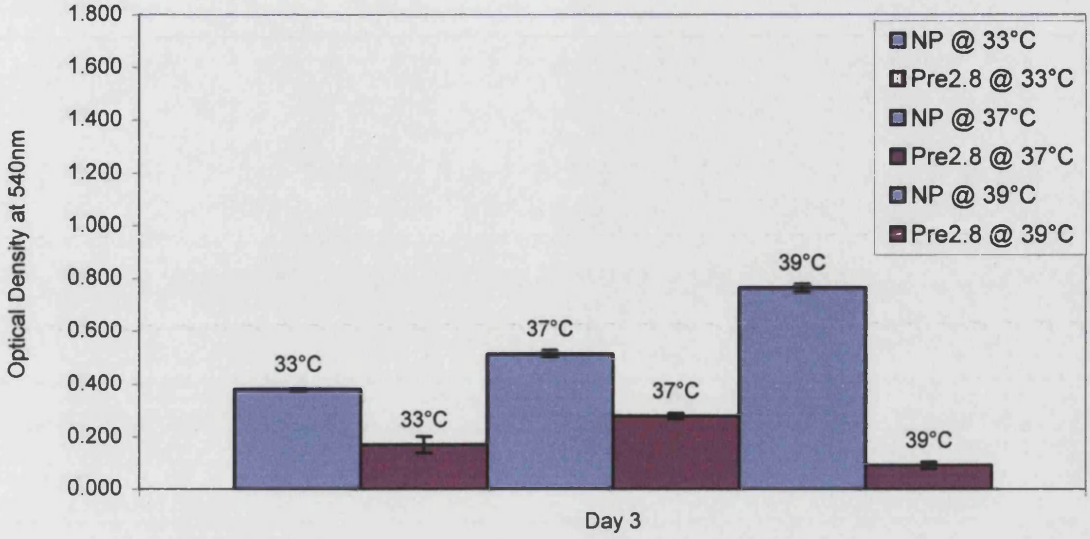

Pre2.8 and 1542-NPTX cells were seeded at a density of 10,000 cells per well and harvested after 3 days for analysis using the MTT assay. The mean and standard error of optical density for 3 experiments were calculated and a histogram with each cell line at 33°C, 37°C and 39°C was obtained.

Figure 4.13: Comparison Of Pre2.8 Cells With 1542-NPTX At Day 10

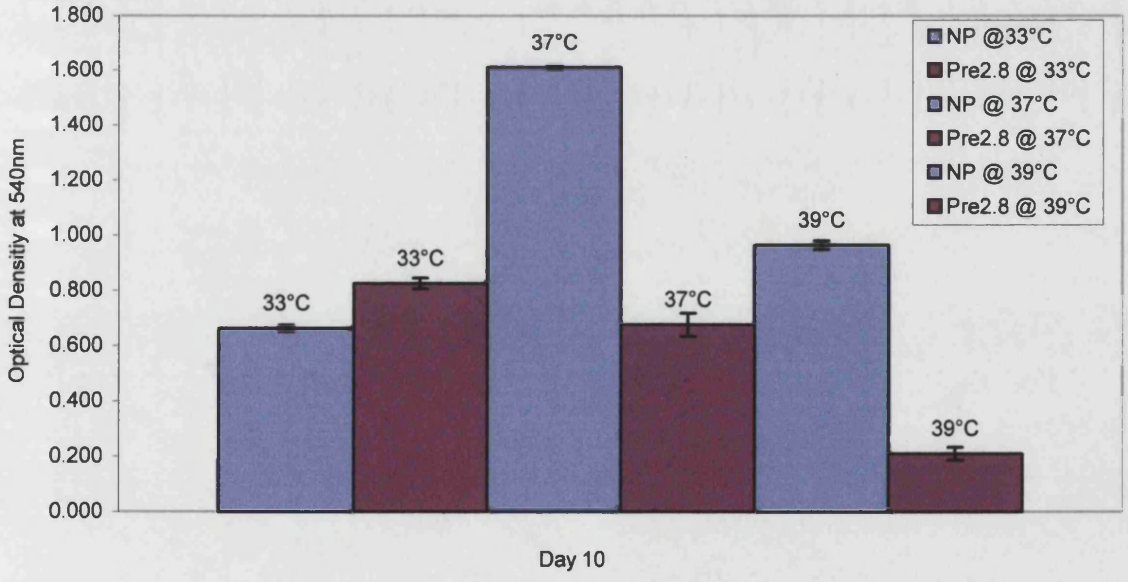

Pre2.8 and 1542-NPTX cells were seeded at a density of 10,000cells per well and harvested after 10 days for analysis using the MTT assay. The mean and standard error of optical density for 3 experiments were calculated and a histogram with each cell line at 33°C, 37°C and 39°C was obtained.

Figure 4.14: Comparison Of S2.13 Cells With 1542-FT At Day 5

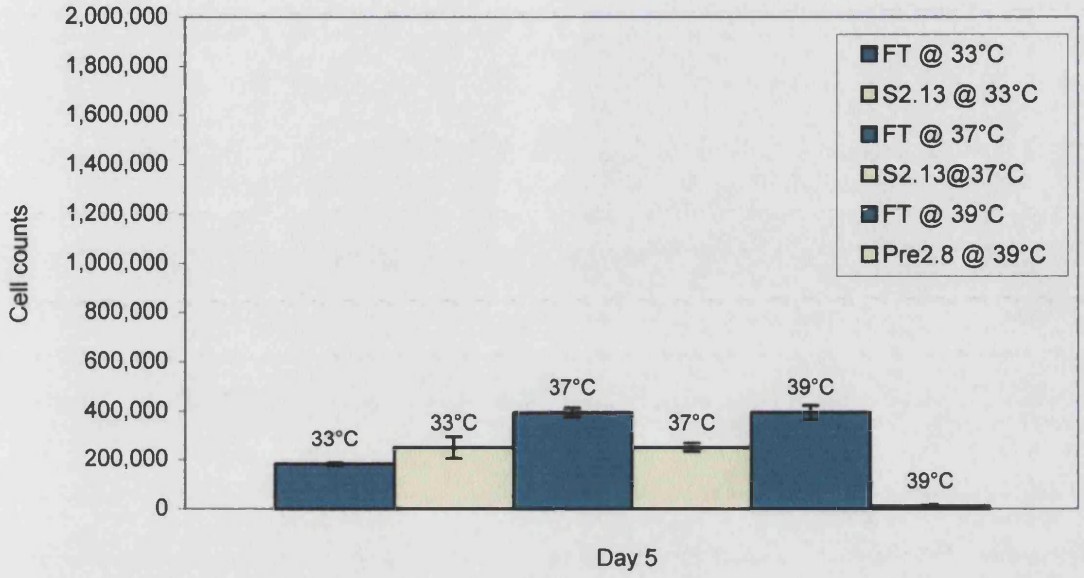

S2.13 cells and 1542-FT cells were seeded at a density of 200,000 cells per 25cm^2 flask and harvested after 5 days for analysis using cell counts. The mean and standard error of cell counts for 3 experiments were calculated and a histogram with each cell line at 33°C, 37°C and 39°C was obtained.

Figure 4.15: Comparison Of S2.13 Cells With 1542-FT At Day 9

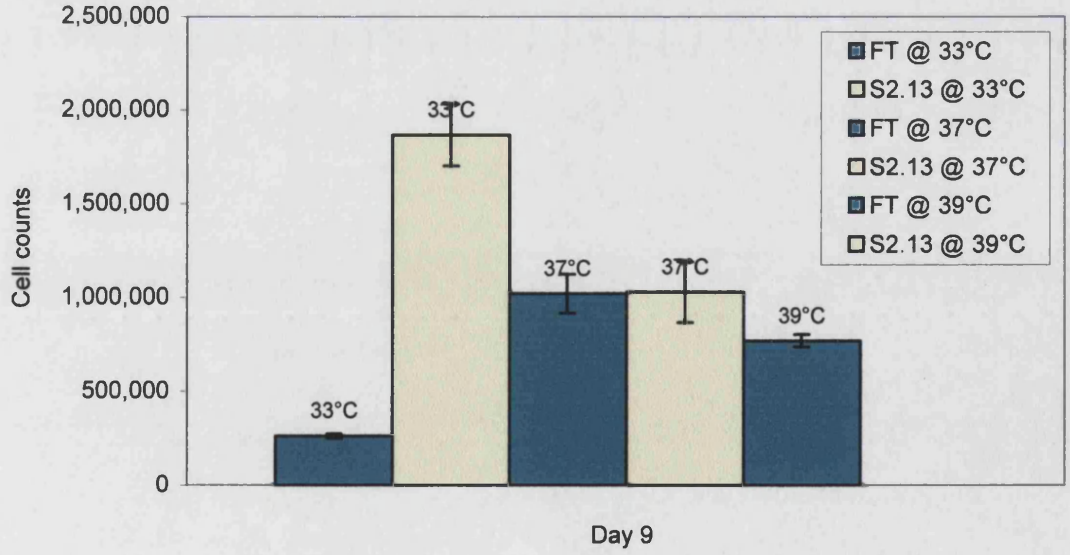

S2.13 cells and 1542-FT cells were seeded at a density of 200,000 cells per 25cm^2 flask and harvested after 10 days for analysis using cell counts. The mean and standard error of cell counts for 3 experiments were calculated and a histogram with each cell line at 33°C, 37°C and 39°C was obtained.

4.4 CELL SIZE DISTRIBUTION

Cell size was determined using a Coulter Counter to measure Pre2.8 cells in suspension. These results were compared to cell size of Pre2.8 and S2.13 cells growing on plastic, using a graticule eyepiece on an inverted microscope.

4.4.1 Beckman Coulter Counter

A size comparison of Pre2.8 cells at 33°C, 37°C and 39°C was carried out using a Coulter Counter. The mean size for 14,767, 14,140 and 8,991 cells measured is 13.25μm, 16.23μm and 16.57μm at 33°C, 37°C and 39°C respectively (figure 4.16). The histogram (figure 4.16) of cell size (μm) shows a significant 22% and 25% increase in cell size (13.25μm to 16.23μm and 16.57μm) when Pre2.8 cells are transferred from 33°C to 37°C and 39°C respectively. No significant difference was seen when cells were transferred to 37°C compared to 39°C. The cell size difference between 37°C and 39°C appeared to be greater by observation under the inverted microscope (figure 3.4). It may be possible that some of the larger cells at 39°C are not able to pass through the Coulter Counter's capillary tube, therefore producing an inaccurate mean cell size value. Alternatively it is possible that highly differentiated cells may not survive trypsinisation as whole cells. This would also account for lack of increase in Pre2.8 cell size at 39°C, using the coulter counter.

The cell size distribution of these cells clearly shows a shift. The majority of cells grown at 33°C are between 10μm and 13μm, which are at the smaller end of the scale (10μm to 21μm). When Pre2.8 cells are transferred to 37°C and 39°C this large peak is not seen. The majority of these cells are distributed between a scale of 13μm and 17μm (figure 4.17).

Figure 4.16: Pre2.8 Cell Size In Suspension

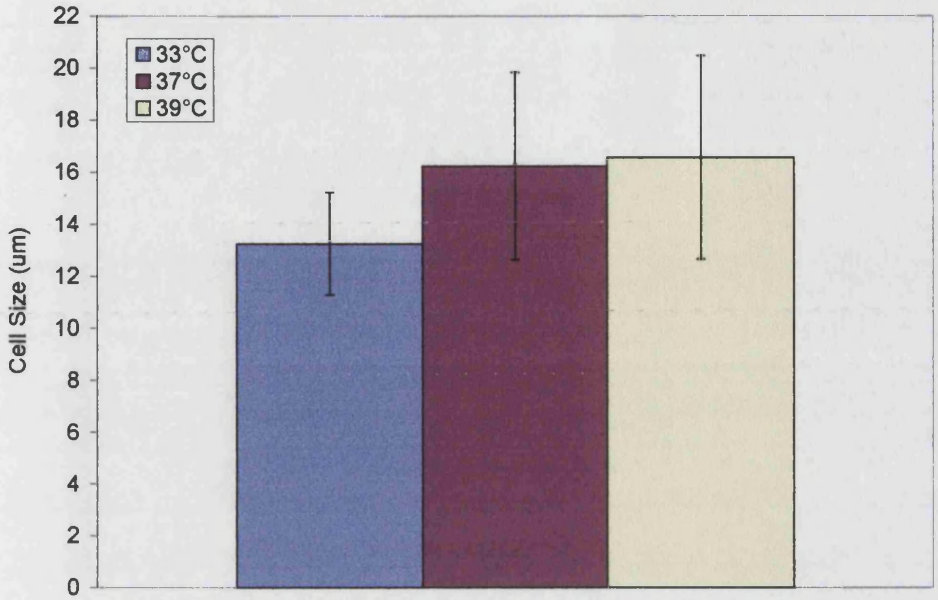

Using a Cell Coulter Counter the mean and standard error for cell size (μm) was calculated for 14,767 Pre2.8 cells in suspension, at 33°C, 37°C and 39°C. A significant increase in cell size of 22% and 25% (13.25μm to 16.23μm and 16.57μm) was observed when Pre2.8 cells were transferred from 33°C to 37°C and 39°C respectively. Unexpectedly no significant difference was observed when cells were transferred to 37°C compared to 39°C.

Figure 4.17: Dot Plot Of Pre2.8 Cell Size Distribution

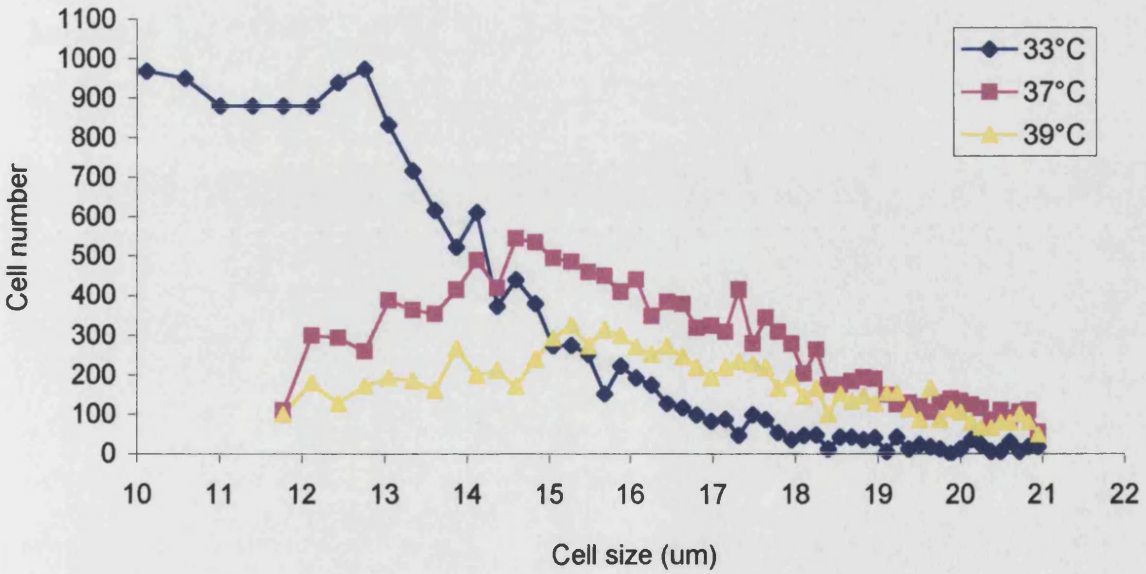

Using a Cell Coulter Counter the cell cycle distribution (cell number versus cell size in μm) was determined for Pre2.8 cells in suspension, at 33°C, 37°C and 39°C.

4.4.2 Graticule And Inverted Microscope

At x200 magnification on the light phase microscope one marking on the graticule eyepiece was equivalent to 5.71μm on the coverslip graticule. The diameter of 100 viable cells and their nuclei were measured from monolayer cultures on a tissue culture plate at 33°C, 37°C and 39°C.

S2.13 stromal cells are much larger than Pre2.8 epithelial cells, 55μm compared to 40μm at 33°C, 64μm compared to 43μm at 37°C and 88μm compared to 52μm at 39°C (see histograms, figure 4.19 and 4.21 for Pre2.8 and S2.13 respectively). Similar comparisons were observed for nucleus size, although the mean nucleus size was approximately half the size of the mean cell size.

4.4.2.1 Pre2.8 Cells

A distribution of cell number versus cell size was determined (figure 4.17). There is a shift in size distribution for Pre2.8 cells. The majority of cells at 33°C and 37°C range between 31μm and 70μm in size while at 39°C cells range between 31μm and 100μm in size.

A histogram of the mean and standard error for 100 Pre2.8 cell and nucleus diameter was determined (figure 4.18). There is a 7% and 12% increase in cell size (40μm to 43μm and 52μm) when Pre2.8 cells are transferred from 33°C to 37°C and 39°C respectively. A 12% and 30% increase in nucleus size of these cells, increasing from 17μm to 19μm and 22μm when transferred from 33°C to 37°C and 39°C respectively.

Figure 4.18: Pre2.8 Cell Size Distribution

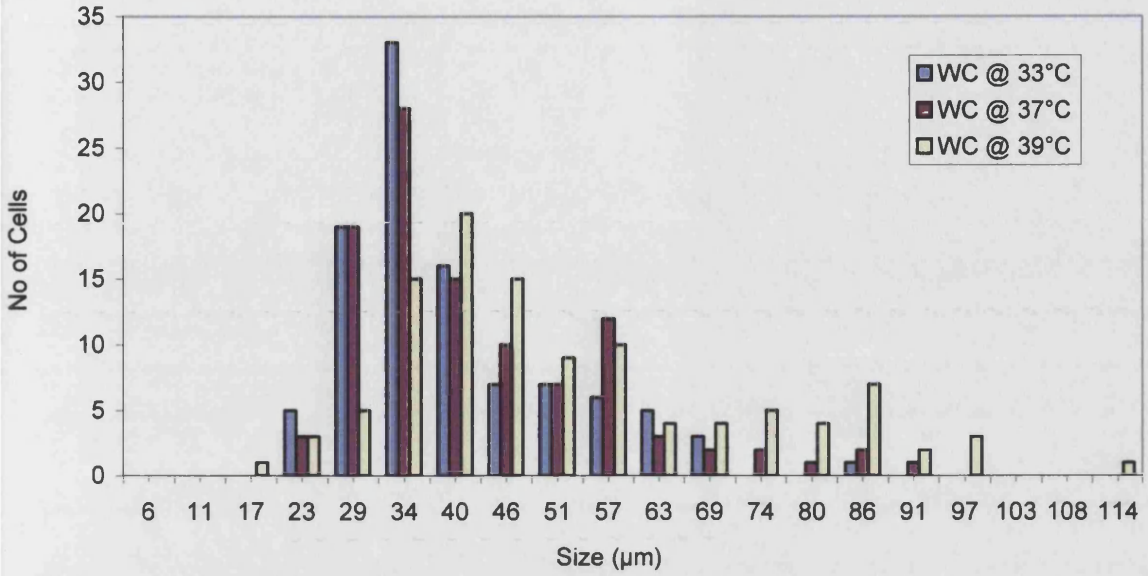

Comparison of whole cell (WC) size distribution for Pre2.8 cells after 7 days grown at 33°C, 37°C and 39°C. Flattened cells were measured using a Graticule under an inverted microscope. The mean and standard error of 100 cells was calculated.

Figure 4.19: Comparison Of Pre2.8 Whole Cell And Nucleus Size At 33°C, 37°C And 39°C

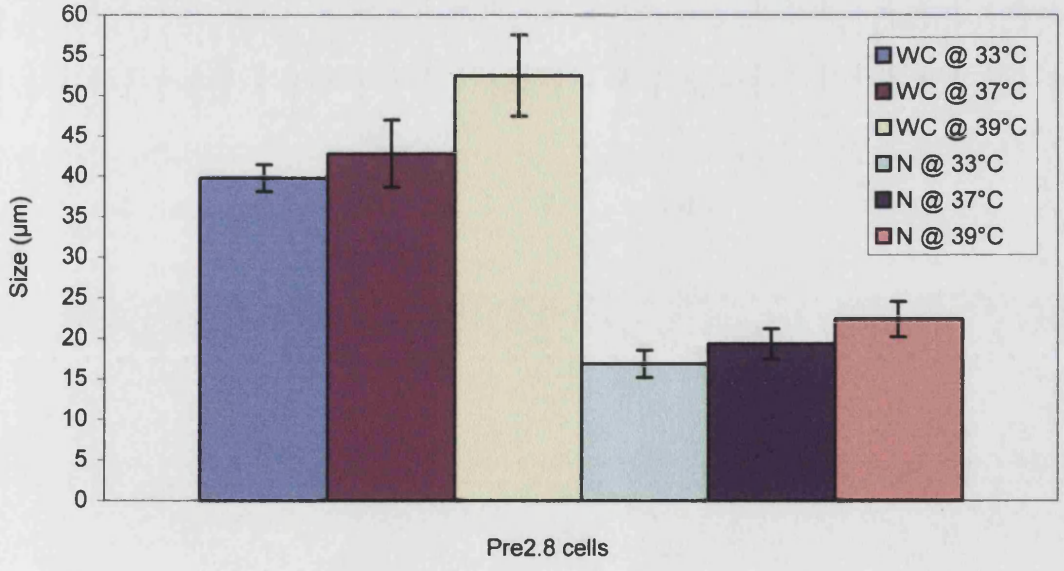

Comparison of whole cell (WC) size and nuclei size (N) for Pre2.8 cells after 7 days grown at 33°C, 37°C and 39°C. Flattened whole cells and their nucleus were measured using a Graticule under an inverted microscope. The mean and standard error of 100 cells was calculated. There is a greater increase in Pre2.8 nuclei size (12% and 30%) than Pre2.8 whole cell size (7% and 12%) from 33°C to 37°C and 37°C to 39°C respectively.

4.4.2.2 S2.13 Cells

A graph of cell size distribution (figure 4.20) shows a size shift when S2.13 cells are transferred from 33°C to 37°C and 39°C. Cells range in size from approximately 30μm to 100μm at 33°C and 37°C and 35μm to 120μm for S2.13 cells.

A histogram of mean and standard error of S2.13 cell and nucleus diameter size shows a 16% and 60% increase when cells are transferred from 33°C to 37°C and 39°C respectively (figure 4.21). The average cell size increases from 55μm to 64μm and 88μm. There is no change in nucleus size from 33°C to 37°C, while a 37% increase is observed when cells are transferred from 33°C to 39°C (25μm to 34μm).

Figure 4.20: S2.13 Cell Size Distribution

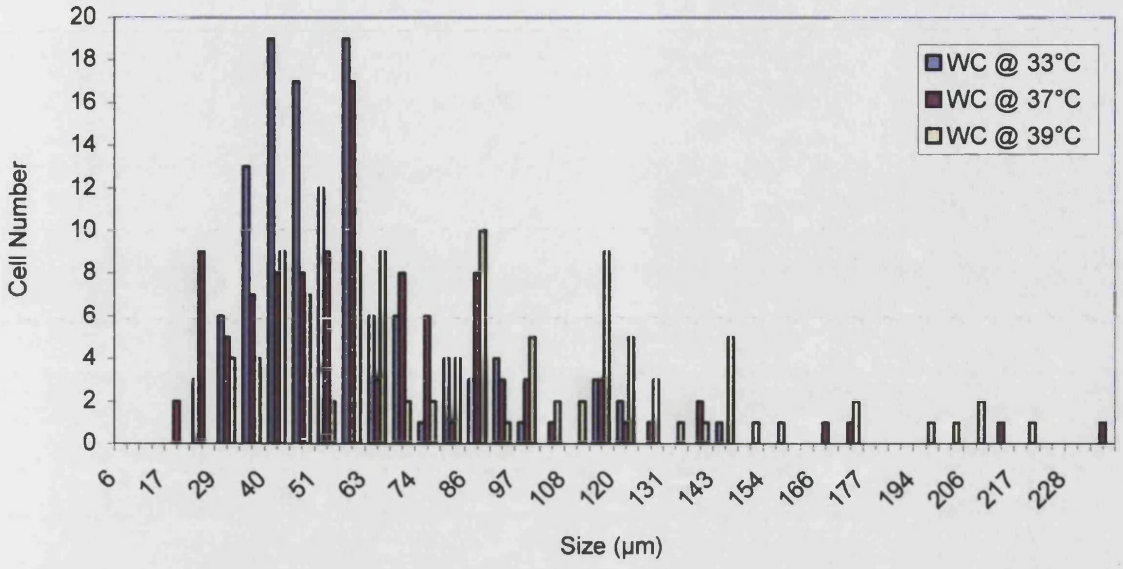

Comparison of whole cell (WC) size distribution for S2.13 cells after 7 days grown at 33°C, 37°C and 39°C. Flattened cells were measured using a Graticule under an inverted microscope. The mean and standard error of 100 cells was calculated.

Figure 4.21: Comparison Of S2.13 Whole Cell And Nucleus Size At 33°C, 37°C And 39°C

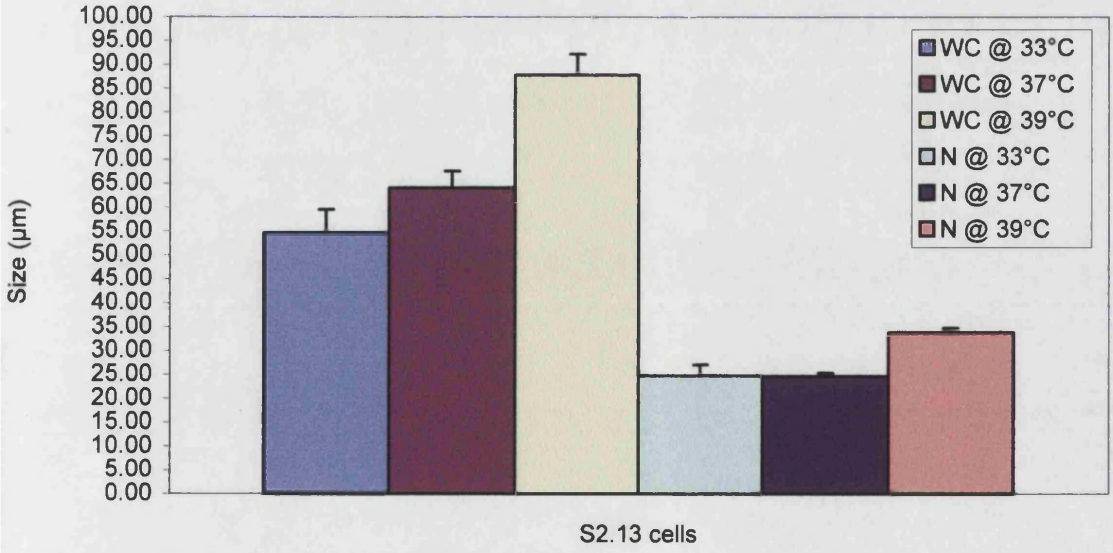

Comparison of whole cell (WC) size and nuclei size (N) for Pre2.8 cells after 7 days grown at 33°C, 37°C and 39°C. Flattened whole cells and their nucleus were measured using a Graticule under an inverted microscope. The mean and standard error of 100 cells was calculated.

4.5 COLONY FORMING EFFECIENCY ON PLASTIC AND IN SOFT AGAR

4.5.1 Colony Forming Efficiency For Pre2.8 Cells On Plastic

Colony forming assays were set up for Pre2.8 cells at a density of 5,000, 10,000, 15,000 and 20,000 cells in triplicate at 33°C and 39°C. The colonies were fixed after 14 days culture (previously optimised protocol for commonly used cell lines within our laboratory) and then counted under a dissecting microscope. In order to avoid counting secondary colonies, only colonies with greater than 50 cells/colony were counted. The results of 5 independent assays are shown in table 4.5. No colonies developed at 39°C. At 33°C, colonies did not develop at a seeding of 5,000 cells, although some cells survived. At a plating density of 20,000 per 5cm dish, the colonies had begun to merge by 14 days and could not be counted. The mean colony forming efficiency was 2.5% and 3.1% for 10,000 and 15,000 cells respectively.

Table 4.5: Colony Forming Efficiency For Pre2.8 Cells At 33°C

10,000	15,000
2.78%±0.10	2.70%±0.29
0.22%±0.18	3.80%±0.50
5.90%±0.43	2.78%±0.22
0.26%±0.17	3.28%±0.39
3.09%±0.10	
2.45%±0.20	**3.14%**±0.35

4.5.2 Anchorage-Independent Growth

The ability of Pre2.8 cells (passage 50) to grow in an anchorage-independent manner was compared with a breast cancer cell line, MDA-MB-435 (Glinsky et al., 1996) and a prostate cancer cell line, PC3 (Kaighn et al. 1979). Cancer cells are known to posess anchorage-independent growth. PC3 cells show anchorage-independent growth in monolayer and soft agar suspension and produce subcutaneous tumors in nude mice (Kaighn et al. 1979). It has previoulely been shown, in our laboratory that MDA-MA-435 and PC3 cell lines produce colonies in semi-solid agar, i.e. anchorage-independent growth, hence they were chosen as good positive controls for these experiments. MDA-MA-435 and PC3 cells were suspended in semi-solid agar in triplicate at 33°C and 37°C at a range of densities. Colony formation was observed after 15 days. Pre2.8 and S2.13 cells did not produce colonies in semi-solid agar, while the MDA-MB-435 and PC3 cancer cell lines had colony-forming ability in agar (data not shown).

CHAPTER 5

RESULTS

DIFFERENTIATION OF MONOLAYER CULTURES

5.1 INTRODUCTION

Pre2.8 and S2.13 cell lines, immortalised using a temperature sensitive SV40 T-antigen construct, were successfully authenticated and characterised (described in chapter 4 and 5). These cell lines should proliferate at 33°C and stop dividing at 37°C or 39°C. The aim of this section is to determine to what extent the cells differentiate when proliferation ceases.

Immunofluorescent and immunocytochemical analyses were carried out to characterise the Pre2.8 and S2.13 cells. Pre2.8 cells were grown on coverslips at 33°C, 37°C and 39°C for 7 days. S2.13 cells were grown at 33°C and 37°C only, as the cells died within 7 days at 39°C. Fluorescent staining was examined using a Hg-arc Zeiss Axiophot fluorescent microscope and extent and intensity of staining was estimated by eye.

5.2 Stromal Cell Markers

Antibodies to vimentin, smooth muscle actin (SMA) and a fibroblast cell surface marker (ASO2) were used to identify stromal cell subtypes (table 5.1 and figure 5.1).

Pre2.8 cells were negative for these markers at all temperatures. S2.13 cells were positive for vimentin and anti-fibroblast antibody (figure 5.1) and negative for SMA. This staining pattern is characteristic of fibroblast cells. There was no background present for SMA or vimentin antibodies. Faint background was seen for fibroblast (ASO2) antibody.

5.3 Epithelial Cell Markers

Cytokeratin expression was used to confirm epithelial cell origin and to look for basal cell (K14 and K17), intermediate cell (K19) and luminal cell differentiation (K8 and K18) cells at 33°C, 37°C and 39°C.

The prostate cancer cell line LNCaP stained for K8 and K18, was weakly positive for K19 and negative for K14 and K17. S2.13 cells were negative for K14 at 33°C and 37°C, while results were inconclusive for K17 (table 5.1). Positive staining was found for K17 which is unexpected as keratins are epithelial cell markers and not stromal.

Nearly all Pre2.8 cells were positive for K14 at all three temperatures. Although all Pre2.8 cells appear to express K17 (figure 5.2), there is a clear intensity difference. At

33°C most cells are only faintly positive whereas at 37°C and 39°C most of the cells express K17 strongly. The number of cells expressing both K14 and K17 (yellow in colour) (figure 5.2) has clearly increased at 37°C and 39°C compared to 33°C. In areas where K17 is most intense, K14 is less intense. The intensity of K14 staining decreased at the two higher temperatures.

K19, an intermediate epithelial marker shows occasional staining at 37°C and 39°C only (figure 5.3). $K14^+$ $K19^-$ staining was observed at 33°C compared to $K14^+$ $K19^+$ found at 37°C and 39°C (figure 5.3). There were small patches of strong $K19^+$ $K14^-$ expression in densely populated Pre2.8 cells at 37°C and 39°C (most obvious at 37°C), indicative of further differentiation at the higher temperatures. K19 and K8 antibodies were sparsely expressed in different cells, when double stained at 37°C compared to extremely sparse co-expression (yellow cells) at 39°C (figure 5.4). All cells at 33°C were negative for K19 with some K8 staining.

The luminal cell markers K8 and K18 were expressed in fewer Pre2.8 epithelial cells at 33°C than at 37°C and 39°C. In double stains for K19 and K8 (figure 5.4) an increase in K8 expression was observed at 37°C and 39°C compared to 33°C. A similar pattern was seen with K14 and K8 (figure 5.5). There appear to be fewer $K14^+$ cells expressing K18 (figure 5.6) than K8 at 33°C and 37°C. Co-expression of K14 and K8 is apparent at 33°C, while $K8^+$ cells are $K14^-$ at 37°C.

Pre2.8 cells have a basal phenotype at 33°C and differentiate into intermediate epithelial cells at 37°C.

5.4 Androgen Expression And Prostate Specific Characteristics Of Pre2.8 And S2.13 Cells

In order to determine if the cells express prostate specific characteristics immunocytochemical staining was carried out for AR, PSA and PAP and results observed under the Nikon Diaphot inverted microscope (table 5.1). Both isoforms of 5α-reductase (type 1 and 2) were examined by RT-PCR.

There was no expression of 5α-R2 (figure 5.7), AR, PSA or PSAP in Pre2.8 or S2.13 cells at any temperature (table 5.1). LNCaP cells were positive for AR, PSA and PSAP antibodies by immunocytochemistry and BPH tissue was positive for 5α-R2, producing a 350bp RT-PCR product (figure 5.7). 5α-R type 1 was expressed in Pre2.8 and S2.13 cells at 33°C, 37°C and 39°C, producing a 170bp fragment (figure 5.7). GAPDH was positive for all Pre2.8 and S2.13 PCR samples, producing a 597bp product.

Table 5.1: Differentiation Pattern Of Pre2.8 Epithelial And S2.13 Stromal Cells

Markers	Positive Control		Neg	Pre2.8			S2.13	
	LNCaP	3T3	Control	33°C	37°C	39°C	33°C	37°C
K14	-	nt	-	+++	+++	+++	-	-
K17	-	nt	-	++	+++	+++	inc	inc
K19	-	nt	-	-	+	+	-	-
K8	+++	nt	-	+	+/++	+/++	nt	nt
K18	+++	nt	-	+	++	++	nt	nt
SMA	nt	+++	-	-	-	-	-	-
Vimentin	nt	+++	-	-	-	-	+++	+++
Fibroblast (ASO2)	nt	+++	Faint background	-	-	-	+++	+++
AR	+++	nt	-	-	-	-	-	-
PSA	+++	nt	-	-	-	-	-	-
PAP	+++	nt	-	-	-	-	-	-

Abbreviations: (nt) not tested; (-) negative expression. Positive staining is expressed as +, ++ or +++ which refers to an estimated amount of staining or quantity of positive stained cells (occasional, moderate or nearly all).

LNCaP and 3T3 cells were only used as positive controls to show that antibodies were active and working correctly. Since LNCaP and 3T3 cells were not being investigated it was not necessary to test them for variation in marker expression at temperatures other than their routine culture temperature.

Figure 5.1: Vimentin And Fibroblast Expression In S2.13 Cells

(A) Vimentin

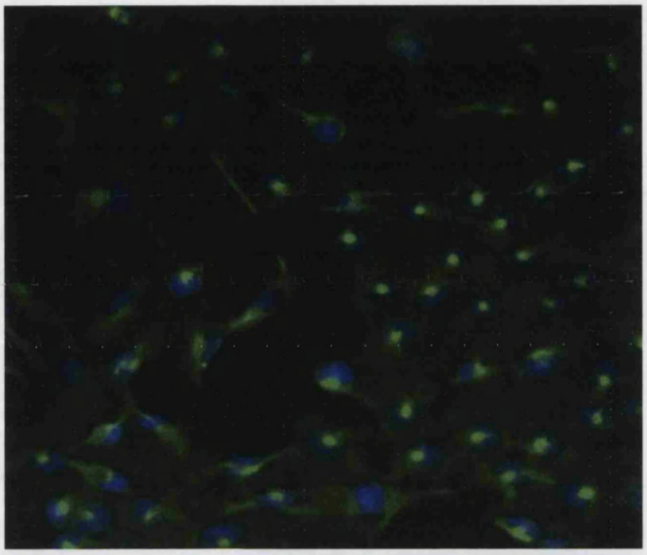

(B) Fibroblast (ASO2)

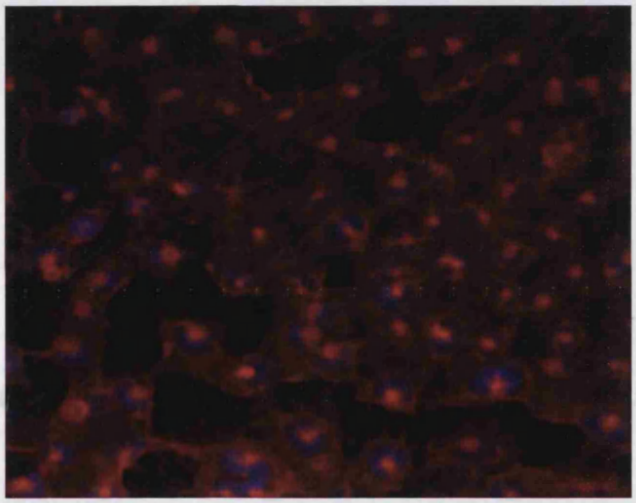

(C) Fibroblast (ASO2)

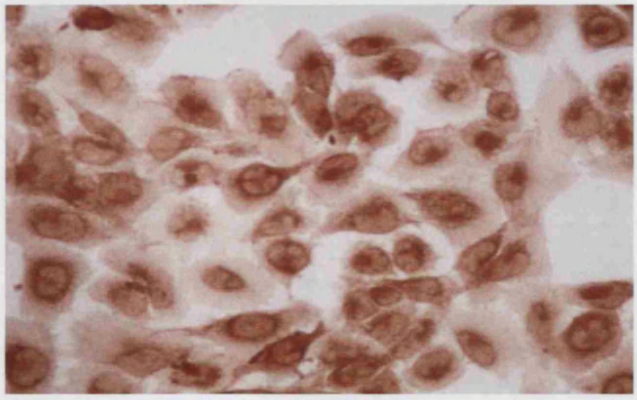

Immunofluorescence (A and B) and immunocytochemistry (C) staining of S2.13 stromal cells (passage 14) that were grown on glass coverslips at 33°C. Nuclei were stained with Hoechst (blue) in A and B. Cells were stained with (A) vimentin (green), (B) ASO2 anti-fibroblast antibody (red) or (C) ASO2 anti-fibroblast antibody (brown). Original magnification was x40 (fluorescence microscope – objective lens).

Figure 5.2: K14 K17 Expression In Pre2.8 Cells

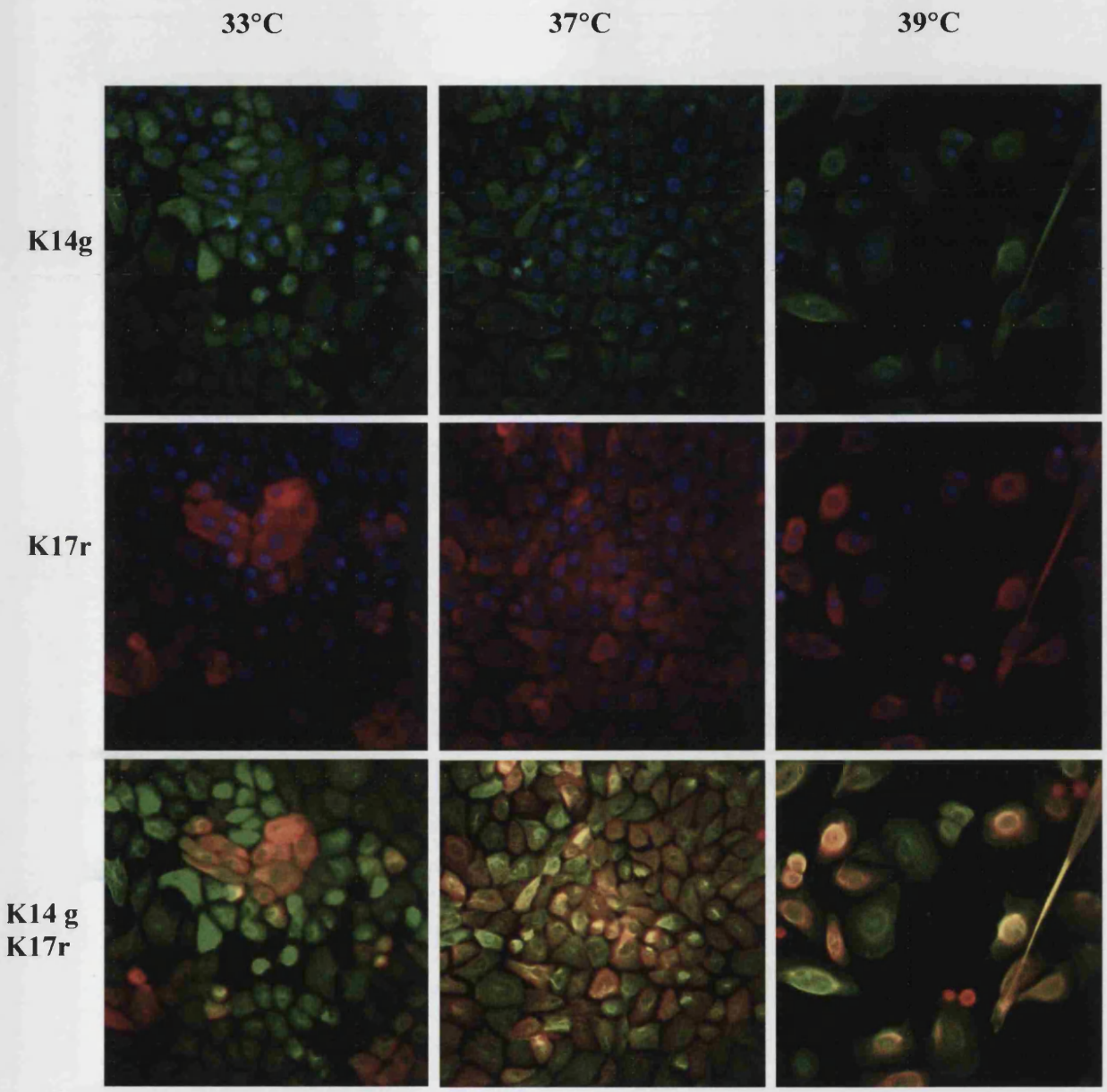

Immunofluorescence staining of Pre2.8 epithelial cells (between passage 48 and 58) grown on glass coverslips at 33°C, 37°C and 39°C. Nuclear Hoechst (blue) staining is shown with K14 and K17 alone, but is not shown with K14/K17 together. Keratin 14 is stained with FITC (green). Keratin 17 is stained with Rhodamine (red). When epithelial cells are double stained with K14 and K17 the colour tends to be yellow (mixture of FITC and Rhodamine). Original magnification was x40 (fluorescence microscope – objective lens).

Figure 5.3: K14 K19 Expression In Pre2.8 Cells

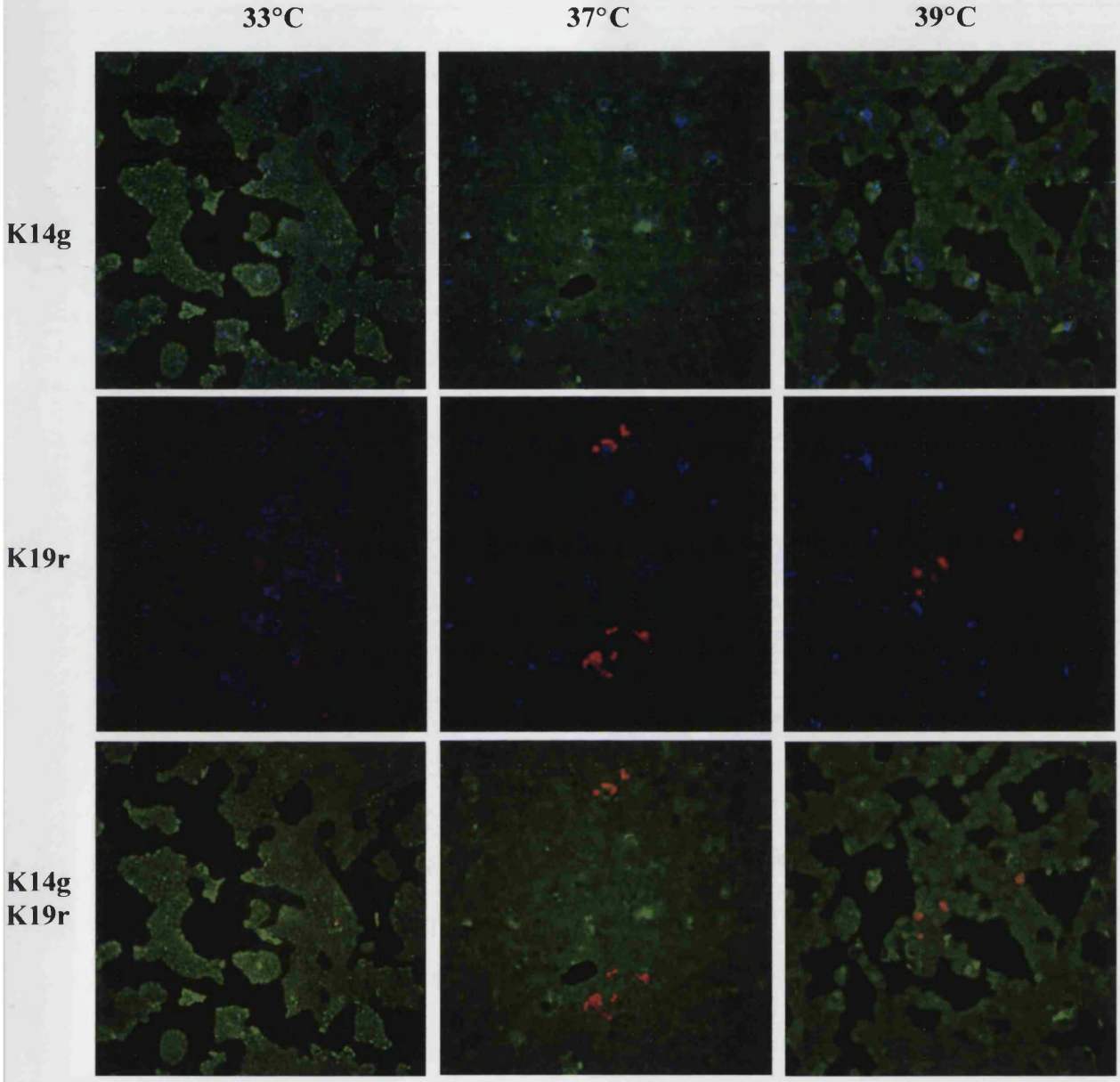

Immunofluorescence staining of Pre2.8 epithelial cells (between passage 48 and 58) grown on glass coverslips at 33°C, 37°C and 39°C. Nuclear Hoechst (blue) staining is shown with K14 and K19 alone, but is not shown with K14/K19 together. Keratin 14 is stained with FITC (green). Keratin 19 is stained with Rhodamine (red). When epithelial cells are double stained with K14 and K19 the colour tends to be yellow (mixture of FITC and Rhodamine). Original magnification was x20 (fluorescence microscope – objective lens).

Figure 5.4: K19 K8 Expression In Pre2.8 Cells

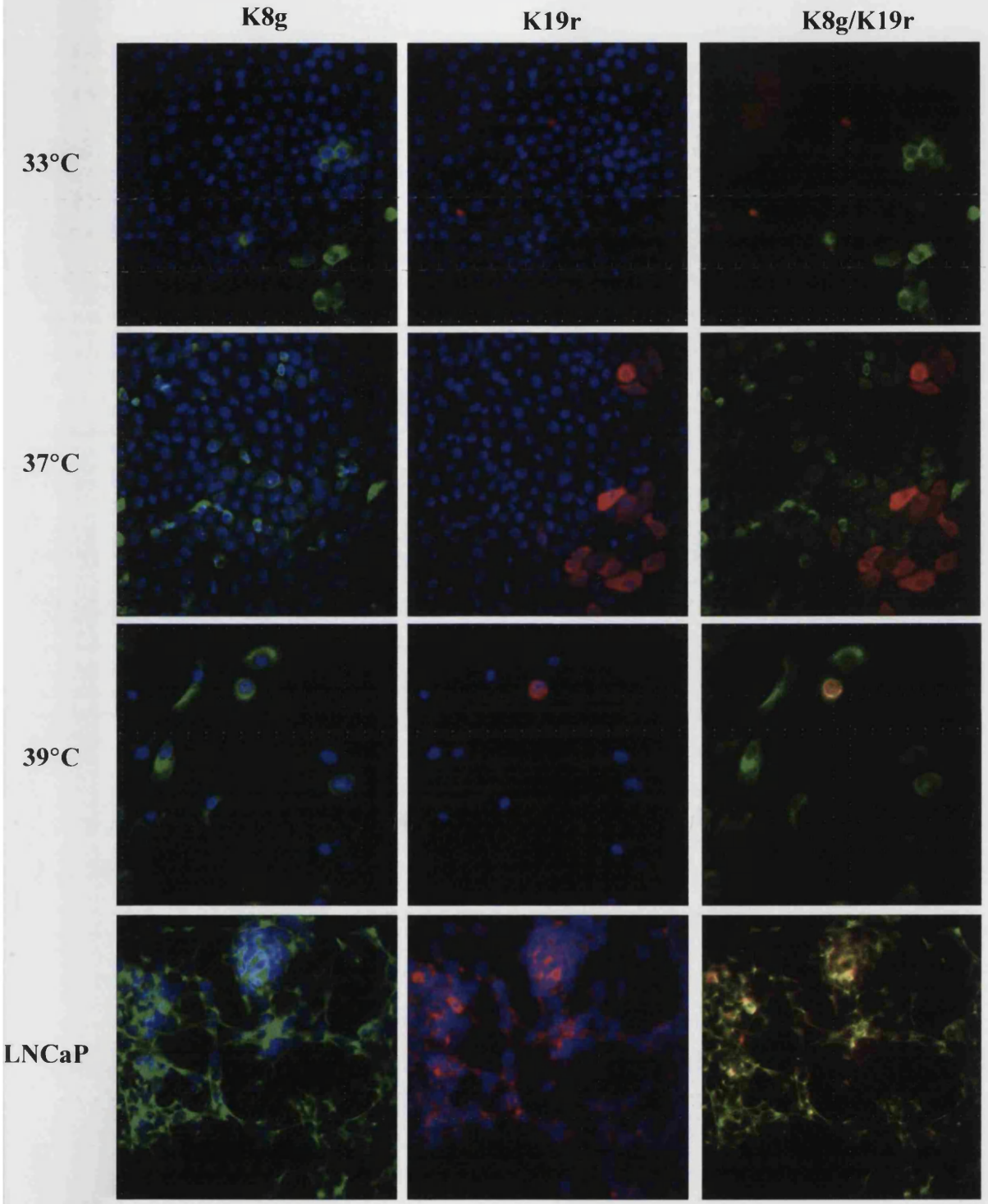

Immunofluorescence staining of Pre2.8 epithelial cells (between passage 48 and 58) grown on glass coverslips at 33°C, 37°C and 39°C. Nuclear Hoechst (blue) staining is shown with K8 and K19 alone, but is not shown with K8/K19 together. Keratin 8 is stained with FITC (green) and Keratin 19 with Rhodamine (red). When epithelial cells are double stained with K8 and K19 the colour tends to be yellow (mixture of FITC and Rhodamine). LNCaP (metastatic prostate cells) luminal cells were used as a positive control for K8 expression. Original magnification was x40 (fluorescence microscope – objective lens).

Figure 5.5: K14 K8 Expression In Pre2.8 Cells

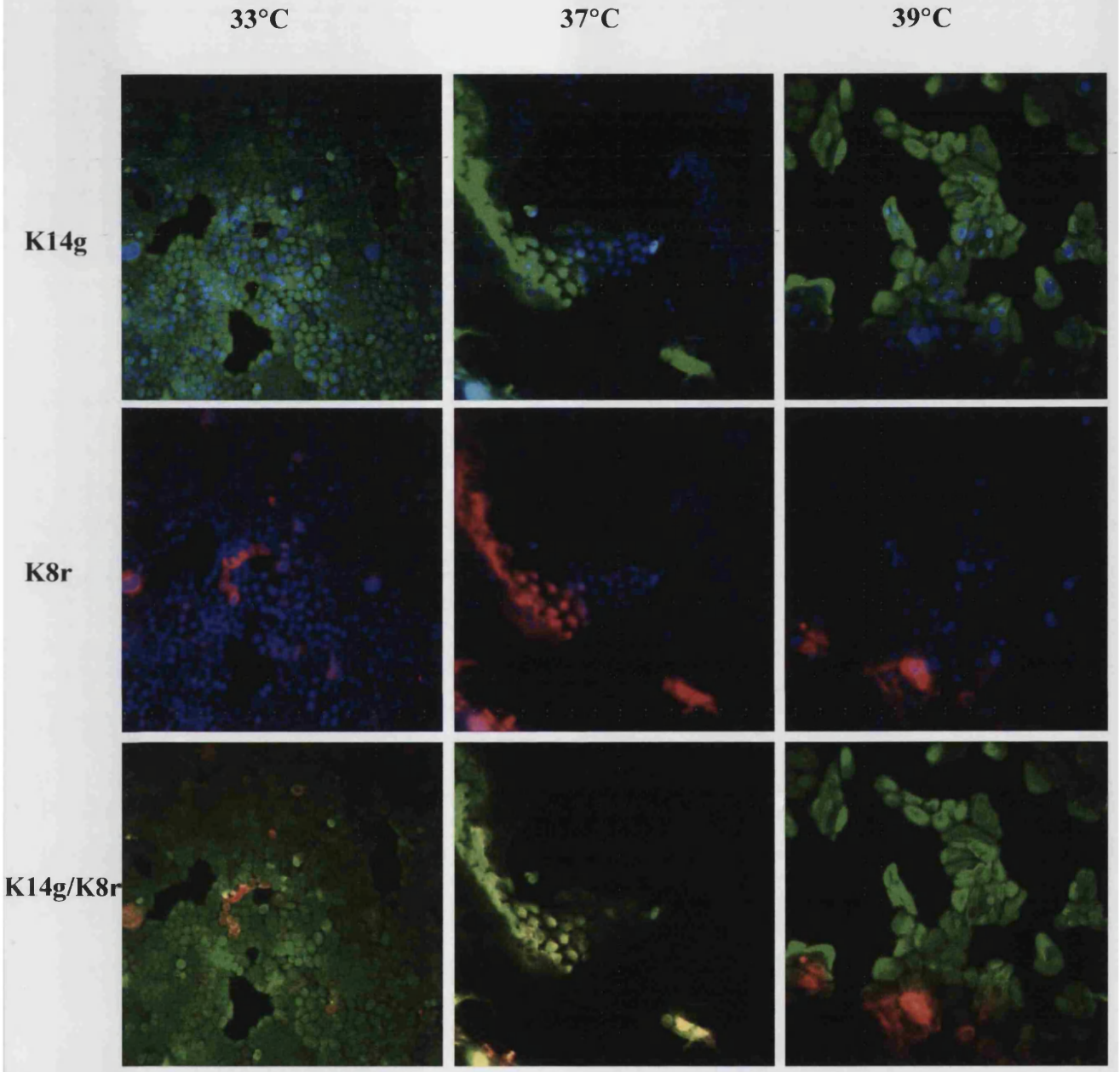

Immunofluorescence staining of Pre2.8 epithelial cells (between passage 48 and 58) grown on glass coverslips at 33°C, 37°C and 39°C. LNCaP (metastatic prostate cells) luminal cells were used as a positive control for K8 expression. Nuclear Hoechst (blue) staining is shown with K14 and K8 alone, but is not shown with K14/K8 together. Keratin 14 is stained with FITC (green). Keratin 8 is stained with Rhodamine (red). When epithelial cells are co-stained with K14 and K8 the colour tends to be yellow (mixture of FITC and Rhodamine). Original magnification was x40 (fluorescence microscope – objective lens).

Figure 5.6: K14 K18 Expression In Pre2.8 Epithelial Cells

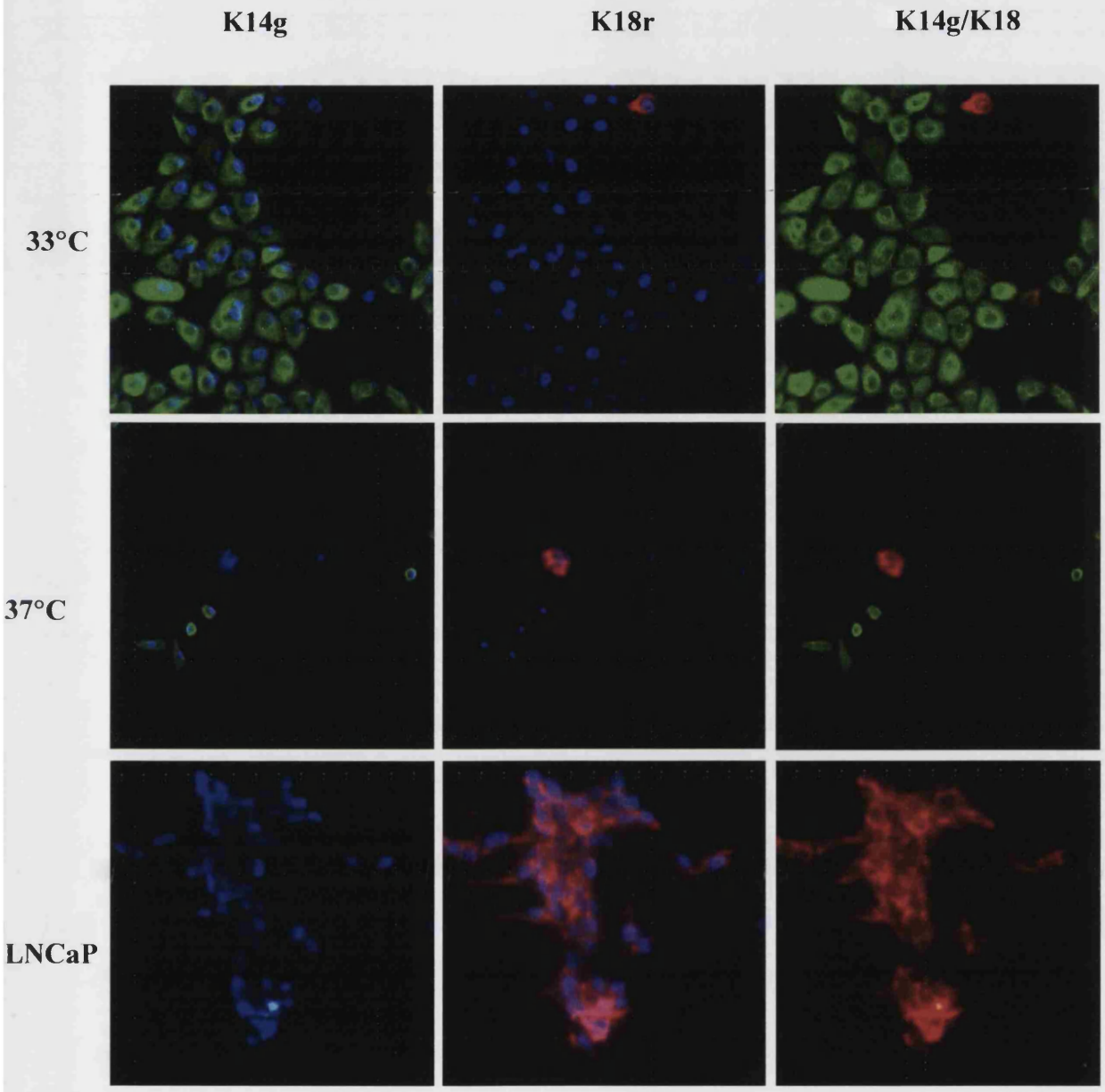

Immunofluorescence staining of Pre2.8 epithelial cells (between passage 48 and 58) grown on glass coverslips at 33°C and 37°C. LNCaP (metastatic prostate cells) luminal cells were used as a positive control for K18 expression and as a negative control for K14. Nuclear Hoechst (blue) staining is shown with K14 and K18 alone, but is not shown with K14/K18 together. Keratin 14 is stained with FITC (green). Keratin 18 is stained with Rhodamine (red). Original magnification at 33°C and with LNCaP cells was x40. Original magnification at 37°C was x20 (fluorescence microscope – objective lens).

Figure 5.7: 5α-Reductase Expression

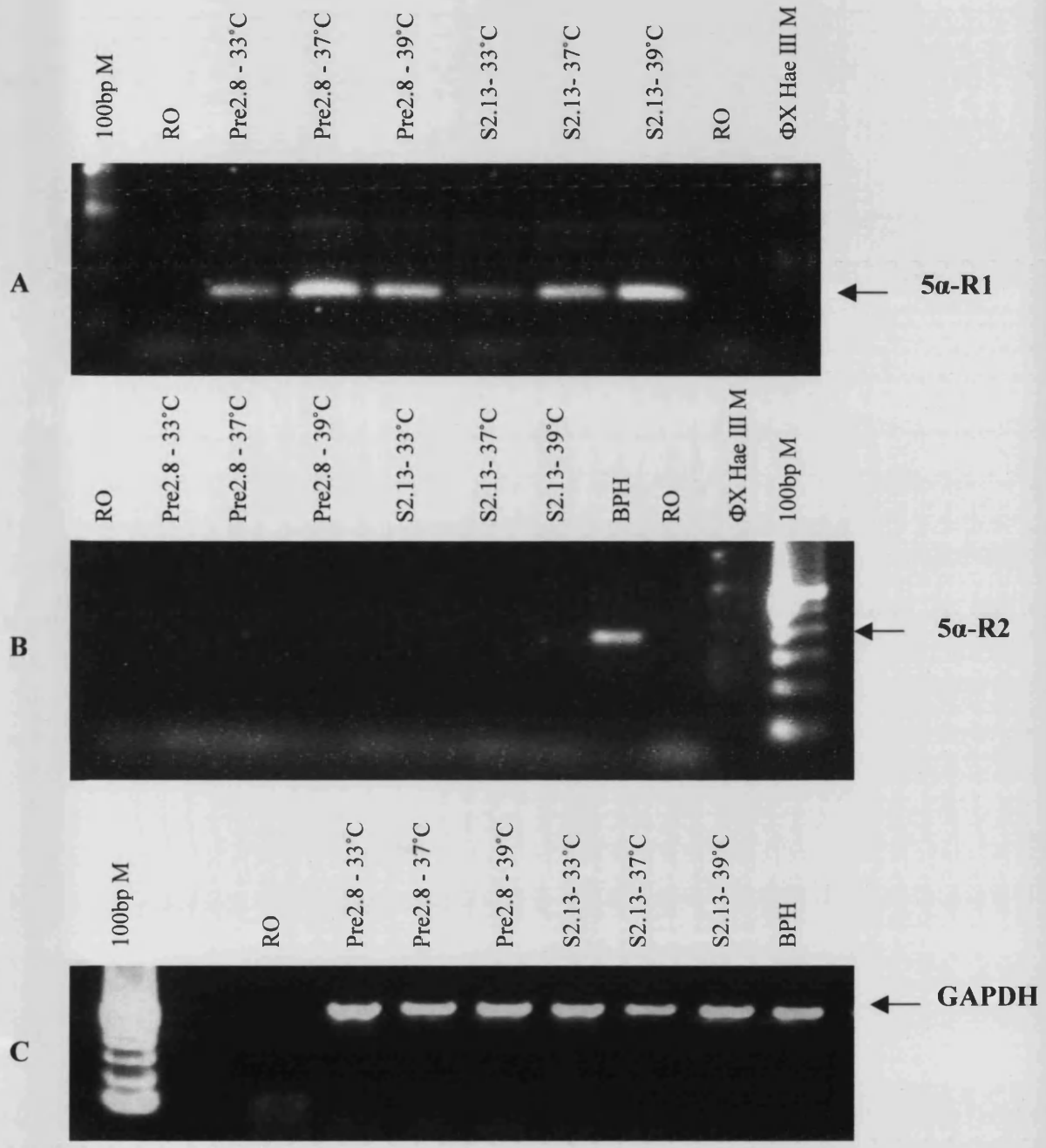

Pre2.8 (between passage 48 and 58) and S2.13 cells (passage 14) were grown in monolayer cultures at 33°C, 37°C and 39°C. Reverse transcribed cDNA was amplified using; 5α-Reductase type 1 primers (A), type 2 primers (B) and GAPDH primers (C). The expected PCR product was 170bp, 350bp and 597bp for 5α-R1, 5α-R2 and GAPDH respectively. Abbreviations: reagent only sample (RO), DNA marker (M), benign prostate hyperplasia (BPH)

CHAPTER 6

RESULTS

3-DIMENSIONAL CULTURES

6.1 INTRODUCTION

The aim of the studies described in Chapter 6 was to investigate the capacity of the Pre2.8 and S2.13 cell lines to form 3-dimensional (3-D) structures in vitro and in vivo, and to determine to what extent these structures reflect the morphology and differentiation of prostate tissue.

Primary cultures of prostate epithelial cells develop 3-D structures in Matrigel in the presence of S2.13-conditioned medium, with evidence of prostate morphology and differentiation (Hudson et al., 2000b). Consequently Matrigel was chosen for this study. Matrigel consists of approximately 60% laminin and other essential components of the basement membrane such as collagen-IV, heparin sulphate proteoglycans, nidogen and varying concentrations of growth factors (Malinda and Kleinman, 1996). Pre2.8 cells were routinely grown in a commercially available serum-free prostate epithelial medium, PrEGM. It has previously been determined that this culture medium supports the growth of prostate epithelial cells (Fry et al., 2000c). S2.13 cells were routinely grown in DMEM (Life Technologies) supplemented with 10% foetal calf serum (FCS). Stromal cells tend not to grow in the absence of serum (Peehl and Stamey, 1986b; Peehl et al., 1988a).

In this chapter attempts to optimise growth conditions for co-cultures of Pre2.8 and S2.13 cells are described. 3-D structures were compared for varying culture conditions. The role of the stroma in the development of 3-D culture by Pre2.8 was investigated. The morphology of the 3-D cultures was studied using immunofluorescence staining for cytokeratins, immunocytochemistry staining for stromal cell markers and prostate-specific differentiation was studied at both protein and mRNA levels. The influence of androgen on the development of 3-D structures by Pre2.8 cells was also studied.

6.2 COMPARISON OF GROWTH OF PRE2.8 AND S2.13 CELLS IN VARIOUS TISSUE CULTURE MEDIA

Before setting up co-cultures of Pre2.8 and S2.13 cells, it was necessary to find a medium that both cell types could happily grow in.

6.2.1 Growth Of Pre2.8 Cells In Serum-Free PrEGM And RPMI-1640 Medium In The Presence And Absence Of Serum

PrEGM is an expensive specialised serum-free epithelial growth medium, whereas RPMI-1640 is a cheap, general-purpose growth medium. To try to reduce costs, the growth of Pre2.8 cells in PrEGM medium was compared to growth in serum-free RPMI and RPMI containing 8% FCS serum (RPMI/FCS) at 33°C, 37°C and 39°C. Comparisons were made of the morphology and cell number after 4 days culture.

Pre2.8 cells died within a few days in serum-free RPMI medium at 37°C and 39°C. At 33°C the epithelial cells were alive after 14 days in serum-free medium, but did not survive passaging. The Pre2.8 cells survived in RPMI/FCS medium at 33°C and 37°C, while at 39°C cells proliferated for about 6 days, but then stopped dividing and were dead by day 20.

The morphology of Pre2.8 cells changed when grown in RPMI/FCS, particularly at 37°C and 39°C (figure 6.1). Some cells were elongated at 33°C and this appearance was more frequent at higher temperatures. At 37°C and 39°C the cells tend to grow as discrete colonies in RPMI/FCS, in contrast to their more scattered appearance in PrEGM.

Figure 6.1: Comparison Of Pre2.8 Cell Morphology In PrEGM And RPMI/FCS Media

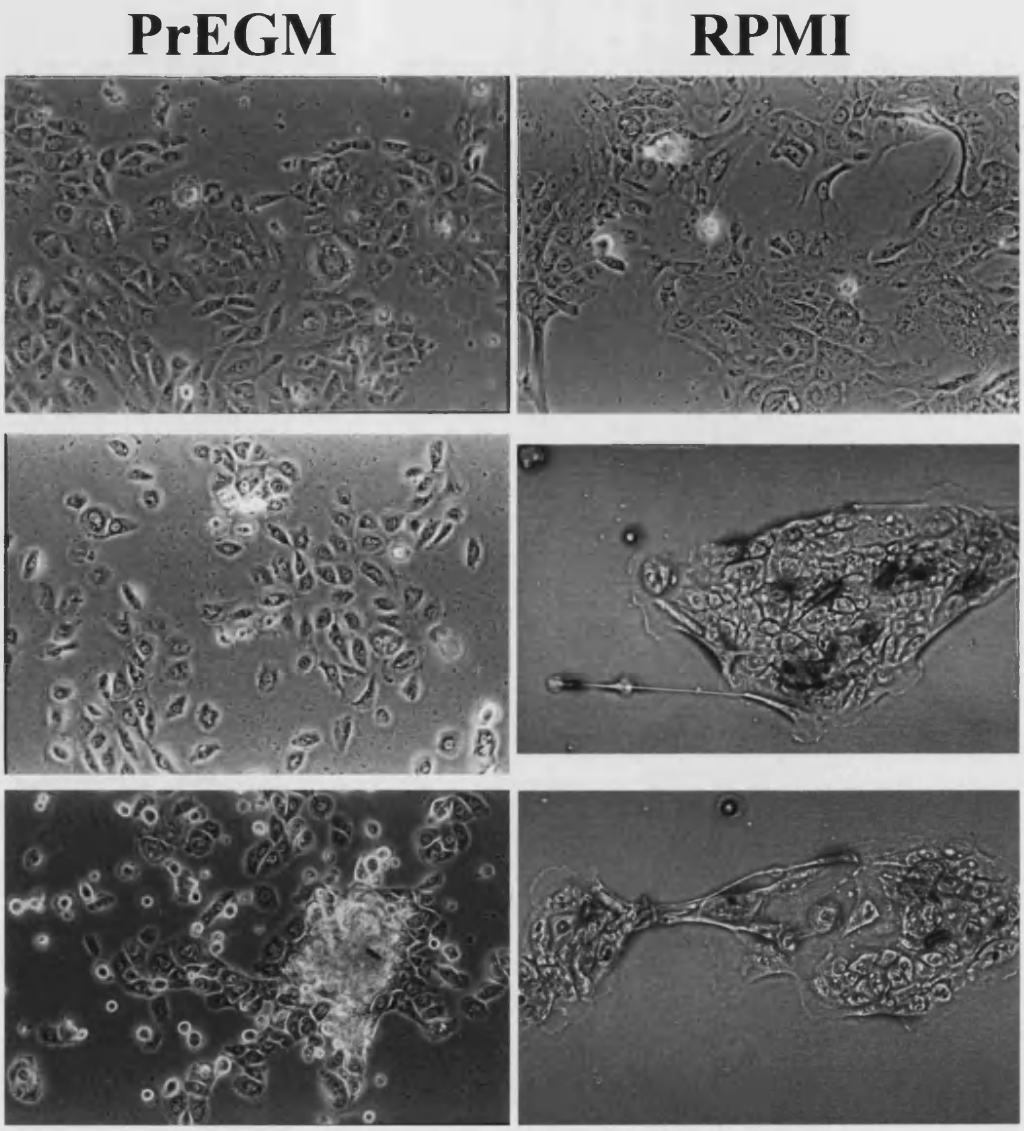

Monolayer cultures of Pre2.8 epithelial cells grown in PrEGM or RPMI/FCS medium for 10 days at 33°C, 37°C and 39°C. Original magnification x20

6.2.2 Proliferation Of Pre2.8 Cells In Various Media

Pre2.8 cells were grown in 4 media: PrEGM, RPMI/FCS, KGM (Keratinocyte-SFM medium), DMEM/FCS and mixtures of these media for 4 days at 33°C. The growth rates were compared using the MTT assay. All assays were repeated 3 times.

RPMI/FCS and DMEM/FCS medium alone and a mixture containing equal volumes of both resulted in the highest growth rates (figure 6.2). PrEGM and KGM, alone or in combination resulted in the lowest growth rates (figure 6.2). Equal volumes of DMEM/FCS (routine S2.13 growth medium) and PrEGM (routine Pre2.8 growth medium) produced approximately half the maximum rate of proliferation achieved with RPMI/FCS alone or DMEM/FCS with RPMI/FCS (figure 6.2).

Figure 6.2:Comparison Of Pre2.8 Cell Proliferation In Different Media At 33°C

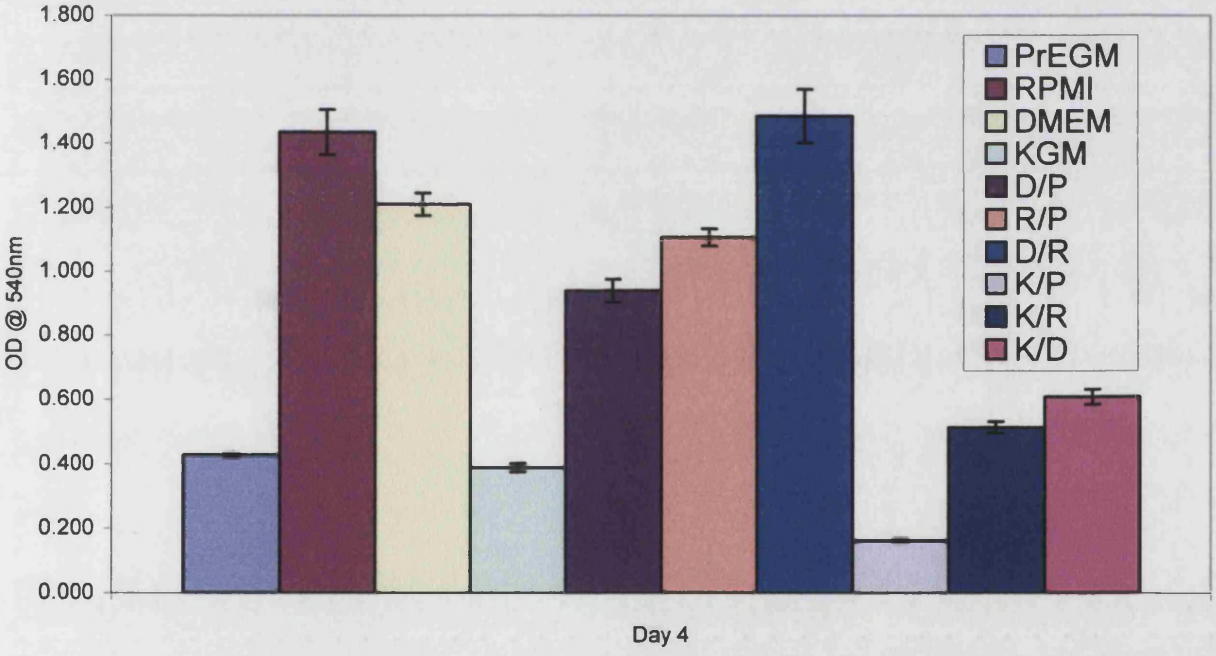

The average and standard error of 3 replicate experiments to compare the growth of Pre2.8 cells with different media combinations. Abbreviations: D/P – DMEM/PrEGM; R/P – RPMI/ PrEGM; D/R – DMEM/ RPMI; K/P – KGM/ PrEGM; K/R – KGM/ RPMI; K/D – KGM/ DMEM

6.2.3 Proliferation Of S2.13 Cells In Various Media

The growth of S2.13 cells was compared in RPMI/FCS, DMEM/FCS (routine S2.13 growth medium), PrEGM (routine Pre2.8 growth medium), DMEM/FCS with PrEGM, RPMI/FCS with PrEGM or RPMI/FCS with KGM (Keratinocyte-SFM medium) medium. The cells were plated at a density of 500,000/T25 flask and grown at 33°C and 37°C. Because S2.13 cells metabolise MTT poorly, comparisons were made using cell counts (figures 6.3 and 6.4). All assays were repeated 3 times.

The highest cell numbers were obtained with a combination of DMEM/FCS with PrEGM and RPMI/FCS with KGM medium at 33°C (figure 6.3). Similar results were obtained at 33°C and 37°C (figure 6.3 and 6.4, respectively).

Conclusion

Pre2.8 and S2.13 grew best in RPMI and DMEM, but RPMI-1640 altered the morphology of Pre2.8 cells. Equal volumes of PrEGM (routine growth medium for Pre2.8 cells) and DMEM (routine growth medium for S2.13 cells) produced similar rates of proliferation for Pre2.8 and S2.13 cells in monolayer cultures, and therefore this mixture was selected for further study.

Figure 6.3: Comparison Of S2.13 Cell Proliferation In Different Media At 33°C

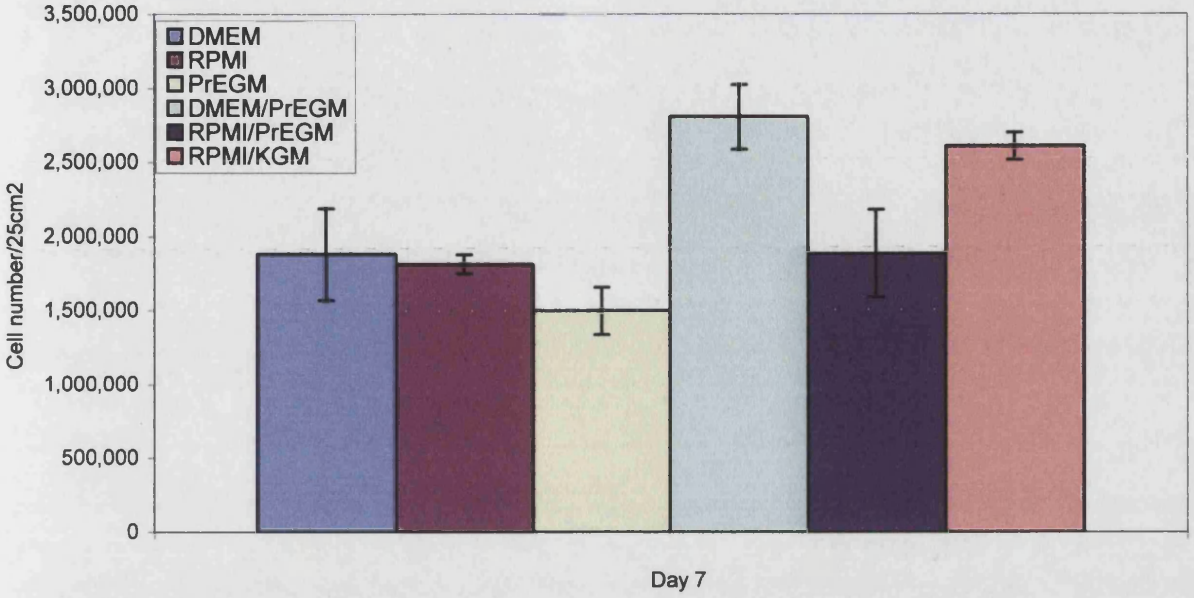

Figure 6.4: Comparison Of S2.13 Cell Proliferation In Different Media At 37°C

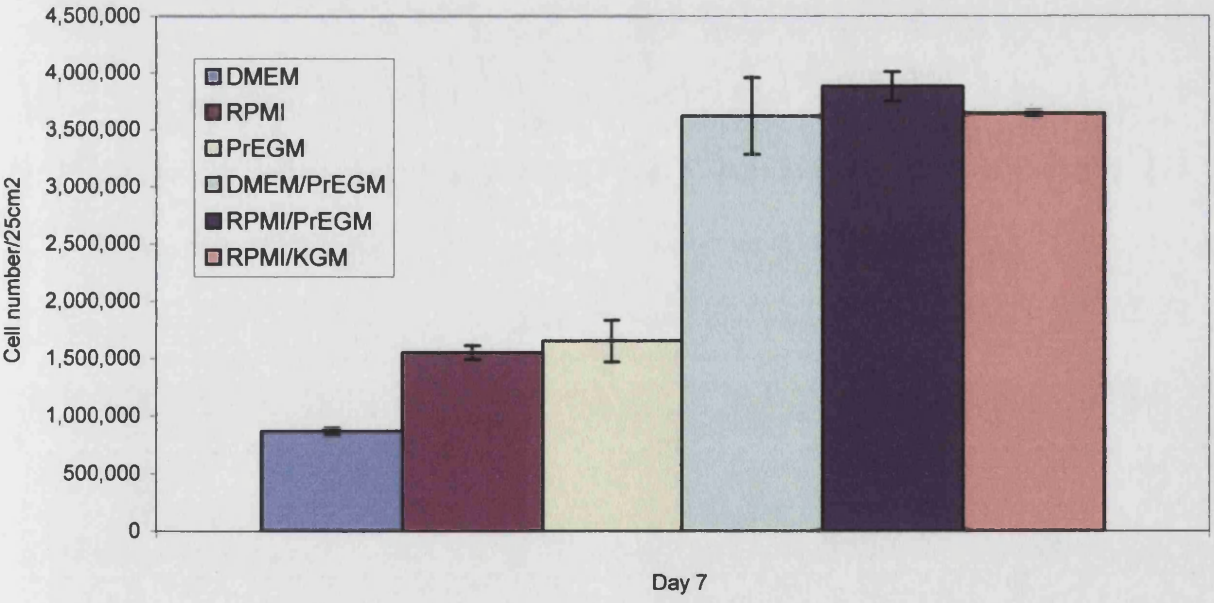

The average and standard error of 3 replicate experiments for comparison of S2.13 cell growth with different media combinations, after 7 days in culture at 33°C (top histogram) and 37°C (bottom histogram).

6.3 EFFECT OF STROMAL CELLS AND CONDITIONED MEDIUM ON THE GROWTH OF PRE2.8 CELLS IN 3-DIMENSIONAL CULTURE

A comparison of the growth of Pre2.8 cells in matrigel (3-D) cultures with equal volumes of PrEGM and DMEM/FCS or PrEGM only was carried out when mixed with S2.13 cells, 3T3 mouse fibroblasts or S2.13 conditioned medium.

Because S2.13 stromal cells grow approximately 4 times faster than Pre2.8 epithelial cells in monolayer culture, initially a Pre2.8/S2.13 ratio of 4:1 was used. Pre2.8 epithelial and S2.13 stromal cells were mixed at a ratio of 4:1 and grown in Matrigel at 33°C, 37°C and 39°C. The morphology of the 3-D cultures was examined under the light phase inverted microscope for up to 20 days of culture (figure 6.5).

Three main types of 3-D structures were observed at each temperature (figure 6.5). At 33°C the cells formed a lattice, consisting of dark clumps of cells connected by fainter tube-like structures. At 37°C cells accumulated together in fewer, larger interconnected organoids. At 39°C the cells formed many small organoids. The co-cultures tended to form lattices in PrEGM alone, and mixtures of small and large organoids in the presence of serum.

The replacement of S2.13 cells with conditioned medium (S2.13 supernatant – cells grown in PrEGM medium) at 33°C and 37°C (table 6.1) (figure 6.6) produced lattices. 3-D structures did not develop when S2.13 cells were grown alone in Matrigel. Very small organoids were seen when Pre2.8 cells only were grown in Matrigel at 33°C and 37°C (figure 6.6). These structures were compared to larger interconnected organoids seen when Pre2.8 and S2.13 cells (ratio of 4:1) were grown in Matrigel in equal volumes of PrEGM and DMEM/FCS (figure 6.6). Similar results were obtained for each of these conditions in the presence and absence of mibolerone. The addition of mibolerone at either 10^{-8} or 10^{-9}M tended to favour the production of small and large organoids (table 6.1, figure 6.6).

The development of 3-D structures was not improved by increasing the concentration of S2.13 cells. When larger numbers of cells (ratios of 1:8 and 1:10) were present the matrigel contracted into a ball.

When 400,000 mouse 3T3 fibroblasts were grown alone in matrigel (3-D) cultures or as a mixture with 100,000 Pre2.8 cells in matrigel cultures, the matrigel contracted into a ball. A ratio of 1:1 for Pre2.8/3T3 cells in matrigel produced 3-D structures similar to Pre2.8/S2.13 matrigel cultures.

Most stromal cells died in Pre2.8/S2.13 matrigel cultures with PrEGM only medium and with equal volumes of PrEGM and DMEM/FCS. Epithelial cell markers (e.g. figures 6.8) stain nearly all cells present in sections of the organoids, except for a few unstained cells (Hoechst^{+}) around the edge of each organoid that are likely to be stromal cells.

6.3.1 Stromal Cell Marker Expression Of 3-Dimensional Cultures

Pre2.8/S2.13, Pre2.8/3T3, S2.13 only and 3T3 only cells grown in matrigel were positive for vimentin and negative for smooth muscle actin (SMA) (table 6.2 and figure 6.7). Pre2.8 only cells were vimentin negative. Prostate tissue sections, NPro2 were vimentin and SMA positive and no background was observed in negative controls. Stromal cells were distributed in an unorganised manner throughout the matrigel.

6.3.2 Keratin Expression Of Pre2.8 Cells In 3-Dimensional Culture

Pre2.8 epithelial and S2.13 stromal cells were mixed at a ratio of 4:1 and grown in Matrigel at 33°C, 37°C and 39°C. 3-Dimensional structures obtained after 20 days in culture were formalin fixed and 7-10μm sections were prepared. Sections were used for immunohistochemistry. All experiments were repeated at least three times. The stained sections were used to study the morphology and degree of differentiation of the 3D structures. RNA was extracted from 3-D structures at 37°C and synthesised into cDNA by reverse transcriptase for PCR analysis of basal and luminal keratin expression.

Pre2.8/S2.13 matrigel cultures had the same cytokeratin pattern at 33°C, 37°C and 39°C (table 6.2). Limited immunocytochemistry could be carried out on 39°C sections due to the small size of spheroids. All secondary antibody controls were negative (table 6.2). Sections of BPH tissue were used for positive controls.

K14/K17 expression

The basal (outer) layer of the organoids was positive for K14 and K17 at 33°C and 37°C (figure 6.8) using double immunofluorescence. K17 was more intensely positive in the

central (luminal) areas of the organoids (figure 6.8). Almost all the cells stained for K17 throughout the organoids.

Pre2.8/3T3 and Pre2.8 only matrigel cultures were positive for K14 and K17 immunofluorescent double staining at 37°C (table 6.2 and figure 6.9). Architecture was similar to Pre2.8/S2.13 organoids, with an outer basal layer and an inner luminal layer.

S2.13 and 3T3 cells grown alone were negative for K14 and K17 (not included in figures). Prostate tissue sections were positive and there was no background present in negative controls (table 6.2 and figure 6.9).

RT-PCR was carried out to confirm the expression of a basal cell marker at the RNA level. Pre2.8/S2.13 co-cultures (1:1 and 1:4) and Pre2.8 only ($1x10^5$ cells) RNA was positive for K5, producing a 350bp fragment as predicted (table 6.4 and figure 6.15). S2.13 alone ($1x10^5$ and $4x10^5$ cells) and LNCaP and DU145 cell lines were negative for K5, as expected. The reagent only samples were negative. The level of RNA expression for K5 was not affected by increasing concentrations of S2.13 stromal cells.

K19 expression

There was limited $K19^+$ stained cells, approximately 1% (figure 6.10).

K8 expression

The percentage of K8 positive cells was difficult to estimate due to difficulty in obtaining satisfactory K8 staining. Immunofluorescent of K8 showed that approximately 10% of the cells are intensely K8 (figure 6.11). Using imunocytochemistry, K8 staining was positive at 33°C and 37°C, although there was faint background staining in the negative control (table 6.2) (figure 6.12). Highly structured organoids at 37°C clearly shows an inner luminal layer with an unstained outer layer, likely to be basal cells (magnification, figure 6.12).

K14/K8 expression

Co-staining of K14 and K8 produced similar results at 33°C, 37°C and 39°C (figures 6.13 and 6.14). These two keratins did not co-stain in the absence of mibolerone, although in the presence of mibolerone K8 was weakly positive in association with K14

(figures 6.13 and 6.14). The difference in K14/K8 co-staining in the presence of mibolerone is particularly clear in cells at 39°C (compare figures 6.13 and 6.14).

K18 Expression

K18 (a luminal epithelial cell marker) immunocytochemistry was negative for all samples including normal prostate tissue sections (NPro2). No conclusion could be made from these results. RT-PCR was carried out to determine K18 expression in Matrigel cultures, Pre2.8/S2.13 (1:1 and 1:4), S2.13 only ($1x10^5$ and $4x10^5$ cells) and Pre2.8 only ($1x10^5$ cells) matrigel cultures (table 6.4 and figure 6.15). A 544bp size fragment was expected. LNCaP cells were positive for K18, but all organoids (Pre2.8/S2.13, S2.13 only and Pre2.8 only) and the DU145 cell line were negative. Reagent only samples were negative.

6.4 EXPRESSION OF PROSTATE-SPECIFIC CHARACTERISTICS BY PRE2.8 CELLS IN 3-DIMENSIONAL CULTURE

Ideally a model of BPH should express nuclear AR and cytoplasmic PSA and PAP in luminal epithelial cells, with secretion of PSA into the medium. Pre2.8 epithelial and S2.13 stromal cells were mixed at a ratio of 4:1 and grown in Matrigel at 33°C, 37°C and 39°C. 3-Dimensional structures obtained after 24 days in culture were formalin fixed and 7-10μm sections were prepared. Sections of the 33°C and 37°C co-cultures were used for immunohistochemistry. Immunohistochemistry could not be carried out on the organoids grown at 39°C, due to their small size. All experiments were repeated at least three times.

RT-PCR was carried out to look for AR and PSA RNA expression in Pre2.8/S2.13 (1:1 and 1:4), S2.13 only ($1x10^5$ and $4x10^5$ cells) and Pre2.8 only ($1x10^5$ cells) matrigel cultures. The expected size fragments on an electrophoresis gel are 526bp (AR) and 362bp (PSA). β-Actin PCR was carried out on all samples to provide PCR amplification and loading controls. The metastatic prostate cell line, LNCaP was used as a positive control for AR and PSA. DU145, a metastatic cell line was included as a negative control for AR and PSA, but it turned out to be weakly positive for both. Reagent only (no template RNA) was used as a PCR contamination control.

6.4.1 Androgen Receptor (AR)

Pre2.8/S2.13 Matrigel sections were positive for AR at 33°C and 37°C in the absence and presence of mibolerone (table 6.2) (figure 6.16). The staining pattern for AR was nuclear and cytoplasmic and it was expressed in all the cells. S2.13 cells alone were unsuccessful and Pre2.8 only sections were negative. Benign prostate sections, NPro2 were positive for AR in the nucleus and there was no background staining in the secondary antibody negative control (figure 6.16).

AR expression was also tested by RT-PCR. The expected size fragment for AR primers is 526bp. The correct size band was found for Pre2.8/S2.13 co-culture, S2.13 only samples and LNCaP positive control (table 6.4 and figure 6.19). Pre2.8 only samples were negative. DU145 had a very faint band at 526bp. Reagent only samples were negative. The level of RNA expression for AR was increased with an increased stromal cell concentration from 100,000 cells seeded to 400,000 cells. This increase in RNA

expression was seen in S2.13/Pre2.8 co-cultures and in S2.13 only matrigel cultures. Equal RNA concentrations were observed for β-actin (table 6.4 and figure 6.19).

6.4.2 PSA

Similar nuclear and cytoplasmic expression was observed for PSA and AR in co-cultures grown at 33°C and 37°C in the absence and presence of mibolerone (table 6.2) (figure 6.17). The prostate tissue section, NPro2 showed PSA staining in the luminal epithelial cells and no background staining was present in negative controls (figure 6.17). A distinct PSA negative area was present in the centre of the organoids, where PSA secretion might be expected. PSA staining was observed in Pre2.8/S2.13 co-cultures, but it consisted of cytoplasmic and nuclear staining (table 6.2).

RT-PCR results for PSA were inconclusive (table 6.4 and figure 6.19). The expected size band for these PSA primers is 362bp. The LNCaP positive control and DU145 produced a band at the correct size, 362bp, but all other samples produced a 500bp fragment. Reagent only controls were negative.

Supernatants from Matrigel and monolayer cultures set-up with Pre2.8 and S2.13 cells grown in PrEGM/DMEM medium with and without mibolerone were tested for PSA. Samples from three different time points at 33°C, 37°C and 39°C were tested (table 6.3). All samples were negative for PSA, while controls (supernatants from the cell line LNCaP) were positive. Supernatant taken from Pre2.8/S2.13, S2.13 only and Pre2.8 only matrigel cultures were negative for PSA expression. If PSA is expressed in these cultures, it is not being secreted into the medium.

6.4.3 PAP

PAP was negative for all Pre2.8/S2.13 co-cultures and other cultures grown at 33°C and 37°C, in the presence or absence of mibolerone. Prostate tissue sections were positive for PAP antibody (table 6.2) (figure 6.18).

6.5 MIBOLERONE

Similar results were obtained in the presence and absence of mibolerone (figures 6.6, 6.13 and 6.14). The effect of mibolerone was studied under the various conditions described in the previous three sections (table 6.2) (figures 6.6, 6.13 and 6.14). The addition of mibolerone at either 10^{-8} or 10^{-9}M tended to favour the production of small and large organoids (table 6.2, figure 6.6) and possibly encourage co-expression of K14 and K8 (table 6.2, figures 6.13 and 6.13).

6.6 CELL PROLIFERATION

The presence of cell proliferation was examined by Ki-67 immunofluorescence. Ki-67 expression was observed in the NPro2 positive control, Pre2.8/S2.13 (4:1 cell ratio), Pre2.8/3T3 (1:1 cell ratio), S2.13 only (100,000 cells seeded) and Pre2.8 only (400,000 cells seeded) matrigel cultures (table 6.2 and figure 6.20). Proliferation appears more concentrated in 3T3/Pre2.8 compared to Pre2.8/S2.13 co-cultures.

Table 6.1: Morphology Of 3-D Cultures

Cell Type	Medium	Temp	Mibolerone	3-D Structures
Pre2.8/S2.13	PrEGM only	33°C	-	Lattice
			+	Small organoids
		37°C	-	Lattice
			+	Small organoids
Pre2.8/S2.13	PrEGM + DMEM/FCS	33°C	-	Small and large organoids
			+	Small organoids
		37°C	-	Large organoids
			+	Small and large organoids
Pre2.8 only	S2.13 conditioned medium (PrEGM). S2.13 supernatant – cells grown in PrEGM medium.	33°C	-	Lattice
		37°C	+	Small organoids
		33°C	-	Lattice
		37°C	+	Small organoids

Table 6.2: Immunohistochemistry Of 3-D Structures At 33°C, 37°C And 39°C

Temp	Sample	Mib	AR	PSA	PAP	K14	K17	K19	K8	K18	SMA	Vim	Ki67
33°C	Pre2.8/S2.13	+	+ *(n+c)*	+ *(n+c)*	-	+	+	-	+	*nt*	*nt*	*nt*	*nt*
	Pre2.8/S2.13	-	+ *(n+c)*	+ *(n+c)*	-	+	+	-	+	*nt*	*nt*	*nt*	*nt*
37°C	Pre2.8/S2.13	+	+ *(n+c)*	+ *(n+c)*	-	+	+	_	+	*nt*	*nt*	*nt*	*nt*
	Pre2.8/S2.13	-	+ *(n+c)*	+ *(n+c)*	-	+	+	-	+	-	-	+	+
	3T3/Pre2.8	-	+	-	-	+	+	-	*nt*	-	-	+	+
	Pre2.8 only	-	*b/g*	*nt*	*nt*	+	+	-	*nt*	-	-	-	-
	S2.13 only	-	*nt*	*nt*	-	-	-	-	*nt*	-	-	*nt*	+
	3T3 only	-	+	-	-	-	-	-	*nt*	-	-	+	+
39°C	Pre2.8/S2.13	+	*nt*	*nt*	*nt*	+	*nt*	*nt*	-	*nt*	*nt*	*nt*	*nt*
	Pre2.8/S2.13	-	*nt*	*nt*	*nt*	+	*nt*	*nt*	-	*nt*	*nt*	*nt*	*nt*
Control	Background		-	-	-	-	-	-	-	-	-	-	-
	Benign prostate (NPro2)		+ *(n)*	+ *(c)*	+ *(c)*	+	+	+	+	-	+	+	+

Abbreviations: AR (androgen receptor); PSA (prostate specific androgen); PAP (prostatic acid phosphatase); K (keratin antibody); SMA (smooth muscle actin); Vim (vimentin); Ki67 (proliferation marker); + (positive); - (negative); *n+c* (nuclear and cytoplasmic cell staining); *nt* (not tested); *b/g* (background staining)

Table 6.3: PSA Level In Co-Culture Supernatant

Set-up				Results		
Temp	Culture type	Sample	Mibolerone	PSA in culture supernatant		
				d11	d18	d19
33oC	3-D	Pre2.8/S2.13	+	-	-	-
	3-D	Pre2.8/S2.13	-	-	-	-
	monolayer	Pre2.8/S2.13	+	-	-	-
	monolayer	Pre2.8/S2.13	-	-	-	
37oC	3-D	Pre2.8/S2.13	+	-	-	-
	3-D	Pre2.8/S2.13	-	-	-	-
	monolayer	Pre2.8/S2.13	+	-	-	-
	monolayer	Pre2.8/S2.13	-	-	-	
39oC	3-D	Pre2.8/S2.13	+	-	-	-
	3-D	Pre2.8/S2.13	-	-	-	-
	monolayer	Pre2.8/S2.13	+	-	-	-
	monolayer	Pre2.8/S2.13	-	-	-	
		Pos control		+	+	+

Table 6.4: Summary Of RT-PCR Results

RNA origin (culture set-up at 37°C)	PSA	AR	K5 (Basal)	K18 (luminal)	β-Actin
	Expected fragment size				
	362bp	526bp	350bp	544bp	
Pre2.8/S2.13 (Culture ratio of 1:1)	pos (500bp)	w pos	pos	neg	pos
Pre2.8/S2.13 (Culture ratio of 1:4)	pos (500bp)	pos	pos	neg	pos
S2.13 only (100,000)	pos (500bp)	w pos	neg	neg	pos
S2.13 only (400,000)	pos (500bp)	pos	neg	neg	pos
Pre2.8 only (100,000)	pos (500bp)	neg	pos	neg	pos
LNCaP positive control	pos (362bp)	pos	neg	pos	pos
DU145	vw pos (362bp)	vw pos	neg	neg	pos
Reagent Only control	neg	neg	neg	neg	neg
Reverse Transcriptase control					neg

Abbreviations: pos – positive; wpos – weak positive; vw pos – very weak positive;

neg- negative

Figure 6.5: Spheroid Development Of 3-D Cultures

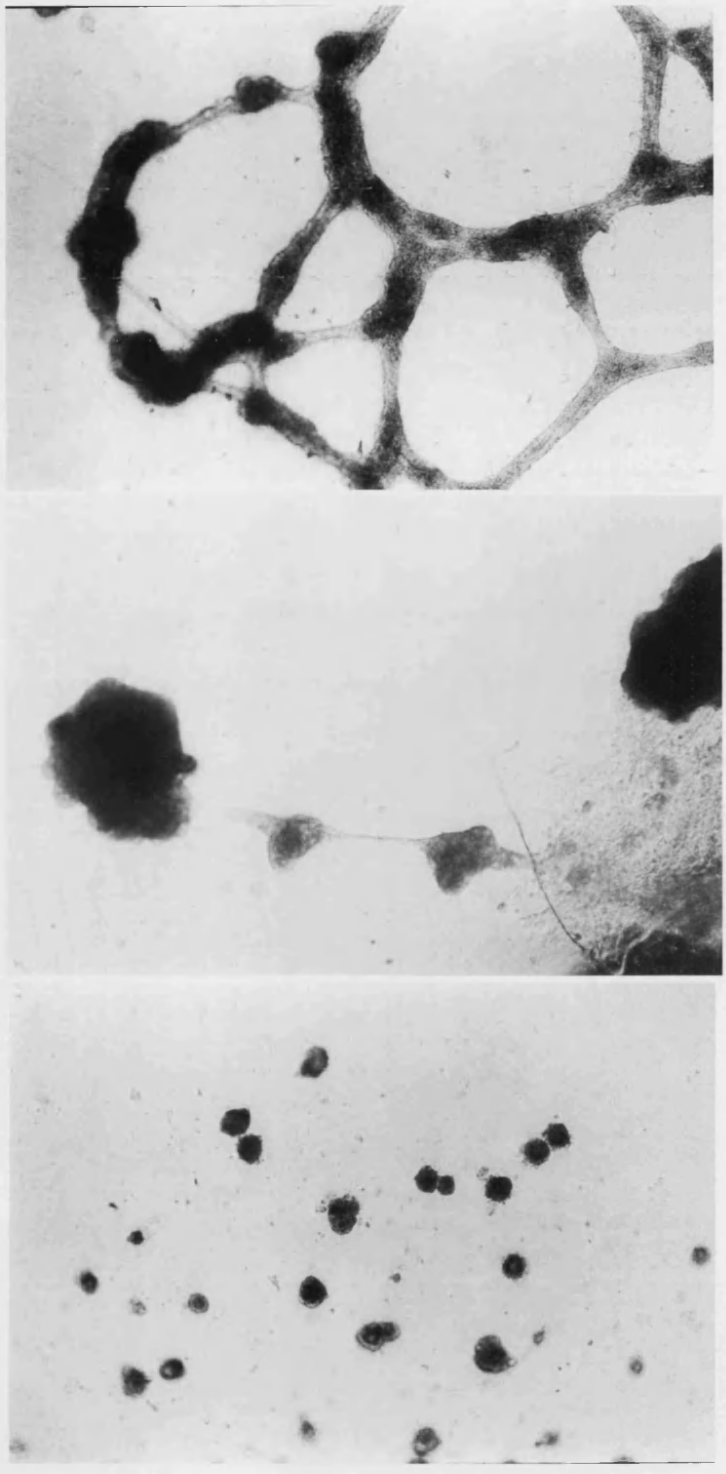

Comparison of organoid (spheroid) development for Pre2.8/S2.13 matrigel (in PrEGM and DMEM/FCS medium) co-cultures at 33°C, 37°C and 39°C, after 20 days in culture. Three main types of 3-D structures were observed; a lattice formation at 33°C, large interconnecting organoids at 37°C and small organoids at 39°C. Original magnification x40 (objective lense).

Figure 6.6: Effects Of Mibolerone On Spheroid Development

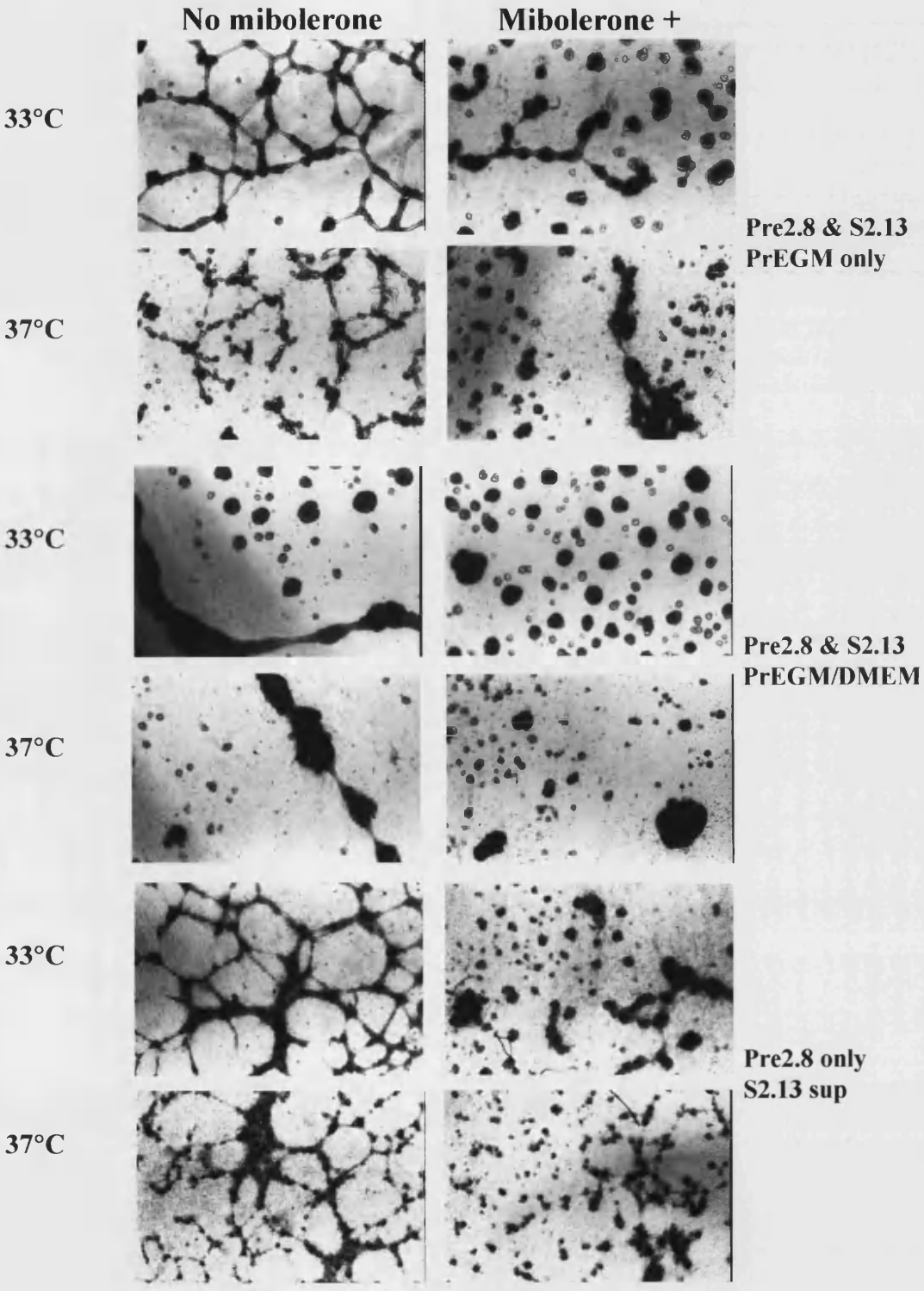

Comparison of organoid (spheroid) development for Pre2.8/S2.13 or Pre2.8 cells only, in matrigel co-cultures at 33°C, 37°C and 39°C, after 20 days in culture. Different culture conditions with and without mibolerone at 33°C and 37°C; 1) Pre2.8 and S2.13 cells in PrEGM medium only; 2) Pre2.8 and S2.13 cells in equal volumes of PrEGM and DMEM/FCS; 3) Pre2.8 cells only in S2.13 conditional PrEGM medium. Original magnification is x40 (objective lense).

Figure 6.7: Vimentin And SMA Expression In 3-D Cultures At 37°C

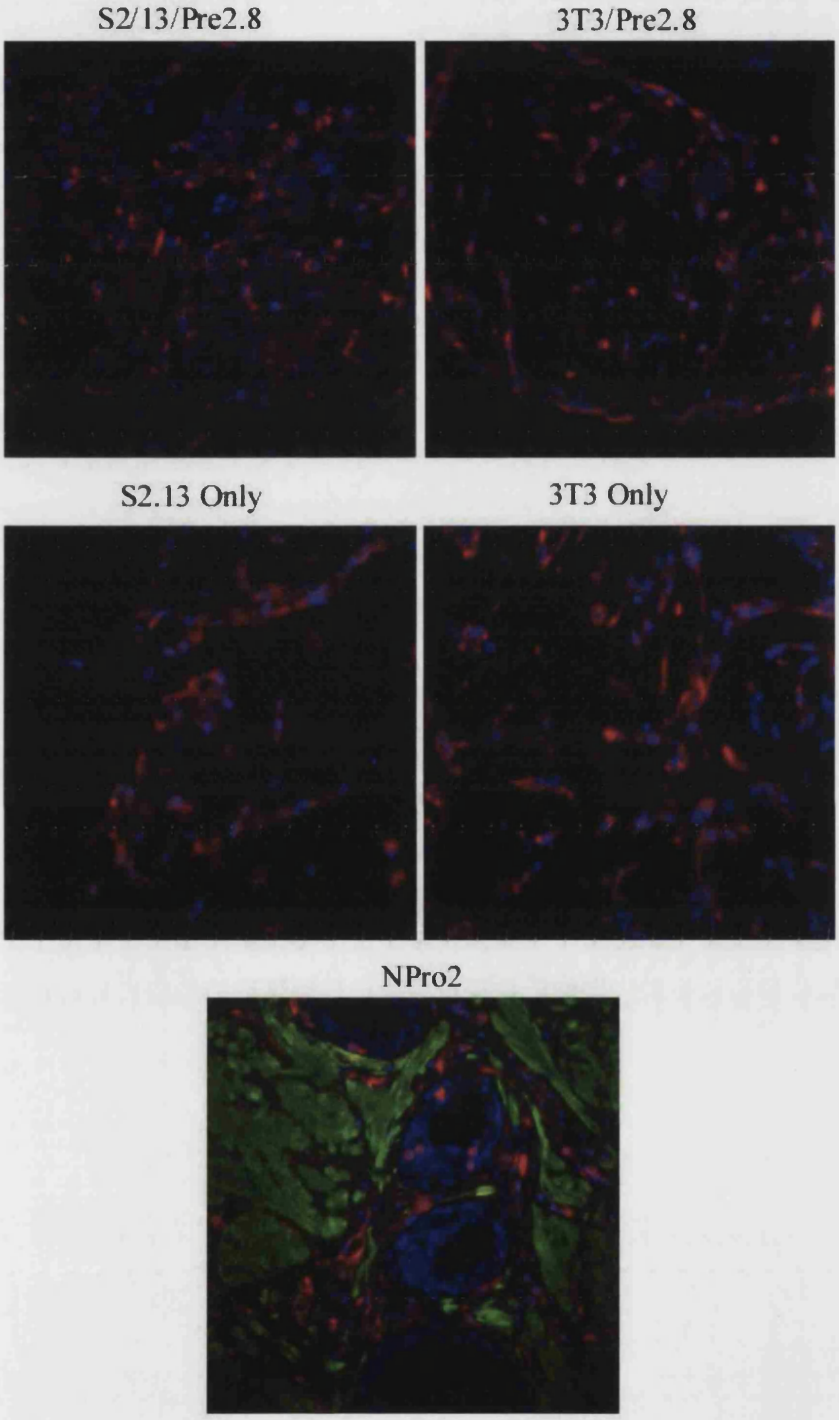

Paraffin sections of day 24 matrigel cultures (in PrEGM and DMEM/FCS medium) at 37°C with varying cell types, S2.13/Pre2.8, 3T3/Pre2.8, S2.13 only and Pre2.8 only cells. Normal prostate tissue (NPro2) sections were used as positive controls: Fluorescence: Vimentin (red); Smooth muscle actin (green); Hoechst (blue). Original Magnification is x40 (fluorescent microscope – objective lense).

Figure 6.8: K14 And K17 Expression In Pre2.8/S2.13 Matrigel Cultures At 37°C

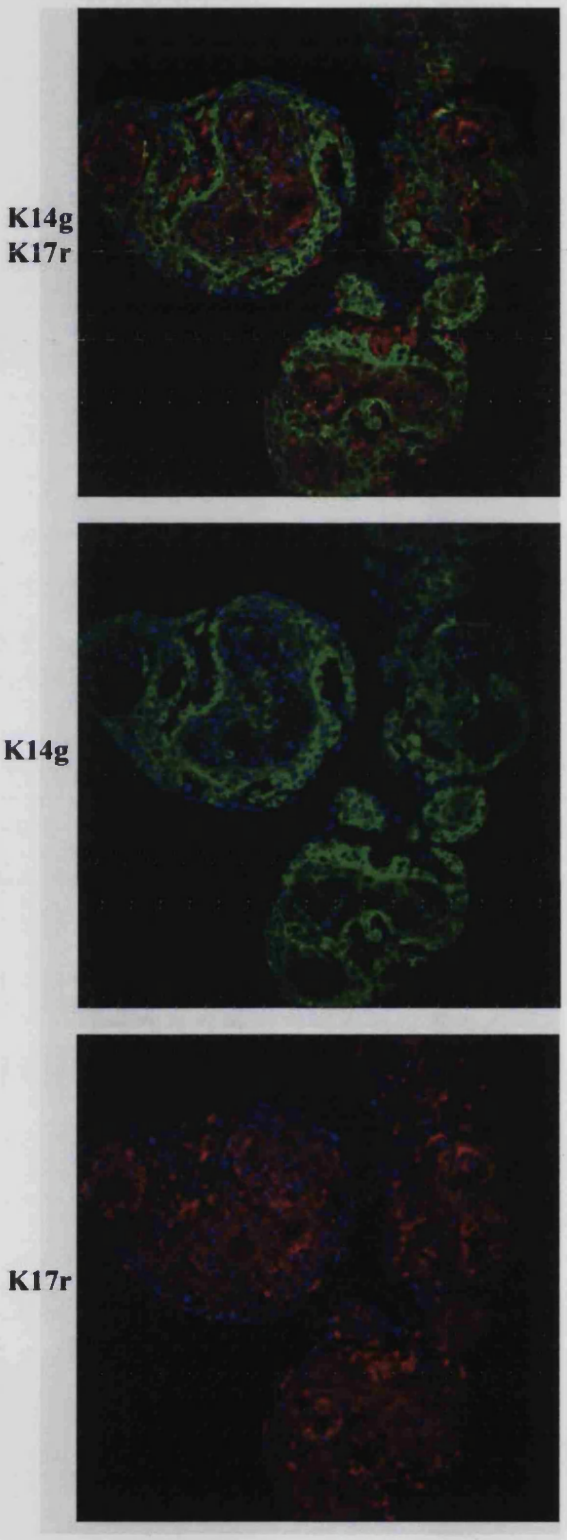

Paraffin sections of Pre2.8/S2.13 matrigel co-cultures (in PrEGM and DMEM/FCS medium) after 3 weeks at 37°C, in the presence of mibolerone, a synthetic DHT. Fluorescence: K14 (green); K17 (red); Hoechst (blue). Original Magnification is x20 (fluorescent microscope – objective lense).

Figure 6.9: K14 And K17 Expression In 3-D Cultures At 37°C

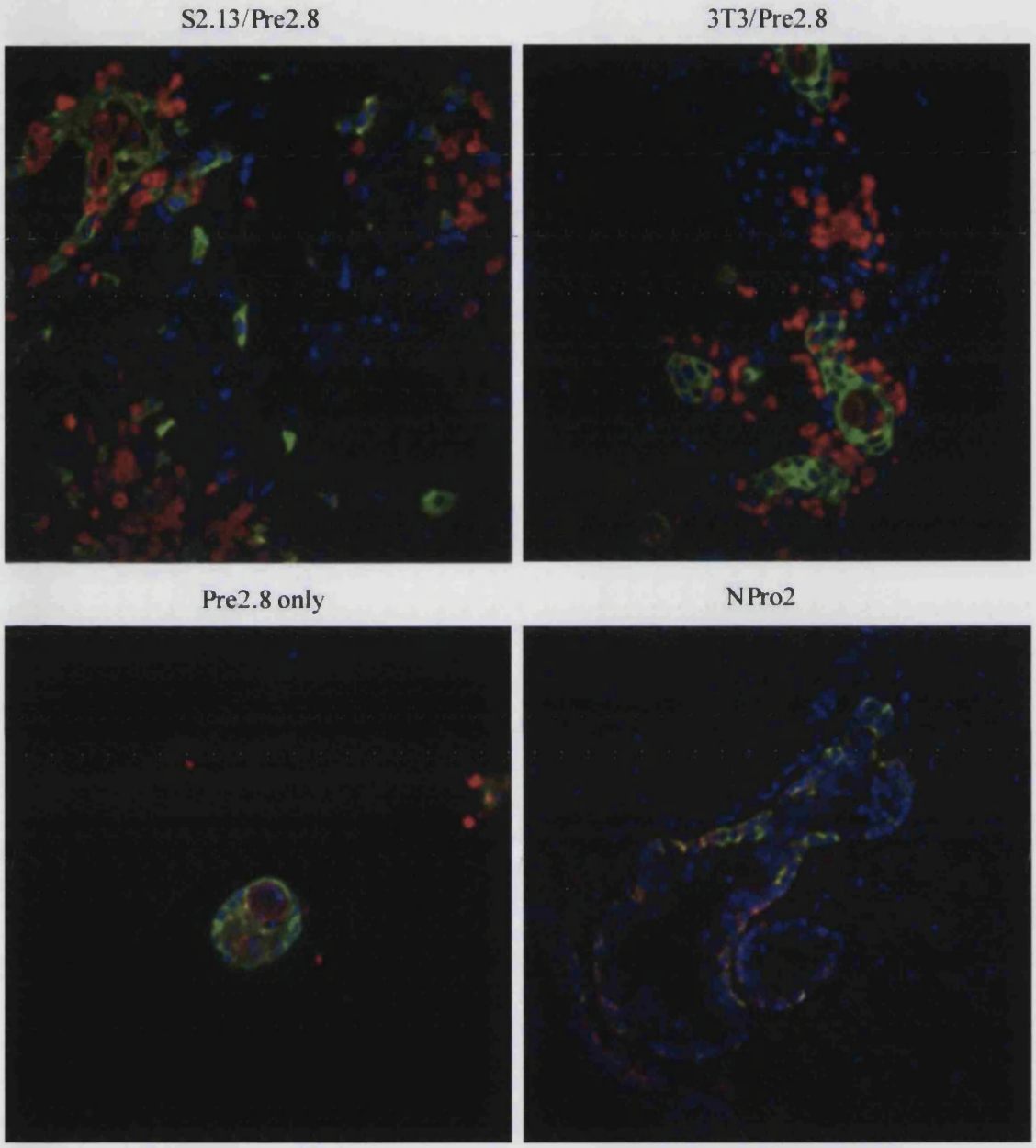

Paraffin sections of 24-day old matrigel cultures (in PrEGM and DMEM/FCS medium) at 37°C with varying cell types, S2.13/Pre2.8, 3T3/Pre2.8 and Pre2.8 only cells. Normal prostate tissue (NPro2) sections were used as positive controls. Fluorescence: K14 (green); K17 (red) and Hoechst (blue). Original magnification was x40 (fluorescent microscope – objective lense).

Figure 6.10: K19 Expression In Pre2.8/S2.13 Matrigel Cultures At 37°C

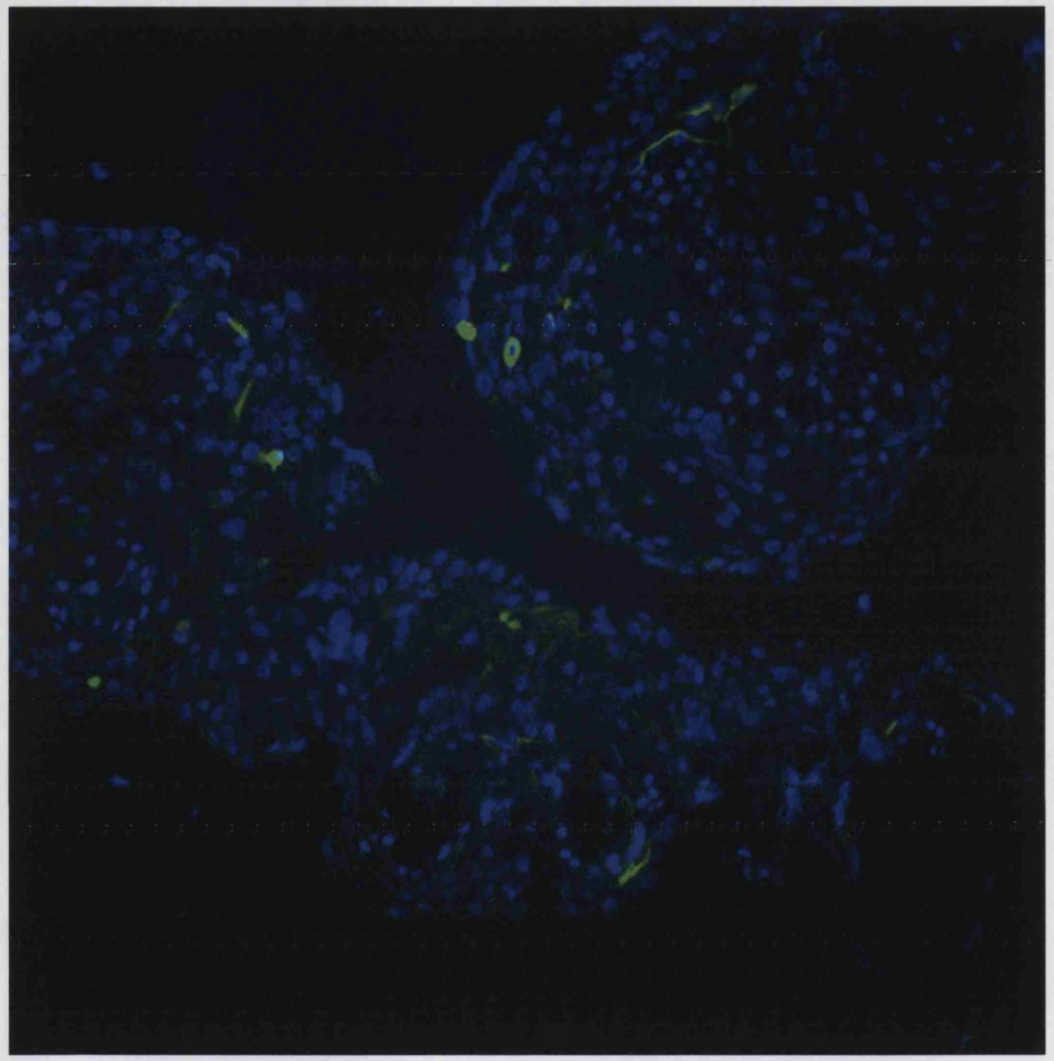

Paraffin section of Pre2.8/S2.13 matrigel co-culture (in PrEGM and DMEM/FCS medium) after 3 weeks at 37°C, in the presence of mibolerone, a synthetic androgen. Immunofluorescence was carried out with nuclear Hoechst (blue) and keratin 19 (green). Original magnification was x20 (fluorescent microscope – objective lense).

Figure 6.11: K8 Expression In Pre2.8/S2.13 Matrigel Cultures At 37°C

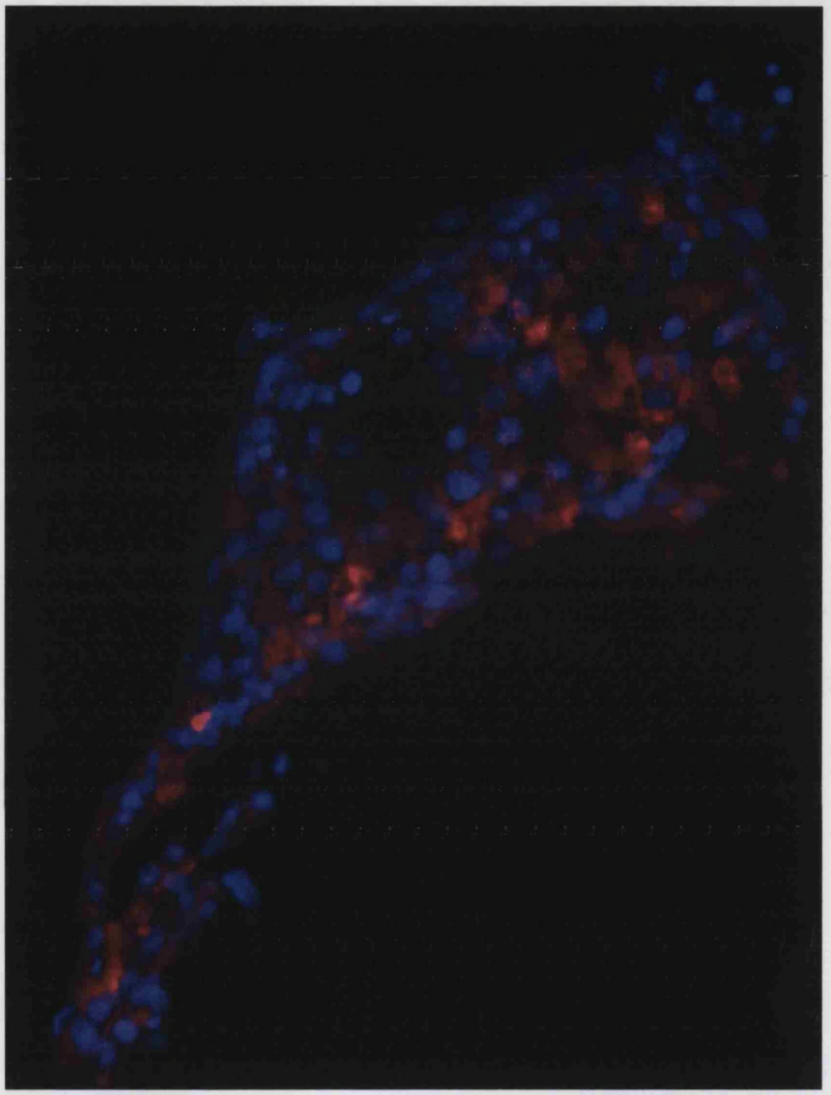

Paraffin section of Pre2.8/S2.13 matrigel co-culture (in PrEGM and DMEM/FCS medium) after 3 weeks at 37°C, in the presence of mibolerone, a synthetic androgen. Immunofluorescence was carried out with nuclear Hoechst (blue) and keratin 8 (red). Original magnification was x20 (fluorescent microscope – objective lense).

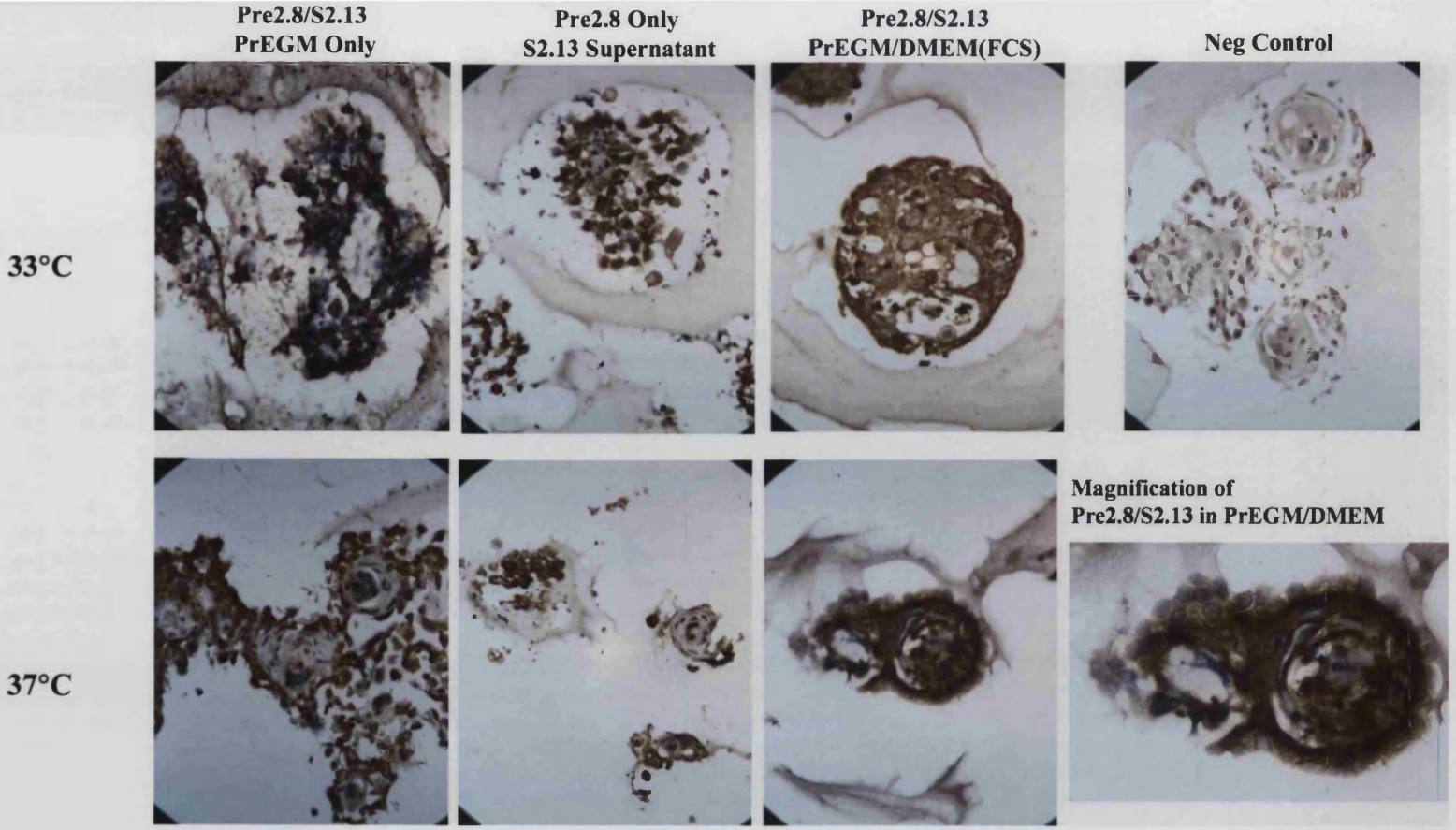

Paraffin sections from 3-D matrigel co-cultures after 3 weeks at 33°C and 37°C, in the presence of mibolerone, a synthetic DHT. Cultures were set up either with Pre2.8/S2.13 cells in PrEGM medium only, Pre2.8 cells only in S2.13 supernatant or Pre2.8/S2.13 in equal volumes of PrEGM and DMEM/FCS. DAB staining: K8 (brown); hematoxylin (blue). Original Magnification is x40 (objective lense).

Figure 6.13: K14 And K8 Expression In Pre2.8/S2.13 Matrigel Cultures Without Mibolerone

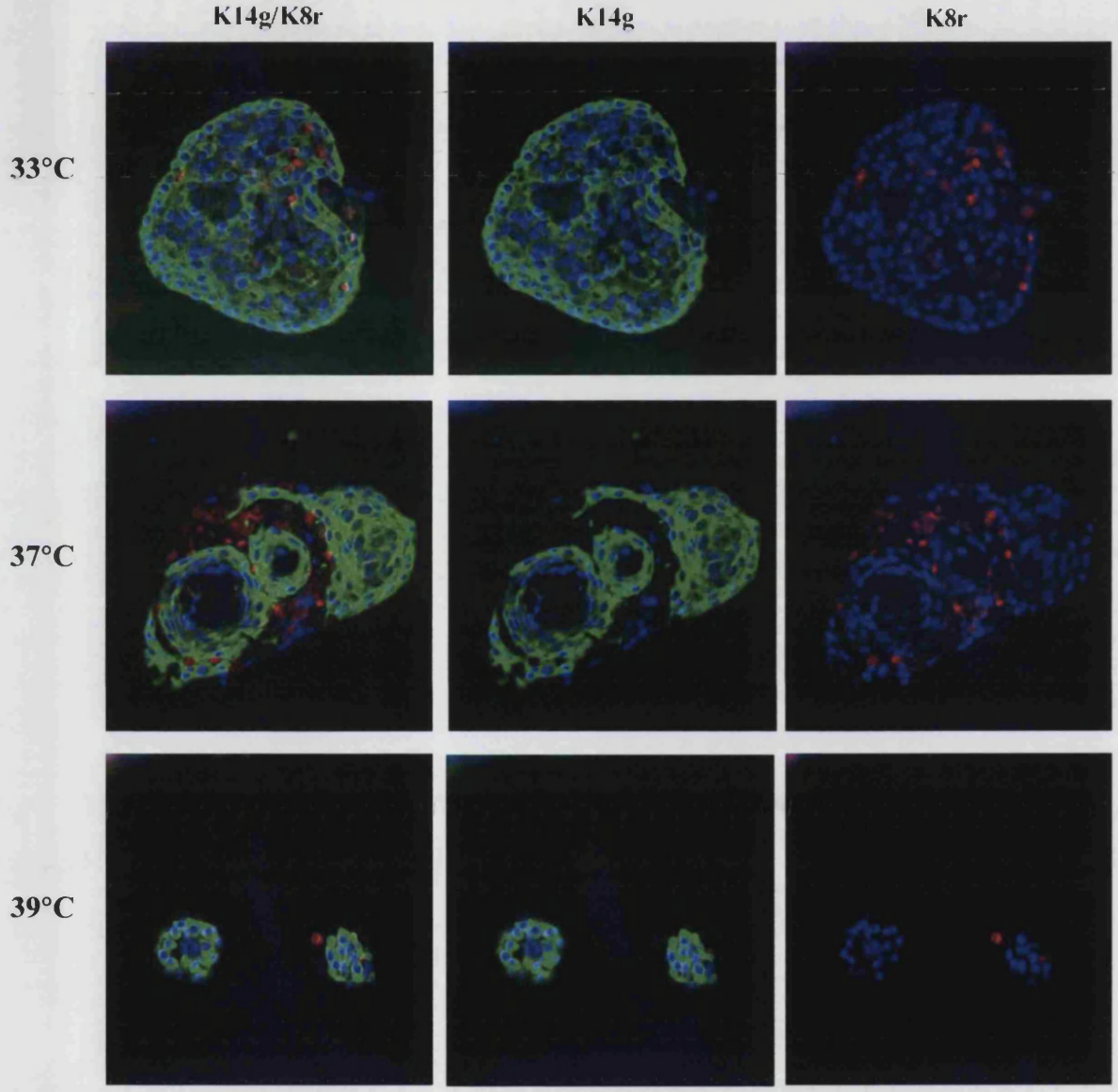

Paraffin sections of Pre2.8 and S2.13 matrigel co-cultures (in PrEGM and DMEM/FCS medium) after 3 weeks at 33°C, 37°C and 39°C, without mibolerone, a synthetic androgen. Fluorescence: K14 (green); K8 (red); Hoechst (blue). Original Magnification is X40 (fluorescent microscope – objective lense).

Figure 6.14: K14 and K8 expression in Pre2.8/S2.13 Matrigel Cultures with Mibolerone

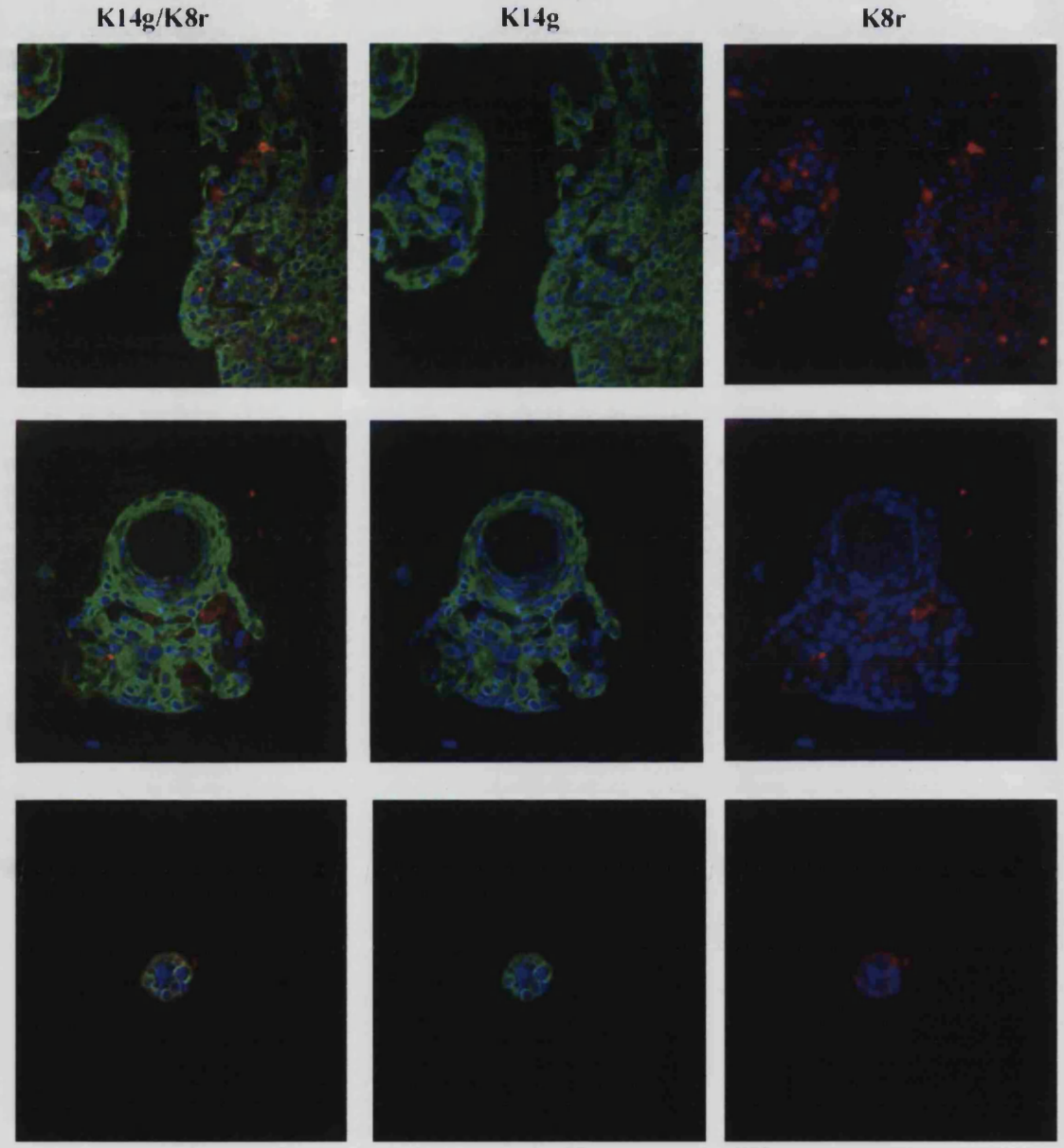

Paraffin sections of Pre2.8 and S2.13 matrigel co-cultures (in PrEGM and DMEM/FCS medium) after 3 weeks at 33°C, 37°C and 39°C, in the presence of mibolerone, a synthetic androgen. Fluorescence: K14 (green); K8 (red); Hoechst (blue). Original Magnification x40 (fluorescent microscope – objective lense).

Figure 6.15: Keratin 5 And Keratin 18 RNA Expression In 3-D Cultures

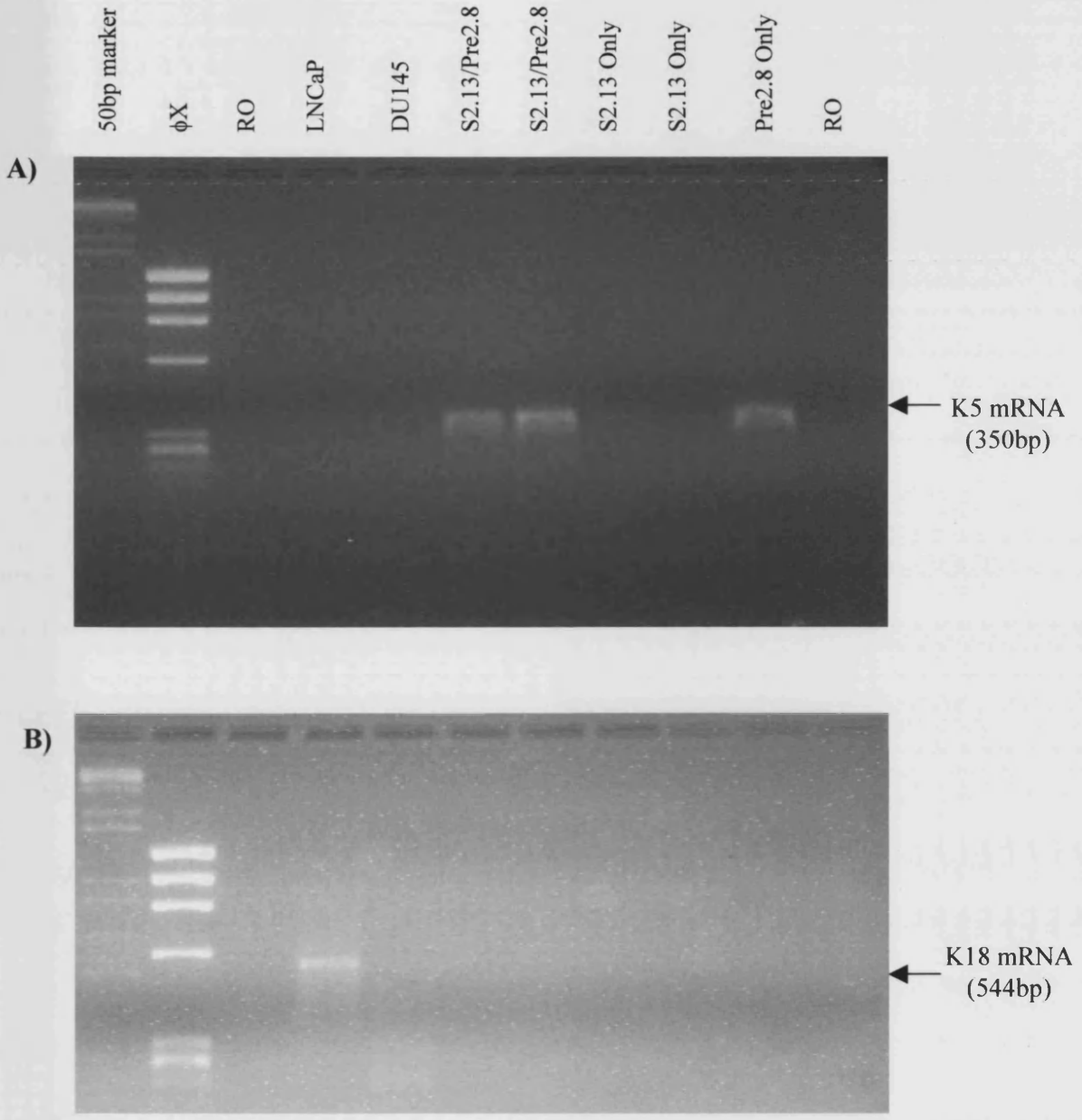

Pre2.8 and S2.13 cells were set up in matrigel cultures together and alone. Reverse transcribed cDNA was amplified using K5 primers (A) and K18 primers (B). The expected PCR product for K5 is 350bp and for K18 is 544bp.

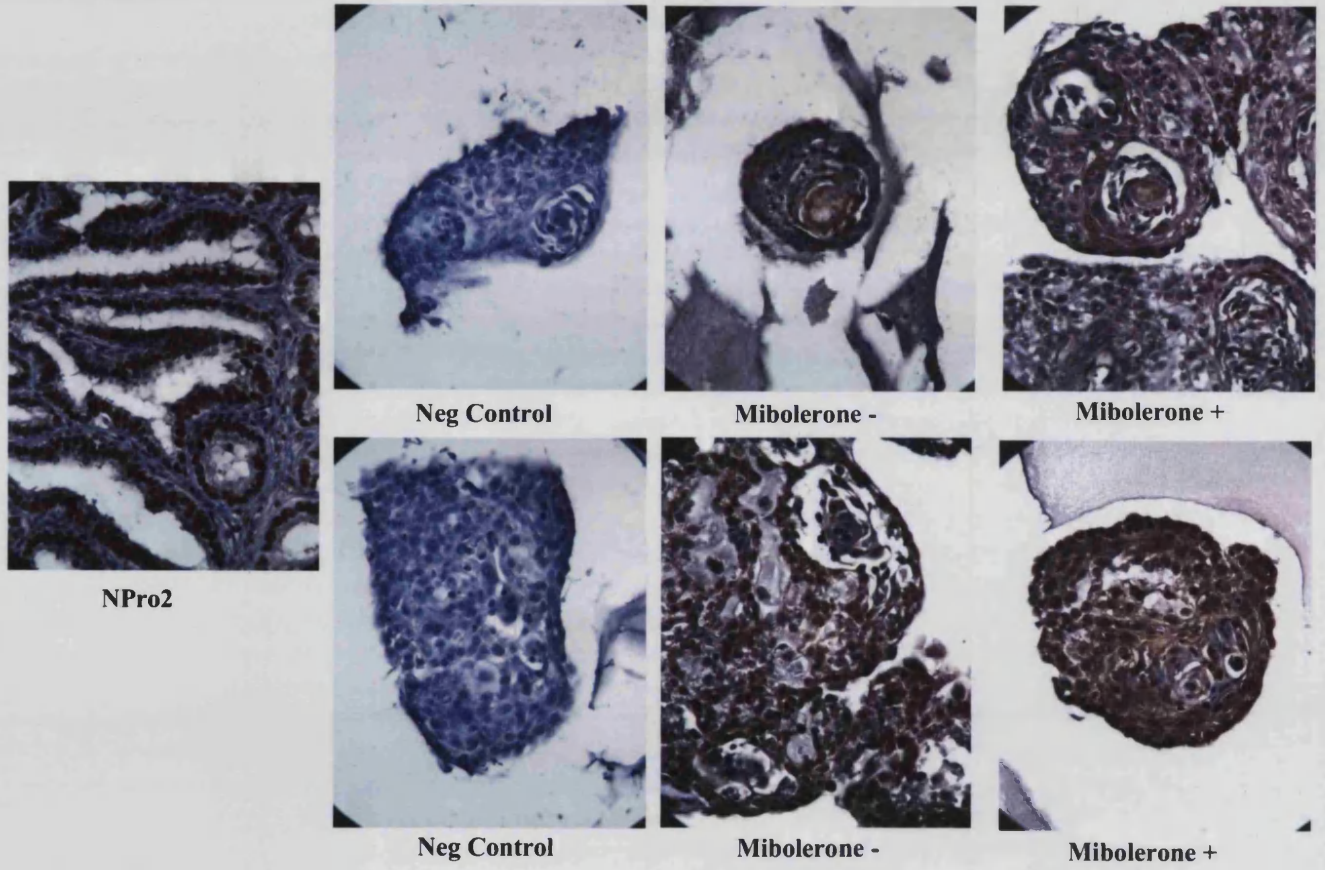

Paraffin sections of day 24, S2.13/Pre2.8 matrigel cultures at 33°C and 37°C. Cultures were set up in the presence and absence mibolerone. Normal prostate tissue (NPro2) sections were used as positive controls. Spheroid sections were used as negative controls (i.e. no primary antibody). DAB staining: AR (brown); Hoechst (blue). Original Magnification is x40 (objective lense).

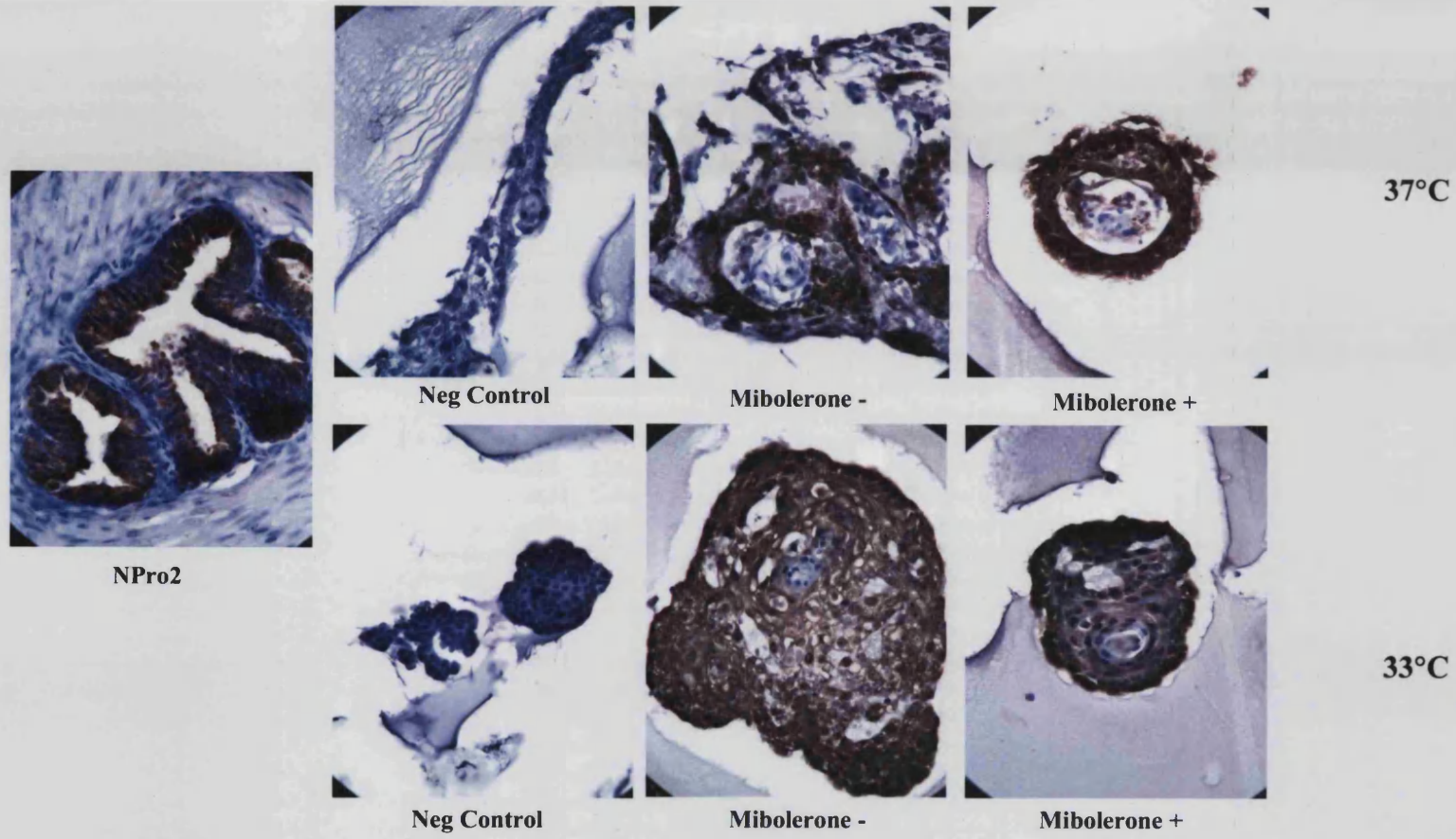

Paraffin sections of day 24, S2.13/Pre2.8 matrigel cultures at 33°C and 37°C. Cultures were set up in the presence and absence mibolerone. Normal prostate tissue (NPro2) sections were used as positive controls. Spheroid sections were used as negative controls (i.e. no primary antibody). DAB staining: PSA (brown); Hoechst (blue). Original Magnification is x40 (objective lense).

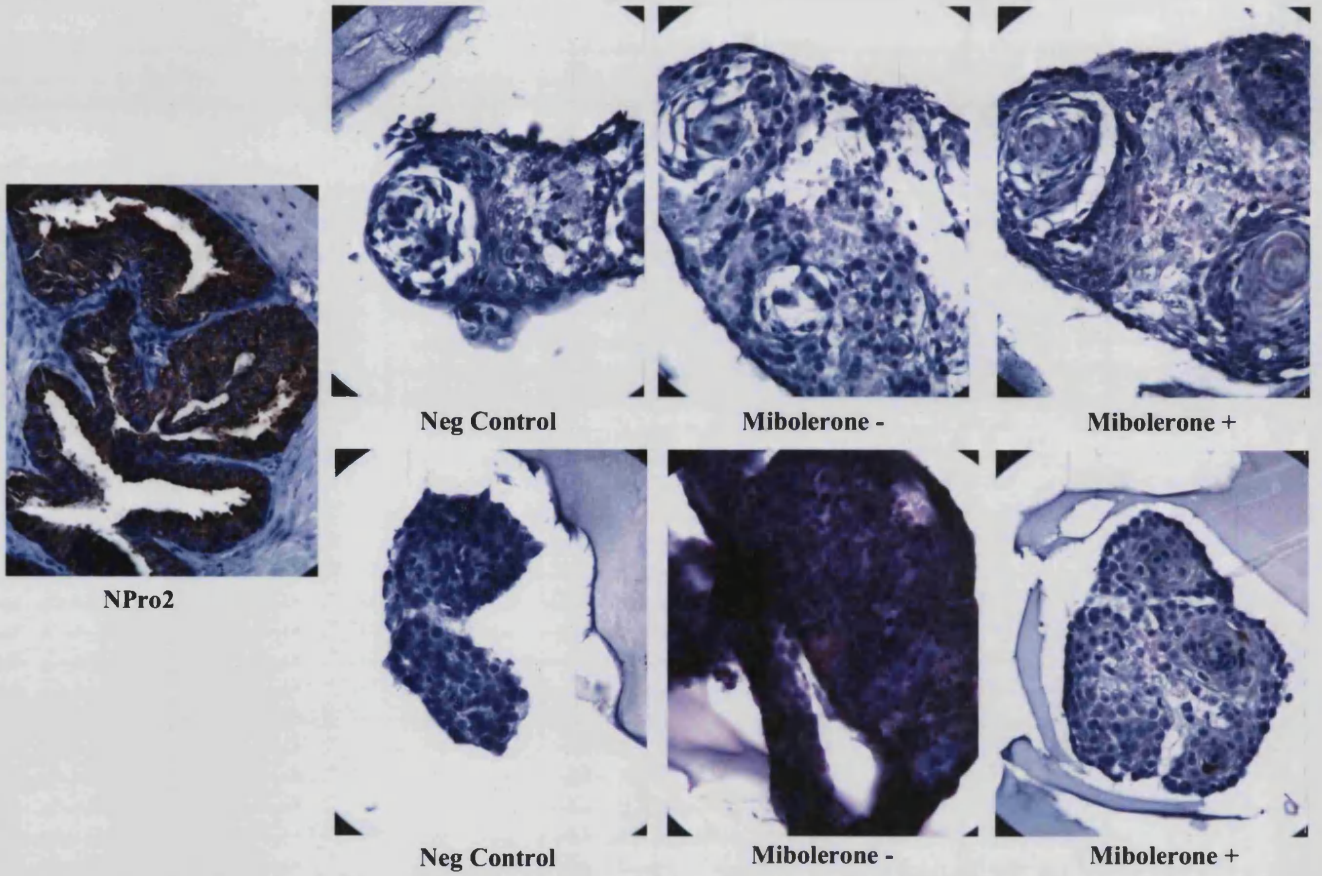

Paraffin sections of day 24, S2.13/Pre2.8 matrigel cultures at 33°C and 37°C. Cultures were set up in the presence and absence mibolerone. Normal prostate tissue (NPro2) sections were used as positive controls. Spheroid sections were used as negative controls (i.e. no primary antibody). DAB staining: PAP (brown); Hoechst (blue). Original Magnification is x40 (objective lense).

Figure 6.19: AR And PSA RNA Expression In 3-D Cultures

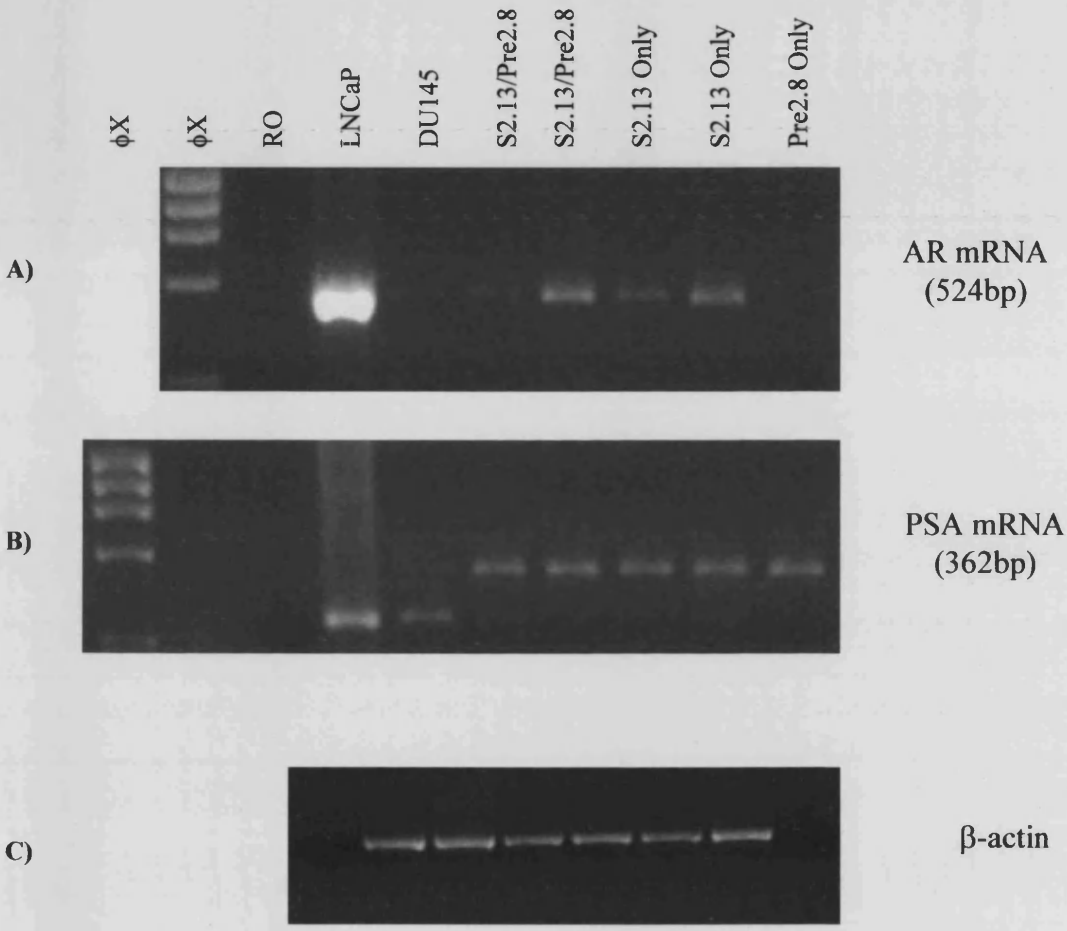

Pre2.8 and S2.13 cells were set up in matrigel cultures together and alone. Reverse transcribed cDNA was amplified using; A) ARAs and ARDa primers, located on exon 1 and exon 4 of AR, respectively and B) PSA. The expected PCR product for AR is 524bp and for PSA is 362bp. C) Equal loading and integrity of the RNA was confirmed by amplification of β-actin mRNA.

Figure 6.20: Proliferation In 3-D Cultures

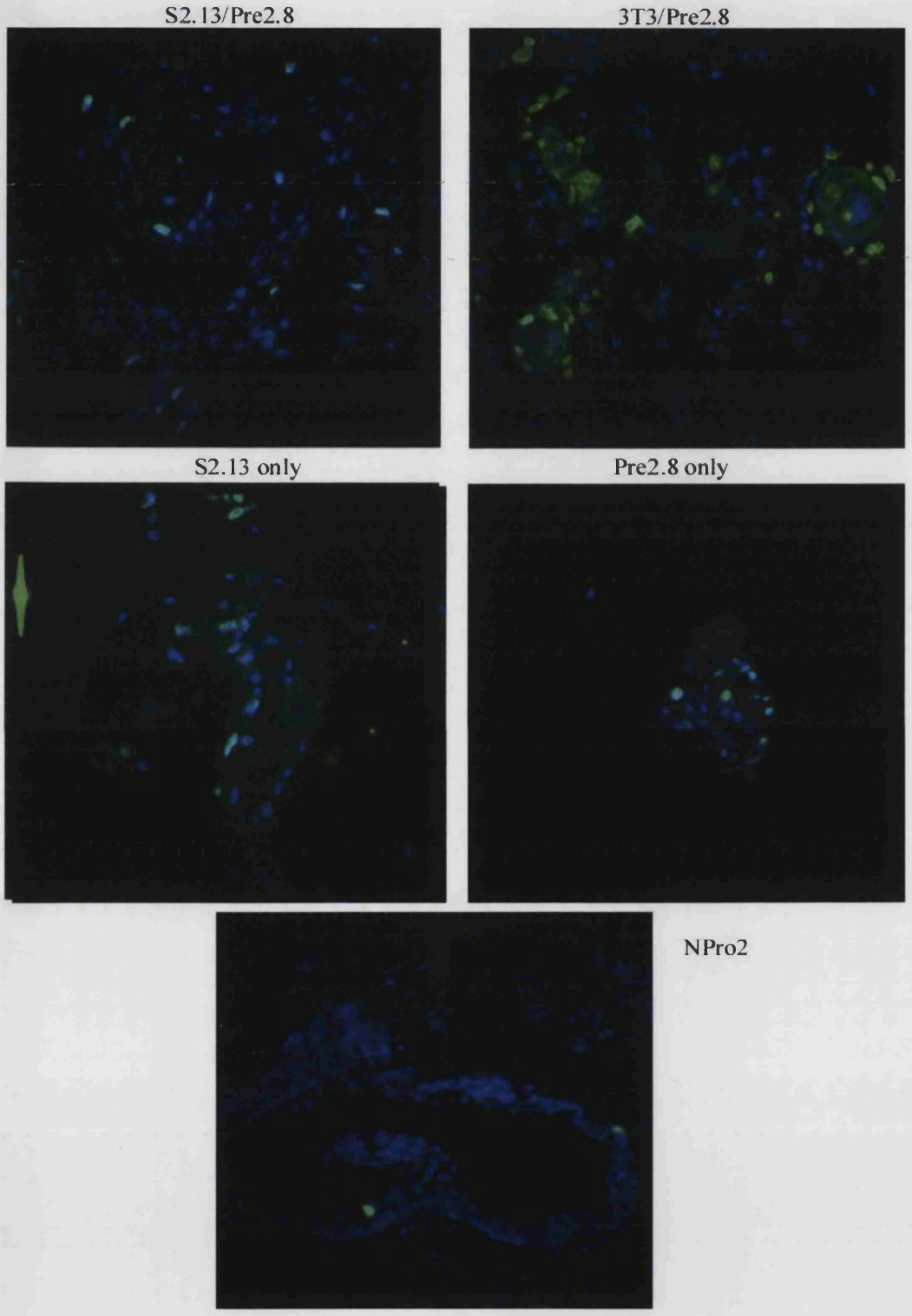

Paraffin sections of day 24 matrigel cultures (in PrEGM and DMEM/FCS medium) at 37°C with varying cell types, S2.13/Pre2.8, 3T3/Pre2.8, S2.13 only and Pre2.8 only cells. Normal prostate tissue (NPro2) sections were used as positive controls. Fluorescence: Ki-67 is green and Hoechst is blue. Original Magnification is x40 (fluorescent microscope – objective lense).

6.7 SUMMARY

In order to develop an in vitro prostate model using normal prostate cell lines, the capacity of Pre2.8 and S2.13 cell lines to form 3-dimensional (3-D) structures in vitro was investigated. The model was based on matrigel cultures using primary prostate cells that produced prostate morphology and differentiation (Hudson et al., 2000b). Initial investigations determined the optimum culture medium for use with both cell lines in matrigel cultures. Conditions were optimised to achieve organoid (spheroid) development most likely to produce morphology and differentiation. During optimisation the role of stroma in matrigel cultures for achieving prostate like characteristics were investigated. The morphology and cell differentiation status of prostate (Pre2.8 and S2.13 BPH cell lines) matrigel (3-D) cultures were investigated using immunofluorescence staining for cytokeratins, immunocytochemistry staining for stromal cell markers and prostate-specific differentiation was studied at both protein and mRNA levels. The influence of androgen (mibolerone, a synthetic androgen) on the development of 3-D structures by Pre2.8 cells was also studied.

3-D structures developed from Pre2.8 cells in Matrigel in equal volumes of PrEGM and DMEM/FCS. The addition of 4% serum resulted in the development of larger organoids. 3-D cultures set-up with Pre2.8 cells grown in PrEGM alone or with conditioned medium developed lattice-like structures. Although larger structures were observed with Pre2.8/S2.13 co-cultures in PrEGM, the cells did not appear to be organised into basal and luminal layers.

Increasing S2.13 cell concentration was not advantageous because the Matrigel contracted and no 3-D structures developed. An alternative cell line, 3T3 mouse fibroblasts, did not improve the ability of Pre2.8 cells to grow in Matrigel. In conclusion, there is no evidence that either the conditioned medium or the addition of the S2.13 stromal cells had a significant influence on the morphology or differentiation of the Pre2.8 cells in 3-D culture.

The structures formed by Pre2.8 cells in Matrigel showed a limited degree of differentiation. They have the potential to form a basal ($K14^+$ $K17^+$) layer surrounding an intermediate or early luminal epithelial layer ($K14^-$ $K17^+$ $K19^-$ $K8^+$). $K14^-$ $K17^+$ and $K8^+$ cells also tend to be scattered in a disorganised fashion throughout the Matrigel.

RT-PCR shows K5 (early basal cell marker) expression but no K18 (late luminal marker), showing limited differentiation occuring.

Although there was some multilayering, little differentiation towards a luminal phenotype was observed. However, positive staining for AR and PSA was observed in the nuclei and cytoplasm. AR is expressed in all cells, from 3-D cultures by immunocytochemistry while RNA expression of AR is found in Pre2.8/S2.13 co-culture and S2.13 only Matrigel cultures, but not in Pre2.8 only Matrigel cultures. PSA was found in the nucleus as well as in the cytoplasm, of 3-D cultures by immunocytochemistry. RT-PCR showed that this PSA expression may be non-specific because a different size band was amplified for 3-D cultures compared to PSA expression in LNCaP positive control, showing that correct primers were used. The particular PSA primer oligonucleotide used for this PCR appears to be annealing to a larger sequence (not expected) that does not have complete homology to the primer sequence (non-specific). AR is expressed in stromal but not epithelial cells in this 3-D model. There is clearly no PSAP expression.

The presence of mibolerone in 3-D cultures appears to inhibit lattice formation and increase organoid formation (figure 6.6), although no difference was observed for cell differentiation or prostate specific characteristics.

In conclusion, a 3-dimensional in vitro model using BPH stromal and epithelial cells from the same patient has been investigated. There are limitations to this model and further optimisation of culture conditions is required. An alternative model such as a collagen sponge may support a greater degree of differentiation.

CHAPTER 7

DISCUSSION

7.1 DISCUSSION

The aim of this project was to establish conditionally immortalised epithelial and stromal cell lines from human prostate tissue that could be used to study prostate differentiation in vitro and in vivo. This study describes the establishment and characterisation of the epithelial cell line Pre2.8 and the stromal cell line S2.13 in monolayer culture. In order to study prostate stromal and epithelial cell interactions S2.13 and Pre2.8 cells were developed into a 3-dimensional model.

7.1.1 Derivation and Authentication and Purity

Two temperature sensitive cell lines, Pre2.8 epithelial and S2.13 stromal cells have been established from BPH tissue, from the same patient. The authenticity of these cell lines was confirmed by showing that the cell lines had the same DNA profile as tissue from the patient from whom the sample was obtained. This finding rules out the possibility of cross-contamination with other cells (Masters et al., 2001). Mycoplasma contamination was ruled out using PCR analysis (Hopert et al., 1993a; Hopert et al., 1993b). Both cell lines were grown for more than 200 population doublings, indicating that they are immortal. The presence of SV40 large T-antigen was confirmed using immunocytochemistry.

Pre2.8 cells were routinely grown in a commercially available serum-free prostate epithelial medium, PrEGM. It has previously been determined that this culture medium supports the growth of prostate epithelial cells (Fry et al., 2000c). Primary cultures from 10 patients became vacuolated and did not survive past 3 weeks in WAJC 404 (McKeehan et al., 1984). Cells from primary cultures of 6 patients grown in mammary epithelial growth medium (MEGM, BioWhittaker UK Ltd) or a combination of MEGM with WAJC 404 or its supplements became squamous after 4-6 weeks and began to detach from the flask. In contrast, cells from 12 patients grown in PrEGM became neither vacuolated nor squamous. Pre2.8 cells grow routinely in PrEGM medium and can be passaged following trypsinisation as long as the cells are centrifuged and washed to remove the trypsin.

S2.13 cells were routinely grown in DMEM (Life Technologies) supplemented with 10% foetal calf serum (FCS). Stromal cells tend not to grow in the absence of serum (Peehl and Stamey, 1986b; Peehl et al., 1988a). Smooth muscle cell (SMC) differentiation can be induced by basic fibroblast growth factor (bFGF) and bovine

pituitary extract (BPE) (Kassen et al., 1996a). Primary smooth muscle cultures gradually lose SMC-specific proteins after 10 passages and develop a myofibroblast phenotype (Zhang et al., 1997). It was thought that horse serum suppresses proliferation of fibroblasts and myofibroblasts. Therefore Zhang et al developed a SMC growth medium, containing horse serum instead of FCS, insulin, dexamethasone and conditioned medium from CRL-5813 and LNCaP tumor cells. Prostatic tumor cells secrete growth factors that stimulate SMC proliferation (Carney et al., 1985; Kooistra et al., 1995b).

The morphologies of both cell lines change when the cells are transferred from 33°C to 39°C, indicating that these cell lines are temperature sensitive. In monolayer cultures at 33°C and 37°C, Pre2.8 epithelial cells are slow growing and have a typical cobblestone appearance, while S2.13 cells are fast growing and have a slightly elongated appearance. Fibroblasts tend to be more obviously elongated in appearance. At 39°C, Pre2.8 cells lose their tightly compact appearance and appear to increase in size. S2.13 cells become more loosely associated and more elongated in appearance at 37°C and 39°C.

Confirmation of the change in cell size of Pre2.8 cells following transfer from 33°C to 39°C was carried out initially using a Coulter Counter, showing a change in cell size from 13.25μm at 33°C to 16.25μm at 37°C and 16.57μm at 39°C. The similarity in cell size found at 37°C and 39°C did not agree with the observations made under the inverted microscope where some cells at 39°C appeared to be larger than at 37°C. Cell size was repeated with adherent cells. The mean size was 40μm at 33°C, 43μm at 37°C and 52μm at 39°C. These findings suggest that the cells become more flattened as the temperature is raised. S2.13 cells were much larger than Pre2.8 cells. A shift in cell size was also seen in these cells, from 55μm to 64μm and 88μm when transferred from 33°C to 37°C and 39°C respectively.

The effect of temperature on the proliferation of Pre2.8 cells was measured to ensure that the immortalisation remained conditional. Pre2.8 cells grow exponentially at 33°C for 17 days, while at 37°C cell growth plateaus much earlier, by day 12. No exponential growth was achieved at 39°C. One important observation is the long lag phase, 2-3 days

before Pre2.8 cells start to divide exponentially. S2.13 cells show a similar pattern. The proliferation rates of these temperature sensitive cell lines are clearly affected when the conformation of the SV40 LTAg is changed at 39°C and 37°C. The growth of conditionally immortalised cell lines was also compared to the growth of cell lines immortalised with wild type HPV. Pre2.8 cells grow faster than the HPV-immortalised 1542- NPTX cells at 33°C, while 1542-NPTX cells grew better at 39°C. Similarly, S2.13 cells did not grow at 39°C, while HPV immortalised 1542-NPFT cells grew well at this temperature.

Colony forming efficiencies provide an indication of stem and transit-amplifying cell fractions within a population (Hudson et al., 2000b). This method also tends to be the preferred method for analysing differences in cell proliferation (colony size) and survival (colony number) within a population. No colonies developed from Pre2.8 cells at 39°C, or when less than 5000 cells were plated at 33°C. Pre2.8 cells grow as a tightly compact monolayer and do not grow well when isolated. The long lag phase may inhibit the survival capacity of these cells under these conditions. Alternatively, these cells may produce autocrine growth factors and need a minimum cell density in order to proliferate.

7.1.2 Cytogenetic Analysis

The karyotype of Pre2.8 and S2.13 cells was analysed by Dr Rod McLeod (DSMZ, Braunschweig, Germany). Using a combination of multicolour fluorescence in situ hybridisation and single locus analysis using bacterial artificial chromosome clones, chromosome rearrangements were studied. Strikingly, both cell lines show amplification of chromosome 20q. In S2.13, chromosome 20 was highly involved in the more complex chromosomal changes and showed the most intense signals.

Pre2.8 cells have a near diploid karyotype with loss of chromosome Y and formation of an isochromosome i(8q), where redistribution of material covered 4q. The long arm of chromosome 20 is inserted into the short arm (p12) of one chromosome 14 and partial duplication of one chromosome 20-homolog.

S2.13 cells have a hypertetraploid karyotype, with many numerical and minor structural changes. Markers of three homogeneous staining regions (HSR) were derived from chromosome 4, 19 and 20.

Although cell lines are prone to genetic instability it is known that many genetic events are likely to be involved in prostate tumorigenesis. It is difficult to distinguish between chromosomal abnormalities occurring due to immortalisation and genetic abnormalities that were present in the primary tissue. Up-regulation of chromosome 20 has been associated with immortalisation and the ability of cells to escape senescence (Cuthill, 1999) (Jarrard and Waldman, 1999).

Some of these findings, particularly alterations of chromosome 20q and the formation of an isochromosome in chromosome 8, i(8) have been observed by other research groups. Gain of chromosome 20 has been associated with many cancer types including prostate, bladder, melanoma, colon, pancreas and breast (Brothman et al., 1990; Richter et al., 1998; Bastian et al., 1998; Korn et al., 1999; Mahlamaki et al., 1997). More specifically amplification of chromosome 20q13 was observed in breast cancer (Tanner et al., 1994) and in other tumor types (Ohyashiki et al., 1992; Mohapatra et al., 1995; Schlegel et al., 1995; Bockmuh et al., 1997). A novel androgen-induced gene, PMEPA1 that encodes a polypeptide with a type 1b transmembrane domain was cloned and characterised (Xu et al., 2000). Database searches showed sequence homology of this gene to genomic clones, RPS-1059C7 and 718J7, which were mapped to chromosome 20 q13.2- q13.33. Using comparative genomic hybridisation, chromosome alterations were found to be possibly associated with clinically defined CaP stage (Wolter et al., 2002). This group found losses at chromosome 13 (q21.1-21.3), 8p21.2, 6q and 16q, and gains at chromosome 17q, 20 (q13.2-13.3) and 9q.

Prostate cancer can be sporadic, familial or hereditary. Sporadic cancers are most widely studied. In a study comparing androgen-sensitive prostate (AS) cancers with androgen-insensitive prostate (AI) cancers, early stage CaP was associated with loss of 8p. Progression of metastatic AI CaP is associated with loss of chromosomes 2q, 5q, 10q, 11q, 13q, 16q, 17q, 20q (Cher et al., 1994). A study of differential gene expression between cell lines, LNCaP (AS) and LNCaP-r (AI) found 3 genes associated with development of AI CaP. An upregulation of the fibronectin (FN) gene, mapped to 2q was found while downregulation of the breast basic conserved gene-1 (BBC1), mapped to 16q and ubiquitin enzyme variant-1 (UEV-1), mapped to 20q was observed.

A hereditary CaP study was carried out to look for the existence of familial clustering and increased hereditary risk (Berry et al., 2000). They carried out a genome wide

search on 162 North American families and found linkage to chromosome 20q13, which they designated as HPC20. Various confirmation studies were unsuccessful in finding confirmation of linkage to these CaP susceptibility loci. No linkage was found for HPC1, CAPB and HPCX in a study of 64 South West European families, although linkage was associated to the PCAP locus (Cussenot and Valeri, 2001) which was originally identified from a study of French and German families. Epidemiology may be an important factor in linkage studies of familial and hereditary CaP. A confirmation study of 20q13 was carried out using 172 families affected by CaP, who were participating in the University of Michigan Prostate Cancer Genetics Project (PCGP) (Bock et al., 2001). No significant evidence for CaP susceptibility for linkage to 20q13 was found, with the exception of black families. Differences between family size, age of CaP diagnosis and ethnic composition could be factors allowing for the lack of 20q13 linkage.

Cytogenetic and array comparative genomic hybridisation and expression analysis was carried out on prostate cancer xenograft (WISH-PC14), derived from a locally advanced tumor (Bar-Shira et al., 2002). Abnormalities were predominantly found on chromosome 8, 20 and X and overexpressed genes were located to chromosome 20q13.

An association of loss of chromosome 8p and gain of chromosome 8q sequences, suggests the formation of isochromosomes, i(8q) in advanced prostate tumors (Macoska et al., 2000). This group found trisomy for chromosome 20 and rearrangements involving chromosomes 3, 4, 8, 9, 10, 16, 17, 18, 19, 21, and 22. They concentrated their studies on numerical and structural alterations of chromosome 8 in two normal prostate epithelium cell lines and three human prostate tumor cell lines. They found loss of 8p in prostate tumor cell lines and two tumor cell lines demonstrated an i(8q) chromosome, as well as rearrangement of chromosome 8 material with either chromosome 20 or 21 for one of the tumor cell lines. Gain of chromosome 8q from q11.2 to q24, although not in the form of an i(8q) was found in one of the normal epithelial cell lines. These authors have shown evidence to support the theory that chromosomal loss of 8p in primary human prostate tumors may not result from simple deletion of all or part of the short arm, but involves 8p loss. This may result from complex structural rearrangements of chromosome 8, which sometimes results in gain of 8q material and this may occur during tumorigenesis.

These studies indicate that chromosomes 20 and 8 alterations may be associated with CaP. The presence of CaP chromosomal alterations, associated with our BPH cell lines, Pre2.8 and S2.13 is unexpected since, BPH is not believed to be a pre-cancerous condition. One explanation is that these genetic changes enable prostate cells to extend their lifespan and have been selected during the immortalisation of the cell lines. Pre2.8 and S2.13 cells do not form colonies in semi-solid agar cultures. It may be useful to repeat this analysis at a later passage level in order to show cell stability and to determine if passaging produces further chromosomal alterations and to see if chromosome 20 and 8 alterations are consistant with with passaging.

7.1.3 Differentiation

The aim of this project was to establish a prostate epithelial and stromal cell model for the study of prostate differentiation in vitro. Most continuous cell lines appear to be relatively undifferentiated cells with the capacity to proliferate, but tend not to differentiate in vitro. We attempted to overcome this limitation by using a temperature sensitive switch for SV40 T-antigen that drives cell proliferation (Jat and Sharp, 1989; Stamps et al., 1994). Immortalised temperature sensitive cells are expected to proliferate at permissive temperatures (33°C), while at non-permissive temperatures (39°C) proliferation should be switched off and cell differentiation is anticipated.

We observed a substantial proliferating population for Pre2.8 cells at 33°C (93% proliferating cells), which substantially decreased when cells were transferred to 37°C (26% proliferating cells) and 39°C (15% proliferating cells), another indication that the temperature sensitive switch was working correctly. It would be interesting to determine if this substantial proliferating population was also observed in the original tissue. It would also be interesting to obtain S2.13 proliferation data for comparison.

To my knowledge there are no other immortalised temperature sensitive prostate cell lines and there is a limited number of immortalised temperature sensitive cell lines established from other human tissues. Most temperature sensitive cell lines have been produced from mouse and rat tissues. Human mammary epithelial cells were immortalised using the temperature sensitive SV40 T-antigen and used to investigate the role of the T-antigen gene and its site of integration in human epithelial cell immortalisation (Stamps et al., 1994). Immortalisation of freshly isolated normal adult human mammary fibroblasts and endothelial cells was unsuccessful using functional

telomerase (hTERT) alone or by using the temperature sensitive (ts) mutant (U19tsA58) of the SV40 LT antigen alone. A combination of hTERT and tsLT-ag generated conditionally immortalised human cells in a reproducible manner (O'Hare et al., 2001). An early optic-nerve progenitor cell model, tsU19-9 was established from postnatal day 2 rats using the ts SV40 LT-antigen. At 33°C these nestin (neuronal precursor marker) expressing cells had a flat epithelial morphology. These cells underwent morphological and antigenic differentiation to cells characteristic of the oligodendrocyte lineage at 39°C (Cohen et al., 1999). Three temperature sensitive human "ovarian surface" cell lines have been established (Leung et al., 2001). This is the area where epithelial ovarian carcinomas develop. At 34°C most cells expressing the epithelial keratin markers varied between cell lines from 20-97%. Collagen type 3, a mesenchymal marker was present in 24-43% of cells. When cell lines were switched to 39°C, proliferation was inactivated and keratin expression was increased to 85-100% in all cell lines, while collagen type 3 expression increased significantly in 2 cell lines.

One hundred neural stem and progenitor cell lines were immortalised, using ts SV40 large T-antigen (A58/U19) from primary hippocampal and cerebellar progenitor cells from embryonic day (E) 16.5 to 17.5 C57BL/10SnJ murine fetuses. From these cell lines a clonal neural stem cell line (MK31) gave rise to 3 of the major CNS cellular elements (neurons, astrocytes and oligodendrocytes). At 33°C single neural stem cells exhibited self-renewal, clonal expansion and both symmetric and asymmetric modes of cell division. When these cells were switched to 39°C they stopped proliferation and successfully differentiated into neuronal, oligodendroglial and astroglial cell lineages, under the influence of specific sets of cytokines (Gokhan et al., 1998). As part of a study on signal transduction pathways leading to neuronal differentiation a hippocampal stem cell line, HiB5 was established from the CNS of the rat, E16 hippocampus using the ts SV40 LT-antigen gene (Renfranz et al., 1991). HiB5 cells have stem cell markers such as nestin and intermediate filament and differentiate into neuronal cells in vivo when implanted into rat brain. They proliferate in response to serum or retinoic acid at 33°C and differentiate into a non-proliferating, neuronal phenotype in response to PDGF (platelet-derived growth factor) at 39°C (Chung et al., 2000; Kwon, 1979).

Masuo Obinata has described a different approach to the establishment of temperature sensitive cell lines (Yanai N and Obinata M, 2001). He hopes that someday all distinct cell types in the body, of which there are 200 known so far, could be separated from

each other to produce a cell bank. He suggests that all cell types could be readily available for analysis in order to answer fundamental questions about the development of different cell types into tissues or organs. A database containing this information could then be established. It would first be necessary to immortalise these cells. In order to overcome the loss of original cell differentiation function they used the tsSV40 LT-antigen, but not directly into each cell type. Instead they produced transgenic mice harbouring the tsSV40 LT-antigen gene derived from tsA58 virus. BamH1 DNA fragment of whole tsSV40 LT-antigen DNA, along with the major histocompatibility complex H-2Kb promoter was injected into fertilised eggs of C57BL/6 mice (Yanai et al., 1991). These transgenic mice were called H2T-transgenic mice. Various tissue cell lines have been established from these H2T-transgenic mice and also from ts transgenic rats (Yanai N and Obinata M, 2001). Most of these cell lines grow at 33°C but cell proliferation is arrested at 39°C, allowing the differentiation functions of these cell lines to be successfully maintained. Some examples of established H2T-transgenic cell lines from different organs of H2T mice are hepatocye cells (Yanai et al., 1991), renal cells (Hosoyamada et al., 1996), colonic epithelial (Tabuchi et al., 2000), tracheal epithelial cells (Sugiyama et al., 1998) and bone marrow stromal cells (Kameoka et al., 1995).

Cell lines have been invaluable as experimental tools for the study of neural and sensory function, particularly in inner ear research. In order to push forward and increase the value of such cell lines, the tsSV40 LT-antigen was used to create temperature sensitive cell lines from different tissues and developmental stages of the inner ear. Sensory cells of the inner ear were immortalised using the $H2K^{b}ts58$ transgenic mouse (Immortomouse)(Holley and Lawlor, 1997). Using this Immortomouse, different cell lines representing different developmental stages can be more readily compared because the immortalising gene is incorporated and expressed in exactly the same way. Alarid et al. targeted the T-antigen gene with promoters that were activated at different stages of development to c reate committed and uncommitted pituitary cell lines. Most of these cell lines have retained their original phenotype (Alarid et al., 1996). These conditionally immortal cell lines differentiate in an ordered manner in terms of gene expression. This provides the potential to study the different effects of various signalling molecules.

Temperature sensitive transgenic mice have been successfully used to establish cell lines that maintain their original phenotype and differentiation can easily be switched

on. This approach may not be beneficial for human prostate research since the mouse prostate is very different from the adult human prostate.

BPH is predominantly a stromal disease (McNeal, 1978) (Rohr and Bartsch, 1980). There are three types of stromal cells in prostate tissue, fibroblasts (vimentin, fibroblast-ASO2), myofibroblasts (vimentin, SMA) and smooth muscle cells (vimentin, SMA, SM-myosin). S2.13 cells are fibroblast cells, expressing vimentin and fibroblast antibody only.

Epithelial cells are responsible for the protective and secretory function of many organs. The function of the prostate is not clear, but it is involved in secretion of PSA and PSAP. Epithelial cells are good models for differentiation and studying stem cells. Stem cells are thought to be located in the basal layer in the adult prostate (Bonkhoff and Remberger, 1996; Robinson et al., 1998b). Prostate epithelium is the site of malignancy. Cytokeratin antibodies have been widely used to determine epithelial cell phenotype and differentiation status. There are two main cell types in prostate epithelium tissue, the basal (K5, K14, K17) and luminal (K8, K18) cells. Pre2.8 cells have stronger K8 and K18 staining at 37°C and 39°C, indicating a more differentiated phenotype at the higher temperatures.

Although there is no definitive evidence for the existence of an intermediate epithelial cell it is now generally accepted. Co-expression of basal and luminal markers in an intermediate phenotype was identified with some cells expressing K14, K5, p63, K17, K19, K8, K18 and GSTpi (Bonkhoff et al., 1994; Bonkhoff and Remberger, 1996; Hudson et al., 2000a; Xue et al., 1998). Keratin 19 expression frequently occurred in basal and in luminal cells of normal, malignant and BPH (Hudson et al., 2001a; Peehl et al., 1996). Hudson et al (2001) suggests that K19 expressing cells represents a population of basal cells in the process of differentiation into luminal cells. They proposed a hypothetical differentiation pathway for human prostate epithelial cells based on patterns of keratin staining. Basal stem cells (K5 and K14 only) give rise to an intermediate transit amplifying population, expressing K19. These cells differentiate into luminal cells with transient co-expression of K19, K8 and K18 before complete differentiation into cells expressing K8 and K18 only. K19 is switched on in Pre2.8, at low levels at 37°C and 39°C, suggesting the presence of an intermediate transit amplifying population.

Evidence contradicting the proposal that K19 is an intermediate epithelial marker and that basal cells are the site for stem cells was found by another group (Wang et al., 2001). They studied the urogenital sinus epithelium, the progenitor of the prostate epithelium precursor, to look for expression of epithelial subtypes. They used cytokeratin markers and other differentiation markers (p63 and GSTpi) and compared its differentiation profile with developing and adult prostate. They suggested that the embryonic urogenital sinus epithelium should be rich in prostatic stem cells, i.e. contain a differentiation marker profile similar to that of prostatic stem cells. Wang et al found a cell population in the foetal urogenital sinus epithelium that only contained the full marker compliment (K14, K5, p63, K19, K8, K18 and GSTpi). They also found a population of cells in the adult prostate with this marker profile. They suggested that the small population of basal/luminal expressing cells are prostate stem cells since they are also found in urogenital sinus epithelium. Otherwise any other proposed stem cell population should be expressed in urogenital sinus epithelium. Their hypothetical cell differentiation model suggests that cells co-expressing K14, K5, p63, K19, K8, K18 and GSTpi give rise to definitive basal cells (K14, K5, p63, K19 and GSTpi positive only) and luminal cells (K8, K18 positive only). On the basis of this theory, Pre2.8 cells may contain stem cells since they express a small population of K14, K17, K19, K8 and K18 positive cells at 37°C and 39°C. This is unlikely otherwise K19 would also be expressed at 33°C. Further investigations need to be carried out in order to clarify the various hypothesis for prostate epithelial cell differentiation. Pre2.8 cells are potentially a good prostate model for this work and for studying proliferation and differentiation.

7.1.4 Androgen Expression

The prostate is an androgen-dependent organ. Testes are the main source of androgen. They synthesise and secrete testosterone into the blood. Testosterone is not the primary androgen responsible for maintenance of the prostate. It is converted to dihydrotestosterone (DHT) by 5α-reductase (5α-R) enzymes (Bartsch et al., 2000). DHT binds with greater affinity than testosterone to the androgen receptor (AR) and this complex is transported to the nucleus. AR is activated and causes upregulation of androgen-sensitive genes to regulate prostate cell growth, differentiation and secretion of various proteins such as PSA and PAP. The androgen receptor remains in the cytoplasm until ligand binding occurs and the dissociation of Heat Shock Proteins

(HSPs) is thought to allow conformational change in the AR and mediate translocation to the nucleus (Gnanapragasam et al., 2000).

There are two 5α-R isoenzymes, type 1 and type 2 and possess approximately 50% sequence homology between them. Type 1 5α-R enzyme is predominantly found in tissues other than the prostate, particularly the skin and liver, while Type 2 is mainly associated with the prostate and both forms are found in serum (Steers, 2001). 5α-R was identified in stromal and epithelial cells in CaP and BPH. Using polyclonal antibodies against 5α-R type 1 and type 2 Bonkhoff et al. showd that 5α-R1 was predominantly expressed in nuclei of secretory luminal cells and 5α-R2 was predominantly expressed in cytoplasm of basal cells. In general 5α-R1 was more abundant than 5α-R2 in stromal and epithelial cells (Bonkhoff and Remberger, 1996; Habib FK et al., 1998).

Mutations in 5α-R2 suggest that this enzyme plays a central role in normal prostate development (Andersson et al., 1991). A non-functional 5α-R2 or AR can cause Pseudohermaphroditism, a condition in men who have small prostates and do not develop BPH. This knowledge led to the production of 5α-R targeting drugs such as Finasteride. Finasteride inhibits 5α-R2 (by 80%-90%) but not 5α-R1, leading to a reduction in prostate volume (Steers, 2001).

Pre2.8 epithelial and S2.13 stromal cells have lost their androgen receptor expression in monolayer cultures. Both cell lines are negative for 5α-R2, AR, PSA and PAP, and are positive for 5α-R1. A reduction of the enzyme 5α-R2 in stromal and basal cells will prevent conversion of testosterone to DHT and hence AR will not be activated to produce PSA and PAP. Pre2.8 do not fully differentiate into luminal cells at 37°C or 39°C, hence secretion of PSA and PAP would not be expected. Using RT-PCR, Habib et al showed that primary cultures expressed both isoforms of 5α-R. Expression of mRNA persisted for 6 passages of primary BPH fibroblast cells, after which expression stopped (Habib FK et al., 1998). It appears that temperature sensitive SV40 LT-antigen immortalisation is not sufficient for these BPH cell lines to maintain all of their original characteristics. The loss of androgen expression and secretory function is likely to be due to monolayer culture conditions or due to the absence of appropriate inductive stromal signals. It would therefore be interesting to examine androgen expression in cultures where Pre2.8 epithelial cells are combined with S2.13 stromal cells. Expression

of PSA and PAP proteins is dependent on the correct cell morphology and architectural organisation being present (Hayward et al., 1992). Matrigel cultures may assist in maintaining the correct architectural organisation.

There are a few immortalised epithelial cell lines and two stromal cell lines that have partially maintained normal prostate function. In general these epithelial cell lines are fully differentiated luminal cells, unlike Pre2.8 cells which are basal epithelial cells at 33°C. NP-2s stromal and NP-2e epithelial cell lines express 5α-R enzymes (Lechner et al., 1978). NP-2e cell line was further transformed to produce 267B1, 272E1 and 272E4 epithelial cells, which showed weak immunostaining for PSA and PAP. These three cell lines were luminal cells ($K8^+$ and $K18^+$) with a mixture of stromal cells ($vimentin^+$ and $actin^+$). The PNT1 luminal epithelial cells line ($K8^+$, $K18^+$ and $K14^-$) were weakly positive for PSA and PAP (Cussenot et al., 1991). BPH-1 luminal cells ($K8^+$, $K18^+$, $K19^+$ and $K14^-$) showed faint AR and PAP immunostaining but could not be confirmed by RT-PCR or Northern blotting (Hayward et al., 1995). PSA was negative by immunostaining. Although Hayward et al suggested 5α-R activity in BPH-1 cells, they have no evidence. They based their result on the presence of DHT, which implies the presence of 5α-R activity. The supernatant of this cell line contained testosterone. RWPE-1 epithelial cells showed AR and PSA expression in response to mibolerone (Webber et al., 1996). RWPE-1 expressed cytokeratins K8, K18, K5 and K14, although K5 and K14 data was not shown. Therefore it is not conclusive whether these cells are fully differentiated or intermediate epithelial cells. BRF-55T luminal epithelial cells ($K8^+$ and $K18^+$) express AR and PSA, although these cells may be pre malignant cells (Iype et al., 1998).

S2.13 cells are fibroblasts unlike Duk50 (Roberson et al., 1995), a smooth muscle cell line and WPMY-1 (Webber et al., 1999), a myofibroblast cell line, both of which express AR. Smooth muscle cells make up most of the stromal tissue and contain a high proportion of androgen receptors in vivo (Planz et al., 1998). This may account for these two cell lines expressing AR and not S2.13 cells.

7.1.5 3-Dimensional Cultures

Stromal-epithelial cell interactions (Timms et al., 1995; Bayne et al., 1998; Liu et al., 1997) and production of basement (Smola et al., 1998) are the principal processes involved in development of normal prostate function and differentiation. In order to

translate these processes into an in vitro model while overcoming the limitations for using primary cells and immortalised monolayer cell cultures, we set up 3-dimensional cultures combining Pre2.8 epithelial and S2.13 stromal cells in matrigel. Laminin plays a major role in extra cellular matrix (ECM) (basement membrane) interactions (Malinda and Kleinman, 1996). Laminin makes up 60% of matrigel, which also consists of collagen 5, other matrix proteins and several growth factors and proteases. Prostate epithelia in matrigel cultures have been shown to form acini capable of secreting prostate specific (Webber et al., 1997).

Temperature sensitive Pre2.8 epithelial and S2.13 stromal cells grew fastest in medium containing 10% serum. Pre2.8 cells in monolayer cultures changed their morphology when grown in RPMI containing 10% serum compared to growth in PrEGM medium. This could suggest that serum contains growth factors, in addition to those present in PrEGM that may be important in prostate epithelial cell proliferation and differentiation.

Three main types of cell clustering developed, lattice formation at 33°C, large inter connecting organoids at 37°C and small organoids at 39°C. The large inter connecting structures most resemble spheroids obtained by Hudson et al from primary type 2 epithelial colonies in matrigel cultures, containing 3T3 conditioned medium (Hudson et al., 2000a). We did not observe side branching in these organoids. Pre2.8 epithelial cells grown in matrigel with S2.13 conditioned medium produced a lattice, showing no resemblance to structures produced by type 2 epithelial colonies. Immortalised epithelial cells in comparison to primary cells appear to have lost a key factor in epithelial cell morphology. Pre2.8, S2.13 matrigel cultures, in PrEGM medium only, produce very small organoids compared to large interconnecting organoids in PrEGM/DMEM-FCS. These results confirm the presence of important growth factors in serum. The presence of mibolerone tended to reduce organoid development to very small structures, with sparse large interconnecting organoids.

Paraffin sections of organoids showed great organisational variation. In general organoids grown at 39°C did not grow large enough to develop acinus structures with distinct basal, luminal or stromal layers. Organoids at 33°C and particularly at 37°C showed greatest potential for prostate like architecture. Early experiments were set up with complete growth factor matrigel, while later experiments were set up with growth factor reduced matrigel. In general earlier experiments produced organised structures

containing acini surrounded by layers of intermediate epithelia ($K14^- K17^+$), which was surrounded by basal cells ($K14^+ K17^+$) that was surrounded by non-epithelial cells, likely to be stromal cells. This organisation appeared to be similar to organised structures observed with type 2 epithelial colonies (Hudson et al., 2000a). Experiments using reduced GF matrigel produced mostly unorganised structures without acini. Unorganised structures expressed both cytokeratins 14 and 17, but K17 was scattered without any organisation. Cytokeratin 8 staining had high background therefore was difficult to determine its location, although in organised spheroids layers of $K8^+$ appeared to be surrounded by a layer of $K8^-$ cells, likely to be basal cells. Cytokeratin 18 was negative by RT-PCR. Growth factors removed from reduced GF matrigel may be critical for correct prostate morphology and differentiation. Hudson et al used complete growth factor matrigel. Stromal cell markers (vimentin $^+$, SMA^-) were only tested in organoids from GF reduced matrigel. Fibroblasts were distributed without any organisation.

Although limited differentiation occurred in Pre2.8/S2.13 matrigel cultures, they do appear to differentiate ($K14^- K17^+$) further than in monolayer cultures. In addition, matrigel cultures permit AR expression, confirmed by immunocytochemistry and RT-PCR analysis. AR staining was found in the cytoplasm and the nucleus. Androgen receptor remains in the cytoplasm until ligand binding occurs and the dissociation of heat shock proteins (HSPs) is thought to allow conformational change in the AR and mediate translocation to the nucleus (Gnanapragasam et al., 2000). Previously, AR expression in primary cultures was observed in the cytoplasm and nuclei (Cussenot et al., 1994b; Robinson et al., 1998a). Cussenot et al suggested that AR expression in the cytoplasm and nuclei is due to partial blockage of this receptor in a non-bound state. Robinson et al suggest that nuclear localisation of the androgen receptor is dependent, in part, on the occupancy of the receptor. Studies on AR in vivo support a ligand-activated transport mechanism, i.e endogenous AR is nuclear in the presence of androgen, and unliganded AR is perinuclear in the cytoplasm (Kemppainen et al., 1992; Georget et al., 1997).

PSA expression observed in the nucleus and cytoplasm was not confirmed by RT-PCR, since the incorrect size band was obtained. PSA positive cells were distributed throughout organoid sections except for distinct PSA negative clusters, consistently situated in the centre of cell clusters. This adds further confusion to these results since it

is expected that PSA would be expressed in the centre of structures where the lumen is expected. This does fit with the unorganised distribution of cytokeratin 8 expressing cells. PSAP was negative by immunocytochemistry and RT-PCR. These results were consistent with type 2 epithelial colonies in matrigel cultures. Type 2 epithelial colonies are thought to contain stem cells.

PNT2-C2, a normal epithelial cell line grown alone in matrigel cultures successfully formed spheroids of cells, but do not form acini, containing a lumen (Lang et al., 2001). These cells maintain their monolayer phenotype. In contrast Webber et al grew RWPE-1 epithelial cells in matrigel and these cells formed spheroids that contained acini that secreted PSA (Webber et al., 1997). Lang et al suggest that formation of acinus-like structures in matrigel is dependent on the differentiation state of the epithelial cells.

Temperature sensitive Pre2.8 and S2.13 cells are thought to stop proliferation and start differentiation at 37°C and 39°C. S2.13 stromal cells express the Ki-67 proliferation marker at 37°C, indicating that the SV40 large T antigen is not being completely inactivated. This may be a limiting factor for normal growth and morphology of epithelial cells in this model.

Urogenital sinus mesenchyme (UGM) induces epithelial differentiation and proliferation and, in turn prostate epithelial cells induce smooth muscle differentiation in UGM (Wong YC et al., 1992). Cunha suggests that once the UGM differentiates into smooth muscle in adulthood, it is the smooth muscle cell that becomes the crucial interactive element in the epithelial microenvironment. S2.13 fibroblast cells do not survive well in these matrigel cultures. Smooth muscle cells make up most of stromal tissue. SM cells contain a high proportion of androgen receptors. These cells are in close proximity to epithelial cells therefore, it is suggested that the stromal, epithelial interaction theory is more likely to be a smooth muscle, epithelial interaction (Planz et al., 1998). Co-culture of epithelial cells with fibroblast cells in matrigel may not be the optimum combination for induction of epithelial cell differentiation and function.

Matrigel is clearly a contributing factor in achieving normal epithelial cell differentiation and function, due to induced expression of AR. The expression of AR in 3-dimensional cultures indicates the presence of 5α-R2 activity. In a study of testosterone metabolism in BPH and CaP (Delos et al., 1998), it was confirmed that 5α-

R2 was predominantly expressed in prostate tissue and primary prostate cultures (Jenkins et al., 1992b). Delos et al observed that 5α-R1 was the isoform preferentially expressed in epithelial cell cultures (freshly isolated and long term). 5α-R2 was preferentially expressed in epithelial matrigel cultures, indicating that matrigel was responsible for changes in enzyme isoform activity. Our results are consistent with Delos et al's findings. In monolayer cultures 5α-R1, not 5α-R2 was observed in both S2.13 and Pre2.8 cells, while 5α-R2 is likely to be expressed in Pre2.8, S2.13 matrigel cultures. Androgen receptor is expressed in luminal cells, not basal cells and in 50% of stromal cells of tissues. Further confirmation of the importance of stromal, epithelial and ECM interactions for normal prostate metabolism, is the expression of AR in matrigel cultures with S2.13 cells alone, but not with Pre2.8 cells alone. When S2.13 and Pre2.8 cells are co-cultured in matrigel AR is expressed. As previously mentioned it is thought that androgens act on smooth muscle cells to maintain epithelial differentiation and in a paracrine manner epithelial cells maintain the differentiated state of smooth muscle cells (Cunha et al., 1997).

To date there are three animal models (Timms et al., 1995; Hayward et al., 1999; Hayward et al., 1997)and one human model (Lang et al., 2001) co-culturing stromal and epithelial prostate cells in matrigel. Lang et al compared epithelial cells alone in matrigel containing serum-free medium, then cultures containing serum and finally the addition of stromal cells. All culture conditions had similar phenotypes except that the addition of stromal cells produced AR expression, which indicates greater differentiation. Epithelial and stromal cells in matrigel cultures, in medium containing serum, oestrogen and DHT produce compact spheroids that are regular in shape and contain a lumen surrounded by one or two epithelial cell layers. The basal layer was not intact. We did not find any significant effect with the addition of mibolerone, but we did not test the effect of oestrogen. In general Lang et al showed that the outer layer of organised spheroids expressed cytokeratin 1, 5, 10 and 14 and the inner layer expressed cytokeratin 18. PSA and PAP was expressed with all culture conditions. Epithelial cell types showed no obvious difference in spheroid formation or morphology for $CD44^+$ basal cells compared to whole population epithelial cells. A population of $CD44^-$ epithelial cells did not grow within matrigel, indicating that basal cells are a contributing factor in epithelial cell growth. Lang et al showed that stroma co-cultured on inserts produced greater spheroid formation compared to stroma mixed with epithelial cells in matrigel or stroma laid on top of matrigel. From these results 3-

dimensional culture set-up may be an important factor. S2.13 stromal cells were directly mixed with Pre2.8 epithelial cells in equal volumes of PrEGM and DMEM-FCS and placed on top of solid matrigel in 24-well culture plates. Lang et al's results suggest that this is not the optimum culture set-up.

Co-cultures of Pre2.8 epithelial and S2.13 stromal cells in matrigel cultures requires further optimisation to achieve terminal epithelial differentiation and production of prostate secretions. The matrigel model established by Lang et al, although very useful is limited because they are primary cells and have a limited lifespan. A continuous supply of primary tissue for these experiments is not achievable. Pre2.8 epithelial and S2.13 stromal are immortalised cell lines, thus providing a continuous supply of cells. Another advantage for the use of Pre2.8 and S2.13 cell lines is that they are temperature sensitive. If it is true that non-basal epithelial cells do not grow in matrigel (Lang et al., 2001), Pre2.8 basal/intermediate epithelial cells are the ideal epithelial population for setting up matrigel cultures. In addition to this it is possible that Pre2.8 cells contain a stem cell population makes them a useful cell line for studying prostate stem cell differentiation. As mentioned above it is likely that S2.13 fibroblasts are not the ideal cells for establishing a prostate model. Replacing S2.13 cells with a smooth muscle cell line would be preferable.

8.0 REFERENCE LIST

Abrahamsson,P.A., Wadstrom,L.B., Alumets,J., Falkmer,S., and Grimelius,L. (1986). Peptide-hormone- and serotonin-immunoreactive cells in normal and hyperplastic prostate glands. Pathol. Res. Pract. *181*, 675-683.

Alarid,E.T., Windle,J.J., Whyte,D.B., and Mellon,P.L. (1996). Immortalization of pituitary cells at discrete stages of development by directed oncogenesis in transgenic mice. Development *122*, 3319-3329.

Ali,S.H. and DeCaprio,J.A. (2001). Cellular transformation by SV40 large T antigen: interaction with host proteins. Semin. Cancer Biol. *11*, 15-23.

Altwein JE. BPH a diagnosis & treatment, Ch 4. 2002. Altwein JE.

Andersson,S., Berman,D.M., Jenkins,E.P., and Russell,D.W. (1991). Deletion of steroid 5 alpha-reductase 2 gene in male pseudohermaphroditism. Nature *354*, 159-161.

Andersson,S. and Russell,D.W. (1990). Structural and biochemical properties of cloned and expressed human and rat steroid 5 alpha-reductases. Proc. Natl. Acad. Sci. U. S. A *87*, 3640-3644.

Aumuller,G. (1983). Morphologic and endocrine aspects of prostatic function. Prostate *4*, 195-214.

Bar-Shira,A., Pinthus,J.H., Rozovsky,U., Goldstein,M., Sellers,W.R., Yaron,Y., Eshhar,Z., and Orr-Urtreger,A. (2002). Multiple genes in human 20q13 chromosomal region are involved in an advanced prostate cancer xenograft. Cancer Res *62*, 6803-6807.

Barry,M.J., Fowler,F.J., Jr., O'Leary,M.P., Bruskewitz,R.C., Holtgrewe,H.L., and Mebust,W.K. (1992). Correlation of the American Urological Association symptom index with self-administered versions of the Madsen-Iversen, Boyarsky and Maine Medical Assessment Program symptom indexes. Measurement Committee of the American Urological Association. J. Urol. *148*, 1558-1563.

Barton,S. (2002). Medical Microbiology, [3rd Edition]. 2002. Associate Editor: Jennings,P.M. Churchill Livingstone publishers.

Bartsch,G., Bruengger,A., de Klerk,D.P., Coffey,D.S., and Rohr,H.P. (1987). Light-microscopic stereologic analysis of spontaneous and steroid- induced canine prostatic hyperplasia. J. Urol. *137*, 552-558.

Bartsch,G., Muller,H.R., Oberholzer,M., and Rohr,H.P. (1979). Light microscopic stereological analysis of the normal human prostate and of benign prostatic hyperplasia. J. Urol. *122*, 487-491.

Bartsch,G., Rittmaster,R.S., and Klocker,H. (2000). Dihydrotestosterone and the concept of 5alpha-reductase inhibition in human benign prostatic hyperplasia. Eur Urol. *37*, 367-380.

Bastian,B.C., LeBoit,P.E., Hamm,H., Brocker,E.B., and Pinkel,D. (1998). Chromosomal gains and losses in primary cutaneous melanomas detected by comparative genomic hybridization. Cancer Res *58*, 2170-2175.

Bayne,C.W., Ross,M., Donnelly,F., Chapman,K., Buck,C., Bollina,P., and Habib,F.K. (1998). Selective interactions between prostate fibroblast and epithelial cells in co-culture maintain the BPH phenotype. Urol. Int. *61*, 1-7.

Bedwal,R.S. and Bahuguna,A. (1994). Zinc, copper and selenium in reproduction. Experientia *50*, 626-640.

Bello,D., Webber,M.M., Kleinman,H.K., Wartinger,D.D., and Rhim,J.S. (1997). Androgen responsive adult human prostatic epithelial cell lines immortalized by human papillomavirus 18. Carcinogenesis *18*, 1215-1223.

Berry,R., Schroeder,J.J., French,A.J., McDonnell,S.K., Peterson,B.J., Cunningham,J.M., Thibodeau,S.N., and Schaid,D.J. (2000). Evidence for a prostate cancer-susceptibility locus on chromosome 20. Am J Hum Genet. *67*, 82-91.

Berry,S.J., Coffey,D.S., Walsh,P.C., and Ewing,L.L. (1984). The development of human benign prostatic hyperplasia with age. J. Urol. *132*, 474-479.

Birkhoff,J.D., Wiederhorn,A.R., Hamilton,M.L., and Zinsser,H.H. (1976). Natural history of benign prostatic hypertrophy and acute urinary retention. Urology *7*, 48-52.

Blaivas,J.G. (1996). Obstructive uropathy in the male. Urol. Clin. North Am. *23*, 373-384.

Bock,C.H., Cunningham,J.M., McDonnell,S.K., Schaid,D.J., Peterson,B.J., Pavlic,R.J., Schroeder,J.J., Klein,J., French,A.J., Marks,A., Thibodeau,S.N., Lange,E.M., and Cooney,K.A. (2001). Analysis of the prostate cancer-susceptibility locus HPC20 in 172 families affected by prostate cancer. Am J Hum Genet. *68*, 795-801.

Bockmuh,I.U., Petersen,S., Schmidt,S., Wolf,G., Jahnke,V., Dietel,M., and Petersen,I. (1997). Patterns of chromosomal alterations in metastasizing and nonmetastasizing primary head and neck carcinomas. Cancer Res. *57*, 5213-5216.

Bonkhoff,H. and Remberger,K. (1996). Differentiation pathways and histogenetic aspects of normal and abnormal prostatic growth: a stem cell model. Prostate *28*, 98-106.

Bonkhoff,H., Stein,U., and Remberger,K. (1994). The proliferative function of basal cells in the normal and hyperplastic human prostate. Prostate *24*, 114-118.

Bonkhoff,H., Wernert,N., Dhom,G., and Remberger,K. (1991). Relation of endocrine-paracrine cells to cell proliferation in normal, hyperplastic, and neoplastic human prostate. Prostate *19*, 91-98.

Bosch,R.J., Griffiths,D.J., Blom,J.H., and Schroeder,F.H. (1989). Treatment of benign prostatic hyperplasia by androgen deprivation: effects on prostate size and urodynamic parameters. J. Urol. *141*, 68-72.

Boyle, P. (1990). Eur Urol. *18[Suppl 5]*, 2-9.

Bright,R.K., Vocke,C.D., Emmert-Buck,M.R., Duray,P.H., Solomon,D., Fetsch,P., Rhim,J.S., Linehan,W.M., and Topalian,S.L. (1997a). Generation and genetic characterisation of immortal human prostate epithelial cell lines derived from primary cancer specimens. Cancer Res *57*, 995-1002.

Bright,R.K., Vocke,C.D., Emmert-Buck,M.R., Duray,P.H., Solomon,D., Fetsch,P., Rhim,J.S., Linehan,W.M., and Topalian,S.L. (1997b). Generation and genetic characterization of immortal human prostate epithelial cell lines derived from primary cancer specimens. Cancer Res. *57*, 995-1002.

Brock and Madigan. (2002). Biology of Microorganisms, [5th edition]. Brock and Madigan.

Brothman,A.R., Ghosn,C., and Werner,E. (1990). Pentasomy 21q in a neonatal case of acute myeloblastic leukemia. Cancer Genet. Cytogenet. *47*, 135-137.

Brothman,A.R., Patel,A.M., Peehl,D.M., and Schellhammer,P.F. (1992a). Analysis of prostatic tumor cultures using fluorescence in-situ hybridization (FISH). Cancer Genet. Cytogenet. *62*, 180-185.

Brothman,A.R., Patel,A.M., Peehl,D.M., and Schellhammer,P.F. (1992b). Analysis of prostatic tumor cultures using fluorescence in-situ hybridization (FISH). Cancer Genet. Cytogenet. *62*, 180-185.

Bryan,T.M. and Reddel,R.R. (1994). SV40-induced immortalization of human cells. Crit Rev. Oncog. *5*, 331-357.

Capella,C., Usellini,L., Buffa,R., Frigerio,B., and Solcia,E. (1981). The endocrine component of prostatic carcinomas, mixed adenocarcinoma- carcinoid tumours and non-tumour prostate. Histochemical and ultrastructural identification of the endocrine cells. Histopathology *5*, 175-192.

Carbone,M. (2001). Introduction. Semin Cancer Biol. *11*, 1-3.

Carney,D.N., Gazdar,A.F., Bepler,G., Guccion,J.G., Marangos,P.J., Moody,T.W., Zweig,M.H., and Minna,J.D. (1985). Establishment and identification of small cell lung cancer cell lines having classic and variant features. Cancer Res *45*, 2913-2923.

Cattoretti,G., Becker,M.H., Key,G., Duchrow,M., Schluter,C., Galle,J., and Gerdes,J. (1992). Monoclonal antibodies against recombinant parts of the Ki-67 antigen (MIB 1 and MIB 3) detect proliferating cells in microwave-processed formalin-fixed paraffin sections. J. Pathol. *168*, 357-363.

Cepko,C.L., Roberts,B.E., and Mulligan,R.C. (1984). Construction and applications of a highly transmissible murine retrovirus shuttle vector. Cell *37*, 1053-1062.

Chancellor,M.B., Blaivas,J.G., Kaplan,S.A., and Axelrod,S. (1991). Bladder outlet obstruction versus impaired detrusor contractility: the role of outflow. J. Urol. *145*, 810-812.

Chang,P.L., Huang,S.T., Wang,T.M., Hsieh,M.L., and Tsui,K.H. (1998). Improvements in the efficiency of care after implementing a clinical- care pathway for transurethral prostatectomy. Br. J. Urol. *81*, 394-397.

Cher,M.L., MacGrogan,D., Bookstein,R., Brown,J.A., Jenkins,R.B., and Jensen,R.H. (1994). Comparative genomic hybridization, allelic imbalance, and fluorescence in situ hybridization on chromosome 8 in prostate cancer. Genes Chromosomes Cancer *11*, 153-162.

Chou,J.Y., Avila,J., and Martin,R.G. (1974). Viral DNA synthesis in cells infected by temperature-sensitive mutants of simian virus 40. J. Virol. *14*, 116-124.

Chung,T., Huang,J.S., Mukherjee,J.J., Crilly,K.S., and Kiss,Z. (2000). Expression of human choline kinase in NIH 3T3 fibroblasts increases the mitogenic potential of insulin and insulin-like growth factor I. Cell Signal *12*, 279-288.

Chyou,P.H., Nomura,A.M., Stemmermann,G.N., and Hankin,J.H. (1993a). A prospective study of alcohol, diet, and other lifestyle factors in relation to obstructive uropathy. Prostate *22*, 253-264.

Chyou,P.H., Nomura,A.M., Stemmermann,G.N., and Hankin,J.H. (1993b). A prospective study of alcohol, diet, and other lifestyle factors in relation to obstructive uropathy. Prostate *22*, 253-264.

Coffey,D.S. and Isaacs,J.T. (1981). Prostate tumor biology and cell kinetics--theory. Urology *17*, 40-53.

Cohen,R.I., Mckay,R., and Almazan,G. (1999). Cyclic AMP regulates PDGF-stimulated signal transduction and differentiation of an immortalized optic-nerve-derived cell line. J Exp Biol. *202*, 461-473.

Costello,L.C. and Franklin,R.B. (1981). Aconitase activity, citrate oxidation, and zinc inhibition in rat ventral prostate. Enzyme *26*, 281-287.

Costello,L.C. and Franklin,R.B. (1994). Effect of prolactin on the prostate. Prostate *24*, 162-166.

Costello,L.C. and Franklin,R.B. (1997). Citrate metabolism of normal and malignant prostate epithelial cells. Urology *50*, 3-12.

Costello,L.C., Liu,Y., and Franklin,R.B. (1996). Testosterone and prolactin stimulation of mitochondrial aconitase in pig prostate epithelial cells. Urology *48*, 654-659.

Cunha,G.R., Sekkingstad,M., and Meloy,B.A. (1983). Heterospecific induction of prostatic development in tissue recombinants prepared with mouse, rat, rabbit and human tissues. Differentiation *24*, 174-180.

Cunha,G.R., Young,P., Hom,Y.K., Cooke,P.S., Taylor,J.A., and Lubahn,D.B. (1997). Elucidation of a role for stromal steroid hormone receptors in mammary gland growth and development using tissue recombinants. J Mammary Gland Biol Neoplasia. *2*, 393-402.

Cussenot,O., Berthon,P., Berger,R., Mowszowicz,I., Faille,A., Hojman,F., Teillac,P., Le Duc,A., and Calvo,F. (1991). Immortalization of human adult normal prostatic epithelial cells by liposomes containing large T-SV40 gene. J. Urol. *146*, 881-886.

Cussenot,O., Berthon,P., Cochand-Priollet,B., Maitland,N.J., and Le Duc,A. (1994a). Immunocytochemical comparison of cultured normal epithelial prostatic cells with prostatic tissue sections. Exp. Cell Res. *214*, 83-92.

Cussenot,O., Berthon,P., Cochand-Priollet,B., Maitland,N.J., and Le Duc,A. (1994b). Immunocytochemical comparison of cultured normal epithelial prostatic cells with prostatic tissue sections. Exp. Cell Res. *214*, 83-92.

Cussenot,O. and Valeri,A. (2001). Heterogeneity in genetic susceptibility to prostate cancer. Europ J of Int Medic *12*, 11-16.

Cuthill,S., Agarwal,P., Sarkar,S., Savelieva,E., and Reznikoff,C.A. (1999). Dominant genetic alterations in immortalization: role for 20q gain. Genes Chromosomes Cancer *26*, 304-311.

Danna,K. and Nathans,D. (1971). Specific cleavage of simian virus 40 DNA by restriction endonuclease of Hemophilus influenzae. Proc. Natl. Acad. Sci. U. S. A *68*, 2913-2917.

Danna,K.J. and Nathans,D. (1972). Bidirectional replication of Simian Virus 40 DNA. Proc. Natl. Acad. Sci. U. S. A *69*, 3097-3100.

Darnell,J.E., Berk,A., Zipursky,S.L., Matsudaira,P., Baltimore,D., and Lodish,H., (1986). Molecular Cell Biology. 4th edition. 815-858. New York: Scientific American Books.

Dean,F.B., Bullock,P., Murakami,Y., Wobbe,C.R., Weissbach,L., and Hurwitz,J. (1987a). Simian virus 40 (SV40) DNA replication: SV40 large T antigen unwinds DNA containing the SV40 origin of replication. Proc. Natl. Acad. Sci. U. S. A *84*, 16-20.

Dean,F.B., Dodson,M., Echols,H., and Hurwitz,J. (1987b). ATP-dependent formation of a specialized nucleoprotein structure by simian virus 40 (SV40) large tumor antigen at the SV40 replication origin. Proc. Natl. Acad. Sci. U. S. A *84*, 8981-8985.

Degeorges A, Hoffschir F, Cussenot O, Gauville C, Le Duc A, Dutrillaux B, and Calvo F (1995). Recurrent cytogenetic alterations of prostate carcinoma and amplification of c-myc or epidermal growth factor receptor in subclones of immortalized PNT1 human prostate epithelial cell line. Int J Cancer *62*, 724-731.

Delos,S., Carsol,J.L., Fina,F., Raynaud,J.P., and Martin,P.M. (1998). 5alpha-reductase and 17beta-hydroxysteroid dehydrogenase expression in epithelial cells from hyperplastic and malignant human prostate . Int J Cancer. *75*, 840-846.

Dermer,G.B. (1978). Basal cell proliferation in benign prostatic hyperplasia. Cancer. *41(5)*, 1857-1862.

di Sant'Agnese,P.A. and Mesy Jensen,K.L. (1984). Somatostatin and/or somatostatin-like immunoreactive endocrine- paracrine cells in the human prostate gland. Arch. Pathol. Lab Med. *108*, 693-696.

di Sant'Agnese,P.A., Mesy Jensen,K.L., and Ackroyd,R.K. (1989). Calcitonin, katacalcin, and calcitonin gene-related peptide in the human prostate. An immunocytochemical and immunoelectron microscopic study. Arch. Pathol. Lab Med. *113*, 790-796.

di Sant'Agnese,P.A., Mesy Jensen,K.L., Churukian,C.J., and Agarwal,M.M. (1985). Human prostatic endocrine-paracrine (APUD) cells. Distributional analysis with a comparison of serotonin and neuron-specific enolase immunoreactivity and silver stains. Arch. Pathol. Lab Med. *109*, 607-612.

Dodson,M., Dean,F.B., Bullock,P., Echols,H., and Hurwitz,J. (1987). Unwinding of duplex DNA from the SV40 origin of replication by T antigen. Science *238*, 964-967.

Dornreiter,I., Hoss,A., Arthur,A.K., and Fanning,E. (1990). SV40 T antigen binds directly to the large subunit of purified DNA polymerase alpha. EMBO J. *9*, 3329-3336.

Dreikorn,K. (2002). The role of phytotherapy in treating lower urinary tract symptoms and benign prostatic hyperplasia. World J. Urol. *19*, 426-435.

Drubin,D.G. and Nelson,W.J. (1996). Origins of cell polarity. Cell *84*, 335-344.

Fetissof,F., Bertrand,G., Guilloteau,D., Dubois,M.P., Lanson,Y., and Arbeille,B. (1986). Calcitonin immunoreactive cells in prostate gland and cloacal derived tissues. Virchows Arch. A Pathol. Anat. Histopathol. *409*, 523-533.

Fetissof,F., Dubois,M.P., Arbeille-Brassart,B., Lanson,Y., Boivin,F., and Jobard,P. (1983). Endocrine cells in the prostate gland, urothelium and Brenner tumors. Immunohistological and ultrastructural studies. Virchows Arch. B Cell Pathol. Incl. Mol. Pathol. *42*, 53-64.

Finlay,C.A., Hinds,P.W., and Levine,A.J. (1989). The p53 proto-oncogene can act as a suppressor of transformation. Cell *57*, 1083-1093.

Franklin,R.B. and Costello,L.C. (1990). Prolactin directly stimulates citrate production and mitochondrial aspartate aminotransferase of prostate epithelial cells. Prostate *17*, 13-18.

Freshney R.I. (1987). Culture of animal cells "A manual of Basic Techniques" 4th edition. A John Wiley & Sons, INC., publication, NY.

Fry,P.M., Hudson,D.L., O'Hare,M.J., and Masters,J.R. (2000a). Comparison of marker protein expression in benign prostatic hyperplasia in vivo and in vitro. BJU. Int. *85*, 504-513.

Fry,P.M., Hudson,D.L., O'Hare,M.J., and Masters,J.R. (2000b). Comparison of marker protein expression in benign prostatic hyperplasia in vivo and in vitro. BJU. Int. *85*, 504-513.

Fry,P.M., Hudson,D.L., O'Hare,M.J., and Masters,J.R. (2000c). Comparison of marker protein expression in benign prostatic hyperplasia in vivo and in vitro. BJU. Int. *85*, 504-513.

Garraway,W.M., Russell,E.B., Lee,R.J., Collins,G.N., McKelvie,G.B., Hehir,M., Rogers,A.C., and Simpson,R.J. (1993). Impact of previously unrecognized benign prostatic hyperplasia on the daily activities of middle-aged and elderly men. Br. J. Gen. Pract. *43*, 318-321.

Gartler,S.M. (1967). Genetic markers as tracers in cell culture. Natl Cancer Inst Monogr. *26*,167-195

George,F.W. and Wilson,J.D. (1986). Hormonal control of sexual development. Vitam. Horm. *43*, 145-196.

Georget,V., Lobaccaro,J.M., Terouanne,B., Mangeat,P., Nicolas,J.C., and Sultan,C. (1997). Trafficking of the androgen receptor in living cells with fused green fluorescent protein-androgen receptor. Mol Cell Endocrinol. *129*, 17-26.

Gerber,G.S. (2002). Phytotherapy for benign prostatic hyperplasia. Curr. Urol. Rep. *3*, 285-291.

Gerdes,J., Lemke,H., Baisch,H., Wacker,H.H., Schwab,U., and Stein,H. (1984). Cell cycle analysis of a cell proliferation-associated human nuclear antigen defined by the monoclonal antibody Ki-67. J. Immunol. *133*, 1710-1715.

Glinsky GV, Price JE, Glinsky VV, Mossine VV, Kiriakova G, and Metcalf JB (1996). Inhibition of human breast cancer metastasis in nude mice by synthetic glycoamines. Cancer Res *56*, 5319-5324.

Gnanapragasam,V.J., Robson,C.N., Leung,H.Y., and Neal,D.E. (2000). Androgen receptor signalling in the prostate. BJU Int. *86*, 1001-1013.

Gokhan,S., Song,Q., and Mehler,M.F. (1998). Generation and regulation of developing immortalized neural cell lines. Methods *16*, 345-358.

Goldstein,J.L. and Wilson,J.D. (1975). Genetic and hormonal control of male sexual differentiation. J. Cell Physiol *85*, 365-377.

Griffiths,D.J. (1996). Pressure-flow studies of micturition. Urol. Clin. North Am. *23*, 279-297.

Griffiths,K., Denis,L., Turkes,A., and Morton,M.S. (1998). Phytoestrogens and diseases of the prostate gland. Baillieres Clin. Endocrinol. Metab *12*, 625-647.

Griffiths,K., Eaton,C.L., Harper,M.E., Peeling,B., and Davies,P. (1991). Steroid hormones and the pathogenesis of benign prostatic hyperplasia. Eur. Urol. *20 Suppl 1*, 68-77.

Guess,H.A., Heyse,J.F., Gormley,G.J., Stoner,E., and Oesterling,J.E. (1993). Effect of finasteride on serum PSA concentration in men with benign prostatic hyperplasia. Results from the North American phase III clinical trial. Urol. Clin. North Am. *20*, 627-636.

Habib FK, Ross M, Bayne CW, Grigor K, Buck AC, Bollina P, and Chapman K (1998). The localisation and expression of 5 alpha-reductase types I and II mRNAs in human hyperplastic prostate and in prostate primary cultures. J Endocrinol. *156*, 509-517.

Habib,F.K., Ross,M., and Bayne,C.W. (2000). Development of a new in vitro model for the study of benign prostatic hyperplasia. Prostate Suppl *9*, 15-20.

Hall,J.A., Maitland,N.J., Stower,M., and Lang,S.H. (2002). Primary prostate stromal cells modulate the morphology and migration of primary prostate epithelial cells in type 1 collagen gels. Cancer Res. *62* , 58-62.

Hansen,J.C. and Deguchi,Y. (1996). Selenium and fertility in animals and man--a review. Acta Vet. Scand. *37*, 19-30.

Hayflick,L. (1965). Tissue cultures and mycoplasmas. Tex. Rep. Biol. Med. *23*, Suppl.

Hayward,S.W., Dahiya,R., Cunha,G.R., Bartek,J., Deshpande,N., and Narayan,P. (1995). Establishment and characterization of an immortalized but non- transformed human prostate epithelial cell line: BPH-1. In Vitro Cell Dev. Biol. Anim *31*, 14-24.

Hayward,S.W., Del Buono,R., Deshpande,N., and Hall,P.A. (1992). A functional model of adult human prostate epithelium. The role of androgens and stroma in architectural organisation and the maintenance of differentiated secretory function. J Cell Sci. *102* , 361-372.

Hayward,S.W., Haughney,P.C., Lopes,E.S., Danielpour,D., and Cunha,G.R. (1999). The rat prostatic epithelial cell line NRP-152 can differentiate in vivo in response to its stromal environment. Prostate *39*, 205-212.

Hayward,S.W., Rosen,M.A., and Cunha,G.R. (1997). Stromal-epithelial interactions in the normal and neoplastic prostate. Br J Urol. *79*, 18-26.

Henttu,P. and Vihko,P. (1989). cDNA coding for the entire human prostate specific antigen shows high homologies to the human tissue kallikrein genes. Biochem. Biophys. Res. Commun. *160*, 903-910.

Hieble,J.P., Caine,M., and Zalaznik,E. (1985). In vitro characterization of the alpha-adrenoceptors in human prostate. Eur. J. Pharmacol. *107*, 111-117.

Hine,I.F. (1981). Block staining of mammalian tissues with hematoxylin and eosin. Stain Technol. *56(2)*, 119-123.

Hockenbery,D.M., Zutter,M., Hickey,W., Nahm,M., and Korsmeyer,S.J. (1991). BCL2 protein is topographically restricted in tissues characterized by apoptotic cell death. Proc. Natl. Acad. Sci. U. S. A *88*, 6961-6965.

Holley,M.C. and Lawlor,P.W. (1997). Production of conditionally immortalised cell lines from a transgenic mouse. Audiol Neurootol. *2*, 25-35.

Holtgrewe,H.L. (1998). Current trends in management of men with lower urinary tract symptoms and benign prostatic hyperplasia. Urology *51*, 1-7.

Honjo,Y., Nangia-Makker,P., Inohara,H., and Raz,A. (2001). Down-regulation of galectin-3 suppresses tumorigenicity of human breast carcinoma cells. Clin Cancer Res. *7(3)*, 661-668.

Hopert,A., Uphoff,C.C., Wirth,M., Hauser,H., and Drexler,H.G. (1993a). Mycoplasma detection by PCR analysis. In Vitro Cell Dev. Biol. Anim *29A*, 819-821.

Hopert,A., Uphoff,C.C., Wirth,M., Hauser,H., and Drexler,H.G. (1993b). Specificity and sensitivity of polymerase chain reaction (PCR) in comparison with other methods for the detection of mycoplasma contamination in cell lines. Journal of Immunological Methods *164*, 91-100.

Horoszewicz,J.S., Leong,S.S., Chu,T.M., Wajsman,Z.L., Friedman,M., Papsidero,L., Kim,U., Chai,L.S., Kakati,S., Arya,S.K., and Sandberg,A.A. (1980). The LNCaP cell line a new model for studies on human prostatic carcinoma. Prog Clin Biol Res *37*, 115-132.

Hosoyamada,M., Obinata,M., Suzuki,M., and Endou,H. (1996). Cisplatin-induced toxicity in immortalized renal cell lines established from transgenic mice harboring temperature sensitive SV40 large T-antigen gene. Arch Toxicol. *70*, 284-292.

Hudson,D.L., Guy,A.T., Fry,P., O'Hare,M.J., Watt,F.M., and Masters,J.R. (2001a). Epithelial cell differentiation pathways in the human prostate: identification of intermediate phenotypes by keratin expression. J. Histochem. Cytochem. *49*, 271-278.

Hudson,D.L., Guy,A.T., Fry,P., O'Hare,M.J., Watt,F.M., and Masters,J.R. (2001b). Epithelial cell differentiation pathways in the human prostate: identification of intermediate phenotypes by keratin expression. J. Histochem. Cytochem. *49*, 271-278.

Hudson,D.L., O'Hare,M., Watt,F.M., and Masters,J.R. (2000a). Proliferative heterogeneity in the human prostate: evidence for epithelial stem cells. Lab Invest *80*, 1243-1250.

Hudson,D.L., O'Hare,M., Watt,F.M., and Masters,J.R. (2000b). Proliferative heterogeneity in the human prostate: evidence for epithelial stem cells. Lab Invest *80*, 1243-1250.

Imperato-McGinley,J., Guerrero,L., Gautier,T., and Peterson,R.E. (1974). Steroid 5alpha-reductase deficiency in man: an inherited form of male pseudohermaphroditism. Science *186*, 1213-1215.

Isaacs,J.T., Brendler,C.B., and Walsh,P.C. (1983). Changes in the metabolism of dihydrotestosterone in the hyperplastic human prostate. J. Clin. Endocrinol. Metab *56*, 139-146.

Isaacs,J.T. and Coffey,D.S. (1989a). Etiology and disease process of benign prostatic hyperplasia. Prostate Suppl *2*, 33-50.

Isaacs,J.T. and Coffey,D.S. (1989b). Etiology and disease process of benign prostatic hyperplasia. Prostate Suppl *2*, 33-50.

Iype,P.T., Iype,L.E., Verma,M., and Kaighn,M.E. (1998). Establishment and characterization of immortalized human cell lines from prostatic carcinoma and benign prostatic hyperplasia. Int. J. Oncol. *12*, 257-263.

Janssen,M., Albrecht,M., Moschler,O., Renneberg,H., Fritz,B., Aumuller,G., and Konrad,L. (2000). Cell lineage characteristics of human prostatic stromal cells cultured in vitro. Prostate *43*, 20-30.

Janssen,P.J., Brinkmann,A.O., Boersma,W.J., and van der Kwast,T.H. (1994). Immunohistochemical detection of the androgen receptor with monoclonal antibody F39.4 in routinely processed, paraffin-embedded human tissues after microwave pre-treatment. J. Histochem. Cytochem. *42*, 1169-1175.

Jarrard,D.F. and Waldman,F.M. (1999). Cancer Res *59*, 2957-2964.

Jat,P.S. and Sharp,P.A. (1989). Cell lines established by a temperature-sensitive simian virus 40 large- T-antigen gene are growth restricted at the nonpermissive temperature. Mol. Cell Biol. *9*, 1672-1681.

Jenkins,E.P., Andersson,S., Imperato-McGinley,J., Wilson,J.D., and Russell,D.W. (1992a). Genetic and pharmacological evidence for more than one human steroid 5 alpha-reductase. J. Clin. Invest *89*, 293-300.

Jenkins,E.P., Andersson,S., Imperato-McGinley,J., Wilson,J.D., and Russell,D.W. (1992b). Genetic and pharmacological evidence for more than one human steroid 5 alpha-reductase. J. Clin. Invest *89*, 293-300.

Kaighn,M.E., Narayan,K.S., Ohnuki,Y., Lechner,J.F., and Jones,L.W. (1979). Establishment and characterization of a human prostatic carcinoma cell line (PC-3). Invest Urol. *17(1)*, 16-23

Kaighn,M.E. (1980). Human prostatic epithelial cell culture models. Invest Urol. *17*, 382-385.

Kaighn,M.E., Reddel,R.R., Lechner,J.F., Peehl,D.M., Camalier,R.F., Brash,D.E., Saffiotti,U., and Harris,C.C. (1989). Transformation of human neonatal prostate epithelial cells by strontium phosphate transfection with a plasmid containing SV40 early region genes. Cancer Res. *49*, 3050-3056.

Kameoka,J., Yanai,N., and Obinata,M. (1995). Bone marrow stromal cells selectively stimulate the rapid expansion of lineage-restricted myeloid progenitors. J Cell Physiol. *164*, 55-64.

Kassen,A., Sutkowski,D.M., Ahn,H., Sensibar,J.A., Kozlowski,J.M., and Lee,C. (1996a). Stromal cells of the human prostate: initial isolation and characterization. Prostate *28*, 89-97.

Kassen,A., Sutkowski,D.M., Ahn,H., Sensibar,J.A., Kozlowski,J.M., and Lee,C. (1996b). Stromal cells of the human prostate: initial isolation and characterization. Prostate *28*, 89-97.

Kellokumpu-Lehtinen,P. and Pelliniemi,L.J. (1988). Hormonal regulation of differentiation of human fetal prostate and Leydig cells in vitro. Folia Histochem. Cytobiol. *26*, 113-117.

Kemppainen,J.A., Lane,M.V., Sar,M., and Wilson,E.M. (1992). Androgen receptor phosphorylation, turnover, nuclear transport, and transcriptional activation. Specificity for steroids and antihormones. J Biol Chem. *267*, 968-974.

King,B.L., Lichtenstein,A., Berenson,J., and Kacinski,B.M. (1994). A polymerase chain reaction-based microsatellite typing assay used for tumor cell line identification. Am. J. Pathol. *144*, 486-491.

Kleinman,H.K., Luckenbill-Edds,L., Cannon,F.W., and Sephel,G.C. (1987a). Use of extracellular matrix components for cell culture. Anal. Biochem. *166*, 1-13.

Kleinman,H.K., Luckenbill-Edds,L., Cannon,F.W., and Sephel,G.C. (1987b). Use of extracellular matrix components for cell culture. Anal. Biochem. *166*, 1-13.

Kohler,G. and Milstein,C. (1975). Continuous cultures of fused cells secreting antibody of predefined specificity. Nature. *256(5517)*, 495-497.

Kooistra,A., Elissen,N.M., Konig,J.J., Vermey,M., van der Kwast,T.H., Romijn,J.C., and Schroder,F.H. (1995a). Immunocytochemical characterization of explant cultures of human prostatic stromal cells. Prostate *27*, 42-49.

Kooistra,A., Konig,J.J., Keizer,D.M., Romijn,J.C., and Schroder,F.H. (1995b). Inhibition of prostatic epithelial cell proliferation by a factor secreted specifically by prostatic stromal cells. Prostate *26*, 123-132.

Korn,W.M., Yasutake,T., Kuo,W.L., Warren,R.S., Collins,C., Tomita,M., Gray,J., and Waldman,F.M. (1999). Chromosome arm 20q gaains and other genomic alterations in colorectal cancer metastatic to liver, as analysed by comparative genomic hybridization and fluorescence in situ hybridization. Genes Chromosomes Cancer *25*, 82-90.

Kwon,Y.K. (1979). Expression of brain-derived neurotrophic factor mRNA stimulated by basic fibroblast growth factor and platelet-derived growth factor in rat hippocampal cell line. Mol Cells *7*, 320-325.

Lang,S.H., Sharrard,R.M., Stark,M., Villette,J.M., and Maitland,N.J. (2001). Prostate epithelial cell lines form spheroids with evidence of glandular differentiation in three-dimensional Matrigel cultures . Br J Cancer. *85*, 599.

Lawson,R.K. (1997). Role of growth factors in benign prostatic hyperplasia. Eur. Urol. *32 Suppl 1*, 22-27.

Lechner,J.F., Narayan,K.S., Ohnuki,Y., Babcock,M.S., Jones,L.W., and Kaighn,M.E. (1978). Replicative epithelial cell cultures from normal human prostate gland. J. Natl. Cancer Inst. *60*, 797-801.

Le Poole.I.C, van den Berg.F.M, van den Wijngaard.R.M, Galloway.D.A, van Amstel.P.J, Buffing.A.A, Smits.H.L, Westerhof.W., and Das.P.K. Generation of a human melanocyte cell line by introduction of HPV E6 and E7 genes. In Vitro Cell Dev. Biol. Anim. 33(1), 42-49.

Lepor H. (2002). Cambells Urology, Ch 47. [7th Edition]. Philidelphia.

Lepor,H., Gup,D.I., Baumann,M., and Shapiro,E. (1988). Laboratory assessment of terazosin and alpha-1 blockade in prostatic hyperplasia. Urology *32*, 21-26.

Leung,E.H., Leung,P.C., and Auersperg,N. (2001). Differentiation and growth potential of human ovarian surface epithelial cells expressing temperature-sensitive SV40 T antigen. In Vitro Cell Dev Biol Anim. *37(8)*, 515-521

Lilja,H. and Abrahamsson,P.A. (1988). Three predominant proteins secreted by the human prostate gland. Prostate *12*, 29-38.

Lin,M.F., DaVolio,J., and Garcia-Arenas,R. (1992). Expression of human prostatic acid phosphatase activity and the growth of prostate carcinoma cells. Cancer Res. *52*, 4600-4607.

Lins,A.M., Micka,K.A., Sprecher,C.J., Taylor,J.A., Bacher,J.W., Rabbach,D.R., Bever,R.A., Creacy,S.D., and Schumm,J.W. (1998). Development and population study of an eight-locus short tandem repeat (STR) multiplex system. J. Forensic Sci. *43*, 1168-1180.

Liu,A.Y., True,L.D., LaTray,L., Nelson,P.S., Ellis,W.J., Vessella,R.L., Lange,P.H., Hood,L., and van den,E.G. (1997). Cell-cell interaction in prostate gene regulation and cytodifferentiation. Proc. Natl. Acad. Sci. U. S. A *94*, 10705-10710.

Lowe,F.C. (2001). Phytotherapy in the management of benign prostatic hyperplasia. Urology *58*, 71-76.

Lytton,B., Emery,J.M., and Harvard,B.M. (1968). The incidence of benign prostatic obstruction. J. Urol. *99*, 639-645.

Ma,Y.L., Fujiyama,C., Masaki,Z., and Sugihara,H. (1997). Reconstruction of prostatic acinus-like structure from ventral and dorsolateral prostatic epithelial cells of the rat in three-dimensional collagen gel matrix culture. J. Urol. *157*, 1025-1031.

Macieira-Coelho,A. and Azzarone,B. (1988). The transition from primary culture to spontaneous immortalization in mouse fibroblast populations. Anticancer Res. *8*, 669-676.

MacLeod,R.A., Spitzer,D., Bar-Am,I., Sylvester,J.E., Kaufmann,M., Wernich,A., Drexler,H.G. (2000). Karyotypic dissection of Hodgkin's disease cell lines reveals ectopic subtelomeres and ribosomal DNA at sites of multiple jumping translocations and genomic amplification. Leukemia. 14(10),1803-14.

Macoska,J.A., Beheshti,B., Rhim,J.S., Hukku,B., Lehr,J., Pienta,K.J., and Squire,J.A. (2000). Genetic characterization of immortalized human prostate epithelial cell cultures. Evidence for structural rearrangements of chromosome 8 and i(8q) chromosome formation in primary tumor-derived cells. Cancer Genet Cytogenet. *120*, 50-57.

Madsen,F.A. and Bruskewitz,R.C. (1995b). Clinical manifestations of benign prostatic hyperplasia. Urol. Clin. North Am. *22*, 291-298.

Madsen,F.A. and Bruskewitz,R.C. (1995a). Clinical manifestations of benign prostatic hyperplasia. Urol. Clin. North Am. *22*, 291-298.

Mahlamaki,E.H., Hoglund,M., Gorunova,L., Karhu,R., Dawiskiba,S., Andren-Sandberg,A., Kallioniemi,O.P., and Johansson,B. (1997). Chromosome genomic hybridization reveals frequent gains of 20q, 8q, 11q, 12p and 17q, and losses of 18q, 9q and 15p in pancreatic cancer. Genes Chromosomes Cancer *20*, 383-391.

Malinda,K.M. and Kleinman,H.K. (1996). The laminins. Int. J. Biochem. Cell Biol. *28*, 957-959.

Masai,M., Sumiya,H., Akimoto,S., Yatani,R., Chang,C.S., Liao,S.S., and Shimazaki,J. (1990). Immunohistochemical study of androgen receptor in benign hyperplastic and cancerous human prostates. Prostate *17* , 293-300.

Masters,J.R., Thomson,J.A., Daly-Burns,B., Reid,Y.A., Dirks,W.G., Packer,P., Toji,L.H., Ohno,T., Tanabe,H., Arlett,C.F., Kelland,L.R., Harrison,M., Virmani,A., Ward,T.H., Ayres,K.L., and Debenham,P.G. (2001). Short tandem repeat profiling provides an international reference standard for human cell lines. Proc. Natl. Acad. Sci. U. S. A *98*, 8012-8017.

Mawhinney,M.G., Schwartz,F.L., Thomas,J.A., and Lloyd,J.W., III (1974). Androgen assimilation by normal and hyperplastic dog prostate glands. Invest Urol. *12*, 17-22.

McConnell,J.D. (1994). Clinical Practice Guidelines. Clinical Practice Guidelines No8 AHCPR publication No 94-0582.

McConnell,J.D. (1998). Campbell's urology., P.C.T.A.B.V.E.D.W.A.J.Walsh, ed. (Philadelphia: WB Saunders Co), pp. 1429-1452.

McConnell,J.D., Barry,M.J., and Bruskewitz,R.C. (1994a). Benign prostatic hyperplasia: diagnosis and treatment. Agency for Health Care Policy and Research. Clin. Pract. Guidel. Quick Ref. Guide Clin. 1-17.

McConnell,J.D., Barry,M.J., and Bruskewitz,R.C. (1994b). Benign prostatic hyperplasia: diagnosis and treatment. Agency for Health Care Policy and Research. Clin. Pract. Guidel. Quick Ref. Guide Clin. 1-17.

McDonnell,T.J., Troncoso,P., Brisbay,S.M., Logothetis,C., Chung,L.W., Hsieh,J.T., Tu,S.M., and Campbell,M.L. (1992). Expression of the protooncogene bcl-2 in the prostate and its association with emergence of androgen-independent prostate cancer. Cancer Res. *52*, 6940-6944.

McKeehan,W.L., Adams,P.S., and Rosser,M.P. (1984). Direct mitogenic effects of insulin, epidermal growth factor, glucocorticoid, cholera toxin, unknown pituitary factors and possibly prolactin, but not androgen, on normal rat prostate epithelial cells in serum-free, primary cell culture. Cancer Res. *44*, 1998-2010.

McNeal,J.E. (1968). Regional morphology and pathology of the prostate. Am. J. Clin. Pathol. *49*, 347-357.

McNeal,J.E. (1978). Origin and evolution of benign prostatic enlargement. Invest Urol. *15*, 340-345.

Menter,D.G., Sabichi,A.L., and Lippman,S.M. (2000). Selenium effects on prostate cell growth. Cancer Epidemiol Biomarkers Prev. *9(11)*,1171-1182.

Merchant,D.J., Clarke,S.M., Ives,K., and Harris,S. (1983). Primary explant culture: an in vitro model of the human prostate. Prostate *4*, 523-542.

Mohapatra,G., Kim,D.H., and Feuerstein,B.G. (1995). Detection of multiple gains and losses of genetic material in ten glioma cell lines by comparative genomic hybridization. Genes Chromosomes Cancer *13*, 86-93.

Nathans,D. and Danna,K.J. (1972). Specific origin in SV40 DNA replication. Nat. New Biol. *236*, 200-202.

Nelson-Rees,W.A., Daniels,D.W., and Flandermeyer,R.R. (1981). Cross-contamination of cells in culture. Science. *212(4493)*, 446-452.

O'Hare,M.J., Bond,J., Clarke,C., Takeuchi,Y., Atherton,A.J., Berry,C., Moody,J., Silver,A.R., Davies,D.C., Alsop,A.E., Neville,A.M., and Jat,P.S. (2001). Conditional immortalization of freshly isolated human mammary fibroblasts and endothelial cells. Proc. Natl. Acad. Sci. U. S. A *98* , 646-651.

Ohyashiki,K., Sasao,I., Ohyashiki,J.H., Murakami,T., Tauchi,T., and Iwabuchi (1992). Cytogenetic and clinical findings of myelodysplastic syndromes with a poor prognosis. An experience with 97 cases. *70*, 94-99.

Ostrowski,W.S. and Kuciel,R. (1994). Human prostatic acid phosphatase: selected properties and practical applications. Clin. Chim. Acta *226*, 121-129.

Ozer,H.L., Banga,S.S., Dasgupta,T., Houghton,J., Hubbard,K., Jha,K.K., Kim,S.H., Lenahan,M., Pang,Z., Pardinas,J.R., and Patsalis,P.C. (1996). SV40-mediated immortalization of human fibroblasts. Exp. Gerontol. *31*, 303-310.

Parsons,R., Anderson,M.E., and Tegtmeyer,P. (1990). Three domains in the simian virus 40 core origin orchestrate the binding, melting, and DNA helicase activities of T antigen. J. Virol. *64*, 509-518.

Peehl,D.M., Leung,G.K., and Wong,S.T. (1994). Keratin expression: a measure of phenotypic modulation of human prostatic epithelial cells by growth inhibitory factors. Cell Tissue Res. *277*, 11-18.

Peehl,D.M. and Sellers,R.G. (1997). Induction of smooth muscle cell phenotype in cultured human prostatic stromal cells. Exp. Cell Res. *232*, 208-215.

Peehl,D.M., Sellers,R.G., and McNeal,J.E. (1996). Keratin 19 in the adult human prostate: tissue and cell culture studies. Cell Tissue Res. *285*, 171-176.

Peehl,D.M. and Stamey,T.A. (1986a). Growth responses of normal, benign hyperplastic, and malignant human prostatic epithelial cells in vitro to cholera toxin, pituitary extract, and hydrocortisone. Prostate *8*, 51-61.

Peehl,D.M. and Stamey,T.A. (1986b). Serum-free growth of adult human prostatic epithelial cells. In Vitro Cell Dev. Biol. *22* , 82-90.

Peehl,D.M., Wong,S.T., and Stamey,T.A. (1988a). Clonal growth characteristics of adult human prostatic epithelial cells. In Vitro Cell Dev. Biol. *24*, 530-536.

Peehl,D.M., Wong,S.T., and Stamey,T.A. (1988b). Clonal growth characteristics of adult human prostatic epithelial cells. In Vitro Cell Dev. Biol. *24*, 530-536.

Peters,D.M., Dowd.N, Brandt.C., and Compton.T. (1996). Human papilloma virus E6/E7 genes can expand the lifespan of human corneal fibroblasts. In Vitro Cell Dev. Biol. May; 32(5), 279-284.

Pipas,J.M. and Levine,A.J. (2001). Role of T antigen interactions with p53 in tumorigenesis. Semin. Cancer Biol. *11*, 23-30.

Planz,B., Kirley,S.D., Wang,Q., Tabatabaei,S., Aretz,H.T., and McDougal,W.S. (1999). Characterization of a stromal cell model of the human benign and malignant prostate from explant culture. J. Urol. *161*, 1329-1336.

Planz,B., Wang,Q., Kirley,S.D., Lin,C.W., and McDougal,W.S. (1998). Androgen responsiveness of stromal cells of the human prostate: regulation of cell proliferation and keratinocyte growth factor by androgen. J Urol. *160*, 1850-1855.

Polat,O., Ozbey,I., Gul,O., Demirel,A., and Bayraktar,Y. (1997). Pharmacotherapy of benign prostatic hyperplasia: inhibitor of 5 alpha- reductase. Int. Urol. Nephrol. *29*, 323-330.

Purkis,P.E., Steel,J.B., Mackenzie,I.C., Nathrath,W.B., Leigh,I.M., and Lane,E.B. (1990). Antibody markers of basal cells in complex epithelia. J. Cell Sci. *97 (Pt 1)*, 39-50.

Renfranz,P.J., Cunningham,M.G., and McKay,R.D. (1991). Region-specific differentiation of the hippocampal stem cell line HiB5 upon implantation into the developing mammalian brain. Cell *66*, 713-729.

Richter,J., Beffa,L., Wagner,U., Schraml,P., Gasser,T.C., Moch,H., Mihatsch,M.J., and Sauter,G. (1998). Patterns of chromosomal imbalances in advanced urinary bladder cancer detected by comparative genomic hybridization. Am. J. Pathol. *153*, 1615-1621.

Riegman,P.H., Vlietstra,R.J., van der Korput,J.A., Romijn,J.C., and Trapman,J. (1989). Characterization of the prostate-specific antigen gene: a novel human kallikrein-like gene. Biochem. Biophys. Res. Commun. *159*, 95-102.

Roberson,K.M., Edwards,D.W., Chang,G.C., and Robertson,C.N. (1995). Isolation and characterization of a novel human prostatic stromal cell culture: DuK50. In Vitro Cell Dev. Biol. Anim *31*, 840-845.

Robinson,E.J., Neal,D.E., and Collins,A.T. (1998a). Basal cells are progenitors of luminal cells in primary cultures of differentiating human prostatic epithelium. Prostate *37*, 149-160.

Robinson,E.J., Neal,D.E., and Collins,A.T. (1998b). Basal cells are progenitors of luminal cells in primary cultures of differentiating human prostatic epithelium. Prostate *37*, 149-160.

Rohr,H.P. and Bartsch,G. (1980). Human benign prostatic hyperplasia: a stromal disease? New perspectives by quantitative morphology. Urology *16*, 625-633.

Ruizeveld de Winter,J.A., Trapman,J., Vermey,M., Mulder,E., Zegers,N.D., and van der Kwast,T.H. (1991). Androgen receptor expression in human tissues: an immunohistochemical study. J. Histochem. Cytochem. *39*, 927-936.

Rundell,K. and Parakati,R. (2001). The role of the SV40 ST antigen in cell growth promotion and transformation. Semin. Cancer Biol. *11*, 5-13.

Saenz-Robles,M.T., Sullivan,C.S., and Pipas,J.M. (2001). Transforming functions of Simian Virus 40. Oncogene *20*, 7899-7907.

Salm,S.N., Koikawa,Y., Ogilvie,V., Tsujimura,A., Coetzee,S., Moscatelli,D., Moore,E., Lepor,H., Shapiro,E., Sun,T.T., and Wilson,E.L. (2000). Transforming growth factor-beta is an autocrine mitogen for a novel androgen-responsive murine prostatic smooth muscle cell line, PSMC1. J. Cell Physiol *185*, 416-424.

Sanda,M.G., Beaty,T.H., Stutzman,R.E., Childs,B., and Walsh,P.C. (1994). Genetic susceptibility of benign prostatic hyperplasia. J. Urol. *152*, 115-119.

Schlegel,J., Stumm,G., Scherthan,H., Bocker,T., Zirngibl,H., Ruschoff,J., and Hofstadter,F. (1995). Comparative genomic in situ hybridization of colon carcinomas with replication error. Cancer Res. *55*, 6002-6005.

Seigel, GM. (1996). Establishment of an E1A- immortalized retinal cell culture. In Vitro Cell Dev Biol Anim. Feb; 32(2), 66-68.

Sensibar,J.A., Pruden,S.J., Kasjanski,R.Z., Rademaker,A., Lee,C., Grayhack,J.T., and Kozlowski,J.M. (1999b). Differential growth rates in stromal cultures of human prostate derived from patients of varying ages. Prostate *38*, 110-117.

Sensibar,J.A., Pruden,S.J., Kasjanski,R.Z., Rademaker,A., Lee,C., Grayhack,J.T., and Kozlowski,J.M. (1999a). Differential growth rates in stromal cultures of human prostate derived from patients of varying ages. Prostate *38*, 110-117.

Servadio,C. (1992). Is open prostatectomy really obsolete? Urology *40*, 419-421.

Shapiro,E., Hartanto,V., and Lepor,H. (1992). Anti-desmin vs. anti-actin for quantifying the area density of prostate smooth muscle. Prostate *20*, 259-267.

Signoretti,S., Waltregny,D., Dilks,J., Isaac,B., Lin,D., Garraway,L., Yang,A., Montironi,R., McKeon,F., and Loda,M. (2000). p63 is a prostate basal cell marker and is required for prostate development. Am. J. Pathol. *157*, 1769-1775.

Sinha,A.A., Wilson,M.J., and Gleason,D.F. (1987). Immunoelectron microscopic localization of prostatic-specific antigen in human prostate by the protein A-gold complex. Cancer *60*, 1288-1293.

Skalli,O., Ropraz,P., Trzeciak,A., Benzonana,G., Gillessen,D., and Gabbiani,G. (1986). A monoclonal antibody against alpha-smooth muscle actin: a new probe for smooth muscle differentiation. J. Cell Biol. *103*, 2787-2796.

Smale,S.T. and Tjian,R. (1986). Inhibition of simian virus 40 DNA replication by specific modification of T-antigen with oxidized ATP. J. Biol. Chem. *261*, 14369-14372.

Smola,H., Stark,H.J., Thiekotter,G., Mirancea,N., Krieg,T., and Fusenig,N.E. (1998). Dynamics of basement membrane formation by keratinocyte-fibroblast interactions in organotypic skin culture. Exp Cell Res. *239*, 399-410.

Stamps,A.C., Davies,S.C., Burman,J., and O'Hare,M.J. (1994). Analysis of proviral integration in human mammary epithelial cell lines immortalized by retroviral infection with a temperature-sensitive SV40 T-antigen construct. Int. J. Cancer *57*, 865-874.

Stamps,A.C., Gusterson,B.A., and O'Hare,M.J. (1992b). Are tumours immortal? Eur. J. Cancer *28A*, 1495-1500.

Stamps,A.C., Gusterson,B.A., and O'Hare,M.J. (1992a). Are tumours immortal? Eur. J. Cancer *28A*, 1495-1500.

Steers,W.D. (2001). 5alpha-reductase activity in the prostate. Urology *58*, 17-24.

Steinberg,M.L. and Defendi,V. (1979). Altered pattern of growth and differentiation in human keratinocytes infected by simian virus 40. Proc. Natl. Acad. Sci. U. S. A *76*, 801-805.

Stone,K.R., Mickey,D.D., Wunderli,H., Mickey,G.H., and Paulson,D.F. (1978). Isolation of a human prostate carcinoma cell line (DU145). Int J Cancer *21*, 274-281.

Sugiyama,N., Tabuchi,Y., Numata,F., Uchida,Y., Horiuchi,T., Ishibashi,K., Ono,S., Obinata,M., and Furusawam,M. (1998). Establishment and characterization of tracheal epithelial cell lines, TM01 and TM02-3, from transgenic mice bearing temperature-sensitive simian virus 40 large T-antigen gene. Cell Struct Funct *23*, 119-127.

Tabuchi,Y., Ohta,S., Arai,Y., Kawahara,M., Ishibashi,K., Sugiyama,N., Horiuchi,T., Furusawa,M., Obinata,M., Fuse,H., Takeguchi,N., and Asano,S. (2000). Establishment and characterization of a colonic epithelial cell line MCE301 from transgenic mice harboring temperature-sensitive simian virus 40 large T-antigen gene. Cell Struct Funct. *25*, 297-307.

Taketa,S., Nishi,N., Takasuga,H., Okutani,T., Takenaka,I., and Wada,F. (1990a). Differences in growth requirements between epithelial and stromal cells derived from rat ventral prostate in serum-free primary culture. Prostate *17*, 207-218.

Taketa,S., Nishi,N., Takasuga,H., Okutani,T., Takenaka,I., and Wada,F. (1990b). Differences in growth requirements between epithelial and stromal cells derived from rat ventral prostate in serum-free primary culture. Prostate *17*, 207-218.

Tanner,M.M., Tirkkonen,M., Kallioniemi,A., Collins,C., Stokke,T., Karhu,R., Kowbel,D., Shadravan,F., Hintz,M., Kuo,W.L., and . (1994). Increased copy number at 20q13 in breast cancer: defining the critical region and exclusion of candidate genes. Cancer Res *54*, 4257-4260.

Tatoud,R., Degeorges,A., Prevost,G., Hoepffner,J.L., Gauville,C., Millot,G., Thomas,F., and Calvo,F. (1995). Somatostatin receptors in prostate tissues and derived cell cultures, and the in vitro growth inhibitory effect of BIM-23014 analog. Mol. Cell Endocrinol. *113*, 195-204.

Taylor-Papadimitriou,J., Purkis,P., Lane,E.B., McKay,I.A., and Chang,S.E. (1982). Effects of SV40 transformation on the cytoskeleton and behavioural properties of human keratinocytes. Cell Differ. *11*, 169-180.

Tchetgen,M.B. and Oesterling,J.E. (1995). The role of prostate-specific antigen in the evaluation of benign prostatic hyperplasia. Urol. Clin. North Am. *22*, 333-344.

Tegtmeyer,P. (1972). Simian virus 40 deoxyribonucleic acid synthesis: the viral replicon. J. Virol. *10*, 591-598.

Terpe,H.J., Stark,H., Prehm,P., and Gunthert,U. (1994). CD44 variant isoforms are preferentially expressed in basal epithelial of non-malignant human fetal and adult tissues. Histochemistry *101*, 79-89.

Tevethia,M.J. and Ripper,L.W. (1977). Biology of simian virus 40 (SV40) transplantation antigen (TrAg) II. Isolation and characterization of additional temperature-sensitive mutants of SV40. Virology *81*, 192-211.

Tevethia,M.J. and Tevethia,S.S. (1977). Biology of simian virus 40 (SV40) transplantation antigen (TrAg) III. Involvement of SV40 gene A in the expression of TrAg in permissive cells. Virology *81*, 212-223.

The Finasteride Study Group. (1993). Finasteride (MK-906) in the treatment of benign prostatic hyperplasia. Prostate *22*, 291-299.

Thigpen,A.E., Silver,R.I., Guileyardo,J.M., Casey,M.L., McConnell,J.D., and Russell,D.W. (1993). Tissue distribution and ontogeny of steroid 5 alpha-reductase isozyme expression. J. Clin. Invest *92*, 903-910.

Thomson,J.A., Pilotti,V., Stevens,P., Ayres,K.L., and Debenham,P.G. (1999). Validation of short tandem repeat analysis for the investigation of cases of disputed paternity. Forensic Sci. Int. *100*, 1-16.

Timms,B.G., Lee,C.W., Aumuller,G., and Seitz,J. (1995). Instructive induction of prostate growth and differentiation by a defined urogenital sinus mesenchyme. Microsc Res Tech. *30*, 319-332.

Todaro,H. and Green,H. (1962). 3T3 mouse fibroblast cell line. not known.

Toji,L.H., Lenchitz,T.C., Kwiatkowski,V.A., Sarama,J.A., and Mulivor,R.A. (1998). Validation of routine mycoplasma testing by PCR. In Vitro Cell Dev. Biol. Anim *34*, 356-358.

Troyanovsky,S.M., Guelstein,V.I., Tchipysheva,T.A., Krutovskikh,V.A., and Bannikov,G.A. (1989). Patterns of expression of keratin 17 in human epithelia: dependency on cell position. J. Cell Sci. *93 (Pt 3)*, 419-426.

Tubaro,A., Carter,S., Hind,A., Vicentini,C., and Miano,L. (2001). A prospective study of the safety and efficacy of suprapubic transvesical prostatectomy in patients with benign prostatic hyperplasia. J. Urol. *166*, 172-176.

Vermeulen,A., Giagulli,V.A., De Schepper,P., Buntinx,A., and Stoner,E. (1989). Hormonal effects of an orally active 4-azasteroid inhibitor of 5 alpha- reductase in humans. Prostate *14*, 45-53.

Walsh,P.C. and Wilson,J.D. (1976). The induction of prostatic hypertrophy in the dog with androstanediol. J. Clin. Invest *57*, 1093-1097.

Wang,Y., Hayward,S., Cao,M., Thayer,K., and Cunha,G. (2001). Cell differentiation lineage in the prostate. Differentiation *68*, 270-279.

Warwick,R. and Williams,P.L. eds. Gray's Anatomy. 973, 191-192. 2002. Longman, Edinburgh.

Watson,J.D., Gilman,M., Witkowski,J., and Zoller,M. (1992). Recombinant DNA. 2nd edition. Scientific American Books, Freeman,W.H. and company, New York.

Watt,K.W., Lee,P.J., M'Timkulu,T., Chan,W.P., and Loor,R. (1986). Human prostate-specific antigen: structural and functional similarity with serine proteases. Proc. Natl. Acad. Sci. U. S. A *83*, 3166-3170.

Webber,M.M., Bello,D., Kleinman,H.K., and Hoffman,M.P. (1997). Acinar differentiation by non-malignant immortalized human prostatic epithelial cells and its loss by malignant cells. Carcinogenesis *18*, 1225-1231.

Webber,M.M., Bello,D., Kleinman,H.K., Wartinger,D.D., Williams,D.E., and Rhim,J.S. (1996). Prostate specific antigen and androgen receptor induction and characterization of an immortalized adult human prostatic epithelial cell line. Carcinogenesis *17*, 1641-1646.

Webber,M.M., Quader,S.T., Kleinman,H.K., Bello-DeOcampo,D., Storto,P.D., Bice,G., DeMendonca-Calaca,W., and Williams,D.E. (2001). Human cell lines as an in vitro/in vivo model for prostate carcinogenesis and progression. Prostate *47*, 1-13.

Webber,M.M., Trakul,N., Thraves,P.S., Bello-DeOcampo,D., Chu,W.W., Storto,P.D., Huard,T.K., Rhim,J.S., and Williams,D.E. (1999). A human prostatic stromal myofibroblast cell line WPMY-1: a model for stromal-epithelial interactions in prostatic neoplasia. Carcinogenesis *20*, 1185-1192.

Weijerman,P.C., Konig,J.J., Wong,S.T., Niesters,H.G., and Peehl,D.M. (1994). Lipofection-mediated immortalization of human prostatic epithelial cells of normal and malignant origin using human papillomavirus type 18 DNA. Cancer Res. *54*, 5579-5583.

Wernert,N., Gerdes,J., Loy,V., Seitz,G., Scherr,O., and Dhom,G. (1988). Investigations of the estrogen (ER-ICA-test) and the progesterone receptor in the prostate and prostatic carcinoma on immunohistochemical basis. Virchows Arch. A Pathol. Anat. Histopathol. *412*, 387-391.

Wessel,R., Schweizer,J., and Stahl,H. (1992). Simian virus 40 T-antigen DNA helicase is a hexamer which forms a binary complex during bidirectional unwinding from the viral origin of DNA replication. J. Virol. *66*, 804-815.

Wilson,J.D. and Siiteri,P.K. (1973). Developmental pattern of testosterone synthesis in the fetal gonad of the rabbit. Endocrinology *92*, 1182-1191.

Wolter,H., Gottfried,H.W., and Mattfeldt,T. (2002). Genetic changes in stage pT2N0 prostate cancer studied by comparative genomic hybridization. BJU. Int. *89*, 310-316.

Wong YC, Cunha GR, and Hayashi N (1992). Effects of mesenchyme of the embryonic urogenital sinus and neonatal seminal vesicle on the cytodifferentiation of the Dunning tumor: ultrastructural study. Acta Anat (Basel). *143*, 139-150.

Wynder,E.L., Rose,D.P., and Cohen,L.A. (1994). Nutrition and prostate cancer: a proposal for dietary intervention. Nutr. Cancer *22*, 1-10.

Xu,L.L., Shanmugam,N., Segawa,T., Sesterhenn,I.A., McLeod,D.G., Moul,J.W., and Srivastava,S. (2000). A novel androgen-regulated gene, PMEPA1, located on chromosome 20q13 exhibits high level expression in prostate. Genomics. *66*, 257-263.

Xue,Y., Smedts,F., Debruyne,F.M., de la Rosette,J.J., and Schalken,J.A. (1998). Identification of intermediate cell types by keratin expression in the developing human prostate. Prostate *34*, 292-301.

Yanai N and Obinata M (2001). Oncostatin m regulates mesenchymal cell differentiation and enhances hematopoietic supportive activity of bone marrow stromal cell lines. In Vitro Cell Dev Biol Anim *37*, 698-704.

Yanai,N., Suzuki,M., and Obinata,M. (1991). Hepatocyte cell lines established from transgenic mice harboring temperature-sensitive simian virus 40 large T-antigen gene. Exp Cell Res *197*, 50-56.

Zeidler,R., Meissner,P., Eissner,G., Lazis,S., and Hammerschmidt,W. (1996). Rapid proliferation of B cells from adenoids in response to Epstein-Barr virus infection. Cancer Res 56(24), 5610-5614.

Zhang,J., Hess,M.W., Thurnher,M., Hobisch,A., Radmayr,C., Cronauer,M.V., Hittmair,A., Culig,Z., Bartsch,G., and Klocker,H. (1997). Human prostatic smooth muscle cells in culture: estradiol enhances expression of smooth muscle cell-specific markers. Prostate *30*, 117-129.

Ziada,A., Rosenblum,M., and Crawford,E.D. (1999). Benign prostatic hyperplasia: an overview. Urology *53*, 1-6.